

Energy Efficiency of P2P and Distributed Clouds Networks

Ahmed Qasim Lawey

Submitted in accordance with the requirements for the degree of
Doctor of Philosophy

The University of Leeds
School of Electronic and Electrical Engineering

June 2015

The candidate confirms that the work submitted is his own, except where work which has formed part of jointly-authored publications has been included. The contribution of the candidate and the other authors to this work has been explicitly indicated below. The candidate confirms that appropriate credit has been given within the thesis where reference has been made to the work of others.

Chapter 3 is based on the work from:

X. Dong, A. Lawey, T. E. H. El-Gorashi, and J. M. H. Elmirghani, “Energy-efficient core networks” *16th IEEE International Conference on Optical Network Design and Modelling (ONDM)*, pp. 1–9, 2012.

Prof. Elmirghani, the supervisor, suggested the study of the energy efficiency of BitTorrent content distribution in IP/WDM networks. The postdoc, Dr El-Gorashi, and the supervisor worked with the student on the MILP model development, results analyses and paper preparation. The PhD student developed the model, obtained and analysed the results, and wrote part I of the joint paper only. This paper includes three parts: energy efficient peer-to-peer networks, energy efficient data compression in optical networks and energy efficient topology design considering embodied energy in optical networks. I contributed the part related to energy efficient peer-to-peer networks only, while X. Dong contributed the other two parts.

And:

A. Lawey, T. El-Gorashi, and J. M. H. Elmirghani, “Energy-efficient peer selection mechanism for BitTorrent content distribution” *IEEE Global Communications Conference (GLOBECOM)*, pp. 1562-1567, 2012.

Prof. Elmirghani, the supervisor, contributed the concept of heterogeneous BitTorrent study. The postdoc, Dr El-Gorashi, and the supervisor worked with the student on the MILP model development, results analyses and paper preparation. The PhD student developed the model and heuristic, obtained and analysed the results, and wrote paper.

And:

A. Lawey, T. El-Gorashi, and J. M. H Elmirghani, "Impact of peers behaviour on the energy efficiency of BitTorrent over optical networks" *14th IEEE International Conference on Transparent Optical Networks (ICTON)*, pp. 1-8, 2012.

Prof. Elmirghani, the supervisor, suggested the study of the impact of peers' behaviour on the energy efficiency of BitTorrent over IP/WDM networks. The postdoc, Dr El-Gorashi, and the supervisor worked with the student on the MILP model development, results analyses, paper preparation and proposed operator controlled seeders to compensate for the leaving peers. The PhD student developed the model and heuristic, obtained and analysed the results, and wrote paper.

And:

A. Q. Lawey, T. E. El-Gorashi, and J. M. Elmirghani, "BitTorrent content distribution in optical networks" *IEEE/OSA Journal of Lightwave Technology*, vol. 32, pp. 3607-3623, 2014.

Prof. Elmirghani, the supervisor, suggested the idea of studying the impact of different topologies on BitTorrent content distribution in IP/WDM networks, the concept of peers that progressively traverse the network nodes to achieve better download rate in an enhanced heuristic, and the concept of location optimisation of operator controlled seeders. The supervisor also suggested the experimental evaluation of BitTorrent in a testbed and drawn its general scheme. The postdoc, Dr El-Gorashi, and the supervisor worked with the student on the MILP model development, results analyses and paper preparation and revision. The PhD student proposed CDN-P2P study, developed the models, heuristics and the experimental testbed, obtained and analysed the results, wrote the paper, and prepared the paper revision.

Chapter 4 is based on the work from:

A. Q. Lawey, T. El-Gorashi, and J. M. H. Elmirghani, "Energy efficient cloud content delivery in core networks" *IEEE Globecom Workshops (GC Wkshps)*, pp. 420-426, 2013.

Prof. Elmirghani, the supervisor, suggested the concept of distributed clouds for content delivery in IP/WDM networks. The postdoc, Dr El-Gorashi, and the supervisor worked with the student on the MILP model development, results analyses and paper preparation. The PhD student proposed the study of different content replication schemes, developed the models, obtained and analysed the results, and wrote the paper.

And:

A. Q. Lawey, T. E. El-Gorashi, and J. M. H. Elmirghani, “Distributed Energy Efficient Clouds Over Core Networks” *IEEE Journal of Lightwave Technology*, vol. 32, pp. 1261-1281, 2014.

Prof. Elmirghani, the supervisor, suggested the study of the impact of different content size on the energy efficiency of content delivery clouds in IP/WDM networks, contributed the concept of storage as a service energy efficiency as a function of content access rate, and proposed the study of non-uniform geo distribution of requesting users on the overall energy efficiency. The postdoc, Dr El-Gorashi, and the supervisor worked with the student on the MILP model development, results analyses and paper preparation and revision. The PhD student developed the models and heuristics, obtained and analysed the results, wrote the paper, and prepared the paper revision.

Chapter 5 is based on the work from:

A. Q. Lawey, T. E. El-Gorashi, and J. M. H. Elmirghani, “Distributed Energy Efficient Clouds Over Core Networks” *IEEE Journal of Lightwave Technology*, vol. 32, pp. 1261-1281, 2014.

Prof. Elmirghani, the supervisor, suggested the study of virtual machines placement in IP/WDM networks. The postdoc, Dr El-Gorashi, and the supervisor worked with the student on the MILP model development, results analyses and paper preparation and revision. The PhD student proposed studying three different VM replication schemes, developed the models and heuristics, obtained and analysed the results, wrote the paper, and prepared the paper revision.

Chapter 6 is based partly on the work from:

A. Q. Lawey, T. E. El-Gorashi, and J. M. H. Elmirghani, “Renewable Energy in Distributed Energy Efficient Content Delivery Clouds” *IEEE International Conference on Communications (ICC), Selected Areas on Communications (SAC) Symposium - Green Communications track*, 2015.

Prof. Elmirghani, the supervisor, suggested the study of the impact of renewable energy availability, represented by wind farms, on distributed content delivery clouds location and content replication schemes. The postdoc, Dr El-Gorashi, and the supervisor worked with the student on the MILP model development, results analyses and paper preparation. The PhD student proposed three different approaches to optimise the use of wind farms renewable energy to power the clouds, developed the model, obtained and analysed the results, and wrote the paper.

This copy has been supplied on the understanding that it is copyright material and that no quotation from the thesis may be published without proper acknowledgement.

© 2015 The University of Leeds and Ahmed Q. Lawey

Acknowledgements

I would like to sincerely thank my supervisor, Professor Jaafar Elmirghani for his inestimable assistance and patience throughout my PhD journey. His insights and valuable advices paved the road toward accomplishing the goals of this work.

I would like to acknowledge Dr. T. H. El-Gorashi, my academic advisor for her worthwhile advices and rewarding discussions.

I would like to acknowledge the Iraqi Ministry of Higher Education for funding my Ph.D. study and for their support.

I wish to express my love and gratitude to my beloved family. I am indebted to my mother Bariqa and uncle Mozahem for their everlasting support and love through all stages of my life and especially during my Ph.D.

Finally I would like to express my love and gratefulness to my wife, Laila, for her support, patience and understanding during the course of my Ph.D.

Abstract

Since its inception, the Internet witnessed two major approaches to communicate digital content to end users: peer to peer (P2P) and client/server (C/S) networks. Both approaches require high bandwidth and low latency physical underlying networks to meet the users' escalating demands. Network operators typically have to overprovision their systems to guarantee acceptable quality of service (QoS) and availability while delivering content. However, more physical devices led to more ICT power consumption over the years. An effective approach to confront these challenges is to jointly optimise the energy consumption of content providers and transportation networks. This thesis proposes a number of energy efficient mechanisms to optimise BitTorrent based P2P networks and clouds based C/S content distribution over IP/WDM based core optical networks.

For P2P systems, a mixed integer linear programming (MILP) optimisation, two heuristics and an experimental testbed are developed to minimise the power consumption of IP/WDM networks that deliver traffic generated by an overlay layer of homogeneous BitTorrent users. The approach optimises peers' selection where the goal is to minimise IP/WDM network power consumption while maximising peers download rate. The results are compared to typical C/S systems. We also considered Heterogeneous BitTorrent peers and developed models that optimise P2P systems to compensate for different peers behaviour after finishing downloading. We investigated the impact of core network physical topology on the energy efficiency of BitTorrent systems. We also investigated the power consumption of Video on Demand (VoD) services using CDN, P2P and hybrid CDN-P2P architectures over IP/WDM networks and addressed content providers efforts to balance the load among their data centres.

For cloud systems, a MILP and a heuristic were developed to minimise content delivery induced power consumption of both clouds and IP/WDM networks. This was done by optimally determining the number, location and internal capability in terms of servers, LAN and storage of each cloud, subject to daily traffic variation. Different replication schemes were studied revealing that replicating content into multiple clouds based on content popularity is the optimum approach with respect to energy. The model was extended to study Storage as a Service (StaaS). We also

studied the problem of virtual machine placement in IP/WDM networks and showed that VM Slicing is the best approach compared to migration and replication schemes to minimise energy.

Finally, we have investigated the utilisation of renewable energy sources represented by solar cells and wind farms in BitTorrent networks and content delivery clouds, respectively. Comprehensive modelling and simulation as well as experimental demonstration were developed, leading to key contributions in the field of energy efficient telecommunications.

Table of Contents

| | |
|---|-----|
| Acknowledgements | i |
| Abstract..... | ii |
| Table of Contents | iv |
| List of Figures..... | ix |
| List of Tables | xiv |
| Chapter 1: Introduction..... | 1 |
| 1.1 Research Objectives..... | 5 |
| 1.2 Original Contributions | 6 |
| 1.3 Related Publications | 8 |
| 1.4 Thesis Structure | 9 |
| Chapter 2: Energy Efficient Core and Content Distribution Networks..... | 11 |
| 2.1 Introduction..... | 11 |
| 2.2 Core Networks | 11 |
| 2.3 IP/WDM Core Network Architecture..... | 12 |
| 2.4 Energy Efficiency of IP/WDM Core Networks..... | 13 |
| 2.5 Content Distribution in Optical Core Networks | 14 |
| 2.5.1 BitTorrent Based P2P Content Distribution..... | 15 |
| 2.5.2 Energy Efficiency of BitTorrent Content Distribution | 17 |
| 2.5.3 Cloud Based Content Distribution | 18 |
| 2.5.4 Energy Efficiency of Cloud Based Content Distribution..... | 21 |

| | | |
|--|--|----|
| 2.5.5 | Energy Efficient Virtual Machines' Placement in the Cloud.. | 23 |
| 2.6 | Mixed Integer Linear Programming Overview | 23 |
| 2.7 | Summary | 26 |
| Chapter 3: Energy Efficient BitTorrent Content Distribution in Optical Core Networks | | |
| | | 27 |
| 3.1 | Introduction..... | 27 |
| 3.2 | Mathematical Model for BitTorrent Systems | 27 |
| 3.3 | Results of the MILP Model | 34 |
| 3.4 | Energy Efficient BitTorrent Heuristic | 43 |
| 3.5 | Enhanced Energy Efficient BitTorrent Heuristic (EEBTv2)..... | 47 |
| 3.6 | Impact of Peers Upload Rate Heterogeneity..... | 49 |
| 3.7 | Impact of Leechers Behaviour | 53 |
| 3.8 | Location Optimisation for OCSs | 59 |
| 3.9 | Impact of Physical Topology | 63 |
| 3.9.1 | AT&T Network..... | 65 |
| 3.9.2 | British Telecom European Network (EU BT)..... | 67 |
| 3.9.3 | Italian Network..... | 68 |
| 3.10 | Hybrid CDN-P2P Architecture | 70 |
| 3.11 | Energy Efficient BitTorrent Experimental Demonstration..... | 80 |
| 3.11.1 | Experimental Setup | 80 |
| 3.11.2 | Experimental Results..... | 81 |
| 3.12 | Summary | 84 |

| | |
|--|-----|
| Chapter 4: Energy Efficient Content Distribution in Distributed Clouds over Optical Core Networks..... | 86 |
| 4.1 Introduction..... | 86 |
| 4.2 MILP for Cloud Content Delivery..... | 86 |
| 4.3 MILP Model Results..... | 93 |
| 4.3.1 Popularity Group Size $PGSp = 3.78$ TB | 97 |
| 4.3.2 Popularity Group Size $PGSp = 0.756$ TB | 105 |
| 4.4 DEER-CD: Energy Efficient Content Delivery Heuristic for the Cloud | 111 |
| 4.5 Energy Efficient Storage as a Service (StaaS)..... | 116 |
| 4.6 Summary..... | 122 |
| Chapter 5: Energy Efficient Virtual Machine Placement in Optical Core Networks | 124 |
| 5.1 Introduction..... | 124 |
| 5.2 Mathematical Model | 124 |
| 5.3 Cloud VM Model Results: | 129 |
| 5.4 DEER-VM: Energy Efficient VM Distribution for the Cloud | 134 |
| 5.5 Summary..... | 138 |
| Chapter 6: Renewable Energy for P2P and Distributed Clouds Networks | 139 |
| 6.1 Introduction..... | 139 |
| 6.2 Renewable Energy for P2P Networks | 140 |
| 6.3 Renewable Energy for P2P Networks MILP | 142 |
| 6.4 Renewable Energy for P2P Networks MILP Results | 145 |

| | | |
|--|---|-----|
| 6.4.1 | MHRT-LSM Approach..... | 146 |
| 6.4.2 | GRT-GSM Approach..... | 147 |
| 6.4.3 | MHRT-GSM Approach..... | 148 |
| 6.4.4 | GRT-LSM Approach..... | 149 |
| 6.4.5 | Quasi Selection Matrix (MHRT-QLSM & MHRT-QGSM) Approaches..... | 152 |
| 6.5 | Renewable Energy for Distributed Clouds Networks..... | 153 |
| 6.6 | Renewable Powered Content Delivery Cloud Model..... | 154 |
| 6.7 | Renewable Powered Content Delivery Cloud Results | 156 |
| 6.7.1 | Approach 1: $\sigma = 1, \theta = 1$ and $\omega = 1$ | 157 |
| 6.7.2 | Approach 2: $\sigma = 1, \theta = 1$ and $\omega = 0$ | 159 |
| 6.7.3 | Approach 3: $\sigma = 100, \theta = 1$ and $\omega = 1$ | 160 |
| 6.8 | Summary..... | 161 |
| Chapter 7: Conclusions and Future Work | | 163 |
| 7.1 | Summary of Contributions..... | 163 |
| 7.2 | Future Work..... | 170 |
| 7.2.1 | Extensions Based On Stated Limitations | 170 |
| 7.2.2 | Re-Connect the Network Dots, From Core to Aggregation to Access | 170 |
| 7.2.3 | Multi-Level Resource Swarms of IP/WDM Networks..... | 171 |
| 7.2.4 | Game Theoretical Approach for Clouds over IP/WDM networks | 171 |

| | |
|--|-----|
| 7.2.5 Energy Efficient Publish/Subscribe for IoT in IP/WDM Networks | 171 |
| 7.2.6 Optimising the Number of Upload Slots' and Their Data Rate for BitTorrent | 172 |
| 7.2.7 Big Data in IP/WDM Networks | 172 |
| 7.2.8 Integrating Queuing Theory with MILP for Content Distribution in Distributed Clouds in IP/WDM Networks | 172 |
| List of Abbreviations | 174 |
| References | 180 |

List of Figures

| | |
|--|----|
| Fig. 2 - 1: IP/WDM network | 13 |
| Fig. 2 - 2: Cloud architecture | 20 |
| Fig. 3 - 1: NSFNET network with links lengths in km | 36 |
| Fig. 3 - 2: Peers selection matrix U_{ijk} | 38 |
| Fig. 3 - 3: Number of hops travelled by traffic resulting from peers selections (MILP) | 39 |
| Fig. 3 - 4: Number of hops between NSFNET nodes | 39 |
| Fig. 3 - 5: Average download rate versus number of seeders per swarm | 40 |
| Fig. 3 - 6: IP/WDM power consumption versus number of seeders per swarm | 41 |
| Fig. 3 - 7: IP/WDM energy consumption versus number of seeders per swarm | 42 |
| Fig. 3 - 8: Energy efficient bittorrent heuristic (EEBT heuristic) | 44 |
| Fig. 3 - 9: Number of hops travelled by traffic resulting from peers selections (EEBT heuristic) | 46 |
| Fig. 3 - 10: The flowchart of the EEBTv2 heuristic | 47 |
| Fig. 3 - 11: The performance of the different bittorrent heuristics (a) Average download rate (b) IP/WDM power consumption (c) IP/WDM energy consumption | 48 |
| Fig. 3 - 12: The average download time of a heterogeneous bittorrent system (CN = 2) | 51 |
| Fig. 3 - 13: IP/WDM energy consumption of a heterogeneous bittorrent system (CN = 2) | 52 |
| Fig. 3 - 14: Percentage of the file downloaded for each group | 54 |

| | |
|--|----|
| Fig. 3 - 15: Average download rate with different number of original seeders | 54 |
| Fig. 3 - 16: IP/WDM power consumption with different number of original seeders | 55 |
| Fig. 3 - 17: IP/WDM energy consumption with different number of original seeders | 56 |
| Fig. 3 - 18: OCSs average upload rate | 58 |
| Fig. 3 - 19: MILP results for OCS (a) Average download rate (b) IP/WDM power consumption (c) IP/WDM energy consumption | 62 |
| Fig. 3 - 20: AT&T network [92], [93], [94] | 65 |
| Fig. 3 - 21: AT&T network results (a) Download rate (b) IP/WDM power consumption (c) IP/WDM energy consumption | 66 |
| Fig. 3 - 22: EU BT network [92], [95], [96] | 67 |
| Fig. 3 - 23: EU BT network results (a) IP/WDM power consumption (b) IP/WDM energy consumption | 68 |
| Fig. 3 - 24: The italian network [92], [97], [98]..... | 69 |
| Fig. 3 - 25: Italian network results (a) IP/WDM power consumption (b) IP/WDM energy consumption | 70 |
| Fig. 3 - 26: CDN-P2P results (a) Total power consumption (b) IP/WDM network power consumption (c) CDN data centre power consumption... | 75 |
| Fig. 3 - 27: File sharing effectiveness | 78 |
| Fig. 3 - 28: Total power consumption (IP/WDM and data centres) with and without load balancing in CDN-P2P..... | 79 |
| Fig. 3 - 29: Experiment racks and connectivity | 81 |
| Fig. 3 - 30: Experimental average download rate and IP/WDM power consumption of original bittorrent experiment (OBT experiment)..... | 82 |

| | |
|--|-----|
| Fig. 3 - 31: Experimental average download rate and IP/WDM power consumption of energy efficient bittorrent experiment (EEBT experiment) | 82 |
| Fig. 3 - 32: Locality for experimental OBT and EEBT | 84 |
| Fig. 4 - 1: Number of users versus time of the day | 94 |
| Fig. 4 - 2: $PGSp = 3.78TB$ (a) Total power consumption (b) IP/WDM power network consumption (c) Cloud power consumption | 98 |
| Fig. 4 - 3: OFR powered on clouds at different times of the day ($PGSp = 3.78 TB$)..... | 101 |
| Fig. 4 - 4 Popularity groups placement under the OPR scheme at 06:00 and 22:00 ($PGSp = 3.78 TB$) | 102 |
| Fig. 4 - 5: Total number of replications per popularity group under the OPR scheme ($PGSp = 3.78 TB$) | 103 |
| Fig. 4 - 6: Number of popularity groups replicated at each node under the OPR scheme ($PGSp = 3.78 TB$) | 104 |
| Fig. 4 - 7: Number of powered on servers in each cloud under the OPR scheme ($PGSp = 3.78 TB$) | 104 |
| Fig. 4 - 8: $PGSp = 0.756 TB$ (a) Total power consumption (b) IP/WDM network power consumption (c) Cloud power consumption | 105 |
| Fig. 4 - 9: OFR powered on clouds at different times of the day ($PGSp = 0.756 TB$) | 106 |
| Fig. 4 - 10: Popularity groups placement under the OPR scheme at 06:00 and 22:00 ($PGSp = 0.756 TB$) | 108 |
| Fig. 4 - 11: Total number of replications per popularity group under the OPR scheme ($PGSp = 0.756 TB$) | 109 |

| | |
|---|-----|
| Fig. 4 - 12: Number of popularity groups replicated at each cloud under the OPR scheme ($PGSp = 0.756 TB$) | 109 |
| Fig. 4 - 13: Number of powered on servers in each cloud under the OPR scheme ($PGSp = 0.756 TB$) | 110 |
| Fig. 4 - 14: The DEER-CD heuristic pseudo-code | 113 |
| Fig. 4 - 15: (a) Total power consumption of the DEER-CD heuristic (b) IP/WDM network power consumption of the DEER-CD heuristic (c) Cloud power consumption of the DEER-CD heuristic..... | 114 |
| Fig. 4 - 16: Total number of replications per popularity group for DEER-CD ($PGSp = 3.78 TB$) | 115 |
| Fig. 4 - 17: Total number of replications per popularity group for DEER-CD ($PGSp = 0.756 TB$)..... | 115 |
| Fig. 4 - 18: Total power consumption of StaaS (b) IP/WDM network power consumption of StaaS (c) Cloud power consumption of StaaS | 120 |
| Fig. 4 - 19: Powered on clouds storage size versus content access frequency for the StaaS optimal scheme (45 MB file size)..... | 122 |
| Fig. 5 - 1: Sample VMs CPU and network utilisation | 131 |
| Fig. 5 - 2: Total power consumption of the different VMs scenarios (b) IP/WDM network power consumption of the different VMs scenarios (c) Cloud power consumption of the different VMs scenarios | 132 |
| Fig. 5 - 3: (a) VMs distribution scheme at 06:00. (b) VMs distribution scheme at 22:00..... | 133 |
| Fig. 5 - 4: DEER-VM heuristic pseudo-code..... | 135 |
| Fig. 5 - 5: DEER-VM total power consumption (b) DEER-VM IP/WDM network power consumption (c) DEER-VM cloud power consumption | 136 |
| Fig. 6 - 1: Illustrative example | 140 |

| | |
|--|-----|
| Fig. 6 - 2: Power consumption versus increasing number of green nodes for the MHRT-LSM approach | 147 |
| Fig. 6 - 3: Power consumption versus increasing number of green nodes for the GRT-GSM approach | 147 |
| Fig. 6 - 4: Power consumption versus increasing number of green nodes for the MHRT-GSM approach..... | 149 |
| Fig. 6 - 5: Power consumption versus increasing number of green nodes for the GRT-LSM approach..... | 150 |
| Fig. 6 - 6: Average hop count versus increasing number of green nodes | 151 |
| Fig. 6 - 7: Relative power consumption of the four approaches | 151 |
| Fig. 6 - 8: Non-renewable power consumption versus increased number of green nodes where no local unchoke is allowed | 153 |
| Fig. 6 - 9: The NSFNET network with wind farms locations..... | 157 |
| Fig. 6 - 10: Clouds power consumption (Approach 1) | 158 |
| Fig. 6 - 11: Number of popularity groups (Approach 1)..... | 158 |
| Fig. 6 - 12: Clouds power consumption (Approach 2) | 159 |
| Fig. 6 - 13: Number of popularity groups (Approach 2)..... | 160 |
| Fig. 6 - 14: Clouds power consumption (Approach 3) | 160 |

List of Tables

| | |
|---|-----|
| Table 3 - 1: Input parameters for the MILP model | 36 |
| Table 3 - 2: Analysed Networks Information | 64 |
| Table 3 - 3: Input Data for the CDN-P2P Model | 74 |
| Table 3 - 4: Demo hardware components | 80 |
| Table 4 - 1: Input Data for the Clouds Models | 94 |
| Table 4 - 2: The power savings gained by the different content delivery clouds models compared to the SNPM model..... | 110 |
| Table 4 - 3: Optimisation gaps between the DEER-CD heuristic and MILP . | 116 |
| Table 5 - 1: Input data for the VM models | 130 |
| Table 5 - 2: Power saving of the different schemes compared to single cloud under geographically non-uniform traffic..... | 134 |
| Table 5 - 3: Optimisation gaps between the DEER-VM heuristic and MILP | 137 |
| Table 6 - 1: Different approaches to deliver a data piece from P1 to P2 and P3 in Fig. 6 - 1 | 141 |
| Table 6 - 2: Input data for renewable energy in P2P networks model..... | 145 |

Chapter 1: Introduction

The Internet is currently witnessing its own version of the Big Bang: it is expanding rapidly in the four dimensions of physical reachability [1], number of users [2], number of attached devices [3], and number of services provided [4]. This expansion manifests itself as growing global traffic, a growth that is estimated to range from 21% [3] to 40% [5] per year, forecasted over the period from 2014 up to 2020. The majority of today's Internet services are content oriented [6], either of a macroscopic nature such as IPTV streaming or of a microscopic nature such as information sharing among Internet of Things (IoT) devices. In either case, the traffic is going to be massively aggregated at core networks due to transporting a small number of large sized content items, e.g. high definition video, or transporting a large number of small sized content items, e.g. sensor updates that sum into a form of Big Data [7]. To support such a large traffic volume with differentiated Quality of Service (QoS), additional intelligent and large capacity equipment has to be deployed across the Internet, especially at Internet Service Provider (ISP) cores. The energy consumption of this equipment is expected to be a major obstacle facing scalable Internet services [8]. In addition there is the negative environmental impact associated with CO₂ emissions from the ICT sector. This is projected to contribute about 2% of the global greenhouse emissions by 2020 [9]. One approach to tackle this problem is to re-examine the basic mechanisms we use to transport and share content across the Internet. Two major approaches have evolved over the years: Peer to Peer (P2P) and Client/Server (C/S) overlay networks. From [5] it is evident that P2P traffic generated mainly by BitTorrent networks; and video services that mostly rely on C/S networks such as YouTube and Netflix, are the major traffic producers in the Internet. It can be argued that the data in [5] may vary over the years, and one content delivery approach could overcome the other if it proved to be cheaper or

more flexible, etc. However, P2P and C/S networks are probably here to stay. For instance, video sharing has shifted over the years from BitTorrent networks to YouTube due to copyright issues [10]; meanwhile, P2P systems are finding their way towards new types of networks such as Vehicular Ad Hoc Networks (VANET) [11] and IoT [12].

Transporting information uses energy at the machines supporting the overlay networks, such as servers and storage, as well as the underlying network layer equipment, such as backbone routers and optical switches. To save energy in an optimal way, we have to consider the interaction between these two layers during energy minimisation as saving energy in one layer might lead to an increase in energy consumption or performance degradation in the other layer. In this thesis we present several mechanisms that can be deployed to jointly minimise the power consumption of BitTorrent based P2P and cloud based C/S overlay networks as well as the underlying physical networks' power consumption. We consider IP/WDM optical core networks as it is most widely deployed network in the ISP cores.

P2P protocols allow end users to share content without the need to centrally host and deliver the content, for example using a centralised content server. Peers in P2P protocols need to establish connections among them so that they can orchestrate content downloading. These connections can be structured in tree like topology or unstructured in mesh like topology. BitTorrent is the most popular form of P2P protocols. Users share content using BitTorrent protocol by distributing pieces of that content among them in unstructured overlay topology. These pieces are selectively sent from one peer to another based a rewarding mechanisms, i.e. a peer is more likely to receive a desired piece if that peer is more likely to send pieces to other peers that they desire. By optimising this peers' selection, we can control the shape of the traffic in the Internet and therefore, provide means to minimise the power consumption of the network by powering off un-utilised resources. Therefore, any success in optimising P2P protocols for energy efficiency would yield considerable energy savings in core networks as P2P traffic is one of the main contributors to the core network traffic, and therefore, its energy consumption.

For P2P systems, this work presents detailed analyses of BitTorrent networks, the original implementation of BitTorrent is considered together with its impact on the energy consumption of IP/WDM networks. As a result an energy efficient

BitTorrent approach is proposed. The approach exploits physical location awareness. It emerged as a result of the Mixed Integer Linear programming (MILP) mathematical optimisation. A heuristic and an experimental testbed were developed and used to verify the MILP optimisation. The goal of the optimisation was to ensure that the BitTorrent peers work at the highest possible performance (i.e. download rates) and lowest possible IP/WDM network energy consumption. The study also investigated a number of factors that can hinder or facilitate IP/WDM network energy saving, such as peer upload rate heterogeneity, peer behaviour after finishing downloading, and physical topology. We also studied the energy efficiency of hybrid CDN-P2P networks, and compared different mechanisms to harness CDN coexistence with P2P swarms.

For cloud networks, we investigated in detail breaking up clouds / data centres and geographically distributing them over the core network to improve the overall network and data centre energy efficiency, hence the term “distributed clouds”. This is a significant departure from current accepted wisdom and trends where larger and larger data centres are traditionally built to accommodate new services under increased content and user numbers. This methodology allows us to co-optimize core optical network energy efficiency with cloud energy efficiency as content/services are not bounded to a limited geographical area and can be migrated/replicated on demand to minimise the overall energy consumption of the core network and the clouds. This investigation has been conducted using mathematical modelling and heuristics. We compared different content replications and evaluated their impact on clouds, network performance, and energy consumption, where we identified the best content replication strategy that can adapt to traffic and content popularity shifts over time. The goal is to satisfy the delivery requirements in terms of perceived download rates while minimising IP/WDM network power consumption. We then studied a limited version of a content delivery scenario, namely Storage as a Service (StaaS) over IP/WDM networks where the goal is to deliver users’ files in an energy efficient manner from nearby clouds based on the rate at which they access their files. Furthermore, Virtual Machine (VM) placement in IP/WDM networks is studied by developing a mathematical model and a heuristic. The goal is to place these VMs at the optimal locations that yield the minimum IP/WDM power consumption while satisfying traffic and CPU utilisation constraints. We studied different VM distribution patterns, and established limits on

the energy efficiency of VM placement for different services and the impact of geographical uniformity/non-uniformity of VM requests, subject to daily traffic variations. Note that these geographically distributed clouds are designed to be managed by a single cloud provider/supplier. However, the work can be potentially extended so that the core network hosts clouds managed by different suppliers where the impact of cooperation vs. conflict on the overall energy efficiency can be evaluated.

Finally, we studied the minimisation of non-renewable energy by introducing renewable energy sources, which are represented by solar cells and wind farms, and investigated the resultant impact on content distribution in BitTorrent based P2P and cloud networks. The goal is to use renewable energy to replace the non-renewable energy in IP/WDM networks for the P2P scenario, and to replace the non-renewable energy in datacentres in the cloud scenario while optimising peer selection (for P2P), content replication (for the clouds), and traffic routing in both cases. We established the trade-offs relating to the influence of renewable energy on peer selection behaviour for P2P and the influence of renewable energy on content replication patterns for the clouds.

We have chosen MILP as the key mathematical basis for energy efficiency evaluation for several reasons. First, MILP is a standard mathematical modelling technique for network flow problems. This is inspired by the success of MILP in modelling transportation problems in industrial logistics. Second, MILP allows flexible extensions for the considered problems by adding new constraints that controls the behaviour of the problem under certain conditions. This has the advantage of allowing MILP to provide solutions and insights that can be harnessed to develop real time heuristic implementations. Third, MILP is already used to evaluate energy efficiency of IP/WDM networks. Therefore, using MILP is a natural choice for this thesis that concentrates on the energy efficiency of IP/WDM networks. The heuristics we developed, as well as the experimental demonstrations based on those heuristics, represent a validation for the MILP solutions as the heuristics working principles are independent of those of the MILP models as will be discussed in more details in Chapters 3, 4 and 5.

1.1 Research Objectives

The following primary objectives were set for the work reported in this thesis:

1. Investigate the energy efficiency of BitTorrent based P2P content distribution in optical core networks represented by an IP/WDM network using mathematical modelling. Based on the insights gained through the mathematical modelling, develop appropriate heuristics that can run in real time environments as well as an experimental demonstration. Finally, compare the results obtained to the traditional client/server approach for homogeneous (user data rates) and heterogeneous cases.
2. Investigate the impact of BitTorrent users' (i.e. peers) altruistic or greedy behaviour on the system performance and energy efficiency and propose a methodology to respond to their behaviour suitable for consideration by the network operator.
3. Study the impact of physical topology on the performance and energy efficiency of BitTorrent systems in IP/WDM networks.
4. Study the energy efficiency of hybrid P2P systems assisted by C/S content delivery in CDN-P2P systems.
5. Assess the impact of the availability of renewable energy on P2P systems' performance and energy efficiency.
6. Investigate centralised vs. distributed cloud computing in IP/WDM core optical networks. Establish the factors that impact the decision of whether to centralise or distribute the cloud. Assess different cloud based services, such as content distribution, storage as a service, and virtual machine placement for processing applications.
7. Assess the impact of the availability of renewable energy on cloud computing and content distribution.

1.2 Original Contributions

The main contributions of this thesis are as follows:

1. The development of a MILP that models the energy consumption of bypass and non-bypass IP/WDM networks subject to traffic generated by file sharing swarms of the original and energy efficient, location aware homogeneous BitTorrent. The model was extended to account for heterogeneous peers as well as including the impact of physical topology. We have shown an average energy saving up to 36% in non-bypass IP/WDM networks employing the energy efficient BitTorrent model compared to C/S model.
2. Two heuristics (EEBT and EEBTv2) were developed for real time implementation of the energy efficient BitTorrent. The first was restricted to a one hop searching radius and the second has an enhanced dynamic search radius to trade energy consumption for better performance. Comparable power savings and performance were achieved by the first and second heuristics, respectively, compared to the MILP.
3. Experimental evaluation of the energy efficient BitTorrent using 14 Cisco switch routers and 14 HP servers to emulate the NSFNET 14 node network. We demonstrated an average 40% power saving in non-bypass IP/WDM networks while maintaining a steady state peer download rate of 1 Mbps.
4. A MILP model was constructed to evaluate the implications of renewable energy on the energy efficient BitTorrent. The renewable energy was generated by solar cells and used to power the IP/WDM core nodes. In the presence of renewable energy we studied the optimum peer selection and the resultant traffic from content sources (seeders and leechers) to content downloaders (leechers only). Six approaches were introduced to harness renewable energy with varying complexities and efficiencies. The results provided evidence for the potential to save up to 36% of non-renewable power when only P2P traffic was optimised.
5. Proposal of upload rate adaptable operator controlled seeders (OCS), evaluated by MILP and a heuristic, to compensate for the greedy behaviour of

some BitTorrent peers where such peers leave the network after finishing downloading, thereby causing lower capacity and performance for the remaining peers. The approach was extended to enable operators to optimise OCSs locations and upload rates to achieve optimal compensation against leechers' behaviour. It was shown that OCSs can help maintain the download rate and save 15% energy compared to the case where leechers stay after finishing the downloading process.

6. Introduction of a MILP for CDN-P2P systems. This includes two different approaches for the hybrid implementation, estimating long term CDN-P2P impact on deferring datacentres' upgrades and quantifying the impact of CDN-P2P systems on datacentres' load balance. One particular approach, H-MinTPC, saved 61% of the total power consumption compared to the CDN-Only architecture.
7. A MILP and a heuristic (DEER-CD) were developed for cloud content delivery over non-bypass IP/WDM networks. We proposed a dynamic replication approach to decide the optimal energy efficient location of content subject to daily traffic variation, as well as the optimal number of clouds, capacity of each cloud in terms of number of servers, internal LAN switches, and upload traffic. The optimal distributed approach demonstrated that network and total power savings of 92% and 43%, respectively, could be achieved for clouds of small sized content, such as music files. Comparable results were obtained for the heuristic.
8. Proposal of a MILP for the minimisation of non-renewable energy through the introduction of renewable energy, represented by wind farms used in content delivery clouds. We minimised the non-renewable energy used in the IP/WDM network and in the cloud as well as the transmission power losses associated with transferring power from wind farms to clouds. Three approaches were compared under different renewable energy availability conditions. The results showed the ability to save 35% of the transmission power while minimising the IP/WDM network non-renewable power consumption.

9. A MILP for energy efficient StaaS over non-bypass IP/WDM networks was introduced. A network power saving of 48% was demonstrated compared to serving content from a single central cloud for large file sizes of 45MB, while lower sized files resulted in lower savings.
10. A MILP and heuristic (DEER-VM) for energy efficient virtual machine placement over non-bypass IP/WDM networks were developed. We studied three VM distribution approaches and established the optimal placement approach. The MILP showed that up to 76% and 25% of the network and total power could be saved, respectively, compared to a single virtualised cloud scenario. Comparable power savings were obtained by placing VMs using the heuristic.

1.3 Related Publications

The original contributions in this thesis are supported by the following publications:

- **Journals**

1. A. Q. Lawey, T. E. El-Gorashi, and J. M. Elmirghani, “BitTorrent content distribution in optical networks” *IEEE/OSA Journal of Lightwave Technology*, vol. 32, pp. 3607-3623, 2014.
2. A. Q. Lawey, T. E. El-Gorashi, and J. M. H. Elmirghani, “Distributed Energy Efficient Clouds Over Core Networks” *IEEE Journal of Lightwave Technology*, vol. 32, pp. 1261-1281, 2014.

- **Conferences**

3. X. Dong, A. Lawey, T. E. H. El-Gorashi, and J. M. H. Elmirghani, “Energy-efficient core networks” *16th IEEE International Conference on Optical Network Design and Modelling (ONDM)*, pp. 1–9, 2012.
4. A. Lawey, T. El-Gorashi, and J. M. H. Elmirghani, “Energy-efficient peer selection mechanism for BitTorrent content distribution” *IEEE Global Communications Conference (GLOBECOM)*, pp. 1562-1567, 2012.

5. A. Lawey, T. El-Gorashi, and J. M. H Elmirghani, "Impact of peers behaviour on the energy efficiency of BitTorrent over optical networks" *14th IEEE International Conference on Transparent Optical Networks (ICTON)*, pp. 1-8, 2012.
 6. A. Q. Lawey, T. El-Gorashi, and J. M. H. Elmirghani, "Energy efficient cloud content delivery in core networks" *IEEE Globecom Workshops (GC Wkshps)*, pp. 420-426, 2013.
 7. A. Q. Lawey, T. E. El-Gorashi, and J. M. H. Elmirghani, "Renewable Energy in Distributed Energy Efficient Content Delivery Clouds" *IEEE International Conference on Communications (ICC), Selected Areas on Communications (SAC) Symposium - Green Communications track*, 2015.
- **Book Chapter**
8. T. E.H. El-Gorashi, A.Q. Lawey, X. Dong and J. M. H. Elmirghani, "Energy Efficient Content Distribution" in "*Communication Infrastructures for Cloud Computing*" ISBN13: 9781466645226, DOI: 10.4018/978-1-4666-4522-6.

1.4 Thesis Structure

Following the introduction in Chapter 1, the rest of the thesis is organised as follows:

Chapter 2 provides an overview of the main topics addressed in this thesis, including core networks with special attention given to IP/WDM networks as the core optical network used in the thesis. Attention is given to content distribution in BitTorrent based P2P and cloud based C/S systems as well as the MILP modelling approach. The chapter reviews the literature on energy efficient IP/WDM networks, energy efficient BitTorrent networks, energy efficient content delivery, and virtual machine placement in clouds networks.

Chapter 3 introduces the BitTorrent systems MILP model and its results. It proposes an energy efficient BitTorrent heuristic and compares its performance to the MILP model. It proposes an extended energy efficient BitTorrent heuristic (EEBTv2) and compares its performance to the first heuristic (EEBT), and then

discusses the impact of leechers' behaviour on the network performance and energy consumption. Following this it introduces a new MILP for studying the impact of peers' behaviour where we optimise the location and upload rates of operator controlled seeders. It investigates the impact of physical network topology on the performance and energy consumption of BitTorrent systems, and the power consumption of a hybrid CDN-P2P network. Finally, an experimental evaluation of EEBT is reported in this chapter and the results are compared to the MILP model.

Chapter 4 introduces the MILP optimisation developed for cloud content delivery, discusses its results, and proposes the DEER-CD real time heuristic. It extends the content delivery model to study StaaS.

Chapter 5 introduces a MILP for virtual machine placement in IP/WDM networks for a distributed cloud scenario and a heuristic (DEER-VM) is proposed.

Chapter 6 introduces two MILPs: the first for minimising non-renewable energy in IP/WDM networks for content distribution using P2P overlay networks. It discusses with an example the different peer selection optimisation approaches subject to solar cell renewable energy. The second MILP optimises the use of wind farm renewable energy to power content delivery clouds. Results are presented for both models and the different approaches are compared in a range of scenarios.

Finally, the thesis is concluded in Chapter 7 which summarises this work's main contributions and gives recommendations for future work.

Chapter 2: Energy Efficient Core and Content Distribution Networks

2.1 Introduction

The work presented in this thesis is centred on the energy efficiency of P2P, represented by the BitTorrent protocol, and distributed clouds in IP/WDM networks. This chapter presents an overview of optical core networks with more detailed descriptions of IP/WDM networks, as well as an overview of BitTorrent and cloud computing for content delivery and virtual machine placement. We also review related work on the energy efficiency of IP/WDM networks, BitTorrent based P2P networks, cloud based C/S networks, hybrid C/S and P2P networks, where work done on joint optimisation of upper layer protocols (P2P and cloud services), lower physical network layers, and renewable energy is reviewed. Finally we describe the optimisation methods used in this thesis.

2.2 Core Networks

Core networks are located at the central part of any telecommunication infrastructure, and are required to connect geographically vast areas. Core networks are typically characterised by high levels of traffic aggregation, minimal reconfigurability, and maximal reliability requisites. The main character of today's Internet is the high volume of packet oriented Internet Protocol (IP) traffic generated mainly by content distribution, such as video content, among Internet users. Therefore, core networks need an IP packet based and high capacity architecture to

cope with Internet demands. To achieve this, IP over WDM (IP/WDM) networks [13] have evolved to comply with this need as each node in the IP/WDM network comprises high end routers capable of achieving packet based traffic engineering to control QoS, latency, and resilience, etc., as well as a high capacity optical physical layer capable of delivering massive traffic volumes through Dense Wavelength Division Multiplexing (DWDM).

2.3 IP/WDM Core Network Architecture

Currently, IP/WDM networks are the main architectures in core networks. This is driven by their natural ability to provide intelligence at the IP layer, through IP routers, and large channel capacity at the optical layer, through DWDM techniques, where a large number of high data rate optical wavelengths are multiplexed over the same fibre. This hybrid architecture allows core network operators to finely tune their network resources, such as IP router ports and optical channels and components to serve diverse kinds of traffic, from constant bit rate to bursty traffic.

IP/WDM networks consist of two layers: the IP layer and the optical layer. In the IP layer, an IP router is used at each node to aggregate data traffic from access networks. Each IP router is connected to the optical layer through an optical switch. Optical switches are connected to optical fibre links where a pair of multiplexers/demultiplexers is used to multiplex/demultiplex wavelengths [14]. Optical fibres provide the large capacity required to support communication between IP routers. Transponders provide Optical Electrical Optical (OEO) processing for full wavelength conversion at each node. In addition, for long distance transmission, Erbium-Doped Fibre Amplifiers (EDFAs) are used to amplify the optical signal on each fibre. Fig. 2 - 1 shows the architecture of an IP/WDM network.

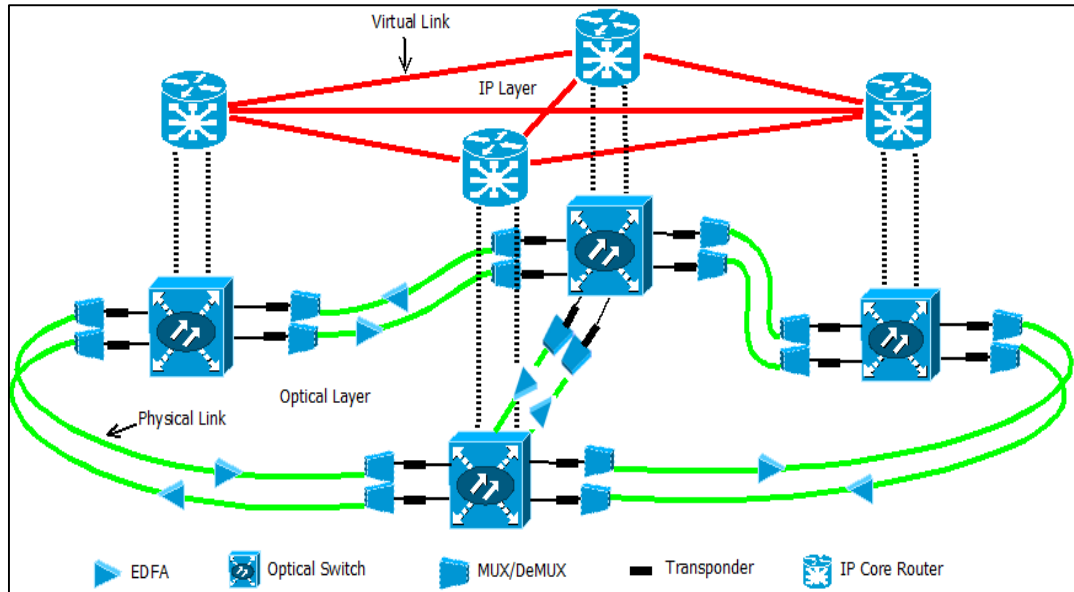


Fig. 2 - 1: IP/WDM network

Two approaches can be used to implement the IP/WDM network, namely, lightpath bypass and non-bypass. In the bypass approach, lightpaths are allowed to bypass the IP layer of intermediate nodes eliminating the need for IP routers, the most power consuming devices in the network, which significantly reduces the total network power consumption compared to the non-bypass approach. However, implementing such an approach involves many technical challenges, mainly the need for long reach, low power optical transmission systems. Other limitations include the loss of electronic processing, and, as such, the advantages of electronic processing at intermediate nodes in terms of grooming, shared protection [15], and deep packet inspection. On the other hand, the forwarding decision in the non-bypass approach is made at the IP layer. Therefore, the incoming lightpaths go through OEO conversion at each intermediate node. The non-bypass approach is implemented in most of the current IP/WDM networks. In addition to its simple implementation, the non-bypass approach allows operators to perform traffic control operations, such as deep packet inspection, and other analysis measures.

2.4 Energy Efficiency of IP/WDM Core Networks

Energy efficiency in core IP/WDM networks is part of global efforts aiming for the goal of greening the Internet [16]. The authors in [17] surveyed the academic and industrial efforts dedicated to the realisation of an energy efficient Internet and

concluded that there are three basic approaches for telecom energy efficiency that have been investigated: (i) re-engineering, (ii) dynamic adaptation, and (iii) sleeping/standby. Re-engineering approaches focus on developing new energy efficient components such as Application Specific Integrated Circuits (ASICs), memory, network links, and lasers. The dynamic adaptation approaches focus on adjusting the maximum capacities of processing and interface components with respect to the actual load imposed on them, such as through Dynamic Voltage and Frequency Scaling (DVFS). Sleeping/standby approaches focus on developing methods to dynamically switch off unused network components or put them in a low power idle mode and turning them on only when necessary, thereby saving power consumption. Several projects were established to tackle the Internet's energy efficiency. The ECONET (low Energy CONsumption NETworks) project [18] ended at September 2013. It investigated standby and capacity scaling for wired network components to save energy when all or part of the network components are not used. Alcatel Lucent promoted the GreenTouch initiative [19] with a broader aim of improving the Internet energy efficiency by a factor of 1000 by 2020 compared to the 2010 energy efficiency levels.

With more attention devoted to IP/WDM networks, the authors in [14] have shown that the lightpath bypass approach reduces the power consumption compared to the non-bypass approach, as bypassing the IP layer at intermediate nodes reduces the number of routers, which are the major power consumers in IP/WDM networks. In [20] the authors focused on reducing the CO₂ emission of backbone IP/WDM networks by introducing renewable energy sources. In [21] a MILP model was developed to optimise the location of datacentres in IP/WDM networks as a means of reducing the network power consumption. In [22] energy-efficient IP/WDM physical topologies were investigated by considering different IP/WDM approaches, nodal degree constraints, traffic symmetry, and renewable energy availability. For a more thorough survey on optical telecommunication energy consumption reduction approaches and trends, the reader is referred to [23].

2.5 Content Distribution in Optical Core Networks

The intrinsic goal behind the creation of the Internet was, and still is in most applications, distributing various kinds of content. Efficient and cost effective

content distribution strategies have played a major role in changing the Internet architecture over the years [24]. Several content providers, such as Google, Facebook, and YouTube, have invested in large datacentres located in diverse geographical locations that are connected to high speed optical networks to meet the ever increasing demands of content hungry users. Such a content distribution strategy is referred to as the Client/Server (C/S) approach where users play the passive role of clients issuing requests while content providers play the active role of content providers delivering acceptable QoS. On the other hand, Peer-to-Peer (P2P) protocols have emerged as an efficient content distribution approach [25]. P2P users play active roles in sharing content among themselves, and the need for a content server is typically not there. Below we review these approaches.

2.5.1 BitTorrent Based P2P Content Distribution

BitTorrent [26], the most popular P2P protocol, is recognised as a successful P2P system based on a set of efficient mechanisms that overcome many challenges other P2P protocols experience, such as scalability, fairness, churn, and resource utilisation. However, some researchers argue that the BitTorrent fairness mechanism is not very effective as it allows free riders to download more content than they provide to the sharing community. Regardless of the academic concerns, BitTorrent traffic accounts for an average of 17% in the Internet [27] and can reach to about 50% of the total upload traffic in some Internet segments [28]. The different percentages represent different popularity for BitTorrent in different geographical areas. For instance, in North America the BitTorrent share is about 52% of the upstream traffic, while in Latin America it was 3.6% at 2011 [28].

The current BitTorrent implementation is based on random graphs since such graphs are known to be robust [26]; yet random graphs mean that BitTorrent is location un-aware, which has represented a burden on ISPs for many years [29] as traffic might cross their networks unnecessarily causing high fees to be paid to other ISPs.

In BitTorrent, file sharing starts by dividing the file to be shared into small pieces, each of 256 kB typically, by the file owner. The file owner generates a corresponding metadata file, called the torrent file that includes essential information about the shared file to help interested users download it. The torrent file is shared

using the HTTP protocol so that users can download it through web pages. The torrent file directs users to a central entity, called the tracker that monitors the group of users currently sharing the content. Such groups are referred to as swarms in BitTorrent terminology and their members as peers. Peers in a swarm are divided into seeders and leechers. Seeders have a complete copy of the file to be shared while leechers have some or none of the file pieces. When contacted by leechers, the tracker returns a list of randomly chosen peers. Leechers select a fixed number of other interested leechers to upload a piece to after the leecher finishes downloading that piece. BitTorrent by default allows each peer (either a seeder or a leecher) to make 4 TCP connections to other leechers in their swarm (we call these connections upload slots). BitTorrent packages can also allow users to choose a different number of upload slots. Upload slots are used to send file pieces to other leechers in the same swarm, i.e. traffic only flows between peers in the same swarm and there is no inter-swarm traffic. This selection process, known as the choke algorithm, is the central mechanism of BitTorrent. Each leecher updates its selection, typically every 10 seconds (also can be configured to be a different period), to select the four peers offering it the highest download rates. On the other hand, seeders select leechers based on their download rates or in a round robin fashion [30]. Tit-for-Tat (TFT) is another implemented mechanism that guarantees fairness by not permitting peers to download more than they upload to other peers.

The BitTorrent protocol employs other mechanisms to ensure its stability and performance, such as the piece selection strategy, implemented by the Local Rarest First (LRF) algorithm, where leechers seek to download the least replicated piece first. The experimental study in [30] has shown that LRF ensures a good replication of pieces in real torrents. An optimal LRF ensures the availability of interesting pieces that peers can always find to download from each other. Another mechanism is the optimistic unchoke algorithm that enables recently arriving peers to download their first piece and allows existing peers to discover better candidates in terms of the download rates they offer.

As stated earlier, BitTorrent has randomness in peer selection, where peers select each other randomly regardless of the impact on the underlying network, and this represents a major concern. For instance, a seeder in a certain ISP network might unchoke a remote leecher in another ISP while overlooking a nearby leecher located

in the same ISP. This generates network cross traffic that results in extra fees to be paid to the other ISP. Such behaviour is referred to as location un-awareness. Several studies proved that by employing locality in peer selection, i.e., prioritising nearby peers over far ones, ISP cross traffic can be reduced while maintaining acceptable performance for BitTorrent [29]. Service support through Nano-datacentres (Nada) has been shown to benefit from location awareness in BitTorrent managed networks [31].

Another dimension of P2P systems is the hybrid Content Delivery Network - Peer-to-Peer (CDN-P2P) [32] architecture, which is an efficient solution for content distribution in terms of cost and performance as it inherits the stability of C/S based CDN and the scalability of P2P based networks, such as BitTorrent. In such systems, users basically connect to each other in a P2P fashion to exchange data with the aid of the CDN datacentres, when the P2P network throughput is not enough to meet the data rate required by the service quality measure. One of the promising applications for this architecture is video streaming, and it is particularly relevant in Video on Demand (VoD).

2.5.2 Energy Efficiency of BitTorrent Content Distribution

Existing research on energy aware BitTorrent has focused on the power consumption of both the network side and the peer side. At the peer side, studies such as the work in [33] suggested elevating the file sharing task to proxies that distribute the content locally to the clients. In [34] the authors used the result of the fluid model in [35] to study the energy efficiency of BitTorrent in steady state. At the network side, the authors in [36] evaluated the energy efficiency of C/S and BitTorrent based P2P systems using a simplified model and concluded that P2P systems are not energy efficient in the network side compared to C/S systems due to the multiple hops needed to distribute file pieces between peers. The study suggested that smart peer selection mechanisms might help reduce the number of hops, and consequently the energy consumption. Similar observations were made in [37], [38] where location un-awareness doubles the utilisation of the access network yielding a higher power consumption. Adding the idle power consumption of the peripherals used for P2P content delivery can double the power consumption in the user's equipment as shown in [16]. However, other researchers in the literature argue that since users of P2P systems only use already powered on peripherals, only the traffic

induced power consumption should be taken into account as in [36]. The authors in [39] studied the performance versus locality trade-offs in BitTorrent like protocols by developing an LP model and a heuristic. Unlike [39], our BitTorrent model takes into account the roles of seeders and leechers, explicitly defines both upload and download capacities; and in our approach the peers' locations refer to the IP/WDM nodes rather than ISPs.

A number of papers have analysed the performance of CDN-P2P architectures in terms of the end users' perceived data rate [40], [41], [42], and they all concluded that it is a potential scheme in terms of cost, capacity, and robustness as it effectively inherits the advantages of both the P2P and CDN architectures. However, little attention has been paid to the power consumption of CDN-P2P architectures at the network side and inside the datacentres. The authors in [43] evaluated a hybrid P2P (HP2P) architecture where videos were delivered from the CDN datacentres or from neighbouring set-top boxes if the videos were available in the local community. They also suggested localised Peer Assisted Patching (PAP) with multicast delivery for highly popular content where newly arrived requests are assigned to the last multicast session while getting the first parts of the video from neighbouring peers who joined early. Both schemes outperform CDN delivery energy efficiency with PAP being more energy efficient than HP2P for popular content. The authors in [44] developed heuristics to analyse the energy efficiency of the hybrid CDN-P2P architecture in IP/WDM networks taking into account content popularity, number of requests, and peer content sharing duration, where they demonstrated 20%-40% energy savings for moderately popular content.

2.5.3 Cloud Based Content Distribution

Cloud computing exploits a range of powerful resource management techniques. It can enable users to share a large pool of computational, network and storage resources available in the Internet. The concept is inherited from research oriented grid computing and was further expanded towards a business model where consumers are charged for the diverse services offered [45]. A recent cloud networking survey commissioned by Cisco [46] has shown that more than 20% of the 1,300 surveyed IT decision makers were willing to deploy over 50% of their total applications into the cloud by the end of 2012. When the survey was carried out in early 2012 only 5% had already been able to migrate at least 50% of their

applications to the cloud. This growth in the tendency to use the cloud as a networked service instead of conventional desktop based applications is expected to be a dominant trend that will shape the future of the Internet [47].

The main concept behind the success of the cloud is virtualisation [48], in which the needed resources are dynamically created over the physical infrastructure in response to incoming requests. This helps both cloud service providers and consumers to cut costs. For the provider, using virtualisation techniques and consolidated services helps to reduce the hardware and operational costs associated with services. For consumers, users, or organisations, an on demand service that is elastic, being able to expand or shrink according to their needs, is a more efficient solution compared to overprovisioning costly local infrastructure that might never or rarely be used.

Cloud services typically come in three flavours [49]:

- **Infrastructure as a Service (IaaS):** The cloud provider manages the physical infrastructure represented by processing, storage, and networks while the users (i.e. customers) provision these resources as virtual machines (VMs) where he/she can run their own operating system and applications as well as possible network control. Amazon EC2 [50] is one of most popular IaaS clouds.
- **Platform as a Service (PaaS):** The cloud provider manages and provisions the physical infrastructure as well as VMs operating systems, while the user has access to programming development platforms that enable the user to write, test, and deploy his/her own applications. Google App Engine [51] is one of the most popular PaaS clouds
- **Software as a Service (SaaS):** Is a more restricted version of PaaS where the applications themselves are also managed by the cloud provider and the user can access these applications through web browsers, for instance. Google Apps [52] is a well-known SaaS cloud.

One of the most important applications that use the concept of the cloud is content distribution. For instance, an IaaS type cloud can free content providers from the cumbersome building and management of their network physical infrastructure and focus on the content distribution service itself, thereby saving time and capital

expenses. For instance, the famous Netflix video streaming service relies on IaaS clouds, such as Amazon EC2, to deliver their content to users. They also employ SaaS and PaaS clouds for specific or customised application development.

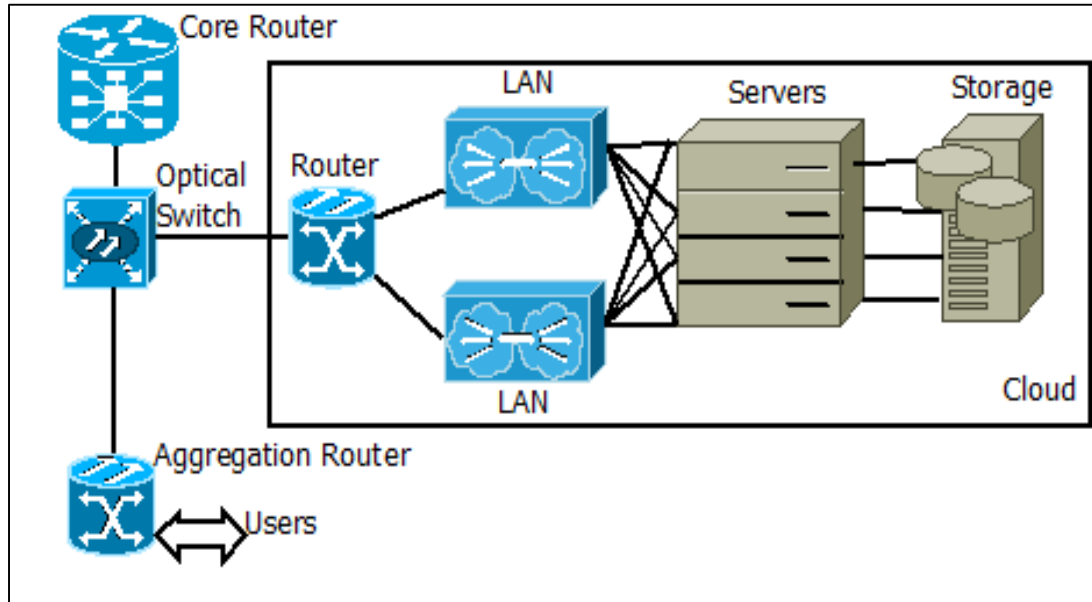


Fig. 2 - 2: Cloud architecture

A typical cloud tailored for content delivery consists of three main parts, namely: content servers, internal LAN, and storage. Clouds are usually built very near to core network nodes to benefit from the large bandwidth offered by such nodes to serve users. Fig. 2 - 2 shows how the different parts inside the cloud are connected and how the cloud is connected to the core network. If the cloud is serving users located at another core node, traffic will flow through the optical switch and core router on its way towards the core network. On the other hand, if the users are located on the same node, the traffic will flow through the optical switch on its path towards the aggregation router where it will be routed to local users. The core/edge network power consumption of the second scenario is limited to the optical switch and aggregation router.

Storage as a Service (StaaS) is another form of cloud based content delivery. It can be viewed as a special case of content delivery service where only the owner or a very limited number of authorised users have the right to access the stored content. Dropbox, Google Drive, Skydrive, iCloud, and Box are examples of cloud based storage. Upon registration for StaaS, users are granted a fixed size of free storage (Quota). DropBox [53], for instance, grants its users 2 GB currently. Different users

might have different levels of utilisation of their StaaS quota as well as different file access frequencies. A large file access frequency has two meanings: either one user accesses it often and/or many authorised users have low/moderate access frequencies to the same file.

2.5.4 Energy Efficiency of Cloud Based Content Distribution

Clouds' elastic management and economic advantages came at the cost of increased concerns regarding their privacy [54], availability [55], and power consumption [56]. Serious concerns were raised about the power consumption of datacentres hosting the clouds [57], leading to significant research efforts being focused on reducing the datacentres' power consumption by exploring opportunities inside the datacentres [58] and/or optimising their locations and traffic patterns [21]. Cloud computing has benefited from the work done on datacentres' energy efficiency. However, the success of the cloud relies heavily on the network that connects the clouds to their users. This means that the expected popularity of the cloud services has implications on network traffic, hence, network power consumption, especially if we consider the total path that information traverses from the cloud storage through its servers, internal LAN, core, aggregation, and access network up to the users' devices. For instance, the authors in [59] have shown that transporting data in public, and sometimes private clouds, might be less energy efficient compared to serving the computational demands by traditional desktops.

Designing future energy efficient clouds, therefore, requires the co-optimisation of both the external network and internal cloud resources. The lack of understanding of this interplay between the two domains of resources might cause eventual loss of power. For instance, a cloud provider might decide to migrate virtual machines or content from one cloud location to another due to low cost or green renewable energy availability; however, the power consumption of the network through which users' data traverses to/from the new cloud location might outweigh the gain of migration.

The authors in [60] studied the design of disaster-resilient optical datacentre networks through integer linear programming (ILP) and heuristics. They addressed content placement, routing, and protection of network and content for geographically distributed cloud services delivered by optical networks. In [61], Mixed Integer

Linear Programming (MILP) models and heuristics were developed to minimise the delay and power consumption of clouds over IP/WDM networks. The authors of [62] exploited anycast routing by intelligently selecting destinations and routes for users' traffic served by clouds over optical networks, as opposed to unicast traffic, while switching off unused network elements. A unified, online, and weighted routing and scheduling algorithm was presented in [63] for a typical optical cloud infrastructure considering the energy consumption of the network and IT resources. In [64], the authors provided an optimisation-based framework, where the objective functions ranged from minimising the energy and bandwidth cost to minimising the total carbon footprint subject to QoS constraints. Their model decides where to build a data centre, how many servers are needed in each datacentre, and how to route requests.

Jointly optimising content distribution for Content Providers (CPs) and traffic engineering for Internet service providers (ISPs) is studied in [65] from the QoS perspective. The authors in [66] studied the same problem from an energy point of view where ISP and CP cooperate to minimise energy. In [67] the authors compared conventional and decentralised server based content delivery networks (CDN), content centric networks (CCN), and centralised server based CDN using dynamic optical bypass where they took the popularity of content into account. In their conventional CDN model, content is fully replicated to all datacentres regardless of content popularity. They showed that CCN is more energy efficient in delivering the most popular content while CDN with optical bypass is more energy efficient in delivering less popular content.

A number of papers have considered means to exploit renewable energy in cloud datacentres [68]. In [20] the authors studied reducing the CO₂ emission of the backbone IP over WDM networks powered by renewable energy sources. The work in [20], as extended in [21], investigated the problem of whether to locate datacentres next to renewable energy or to transmit renewable energy to datacentres. In [69] the authors introduced renewable energy aware virtual machine migration heuristics. The authors in [70] developed two algorithms to route connections supporting cloud computing services so the CO₂ emissions of the network were reduced.

A key difference between our content distribution model and the work done in the literature is the extensive study of the impact of content popularity among different locations where we compare content replication schemes.

2.5.5 Energy Efficient Virtual Machines' Placement in the Cloud

Machine virtualisation provides an economical solution to efficiently use the physical resources, opening the door for energy efficient dynamic infrastructure management as highlighted by many research efforts in this field. The authors in [71] studied the balance between server energy consumption and network energy consumption to present an energy aware joint Virtual Machine (VM) placement method for inside datacentres. The authors in [72] proposed the use of multiple copies of active VMs to reduce the resource requirement of each copy of the VM by distributing the incoming requests among the VMs to increase the energy efficiency of the consolidation and VM placement algorithm. They considered heterogeneous servers in the system and used a two dimensional model that considers both computational and memory bandwidth constraints. The authors in [73] proposed a MILP formulation that virtualises the backbone topology and places the VMs in several cloud hosting datacentres that are interconnected over an optical network with the objective of minimising power consumption.

2.6 Mixed Integer Linear Programming Overview

Throughout this thesis, we use a form of mathematical optimisation, Mixed Integer Linear Programming (MILP), which can be used to determine the maximum/minimum of a linear function subject to one or more inequalities and/or equalities (constraints) [74]. MILP has several applications in transportation, assignment, group formation, scheduling, packing, flow problems, and more [75]. Like any optimization technique, MILP cannot be used for all kinds of problems. For instance, (i) MILP cannot be used in situations where the input parameters has uncertain ranges, (i) it cannot be used in problems where input parameters can change during the solution, (iii) not all problems can be linearized. On the other hand, MILP can make a difference if the problems are tractable. For instance sensitivity analysis is straight-forward by changing the input parameters and monitoring its impact on the optimal variables values. MILP gives insights regarding

the optimal approach to be implemented to attain a certain goal, such as the optimal group formation or task assignment. This can be done by monitoring MILP outcome for a range of input parameters and extract knowledge about the generic behavior of the problem. This knowledge can be then used to construct real time heuristics that mimic MILP behavior in realistic environments.

MILP typically consists of four elements:

- **Objective function:** A linear mathematical function to be minimised or maximised that represents the aim of the optimisation process, such as minimising network energy or maximising client download rate.
- **Variables:** These are the decision variables that the model optimises so that the objective function achieves its peak or lowest value. In MILP, variables can be continuous, integer, or binary, hence the name ‘mixed’. Typical variables in this thesis include peer selection and the location of the cloud in an IP/WDM network together with the optimum routes and the amount of traffic flow per route.
- **Parameters:** These are fixed value numbers that are given as an input to the optimisation process and are not to be optimised. Typical parameters in this thesis are the power consumption values of different network devices.
- **Constraints:** These can be in the form of equality or inequality expressions and serve the purpose of conditioning and limiting certain solutions of the problem to be optimised. One typical constraint in this thesis is capacity constraints on network links.

To illustrate the working principles of MILP, consider the following typical example from [76]:

Maximize: $25xb + 30xc$

Subject to:

$$(1/200)xb + (1/140)xc \leq 40$$

$$0 \leq xb \leq 6000$$

$$0 \leq xc \leq 4000$$

where xb and xc are the variables to be optimised. These could be the number of tons of bands (xb), and tons of coils (xc) to be produced by a steel factory as in [76]. Parameters in this problem are the profit per ton of bands (\$25) and profit per ton of coils (\$30). The objective function is to maximise the total profit of the factory per week: $25 \, xb + 30 \, xc$. Without constraints, the idealised answer is that the factory should produce infinite tons of bands and coils per week in order to maximise profit. However, in reality the factory production is limited by the labour hours available per week and the current booked orders. These limitations represent the constraints of the problem. Production rates for this particular factory are 200 and 140 tons per hour for the bands and coils, respectively. Therefore, the total working hours for the factory per week is $(1/200) \, xb + (1/140) \, xc$, which should be less or equal to a limit of 40 labour hours per week {i.e. $(1/200) \, xb + (1/140) \, xc \leq 40$ }. On the other hand, the factory offered bookings are limited to 6000 and 4000 tons for band and coils, respectively.

In this particular example, the optimal answer is $xb = 6000$ and $xc = 1400$. This is because bands are more profitable than coils as $25 \cdot 6000 > 30 \cdot 4000$. Therefore, the factory should produce the largest possible tons of bands (6000 tons) for 30 hours and the rest 10 hours are used to produce coils. Being a simple example, the answer can be intuitively checked by hand, however, problems with more variables such as the ones considered in this thesis are hard to solve without a computerised solvers.

Several algorithms have been developed to solve linear optimisation problems, such as Simplex, Dual Simplex, Newton Barrier, Branch and Bound method, and others. Each method uses a different concept, and they are reviewed in [77].

The existence of integers in MILP makes the problem solution hard [78] (belonging to NP-Hard class) and takes a long time to solve. However, by relaxation, i.e. demanding that all integer variables are transformed into continuous variables, a near optimal fast solution can be found usually. This method is consistently used throughout this thesis and in the literature in this research field [79], [80].

To solve MILP problems, the IBM ILOG CPLEX optimisation studio is typically used. CPLEX is used to solve the MILP models in this thesis. AMPL (A

Mathematical Programming Language) [81] is used to access the CPLEX solver, it provides a means to connect the model and its data files with CPLEX.

2.7 Summary

This chapter presented an overview of optical core networks, specifically IP/WDM networks, as well as different content distribution approaches such as P2P and C/S based approaches in the cloud. We have reviewed the work done in the literature on the energy efficiency of IP/WDM networks, P2P overlay networks, and cloud datacentres. Unlike the work done in the literature, our aim is to provide detailed analyses of the impact of the overlay content distribution either using P2P or cloud infrastructure on the energy consumption of IP/WDM core networks. For P2P systems, this is done by optimising peer selections for P2P networks to harvest the underlying awareness of the physical network as well as optimising the network routing subject to different factors, such as peer behaviour, physical topology, and other factors to be detailed in their corresponding sections of the thesis. For cloud systems, optimising cloud location, network routing, content, and virtual machine placement are used to minimise both cloud and network power consumption jointly. We will study in detail the impact of renewable energy availability on P2P and distributed content delivery cloud systems later in this thesis.

Chapter 3: Energy Efficient BitTorrent Content Distribution in Optical Core Networks

3.1 Introduction

The lack of basic locality awareness in the original BitTorrent implementations is already known to cause drastic impact on ISPs networks due to cross-node traffic. In this chapter we study the impact of locality un-awareness in BitTorrent on the energy consumption of IP/WDM networks through MILP modelling first. Then we look at peers selection to see whether optimising them can yield energy saving in bypass and non-bypass IP/WDM networks. Based on the model results, we develop heuristics to allow implementing the model insights in real time environments. Different factors that impact the performance and energy efficiency of BitTorrent networks are studied, such as the impact of upload rates heterogeneity, peers behaviour, physical topology, and CDN support in CDN-P2P systems. Finally we revisit our energy efficient heuristic through an experimental demonstration testbed to evaluate its performance in the lab and to draw conclusions from the demo results compared to the optimal MILP model results.

3.2 Mathematical Model for BitTorrent Systems

As mentioned in chapter 1, BitTorrent is the dominant P2P protocol. It accounted for about 90% of P2P traffic at 2011 [28]. As P2P traffic is one of the main

contributor for the core network traffic profile, optimising BitTorrent for energy efficiency would result in considerable energy savings in core networks. However, before optimising the BitTorrent protocol, it is an important first step to investigate the impact of the original protocol implementation on core network energy consumption. Therefore, in this section we start by mathematically studying the original BitTorrent implementation, characterised by random peers selection, then we model an energy efficient variant that reduces traffic flow through network nodes, allowing us to power off underutilised component, and hence, saving energy.

Peer selection in BitTorrent protocol is the mechanism by which peers choose which other peers to communicate with, based on other peers rewarding history. The original BitTorrent implementation favours random peers' selection as it is not optimised to be aware of the physical underlying networks. This will be well demonstrated in Fig. 3 - 2. As these peers are distributed over cities connected by the core network nodes, traffic generated by random peer selection will cause huge traffic to cross between core network nodes, a major cause for power consumption as more telecommunication equipment have to be installed and powered on to deliver the increased traffic. Therefore, optimising the peer selection where peers prefer other nearby peers over far ones is one approach we can investigate to mitigate the impact of BitTorrent protocol on core networks power consumption.

Due to its dynamic nature, the mathematical modelling of BitTorrent was always an intricate task. External factors such as peers arrival/departure as well as internal factors attributed to different mechanisms such as the choke algorithm, the LRF algorithm, fairness and optimistic unchoke have motivated many researchers to study BitTorrent through measurements [82] or simulation [83] studies. However, few mathematical models were developed to study BitTorrent such as the stochastic fluid model in [84] and the branching process model in [85].

In this section, we develop a MILP model to study the impact of peer selection on the power consumption of BitTorrent over bypass and non-bypass IP/WDM networks. In our model peers locations refer to nodes in the IP/WDM network rather than ISPs connections, i.e. the model tries to minimise traffic between nodes. The objective function of the model considers maximising the download rate while the network power consumption is minimised. We assume optimal LRF, where peers do always have interesting file pieces. We also assume a flash crowd scenario for

BitTorrent, the most challenging phase for content providers [29], where the majority of leechers arrive soon after a popular content is shared. For simplicity, we do not consider optimistic unchoke in the MILP model.

Under the bypass approach, the total network power consumption (NPC) is composed of:

- 1) The power consumption of router ports

$$\sum_{i \in N} Prp \cdot Q_i + Prp \cdot \sum_{i \in N} \sum_{j \in N: i \neq j} C_{ij}$$

- 2) The power consumption of transponders

$$\sum_{m \in N} \sum_{n \in N: m_m} Pt \cdot W_{mn}$$

- 3) The power consumption of EDFAs

$$\sum_{m \in N} \sum_{n \in N: m_m} Pe \cdot A_{mn} \cdot F_{mn}$$

- 4) The power consumption of optical switches

$$\sum_{i \in N} PO_i$$

- 5) The power consumption of Multi/Demultiplexers

$$\sum_{m \in N} \sum_{n \in N: m_m} Pmd \cdot F_{mn}$$

The model can be extended to study the power consumption under the non-bypass approach by redefining the IP router ports power consumption as follows:

$$\sum_{i \in N} Prp \cdot Q_i + Prp \cdot \sum_{m \in N} \sum_{n \in N: m_m} W_{mn}$$

In the following, we declare the sets, parameters and variables used in above equations and the developed model to follow:

Sets:

| | |
|-----------|---|
| N | Set of IP/WDM nodes |
| Nm_i | Set of neighbours of node i |
| Sw | Set of swarms |
| P_k | Set of peers in swarm k |
| Sd_k | Set of seeders in swarm k |
| L_k | Set of leechers in swarm k |
| Pn_{ik} | Set of peers of swarm k located in node i |

Parameters:

| | |
|----------|---|
| $ N $ | Number of IP/WDM nodes |
| Prp | Power consumption of a router port |
| Pt | Power consumption of a transponder |
| Pe | Power consumption of an EDFA |
| PO_i | Power consumption of the optical switch in node i |
| Pmd | Power consumption of a multiplexers/ demultiplexers |
| W | Number of wavelengths in a fibre |
| B | Bit rate of a wavelength |
| S | Span distance between EDFAs |
| D_{mn} | Distance between node pair (m,n) |
| A_{mn} | Number of EDFAs between node pair (m,n) |

| | |
|------------|--|
| SN | Number of swarms |
| PN | Number of of peers in a single swarm |
| DN | Number of seeders in a single swarm |
| LN | Number of leechers in a single swarm |
| Np_{ik} | The node of peer i that belongs to swarm k |
| SLN | Number of upload slots |
| Up | Upload capacity for each peer |
| SR | Upload rate for each slot, $SR = Up/SLN$ |
| Dp | Download capacity of each peer |
| F | File size in Gb |
| L_r^{sd} | Regular traffic demand between node pair (s,d) |

Variables (All are non-negative real numbers):

| | |
|----------------|---|
| C_{ij} | Number of wavelengths in the virtual link (i,j) |
| L_k^{sd} | Traffic demand between node pair (s,d) generated by peers of swarm k . |
| L_{ijk}^{sd} | Swarm k traffic demand between node pair (s,d) traversing virtual link (i,j) |
| L_{ij}^{sd} | The regular traffic flow between node pair (s,d) traversing virtual link (i,j) |
| W_{mn}^{ij} | Number of wavelength channels in the virtual link (i,j) that traverse physical link (m,n) |
| W_{mn} | Total number of wavelengths in the physical link (m,n) |
| F_{mn} | Total number of fibres on the physical link (m,n) |

| | |
|-------------|--|
| Q_i | Number of aggregation ports in router i |
| U_{ijk} | $U_{ijk} = 1$ if peer i unchokes peer j in swarm k , otherwise $U_{ijk}=0$ |
| $Avdr_{ik}$ | Download rate of peer i that belongs to swarm k |

In the following, we present the MILP model that maximises the peers download rate and minimises the network power consumption, subject to flow, capacity and BitTorrent constraints, as follows:

Objective: Maximise

$$\begin{aligned}
\alpha \cdot \left(\sum_{k \in Sw} \sum_{i \in L_k} Avdr_{ik} \right) - \beta \cdot \left(\sum_{i \in N} Prp \cdot Q_i + Prp \cdot \sum_{i \in N} \sum_{j \in N: i \neq j} C_{ij} \right. \\
+ \sum_{m \in N} \sum_{n \in Nm_m} Pt \cdot W_{mn} \\
+ \sum_{m \in N} \sum_{n \in Nm_m} Pe \cdot A_{mn} \cdot F_{mn} \\
\left. + \sum_{i \in N} PO_i + \sum_{m \in N} \sum_{n \in Nm_m} Pmd \cdot F_{mn} \right)
\end{aligned} \tag{3-1}$$

Subject to:

$$\begin{aligned}
L_k^{sd} = \sum_{i \in Pn_{sk}} \sum_{j \in Pn_{dk}: j \in L_k} SR \cdot U_{ijk} \\
\forall k \in Sw \forall s, d \in N: s \neq d,
\end{aligned} \tag{3-2}$$

$$\begin{aligned}
\sum_{j \in N: i \neq j} L_{ijk}^{sd} - \sum_{j \in N: i \neq j} L_{jik}^{sd} = \begin{cases} L_k^{sd} & \text{if } i = s \\ -L_k^{sd} & \text{if } i = d \\ 0 & \text{otherwise} \end{cases} \\
\forall k \in Sw \forall s, d, i \in N: s \neq d,
\end{aligned} \tag{3-3}$$

$$\begin{aligned}
\sum_{j \in N: i \neq j} L_{ij}^{sd} - \sum_{j \in N: i \neq j} L_{ji}^{sd} = \begin{cases} L_r^{sd} & \text{if } i = s \\ -L_r^{sd} & \text{if } i = d \\ 0 & \text{otherwise} \end{cases} \\
\forall s, d, i \in N: s \neq d,
\end{aligned} \tag{3-4}$$

$$\sum_{s \in N} \sum_{d \in N: s \neq d} \left(L_{ij}^{sd} + \sum_{k \in Sw} L_{ijk}^{sd} \right) \leq C_{ij} \cdot B$$

$$\forall i, j \in N: i \neq j,$$
(3-5)

$$\sum_{n \in Nm_m} W_{mn}^{ij} - \sum_{n \in Nm_m} W_{nm}^{ij} = \begin{cases} C_{ij} & \text{if } m = i \\ -C_{ij} & \text{if } m = j \\ 0 & \text{otherwise} \end{cases}$$

$$\forall i, j, m \in N: i \neq j,$$
(3-6)

$$\sum_{i \in N} \sum_{j \in N: i \neq j} W_{mn}^{ij} \leq W \cdot F_{mn}$$

$$\forall m \in N \quad \forall n \in Nm_m,$$
(3-7)

$$\sum_{i \in N} \sum_{j \in N: i \neq j} W_{mn}^{ij} = W_{mn}$$

$$\forall m \in N \quad \forall n \in Nm_m,$$
(3-8)

$$Q_i = \frac{1}{B} \cdot \sum_{d \in N: i \neq d} \left(L_r^{id} + \sum_{k \in Sw} L_k^{id} \right)$$

$$\forall i \in N,$$
(3-9)

$$Avdr_{ik} = \sum_{j \in P_k: i \neq j} SR \cdot U_{jik}$$

$$\forall k \in Sw \quad \forall i \in L_k,$$
(3-10)

$$Avdr_{ik} \leq Dp$$

$$\forall k \in Sw \quad \forall i \in L_k,$$
(3-11)

$$\sum_{j \in L_k, i \neq j} U_{ijk} \leq SLN$$

$$\forall k \in Sw \quad \forall i \in P_k,$$
(3-12)

$$SR \cdot U_{ijk} = SR \cdot U_{jik}$$

$$\forall k \in Sw \quad \forall i, j \in L_k \quad i \neq j.$$
(3-13)

Equation (3-1) gives the model objective where the download rate is maximised while minimising IP/WDM network power consumption. Note that parameter α is used to scale the average download rate so that it becomes comparable to the

network power consumption, and furthermore allows the emphasis placed on download rate to be varied. Note also that setting $\beta = 0$ in Equation (3-1) gives the original implementation of BitTorrent (OBT) where the objective is to only maximise the download rate. In this case (*i. e.* $\beta = 0$), we use the MILP model to determine the transit traffic between nodes given by the variable L_k^{sd} . Then we optimise routing of the transit traffic over the IP/WDM network using the model in [21], [14] where L_k^{sd} is an input parameter in this case.

Constraint (3-2) calculates the transient traffic between IP/WDM nodes due to BitTorrent swarms based on peers' selection. Constraints (3-3) and (3-4) are the flow conservation constraints for swarms traffic and regular traffic, respectively. They ensure that the total incoming traffic is equal to the total outgoing traffic for all nodes except for the source and destination nodes. Constraint (3-5) ensures that the traffic (regular and BitTorrent) traversing a virtual link does not exceed its capacity. Constraint (3-6) represents the flow conservation for the optical layer. It ensures that the total number of outgoing wavelengths in a virtual link is equal to the total number of incoming wavelengths except for the source and destination nodes of the virtual link. Constraints (3-7) and (3-8) represent the physical link capacity constraints. Constraint (3-7) ensures that the number of wavelength channels in virtual links traversing a physical link does not exceed the capacity of fibres in the physical links. Constraint (3-8) ensures that the number of wavelength channels in virtual links traversing a physical link is equal to the number of wavelengths in that physical link. Constraint (3-9) calculates the number of aggregation ports for each router. Constraint (3-10) calculates the download rate for each peer according to the upload rate it receives from other peers selecting it while constraint (3-11) limits the download rate of a leecher to its download capacity. Constraint (3-12) gives the limit on the number of upload slots for each peer so that the total upload rate does not exceed the peers upload capacity. Constraint (3-13) represents fairness in BitTorrent where each leecher reciprocates equally to other leechers selecting it.

3.3 Results of the MILP Model

We compare the energy-efficient BitTorrent (EEBT) with the current implementation of BitTorrent (OBT) and C/S systems. We consider the same content

distribution scenario for the different systems where 160k groups of downloaders, each downloading a 3 GB file, are distributed randomly over the NSFNET network nodes. Each group consists of 100 members. We chose 160k swarms as NSFNET represents a continental network connecting large states in the US, therefore, the need to model a large number of swarms. Given our input parameters, 160k swarms contribute about 50% of the total traffic in NSFNET. This is because the average regular traffic demand between each node pair in the NSFNET on different time zones is 82 Gbps [21]. Hence, with 160k swarms and 100 peers per swarm, each of 1 Mbps upload capacity, the BitTorrent distribution scenario results in 16 Tbps of aggregate traffic, however some peers communicate with peers in their own node. Therefore the aggregate BitTorrent traffic that contributes to cross-node traffic is found to be 14.9 Tbps which corresponds to an average node-to-node BitTorrent traffic of about 82 Gbps, equal to regular traffic. Thus, it accounts for 50% of the total traffic in the NSFNET network. We chose NSFNET as it represents a well-known core network in the US for researchers with data regarding its topology and average traffic demands available online [86]. However the impact of other topologies will be analysed later in Section 3.9.

For the BitTorrent scenario, we refer to the downloader groups as swarms and their members as peers. Each swarm has 100 peers. For this section, we consider a homogeneous system where all peers have an upload capacity of 1 Mbps. This capacity reflects typical P2P users in the Internet [84]. Solving the MILP model on a PC does not scale to produce results for a large network with 160k swarms. Therefore to define a tractable problem, we solve the model for 20 swarms and assume that the network contains 8k replicas of these 20 swarms. The traffic resulting from the 160k swarms is obtained by scaling the traffic of the 20 swarms.

For fair comparison, the number of downloaders in the C/S scenario is assumed to be equal to the number of leechers in the BitTorrent scenario, and seeders are replaced by one or more data centres with an upload capacity equal to the total upload capacity of all peers in the BitTorrent scenario. This ensures that the upload capacity and download demands are the same for both scenarios and therefore, the power consumption only depends on how the content is distributed.

The NSFNET used to evaluate the different systems is depicted in Fig. 3 - 1. It consists of 14 nodes and 21 bidirectional links.

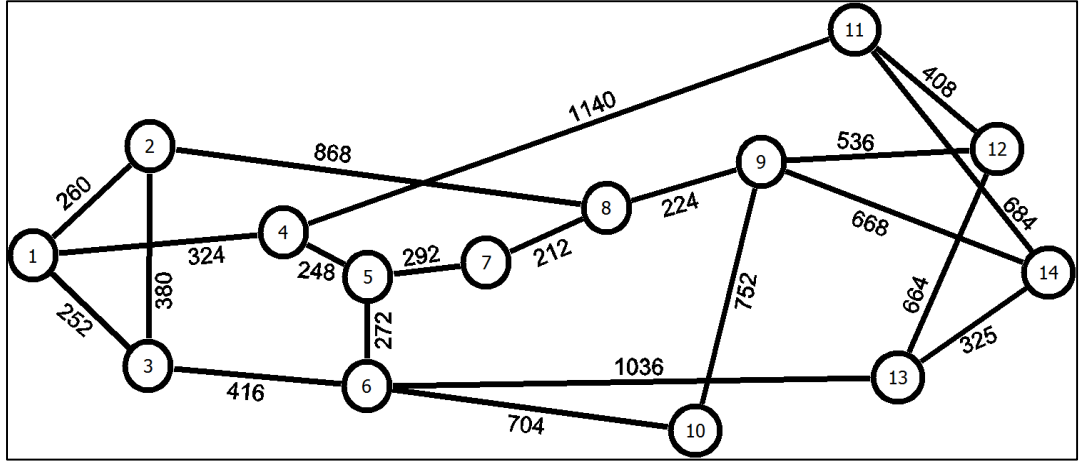


Fig. 3 - 1: NSFNET network with links lengths in km

| | |
|---|-------------------|
| Power consumption of a router port (Prp) | 1000 W [87], [14] |
| Power consumption of transponder (Pt) | 73 W [14] |
| Power consumption of an optical switch (PO_i) $\forall i$ | 85 W [88] |
| Power consumption of EDFA (Pe) | 8 W [89] |
| Power consumption of a Mux/Demux (Pmd) | 16 W [90] |
| No. of wavelengths in a fibre (W) | 16 |
| Bit rate of each wavelength (B) | 40 Gbps |
| Span distance between EDFAs (S) | 80 km |
| Number of modelled swarms (SN) | 20 |
| Number of peers in single swarm (PN) | 100 |
| Number of upload slots (SLN) | 4 |
| Upload capacity for each peer (Up) | 0.001 Gbps |
| Download capacity for each peer (Dp) | 0.01 Gbps |
| Number of data centres (DCN) | 5 |
| Factor of average download rate (α) | 1,000,000 |
| Factor of power consumption (β) | 0 or 1 |

Table 3 - 1: Input parameters for the MILP model

We consider the C/S system with 5 data centres located optimally [21] at nodes 3, 5, 8, 10 and 12 with a total upload capacity of 16 Tbps. We used the model in [21] to evaluate the performance of the C/S system. Table 3 - 1 gives the input parameters of the model.

The router ports power consumption and number of wavelength per fibre is based on [14], note that the power consumption of the IP router port takes into account the power consumption of the different shared and dedicated modules in the IP router such as the switching matrix, power module and router processor. The eight-slot CRS-1 consumes about 8 kW and therefore the power consumption of each port is given as 1 kW.

The ITU grid defines 73 wavelengths at 100 GHz spacing, or alternatively double this number approximately at 50 GHz channel spacing. Wavelengths represent the channels at which traffic is aggregated and sent to remote nodes. As the space between channels increases, the number of channels decreases accordingly. In more recent studies [91] we have adopted lower router power per port, 440 W, based on Alcatel-Lucent designs. Also a larger (>16) number of wavelengths per fibre is possible at 100 GHz or 50 GHz spacing, however with super channels and the introduction of 400 Gbps and envisaged 1 Tb/s and possibly flexigrid developments, the number of channels may fall. Also note that a larger number of wavelengths per fibre will reduce the number of fibres and hence EDFAs, but the power consumption of the latter is small. To facilitate comparison with previous studies we have adopted the power consumption figures in [14], [21]. Note that the data rate of router ports is the same as the wavelength rate (40 Gbps).

We evaluate the average download rate, power and energy consumption under different number of seeders (15 to 95 seeders per swarm). Increasing the number of seeders reflects the increased download capacity for the swarms. However, the total number of peers is fixed at 100 peers per swarm to maintain the same total upload capacity at 16 Tbps. The authors in [83] have calculated the optimal average download rate for a leecher, considering optimal LRF which results in peers with interesting file pieces in a swarm, as:

$$Avdr = U_p + \sum_{s=1}^{DN} U_p / LN. \quad (3-14)$$

We compare the performance of the BitTorrent model to the optimal performance deduced by (3-14).

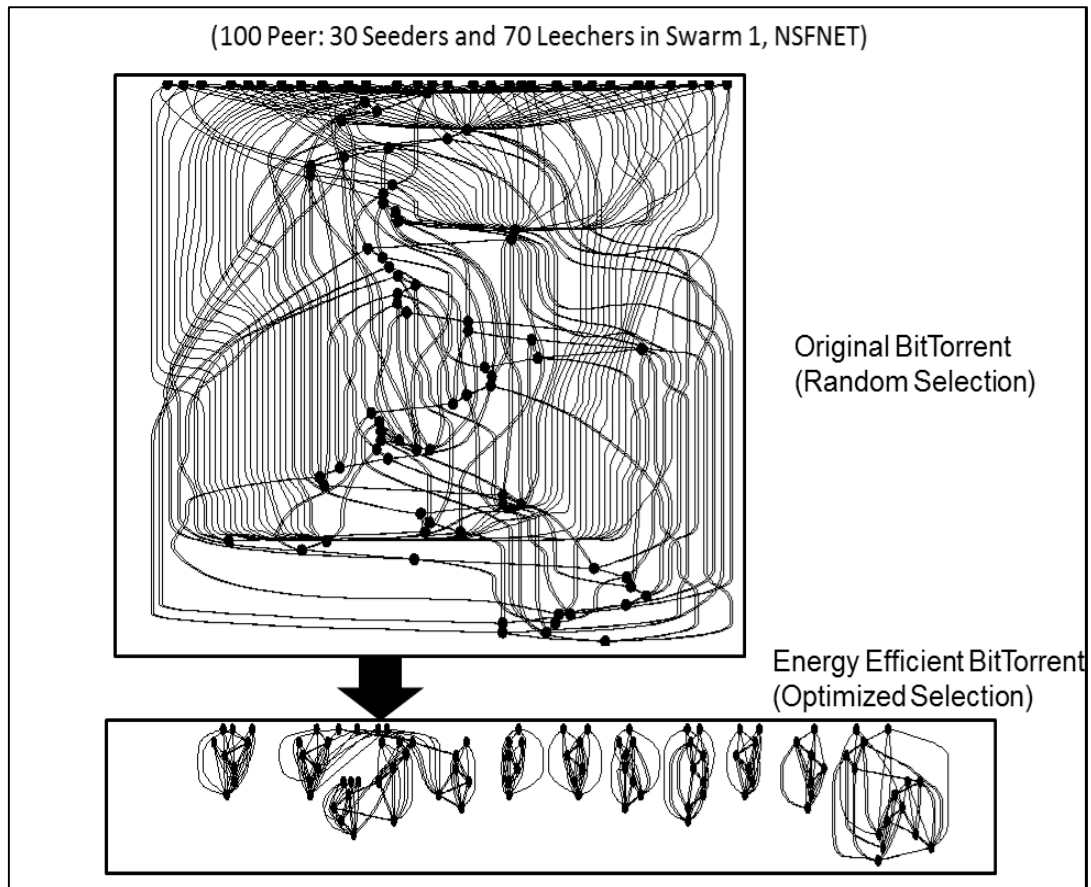


Fig. 3 - 2: Peers selection matrix U_{ijk}

To illustrate the selection behaviour of BitTorrent, Fig. 3 - 2 visualises the selection matrix U_{ijk} of a sample single swarm of 30 seeders and 70 leechers. The dots in the graph represent peers.

It is obvious that peer selection in OBT (*i.e.* $\beta = 0$) is random, as peers have no sense of location; therefore, a peer might select a far peer while neglecting a nearby one. Examining the peer selection for EEBT (*i.e.* $\beta = 1$), we noticed that peers favour those who are near to them in terms of number of hops as fewer hops yield less network power consumption.

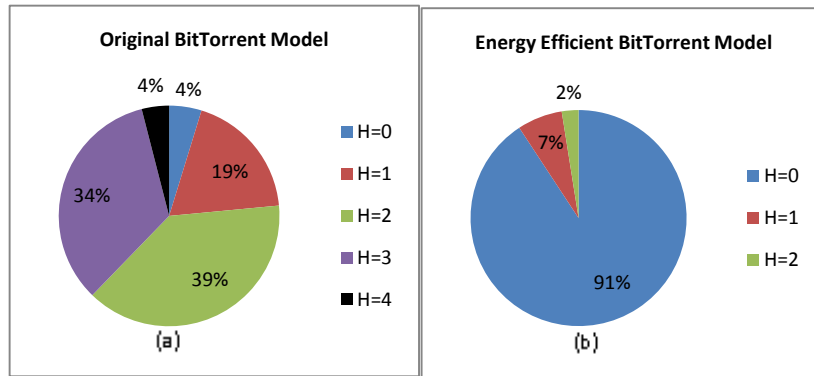


Fig. 3 - 3: Number of hops travelled by traffic resulting from peers selections (MILP)

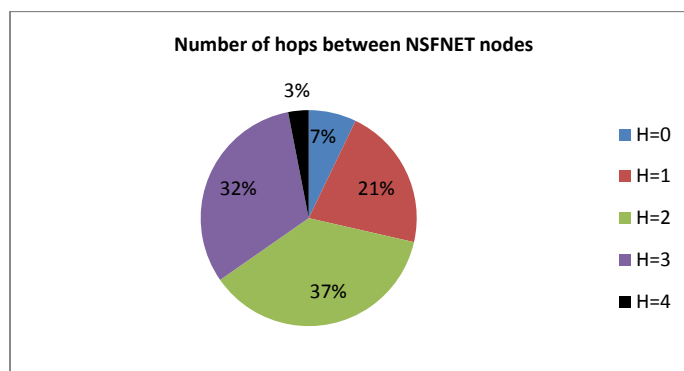


Fig. 3 - 4: Number of hops between NSFNET nodes

In Fig. 3 - 3 we further highlight the locality behaviour of the BitTorrent models by showing the number of hops (H) travelled by traffic resulting from peers' selections for the same swarm shown in Fig. 3 - 2. Location un-awareness in OBT (Fig. 3 - 3 (a)) resulted in only 4% of the demands satisfied locally and 19% served by peers located in neighbouring nodes. On the other hand, EEBT (Fig. 3 - 3 (b)) served 91% of the demands locally and 7% from neighbouring nodes. As the OBT is based on random selection, the number of hops travelled by traffic between peers follows a similar distribution to the distribution of number of hops between nodes in NSFNET shown in Fig. 3 - 4.

Note that peers selection behaviour for the EEBT is independent of whether we model it over bypass or non-bypass IP/WDM network as selecting nearby peers saves power in intermediate router ports and optical components under the non-bypass approach and save power consumption of optical components under the bypass approach.

In the following we present and analyse the average download rate, power and energy consumption for OBT and its energy efficient version, EEBT.

Power savings are calculated at each number of seeders case and eventually averaged over the whole range to obtain the average power savings as increasing/decreasing number of seeders/leechers represents a scenario where leechers turn gradually into seeders after finishing downloading the file. The heuristic part of the results will be discussed in the next section.

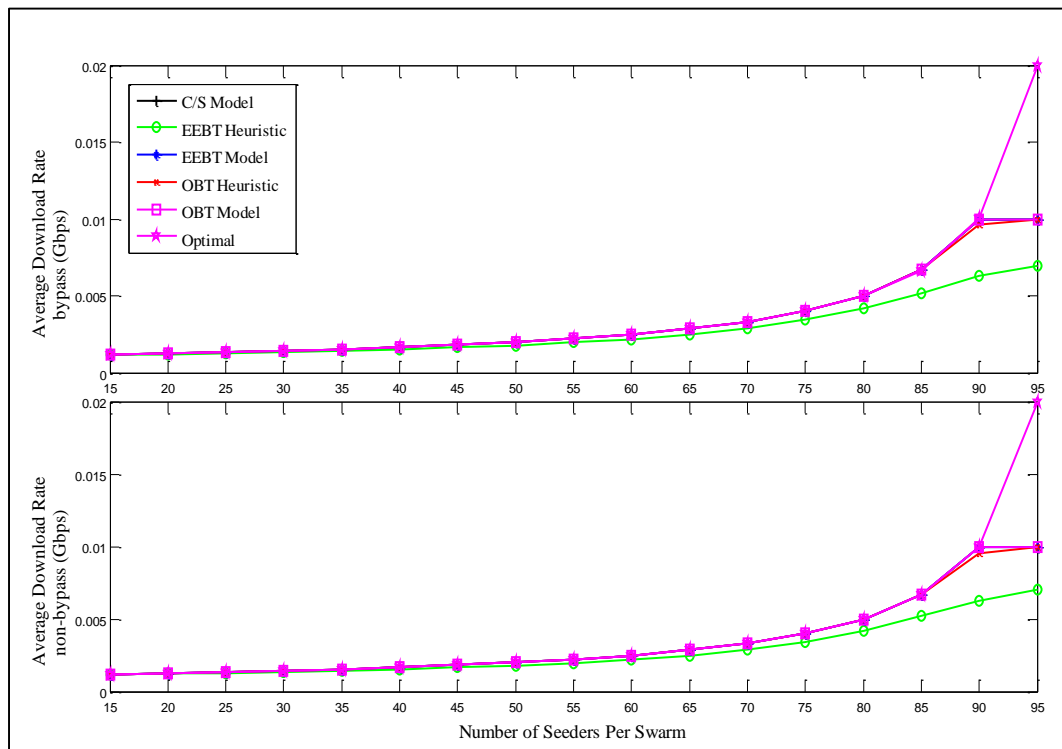


Fig. 3 - 5: Average download rate versus number of seeders per swarm

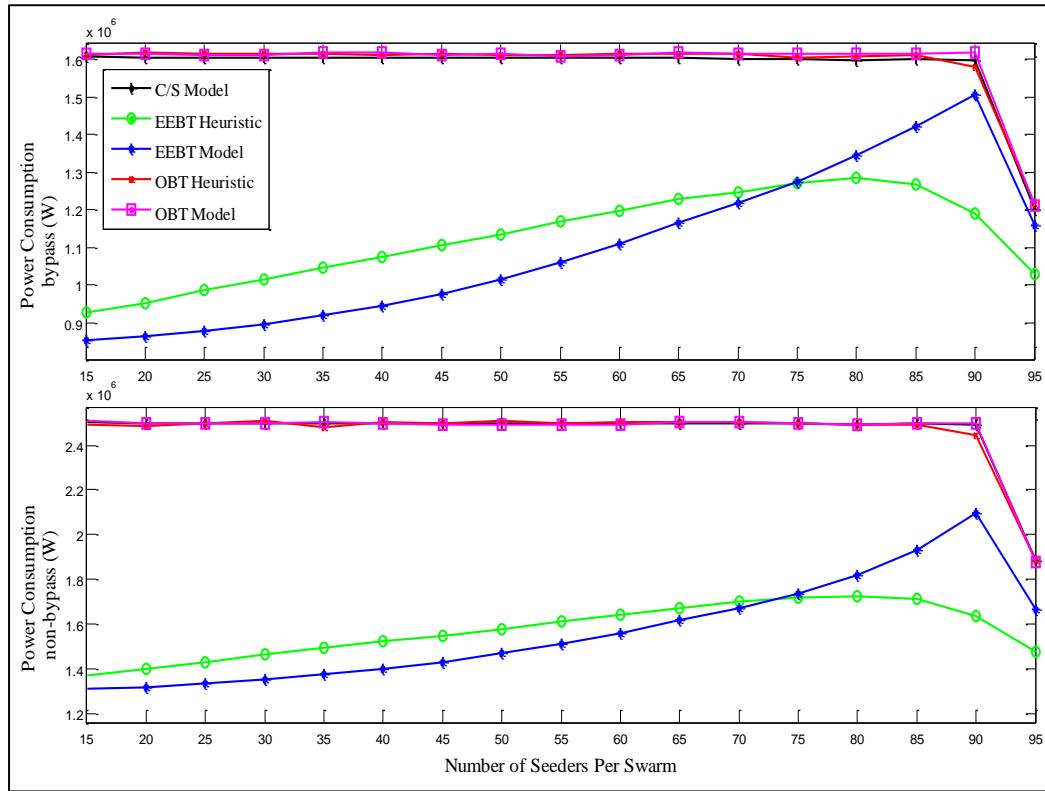


Fig. 3 - 6: IP/WDM power consumption versus number of seeders per swarm

For the bypass approach, the results shown in Fig. 3 - 5 reveal that OBT and EEBT models and a typical C/S model of 5 data centres achieve near optimal performance in terms of the average download rate. Fig. 3 - 6, however, shows that while the OBT consumes similar power in the network side as the C/S model, EEBT reduces the network power consumption by about 30% compared to the C/S and the OBT models. For 90 seeders per swarm (10 leechers), the download rate reaches the maximum download capacity of the leechers; therefore, any further increase in the number of seeders will not result in improving the average performance. For 95 seeders per swarm, the network only needs a total upload rate of 0.05 Gbps which can be satisfied by only 50 peers, resulting in 50% decline in upload traffic in the network and consequently lower power consumption as shown in Fig. 3 - 6.

As discussed in Section 3.2, we do not consider the optimistic unchoke in the MILP model. Note that considering the optimistic unchoke may result in more traffic between IP/WDM nodes and consequently higher power consumption, if the optimistic slots increase the total capacity of the peers. On the other hand, optimistic unchoke and the seeders choke algorithm within EEBT will be constrained by

locality; therefore, we expect them to contribute less to energy consumption for EEBT.

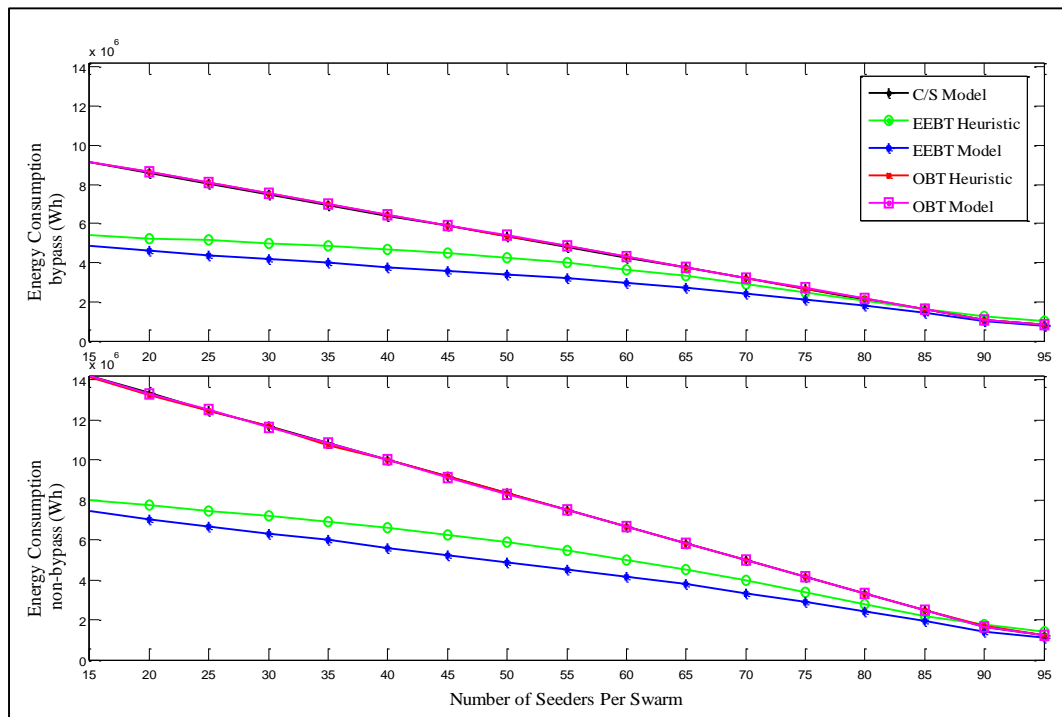


Fig. 3 - 7: IP/WDM energy consumption versus number of seeders per swarm

To evaluate the energy consumption under a particular number of seeders, we multiply the power consumption by the average download time (calculated by dividing the file size by average download rate). Fig. 3 - 7 shows that the energy consumption decreases as the number of seeders increases due to the decrease in the average download time. As mentioned, Fig. 3 - 6 (power) shows a sudden drop at 95 seeders (5 leechers), however, Fig. 3 - 7 (energy) does not show that. This is due to the download capacity limit of 10 Mbps per peer which reduces the download rate for the 5 leechers from 20 Mbps to 10 Mbps; (At 95 seeders (i.e. 5 leechers)), the average download rate per leecher should be $100 \times 1 \text{ Mbps} / 5 = 20 \text{ Mbps}$ which is double the download capacity per leecher ($Dp = 10 \text{ Mbps}$, Table 3 - 1)). This means that the power at 95 seeders is multiplied by a longer time duration, (0.67 hours rather than 0.33 hours), due to the lower download rate and consequently this slopes the energy curve up compared to other cases and prevents the reproduction of the drop in power consumption curve. The energy consumption savings achieved by the EEBT compared to the C/S model are similar to the power consumption savings as the different models achieve similar download rates.

The download rates under the non-bypass approach show similar trends to those observed under the bypass approach (Fig. 3 - 5) as the download rate is independent of the optical layer approach. Fig. 3 - 6 shows that the non-bypass approach consumes more power compared to the bypass case as the non-bypass approach requires router ports (the major power consumers in the network) at intermediate nodes. The EEBT model under the non-bypass approach achieves power and energy savings of 36% compared to the C/S and the OBT models.

From Fig. 3 - 7 we can estimate the energy required to distribute a file using the C/S and BitTorrent content distribution schemes. As mentioned earlier, the content distribution traffic represents 50% of the total network traffic, therefore we can assume that content traffic is roughly responsible for 50% of the network total energy consumption. Considering the total number of downloaders in the network, the C/S system requires 1237 Joules and 1928 Joules approximately to deliver one file of 3 GB under the bypass and non-bypass approaches, respectively. On the other hand the EEBT model reduces the energy per file to 871 Joules and 1247 Joules approximately under the bypass and non-bypass approaches, respectively, given our input parameters.

3.4 Energy Efficient BitTorrent Heuristic

Examining the results of the EEBT model shows that the majority of peers selected by any leecher are located within the leecher local node to minimise energy consumption as spanning the neighbouring nodes can increase the power consumption of the network unnecessarily. Such localised selection did not affect the achieved average download rates. The TFT mechanism (implemented in the model by the fairness constraint (3-13)) ensures that the download rate a leecher gets from other leechers is limited to its upload capacity. Therefore, as all leechers are assumed to have the same upload capacity, spanning to peers in neighbouring nodes does not grant leechers higher download rates than what they can achieve from leechers in the local node as long as a sufficient number of leechers (at least 5 leechers, as $SLN = 4$) are available in the local node. The results also reveal that seeders may select remote leechers (when there is an insufficient number of local leechers) to help them maintain their optimal download rate.

We developed an EEBT heuristic based on the above observations. The heuristic flow chart is shown in Fig. 3 - 8.

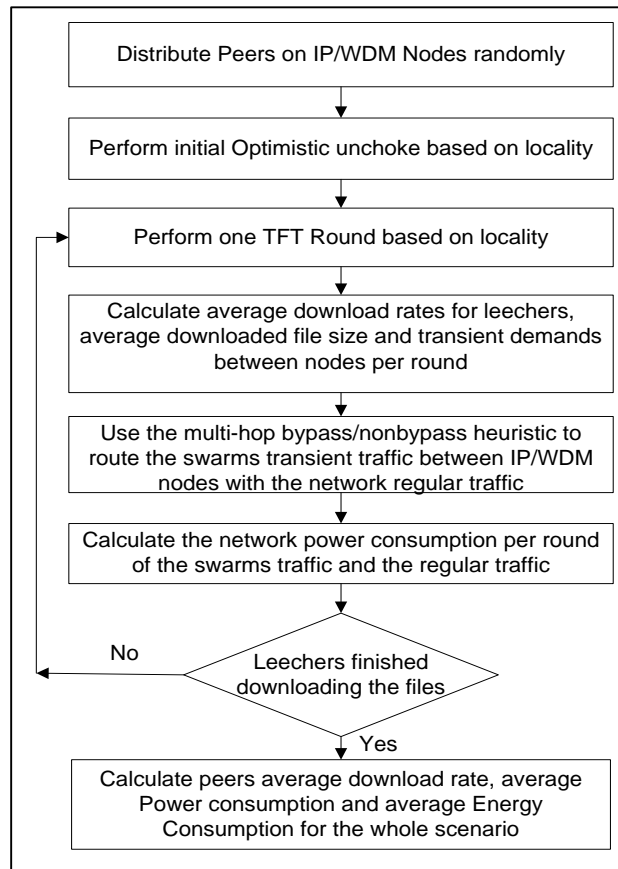


Fig. 3 - 8: Energy efficient BitTorrent heuristic (EEBT heuristic)

The heuristic begins with randomly distributing peers over IP/WDM nodes. We use the same random distribution for both the model and heuristic to retain a fair comparison. Peers start with optimistic unchoke since they have no prior knowledge of each other's characteristics. The optimistic unchoke is constrained by locality where seeders span the neighbourhood nodes and leechers are clustered in their local nodes as long as a sufficient number of local peers is available (5 or more), otherwise, leechers explore neighbouring nodes as well to maximise their download rates. The unchoke rounds then start and are repeated every 10 seconds [26]. The TFT mechanism ensures each leecher reciprocates to those who upload to it and chokes those who do not. TFT is applied based on locality as well. Note that leechers fill any empty upload slots after each TFT round by another optimistic unchoke. The average download rate, downloaded file size and transient traffic resulting from seeders unchoking leechers on remote nodes are calculated for each round. The multi-hop bypass heuristic [21], [14] is used to route the swarms' transient traffic

between IP/WDM nodes with the network regular traffic. Rounds are repeated until all leechers finish downloading their files. Finally, the average performance is calculated.

The results of the EEBT heuristic are shown in Fig. 3 - 5, Fig. 3 - 6, and Fig. 3 - 7. The model tries to maintain the optimal download rate by allowing peers to go beyond their neighbouring nodes for peer selection at high number of seeders (low number of leechers) while the heuristic limits peers to neighbouring nodes (one hop) which might not be enough to select a sufficient number of leechers. The one-hop leechers may also already suffer from decreased download rates, as their peer selection is restricted to their local and neighbouring nodes. This results in lower download rates for leechers as well as lower network power consumption compared to the C/S model at high number of seeders due to reduced transient traffic between nodes.

Under the bypass approach, EEBT achieves 28% reduction in power consumption compared to the C/S model with a reduction in the download rate by 13%. The heuristic power savings are comparable to the saving obtained through the MILP optimisation.

Fig. 3 - 6 shows that EEBT power consumption decreases when the number of seeders is more than 75 seeders as the achieved download rate is lower than the optimal download rate as shown in Fig. 3 - 5.

As the heuristic download rate decreases at high number of seeders, i.e. leechers need more time to download their files; the reduction in power consumption does not necessarily mean a parallel reduction in energy consumption as well. For a number of seeders equal to 85 and more, the energy consumption of the heuristic exceeds the C/S model by about 13% (Fig. 3 - 7). Therefore, the average energy consumption savings achieved by EEBT are limited to 15% compared to the C/S model. The energy results in Fig. 3 - 7 are a better basis for comparison as they reflect the power consumption and the downloading time.

Under the non-bypass approach, EEBT heuristic achieves comparable power savings to the MILP model (36% power saving and 25% energy saving compared to the C/S MILP model).

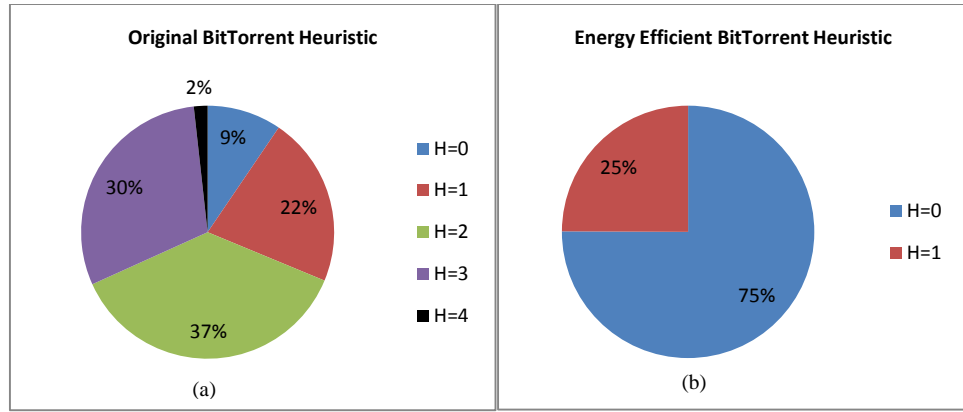


Fig. 3 - 9: Number of hops travelled by traffic resulting from peers selections (EEBT heuristic)

Fig. 3 - 9 shows the number of hops travelled by the traffic resulting from the EEBT heuristic peers selection mechanism for the same swarm shown in Fig. 3 - 2. The number of hops travelled by the traffic between peers for the OBT heuristic (Fig. 3 - 9(a)) also follows a similar distribution to the distribution of number of hops between nodes in NSFNET shown in Fig. 3 - 4.

On the other hand, under the EEBT heuristic (Fig. 3 - 9(b)) the majority (75%) of peers selections are within local nodes ($H=0$). This is because we only allow leechers to cross to neighbouring nodes if number of local peers is less than 5 as mentioned in our heuristic. As we have 70 leechers, then about 5 leechers are available in each node on average plus some seeders, therefore, only a limited number of leechers cross their local nodes (when the number of their local peers falls below the average of 5 peers). However, seeders in our heuristic have more freedom to scan both local and neighbouring nodes equally likely and since the average nodal degree in NSFNET is about 2, a seeder is more likely to select a leecher located in a neighbouring node ($H=1$) rather than local node ($H=0$). Therefore, the percentage of traffic travelling one hop ($H=1$) under the EEBT heuristic rises from 7% (for the EEBT model in Fig. 3 - 3(b)) to 25%. In addition to the multi-hop heuristic being less efficient in routing traffic compared to the MILP model, the increase in H ($H=1$ hop) explains the increase in EEBT power consumption compared to the model for a number of seeders less than 75 as shown in Fig. 3 - 6.

3.5 Enhanced Energy Efficient BitTorrent Heuristic (EEBTv2)

The heuristic presented in the previous section is a one hop heuristic, meaning that leechers and seeders can search for other leechers in a maximum of one hop distance. As we have seen, this led to degraded performance when the number of leechers is small, as the average hop distance between them will be higher than one, due to the uniform distribution of leechers among the network nodes.

In this section we enhance the performance of the EEBT heuristic by allowing leechers to extend their selection beyond the local or neighbourhood nodes when the number of peers in their search area falls below the number of upload slots ($SLN = 4$). To implement such heuristic, leechers need to have full knowledge of the distribution of other leechers in the network which can be provided by the tracker.

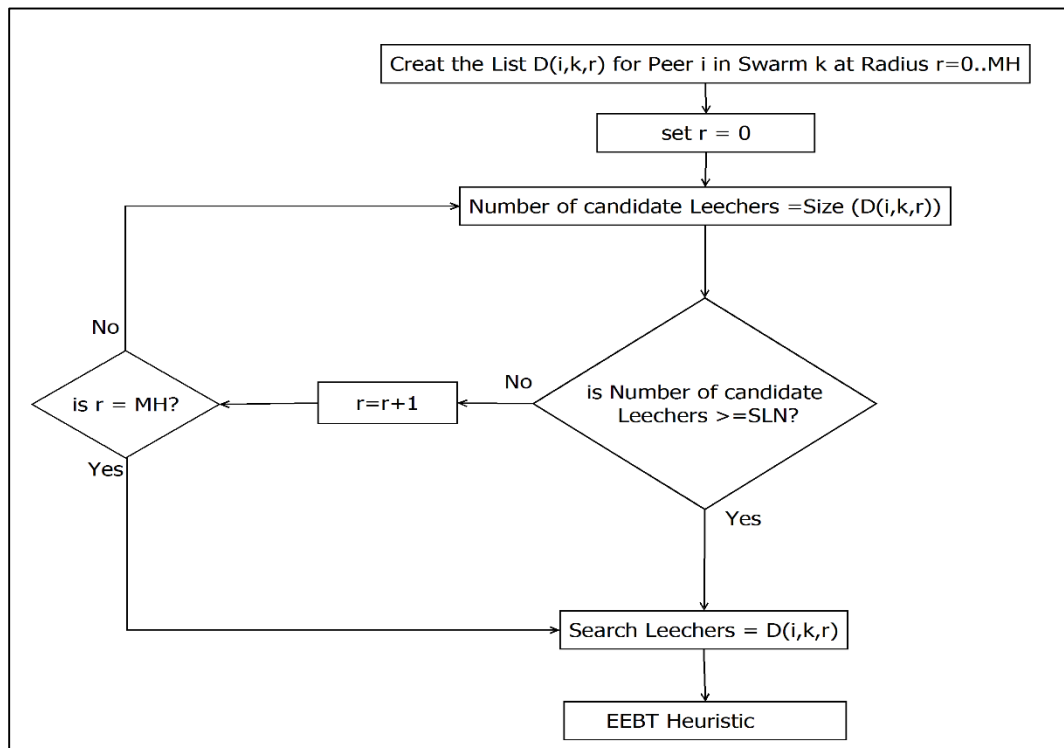


Fig. 3 - 10: The flowchart of the EEBTv2 heuristic

We define a parameter called *Radius* that can have a value between 0 and the maximum number of hops in the network (MH) where $Radius = 0$ refers to the local node. Each peer i in swarm k creates a list, $D(i, k, r)$, which contains the other leechers that are located in the nodes that lie within $Radius \leq r$.

For instance, in NSFNET, for $Radius = 1$, a leecher in node 1 will list all the other leechers that belong to the same swarm located in node 1, 2, 3 and 4, as nodes 2, 3 and 4 are one hop neighbours of node 1. We refer to the enhanced heuristic as Enhanced Energy Efficient BitTorrent (EEBTv2). Fig. 3 - 10 shows the flowchart of the EEBTv2 heuristic, leechers search for other leechers to unchoke by searching in progressive values of $Radius$ until enough leechers are found. This ensures that each leecher will have at least SLN leechers to TFT with.

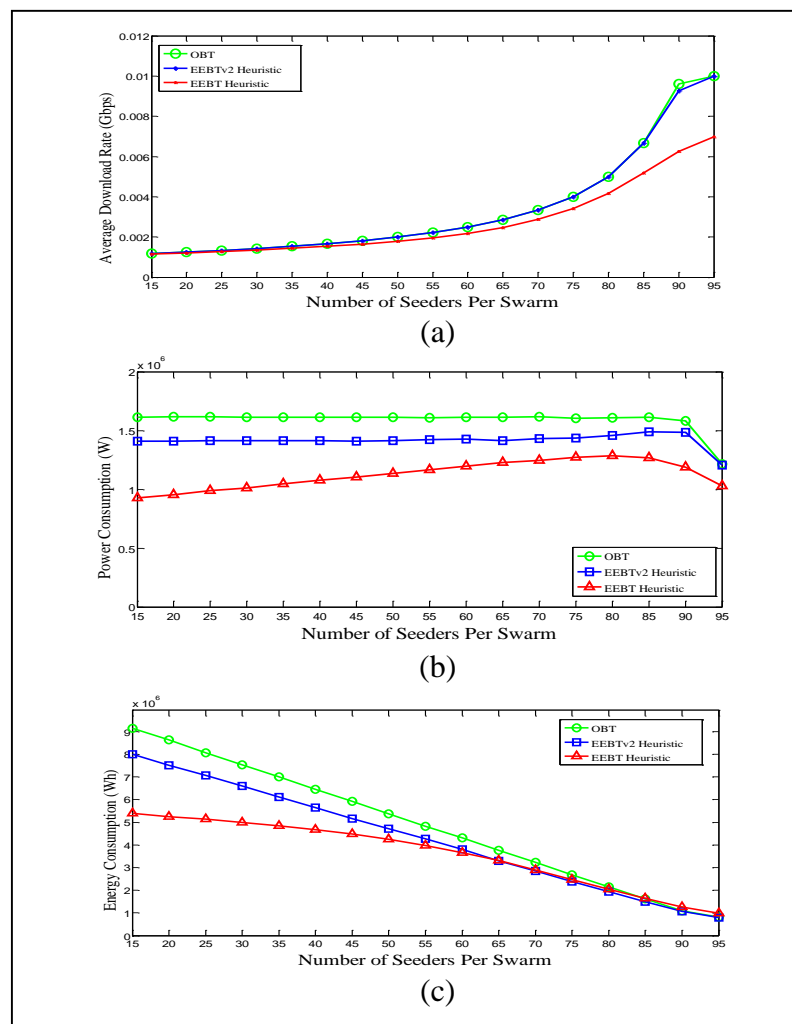


Fig. 3 - 11: The performance of the different bittorrent heuristics (a) Average download rate (b) IP/WDM power consumption (c) IP/WDM energy consumption

Fig. 3 - 11 compares the performance of the EEBTv2 heuristic to the EEBT and the OBT heuristics over the NSFNET network. The EEBTv2 heuristic achieves a download rate comparable to that of the OBT heuristic as shown in Fig. 3 - 11(a) which is a rate higher than that achieved by the EEBT. To achieve such download rate, leechers in the EEBTv2 heuristic have to traverse more hops to connect to other

leechers compared to the EEBT heuristic, reducing the power consumption saving achieved compared to the OBT heuristic from 29% achieved by the EEBT heuristic to 11%, as shown in Fig. 3 - 11(b).

Because of the high download rate achieved by the EEBTv2 heuristic, the difference in energy consumption between the two heuristics is reduced. While the EEBT heuristic saves about 17% energy compared to the OBT, the EEBTv2 heuristic achieves 11% energy savings as shown in Fig. 3 - 11(c). At high number of seeders (corresponding to low number of leechers) the EEBTv2 heuristic, Fig. 3 - 11(c), consumes lower energy compared to the EEBT as the download rate of the EEBT is degraded by 13%, as mentioned in Section 3.4

3.6 Impact of Peers Upload Rate Heterogeneity

Heterogeneous systems exhibit new features that might affect the overall performance of BitTorrent, such as the clustering phenomenon [92] in which peers that belong to the same upload class congregate together. This behaviour is a consequence of the choke algorithm's fairness mechanism as peers choke those who reciprocate at lower rates. Eventually, the peer selection mechanism will be biased by upload capacities. Here clusters with higher upload capacities become more likely to finish before clusters of lower upload capacities.

For heterogeneous BitTorrent systems, we assume the following:

- While all seeders stay in the network for the whole time, leechers of each class leave as soon as they finish downloading. This represents the worst case scenario as the departure of leechers after finishing downloading decreases the capacity of the system, hence raising the energy consumption.
- Classes are defined in a descending order where $Class_1$ has the highest upload capacity and $Class_{cn}$ has the lowest upload capacity.
- The number of phases is equal to the number of classes. At phase t , classes $Class_t \dots Class_{CN}$ coexist in the swarm and $Class_t$ finishes downloading at the end of phase t and leaves the network. Therefore, in the first phase ($t = 1$) all

classes coexist while in the last phase ($t = cn$) only the class with the lowest upload capacity ($Class_{CN}$) remains.

We define the following sets and parameters in the model:

Sets:

| | |
|-----------|--|
| T | Set of downloading phases |
| PC_{ck} | Set of peers of class c in swarm k |

Parameters:

| | |
|-----------|---|
| CN | Number of Classes |
| PCN_c | Number of peers in class c for all swarms |
| $Class_c$ | Class c upload capacity, in Gbps |

Note that the rest of the sets, parameters and variables are the same as those defined in Section 3.2 with the subscript t added to every variable in order to signify the phase value. For instance, the variable $Avdr_{ik}$ is replaced by $Avdr_{ikt}$, and network power consumption NPC is replaced by NPC_t ...etc. We also need the same objective function summed over the t index and the same set of constraints of Section 3.2, plus the following one:

$$\begin{aligned}
 &U_{ijkt} = 0 \\
 &\forall t \in T, \quad \forall c \in \{1 \dots t-1\}, \quad \forall k \in Sw, \forall i, j \in P_k: \\
 &\quad t \neq 1 \quad j \notin Sd_k \quad i \neq j \quad Up_{jk} = Class_c.
 \end{aligned} \tag{3-15}$$

Constraint (3-15) ensures that at each phase t , leechers who finished downloading in the previous phases do not participate in the peer selection mechanism in phase t given by U_{ijkt} . Note that in the first phase ($t = 1$) all leechers coexist in the network.

The average download rate for class c at phase t is given as follows:

$$CDr_{tc} = \frac{1}{PCN_c} \cdot \sum_{k \in Sw} \sum_{i \in PC_{ck}: i \in P_k, i \notin Sd_k} Avdr_{ikt}, \tag{3-16}$$

The size of the remaining file pieces to be downloaded by class c at phase t is:

$$F_{tc} = F - \sum_{k=1}^{t-1} PD_k \cdot CDr_{kc}, \quad (3-17)$$

Equations (3-16) and (3-17) are used to deduce the duration of each phase (PD_t) which is defined as the time required by the class of the highest capacity among the co-existing classes in that phase, c_{max} , to finish downloading the remaining part of the file, calculated as follows:

$$PD_t = \frac{F_{tc_{max}}}{CDr_{tc_{max}}}, \quad (3-18)$$

where $c_{max} = t$. From (3-18) we can estimate the average download time (ADT) for our scenario as:

$$ADT(Hours) = \sum_{t=1}^{cn} PD_t / 3600. \quad (3-19)$$

We evaluate a heterogeneous BitTorrent system with two classes ($CN = 2$), low upload capacity class of 0.001 Gbps and high upload capacity class of 0.005 Gbps. We consider 15 seeders in the network and evaluate the performance for different number of leechers (85 to 5). We also compare this heterogeneous system to the C/S model and two homogenous BitTorrent systems, one with 0.001 Gbps upload capacity and another one with 0.005 Gbps upload capacity.

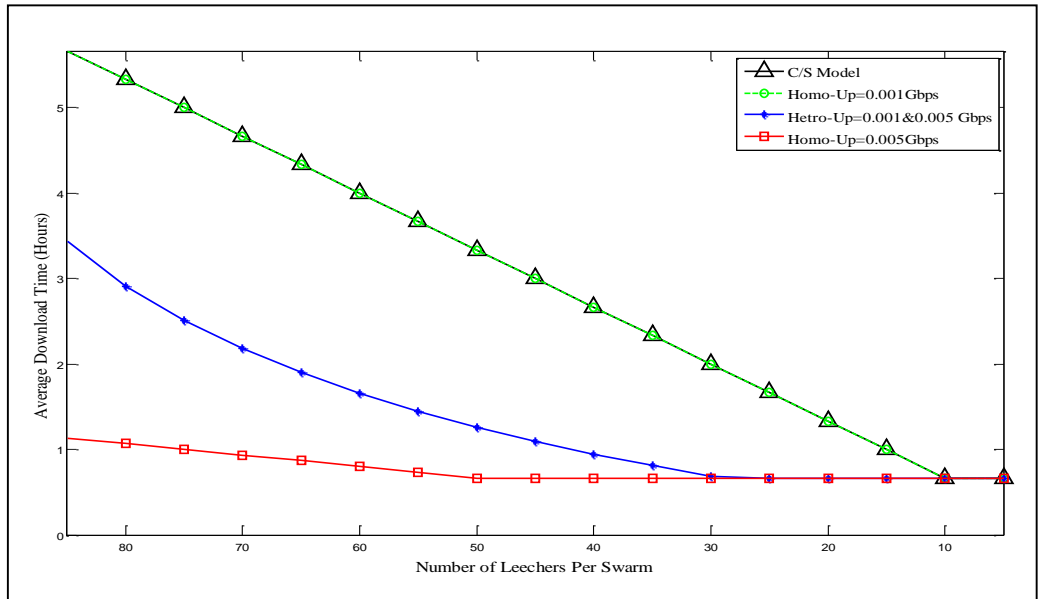


Fig. 3 - 12: The average download time of a heterogeneous BitTorrent system ($CN = 2$)

Fig. 3 - 12 shows the average download time for peers considering different number of leechers. The download time has been reduced by 49% compared to the C/S system. This is because more seeders select the remaining slow leechers when fast leechers leave, leading to an increase in the capacity of the network and hence shorter download time.

The network energy consumption at each phase is calculated by multiplying the network power at that phase (NPC_t) by the phase duration (PD_t). Hence, the total energy consumption (EC) for our scenario is given as:

$$EC(Wh) = \sum_{t=1}^{cn} NPC_t \cdot PD_t / 3600. \quad (3-20)$$

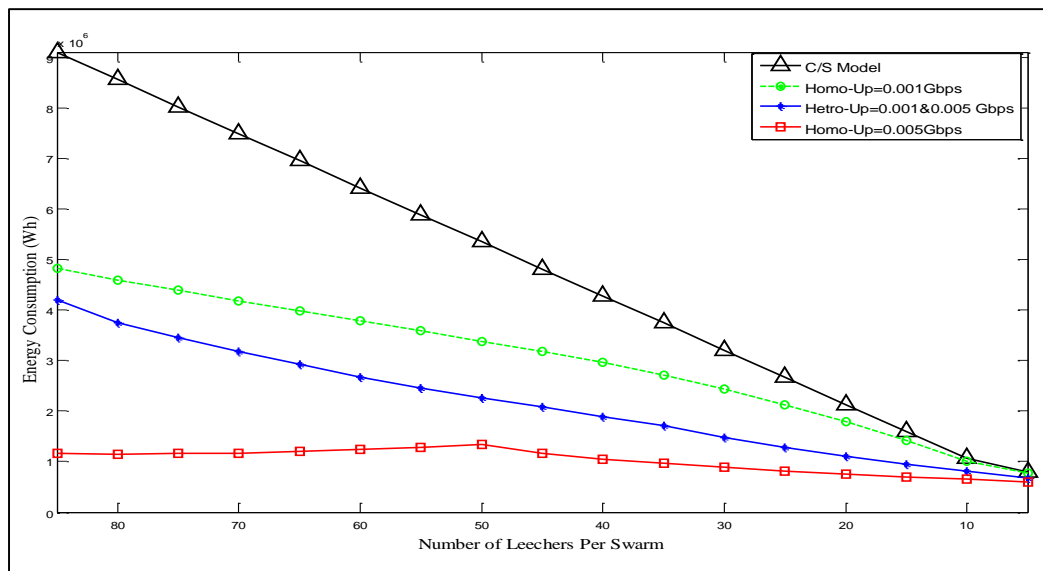


Fig. 3 - 13: IP/WDM energy consumption of a heterogeneous BitTorrent system ($CN = 2$)

The energy consumption of the network follows a trend similar to that of the download time as shown in Fig. 3 - 13. The heterogeneous model resulted in 50% energy savings compared to the C/S model. The high power consumption caused by fast peers impacts the network for a short time as fast peers group together, biased by their upload capacity which leads to lower energy consumption. On the other hand, slow leechers benefit from the departure of fast leechers as more seeders will select them, Fig. 3 - 12, reducing time as well as energy consumption.

3.7 Impact of Leechers Behaviour

Even homogeneous peers in BitTorrent may finish downloading at different times under certain condition, such as arrival pattern. In Section 3.2 we assumed that all peers arrive to the network as soon as a popular content is shared and therefore they all finish almost at the same time as peers are homogenous in terms of their upload capacity. However, peers might arrive in the network at different points in time and therefore they finish at different times. After they finish downloading their files, leechers might stay to seed or they might leave the network as they do not have the incentive to participate in sharing their files. In this section, we investigate the impact of leechers' behaviour on the network performance and energy consumption. We also investigate how seeders can adapt to the behaviour of leechers to maintain the network energy consumption and performance.

The model in Section 3.2 is used to compare the network performance and energy consumption under two scenarios. While in the first scenario leechers stay to seed after finishing downloading, the second scenario assumes leechers leave the network as soon as they finish downloading. We fix the number of seeders (original seeders) and decrease the number of leechers from 85 to 5 leechers. All peers are also assumed to have an upload capacity of 1 Mbps.

Our evaluation is based on the assumption that leechers arrive to the network in groups, each of 5 leechers, at different time intervals until the entire number of leechers reaches 85. Therefore, at a certain time, each group would have downloaded a different percentage of the file depending on their arrival time. We assume that the arrival behaviour results in an idealised linear relationship between group index and the downloaded percentage of the file as depicted in Fig. 3 - 14. However, other relations reflecting different arrival scenarios might be considered as an extension to this work.

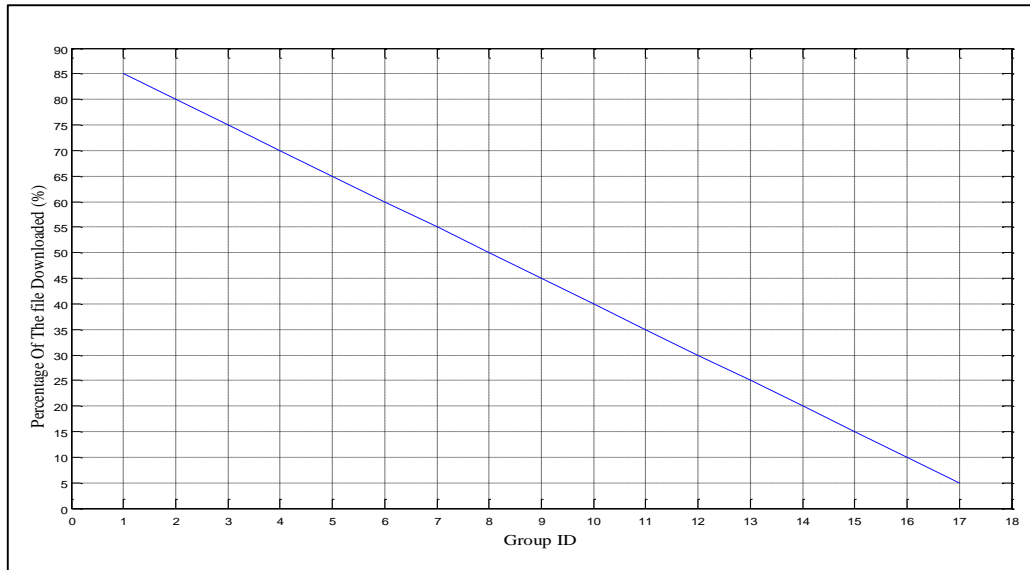


Fig. 3 - 14: Percentage of the file downloaded for each group

Fig. 3 - 15 displays the average download rate for leechers with different number of original seeders, 15, 50 and 95, assuming that leechers leave after finishing downloading. Fig. 3 - 15 also shows the performance under the scenario where the swarm starts with 15 original seeders but leechers stay in the network to seed after finishing downloading. The download rate achieved increases as more peers (original seeders and staying leechers) are available to seed. Under the scenario where leechers leave after finishing, the performance of the network with different number of original seeders is a shifted version of the case where leechers stay in the network to seed after finishing downloading.

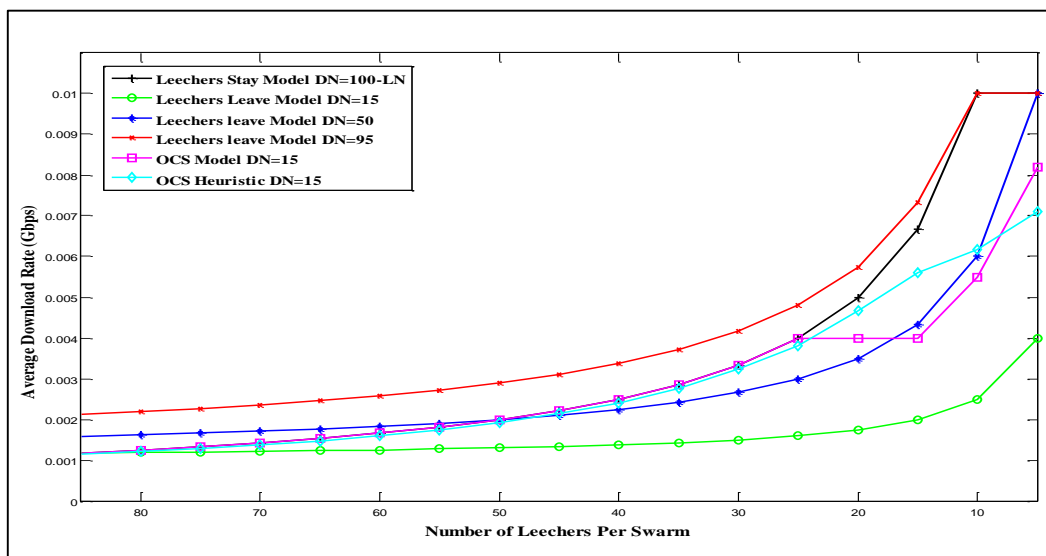


Fig. 3 - 15: Average download rate with different number of original seeders

Fig. 3 - 16 shows the power consumption of the network. As expected, the higher average download rate obtained with higher number of original seeders where leechers leave after finishing results in higher power consumption.

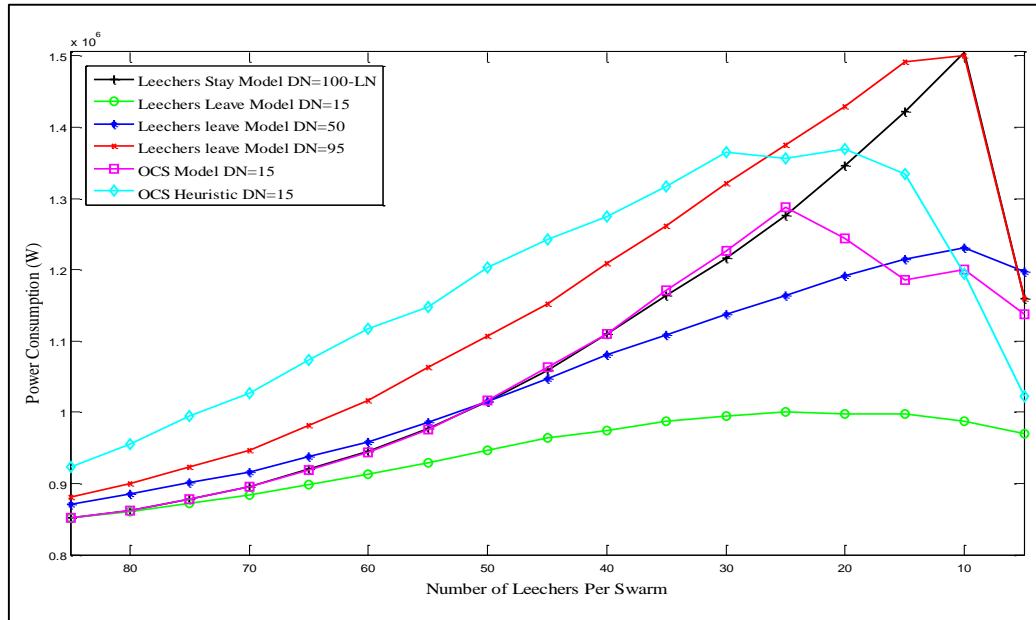


Fig. 3 - 16: IP/WDM power consumption with different number of original seeders

However, as discussed earlier, higher download rates mean also less downloading time which, as Fig. 3 - 17 reveals, leading to less energy consumption. The energy consumption is calculated by multiplying the power consumption at a particular number of leechers by the time required for the group with the highest percentage of the file to finish downloading. The network experiences high energy consumption at 85 leechers and then the energy significantly drops at 80 leechers. This is due to the fact that the first group with 85% of the file downloaded needs to download the remaining 15% while other groups in subsequent steps need to download only 5%, therefore the first group takes longer time to leave the network.

The departure of leechers after finishing downloading increases the energy consumption if the number of original seeders is low to moderate. With 15 original seeders, the energy efficient model consumes 61% more energy when leechers leave the network after finishing downloading compared to the scenario where leechers stay to seed after finishing downloading. The increase is limited to about (3%) with 50 original seeders. The energy consumption is reduced by 22% when the number of original seeders rises to 95.

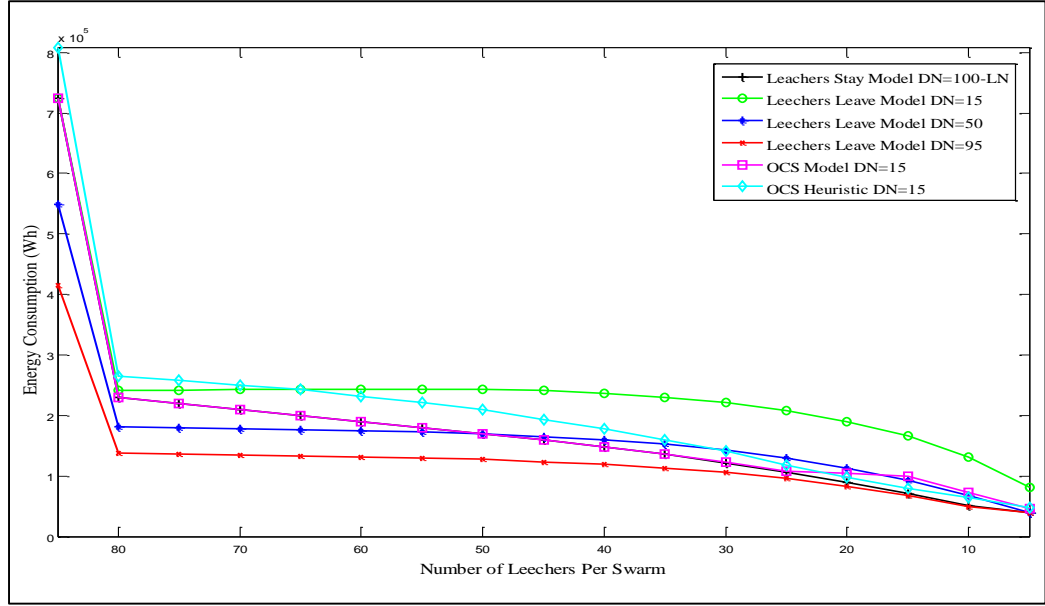


Fig. 3 - 17: IP/WDM energy consumption with different number of original seeders

From the results above, we observe that to approach the performance of the case when leechers stay to seed after finishing downloading, the seeders should account for 50% to 95% of the total number of peers. However, swarms might not be able to provide such a large number of seeders. In a managed environment where an operator can control its own seeders, operators can increase the upload rates of their seeders to compensate for the impact of leechers departure on the energy consumption. To address this problem formally we extend the model in Section 3.2. The model considers U_{ijk} at each particular number of leechers as an input parameter and tries to maintain it by optimising the seeders upload rate Up_s to compensate for leechers leaving the swarm. These variable upload rate seeders are called Operator Controlled Seeders (OCSs).

The extended model redefines the following parameters and variables:

Parameters:

U_{ijk} $U_{ijk} = 1$ if peer i unchokes peer j in swarm k , otherwise $U_{ijk} = 0$

Up_l Upload rate for leechers, 0.001 Gbps

Variables (All are non-negative real numbers):

Up_s Upload rate for OCSs

SR_{ik} Upload rate for each slot of peer i in swarm k

The model is defined as follows:

Objective: Similar to the objective in Section 3.2

Subject to: Similar constraints of Section 3.2 considering the redefined variables and parameters above plus the following:

$$Up_s \leq Dp, \quad (3-21)$$

$$SR_{ik} = Up_l / SLN \quad (3-22)$$

$$\forall k \in Sw \quad \forall i \in L_k,$$

$$SR_{ik} = Up_s / SLN \quad (3-23)$$

$$\forall k \in Sw \quad \forall i \in Sd_k,$$

$$\frac{1}{LN \cdot SN} \cdot \sum_{k \in Sw} \sum_{i \in L_k} Avdr_{ik} \leq Up_l + \sum_{s=1}^{100-LN} Up_l / LN. \quad (3-24)$$

Constraint (3-21) ensures that the upload rate of OCSs does not exceed their download capacity as this will be unrealistic for the majority of the clients' network connections. Constraints (3-22) and (3-23) ensure that only OCSs are allowed to raise their upload rate. Constraint (3-24) limits the average download rate for the peers to the value deduced by equation (3-14) as this is the target the model tries to maintain by optimising OCSs upload rate.

Fig. 3 - 15 shows the average download rate for peers obtained from optimising the upload rate of the 15 OCSs when leechers leave the network after finishing. The model manages to maintain the average download rate for a number of leechers as high as 35. When the number of leechers is lower than 35, the download rate deviates. This is because the increase in the seeders upload rate in this case is limited by the leechers reaching their maximum download capacity. Recall that the extended model optimises the upload rates of OCSs given U_{ijk} as an input parameter.

Fig. 3 - 18 reveals that OCSs need to achieve a maximum upload rate 0.005 Gbps to compensate for leechers leaving the network making this approach more efficient and realistic compared to deploying a high number of seeders with lower upload rate.

Fig. 3 - 16 shows the power consumption of the model obtained by optimising the upload rate of OCSs. It exhibits similar trends to those of the average download rate. Both scenarios where leechers stay to seed after finishing or OCSs adapt their upload rates in response to leechers leaving consume more power compared to the scenario where seeders do not adapt their upload rate in response to leechers leaving.

However, as the time required to download the file is reduced, optimising the OCSs upload rate to adapt to leechers leaving reduces the increase in energy consumption compared to the scenario where leechers stay to seed (Fig. 3 - 17) from 61% (seeders do not adapt their upload rate) to 7%.

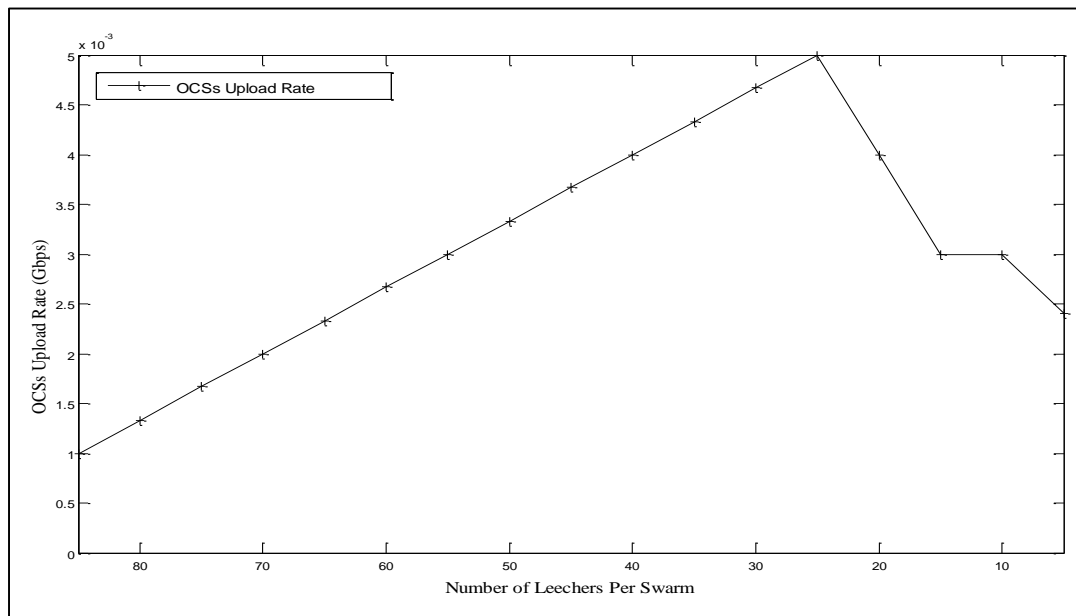


Fig. 3 - 18: OCSs average upload rate

To enable practical implementation of the OCSs approach, we added a function to the EEBT heuristic in Fig. 3 - 8 to calculate the average upload rate of seeders as leechers leave the network. The relationship between the number of leechers and the seeders upload rate, shown in Fig. 3 - 18, can be deduced from the fact that the total upload capacity for all peers in the network is equal to the total download demand of leechers, hence:

$$S_{avur} = \frac{LN \cdot (T_{avdr} - Up_l)}{DN}. \quad (3-25)$$

where S_{avur} represents the OCSs average upload rate and T_{avdr} is the target average download rate for leechers. If we set T_{avdr} to the average download rate for the scenario where leechers stay to seed (Fig. 3 - 15), then S_{avur} obtained from (3-25) will be very close to the corresponding value for the seeders average upload rate of Fig. 3 - 18.

The results of the EEBT heuristic with OCSs upload rate adaptation are shown in Fig. 3 - 15, Fig. 3 - 16 and Fig. 3 - 17. The simple heuristic achieves comparable performance to the MILP model with no more than 8% reduction in the average download rate compared to the case when leechers stay to seed. The power/energy consumption of the heuristic has increased by only 12% compared to the model (Fig. 3 - 16 and Fig. 3 - 17).

3.8 Location Optimisation for OCSs

In this section we extend the work in the previous section, to further optimise the location of OCSs as well as their upload rate in case leechers start to leave the network after finishing downloading. The work in Section 3.7 does not optimise the location of OCSs and assumes they are uniformly distributed in the network.

To implement rate and location optimisation, we define the following necessary variables:

Variables (All are non-negative real numbers):

US_{isjk} The upload traffic sent from the OCS i in node s to leecher j , where both the OCS and the leecher are in swarm k

USb_{isjk} $USb_{isjk} = 1$ if OCS i in node s unchokes leecher j , where both the OCS and the leecher are in swarm k , otherwise $USb_{isjk} = 0$

SL_{isk} $SL_{isk} = 1$ if OCS i is located in node s in swarm k , otherwise $SL_{isk} = 0$

Objective: Similar to the objective of the model in Section 3.2

Subject to: Constraints (3-2)-(3-9), (3-11)-(3-13), plus the following:

$$Avdr_{jk} = \sum_{i \in L_k, i \neq j} SR \cdot U_{ijk} + \sum_{i \in Sd_k} \sum_{s \in N} US_{isjk}$$

$$\forall k \in Sw \quad \forall j \in L_k, \quad (3-26)$$

$$US_{isjk} \cdot M1 \geq USb_{isjk}$$

$$\forall k \in Sw \quad \forall i \in Sd_k \quad \forall j \in L_k \quad \forall s \in N, \quad (3-27)$$

$$US_{isjk} \leq M2 \cdot USb_{isjk}$$

$$\forall k \in Sw \quad \forall i \in Sd_k \quad \forall j \in L_k \quad \forall s \in N, \quad (3-28)$$

$$\sum_{j \in L_k} USb_{isjk} \geq SL_{isk}$$

$$\forall k \in Sw \quad \forall i \in Sd_k \quad \forall s \in N, \quad (3-29)$$

$$\sum_{j \in L_k} USb_{isjk} \leq M \cdot SL_{isk}$$

$$\forall k \in Sw \quad \forall i \in Sd_k \quad \forall s \in N, \quad (3-30)$$

$$\sum_{s \in N} SL_{isk} = 1$$

$$\forall k \in Sw \quad \forall i \in Sd_k, \quad (3-31)$$

$$\sum_{s \in N} \sum_{j \in L_k} USb_{isjk} \leq SLN$$

$$\forall k \in Sw \quad \forall i \in Sd_k, \quad (3-32)$$

$$US_{isjk} \geq SR \cdot USb_{isjk},$$

$$\forall k \in Sw \quad \forall i \in Sd_k \quad \forall j \in L_k \quad \forall s \in N, \quad (3-33)$$

$$\frac{1}{LN \cdot SN} \cdot \sum_{k \in Sw} \sum_{i \in L_k} Avdr_{ik} \leq Up + \sum_{s=1}^{PN-LN} Up_l / LN, \quad (3-34)$$

$$\sum_{s \in N} \sum_{j \in L_k} US_{isjk} \leq Dp$$

$$\forall k \in Sw \quad \forall i \in Sd_k, \quad (3-35)$$

Constraint (3-26) calculates the total download rate for each leecher by summing the download rates the leecher obtains from other leechers and OCSs. Constraints (3-27) and (3-28) determine whether the OCS i in node s unchokes leecher j in the same

swarm k . $M1$ and $M2$ are large enough numbers with units of 1/Gbps and Gbps, respectively, and they ensure that $USb_{isjk} = 1$ if $US_{isjk} > 0$, otherwise $USb_{isjk} = 0$. Constraints (3-29) and (3-30) determine the location of OCS i in swarm k . M is a large enough unitless number that ensures $SL_{isk} = 1$ if $\sum_{j \in L_k} USb_{isjk} > 0$, otherwise $SL_{isk} = 0$. Constraint (3-31) ensures that there is only one copy of each OCS in the network. Constraint (3-32) limits the total number of upload slots of OCSs to the maximum allowed number of upload slots, defined by SLN . Constraint (3-33) ensures that the upload rate for each slot for OCSs is not less than the defined slot rate for leechers (SR). However, OCSs are allowed to increase their upload slots rates beyond SR . Constraint (3-34) ensures that the average download rate for all leechers equals to the optimal download rate. This will force the OCSs to increase their upload rate in case leechers leave the network after finishing downloading. Constraint (3-35) limits the maximum upload rate for OCSs to their download capacity as it is unrealistic to have a peer with more upload capacity than its download capacity.

Our evaluation is based on the assumption that leechers arrive to the network in groups, each of 10 leechers, at different time intervals until the total number of leechers reaches 85. We also assume that the arrival behaviour results in a linear relationship between group index and the downloaded percentage of the file, similar to Section 3.7.

Fig. 3 - 19 compares the performance of the EEBT model, where OCS are optimally located, to the results of the three schemes considered in Section 3.7, where (i) leechers stay, (ii) leechers leave with no OCS, and (iii) uniformly distributed OCS compensate for the reduction in the download rate after leechers leave.

The different schemes are compared in a scenario where the swarm has 15 OCS and 85 leechers. Leechers finish downloading in groups of 10 and either leave the network or stay to act as seeders.

Fig. 3 - 19(a) shows that optimally locating the OCS nodes achieved similar download rate to the case of leechers staying. Moreover, the new scheme saves 15% and 40% power consumption compared to the scheme where leechers stay and leechers leave and no OCS are introduced, respectively as shown in Fig. 3 - 19(b).

This is because the new scheme, unlike the uniform distribution of OCS where some nodes might end up with no OCS, places an OCS in each node which minimises the cross traffic due to OCS to leechers selections.

Note also that the scenario of leechers leaving with no OCS has the highest energy consumption in spite of the fact that it does not have the highest power consumption. This is because this scenario has the lowest download rate (Fig. 3 - 19(a)) as leaving peers are not replaced by OCS and the swarm loses upload capacity and consequently low download rates and high download times are observed. This eventually leads to high energy consumption as shown in Fig. 3 - 19(c).

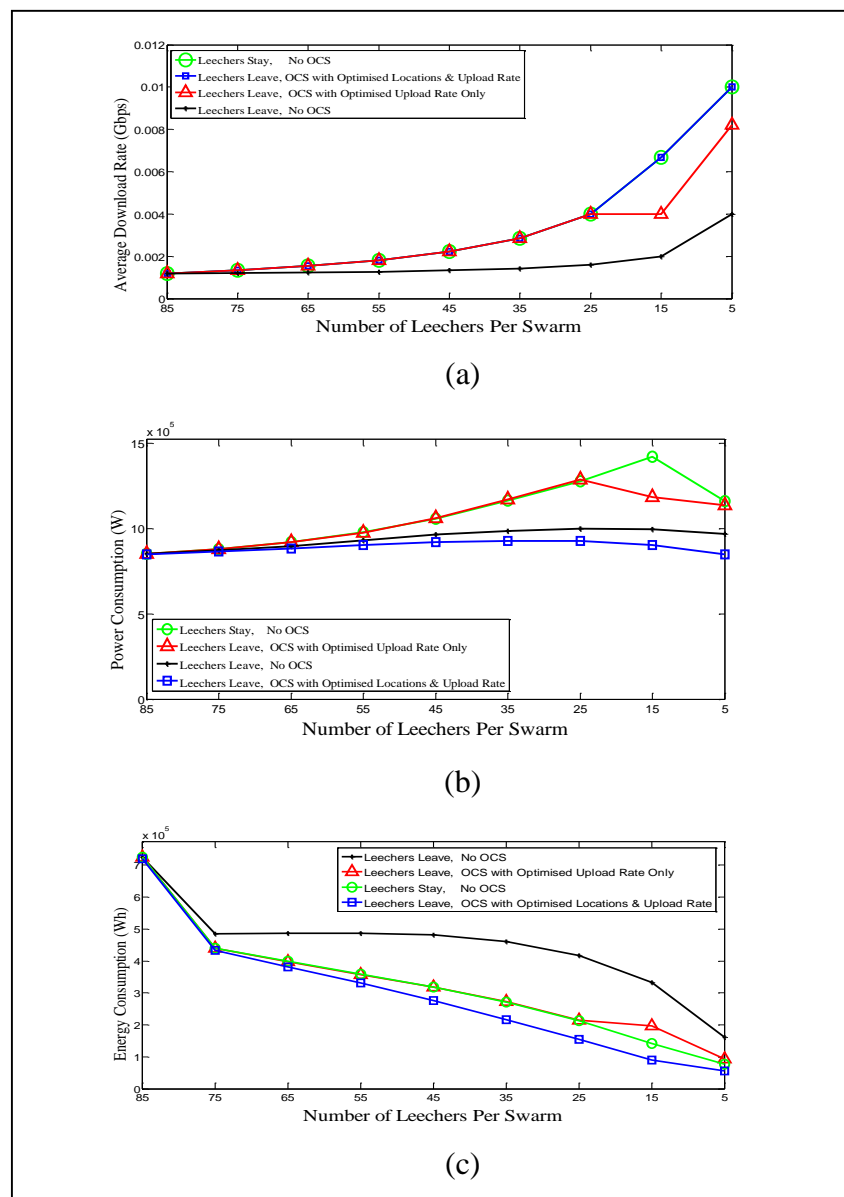


Fig. 3 - 19: MILP results for OCS (a) Average download rate (b) IP/WDM power consumption (c) IP/WDM energy consumption

3.9 Impact of Physical Topology

In this section we study the impact of the network topology on the energy efficiency of BitTorrent over bypass IP/WDM networks. We consider three topologies of different number of nodes and average hop counts, namely, the AT&T network in USA, the British Telecom network in Europe (EU BT), and the Italian network. These topologies are chosen as they allow us to: (i) investigate the impact of large number of nodes (AT&T) compared to NSFNET (ii) investigate the impact of number of hops given similar number of nodes (EUBT and Italian Network). As BitTorrent peers are distributed and cause communication among core nodes, their energy efficiency relies on the nature of core nodes topology which gives insights regarding the physical conditions at which more power savings can be achieved.

We consider the same content distribution scenario for the different schemes (BitTorrent and C/S schemes) over the NSFNET topology as in Section 3.2 where 160k groups of downloaders, each downloading a 3 GB file, are distributed randomly over the network nodes. Each group consists of 100 members.

We also assume the same average regular traffic and BitTorrent cross-node traffic demands between each node pair in the NSFNET considering different time zones, which is 82 Gbps as in Section 3.3 . The scenario we considered represents a future scenario with approximately double the current level of network traffic. Note that traffic is currently growing at 30%-40% per year [93] and therefore traffic doubles every two years approximately.

To study the performance over the different topologies, we estimate the average regular traffic between node pairs, ART_n , based on the traffic of the NSFNET topology:

$$ART_n = \left(\frac{P_n}{P_{NSFNET}} \right) \cdot ART_{NSFNET} \text{ Gbps.} \quad (3-36)$$

where P_n is the population of users in topology n and P_{NSFNET} , is the population of users in the NSFNET which is considered to be equal to the USA population, ART_{NSFNET} is the average regular traffic demands between node pairs in NSFNET Table 3 - 2. We use ART_n to generate the elements of the regular traffic matrix,

denoted as RTN_{sd} , randomly and uniformly distributed between $[10, (2 \cdot ART_n - 10)]$ Gbps.

The number of swarms, NS_n , is calculated based on the fact that the total swarm traffic should be equal to the total regular traffic so that each contribute 50% of the total traffic in the network. Similar to Section 3.3, we solve the MILP model for 20 swarms and assume that the network contains 8k replicas of these 20 swarms, i.e. a total of 160k swarms so the swarms contribute 50% of the total traffic in the network. To obtain the total number of swarms for each of the topologies considered in this section, the 20 swarms are scaled by the ratio between the total regular traffic and the total swarms' traffic. So NS_n is given as:

$$NS_n = 20 \cdot \left(\frac{\sum_{s \in N} \sum_{d \in N} RTN_{sd}}{\sum_{s \in N} \sum_{d \in N} STN_{sd}} \right) \quad (3-37)$$

where STN_{sd} is the swarms traffic between nodes s and d due to running the OBT model with 20 swarms. The resulting regular traffic and number of swarms are summarised in Table 3 - 2.

For the C/S scheme, the model in [21] is again used to optimally locate 5 data centres in the different topologies and evaluate the performance of the C/S scheme. Note that we assume different data centres have different content, i.e. content is not replicated, and all the content is equally popular. The results are obtained against increasing number of seeders (from 25 to 95) in steps of 10 where the number of leechers decreases accordingly to maintain the total number of peers in all cases at $PN = 100$ peers (Table 3 - 1). For instance, if the number of seeders is 55 in a figure, this means that the number of leechers is 45.

| Network | Country | Population (Million) | No. of Nodes | No. of Links | Avg. Hop Count | Avg. Regular Traffic (Gbps) | No. of Swarms |
|---------|---------|----------------------|--------------|--------------|----------------|-----------------------------|---------------|
| NSFNET | USA | 314 | 14 | 21 | 2 | 82 | 160,000 |
| AT&T | USA | 314 | 25 | 54 | 2.5 | 82 | 509,400 |
| EU BT | Europe | 406 | 21 | 34 | 2 | 105.8 | 464,740 |
| Italian | Italy | 61 | 21 | 36 | 3 | 15.9 | 70,000 |

Table 3 - 2: Analysed Networks Information

3.9.1 AT&T Network

The AT&T network [94], [95] projected on USA map [96], shown in Fig. 3 - 20, consists of 25 nodes and 54 bidirectional links. As the AT&T network is located in USA; it is considered to have the same population and average regular traffic between node pairs as the NSFNET. However, due to its higher number of nodes compared to the NSFNET, the total regular traffic in this network will be higher. Therefore, 509,400 swarms are assumed for this network as shown in Table 3 - 2. The 5 data centres of the C/S system are optimally located at nodes 11, 13, 14, 17 and 24 to minimise power consumption using our data centres MILP in [21].

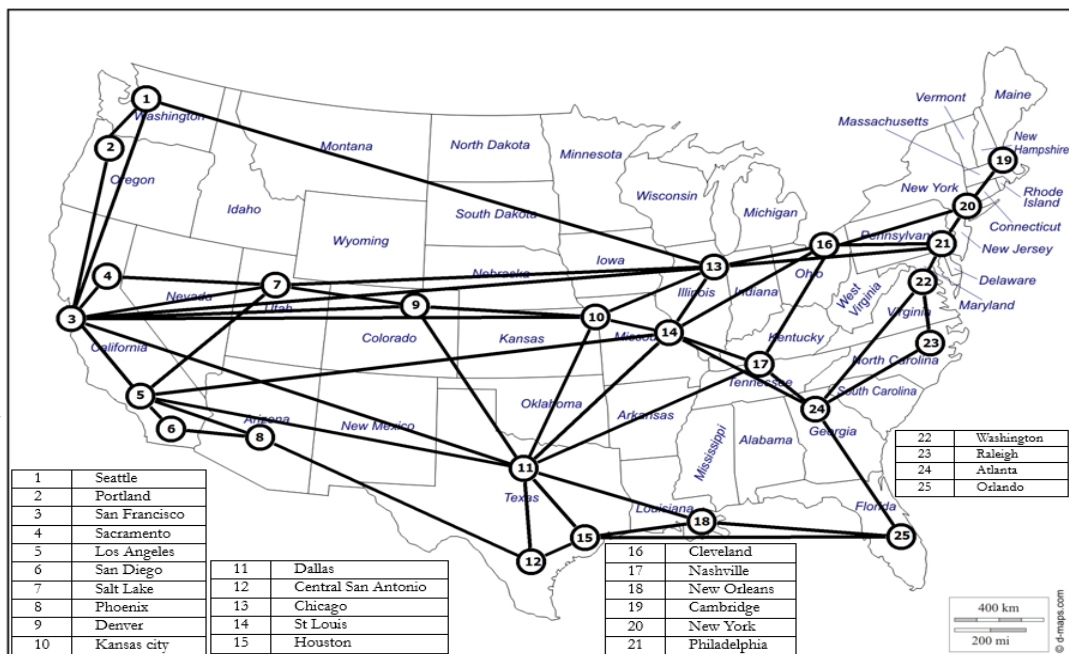


Fig. 3 - 20: AT&T network [94], [95], [96]

Fig. 3 - 21 compares the performance of the OBT, EEBT and C/S models over the AT&T network. Similar trends to those observed for the NSFNET network in Section 3.3 are observed for the AT&T network. Fig. 3 - 21(a) shows that the three schemes: OBT, EEBT and C/S achieve the optimal download rates. However, they consume different amounts of power as shown in Fig. 3 - 21(b). The OBT scheme has the highest power consumption as it yields the highest cross traffic between nodes due to its locality un-awareness. The C/S scheme consumes slightly less power compared to the OBT as downloaders consume no power in the core network when they download from a local data centre in their node, yielding 1% power saving compared to the OBT. The EEBT scheme is the most energy efficient scheme among the schemes considered as it considers the peers' locations, resulting in 19%

power saving compared to the OBT scheme. The lower power saving achieved by the EEBT scheme over the AT&T (19%) network compared to the savings over the NSFNET (30%, Section 3.3) is due to the higher number of nodes which leads to having a smaller number of localised peers per node, hence, higher likelihood that leechers connect with peers across the network to achieve the optimal download rate [83]. As noticed in Section 3.3, the decline in power consumption at 95 seeders is because the remaining 5 leechers only require a total download rate of 0.05 Gbps due to their download capacity limit which can be satisfied by only 50 peers (the 5 leechers plus 45 seeders out of the 95 seeders) in the BitTorrent scheme, resulting in 50% lower P2P upload traffic in the network and consequently lower power consumption as shown in Fig. 3 - 21(b). For C/S scheme the servers will push less traffic as well to satisfy the lower demanded traffic by the 5 downloaders.

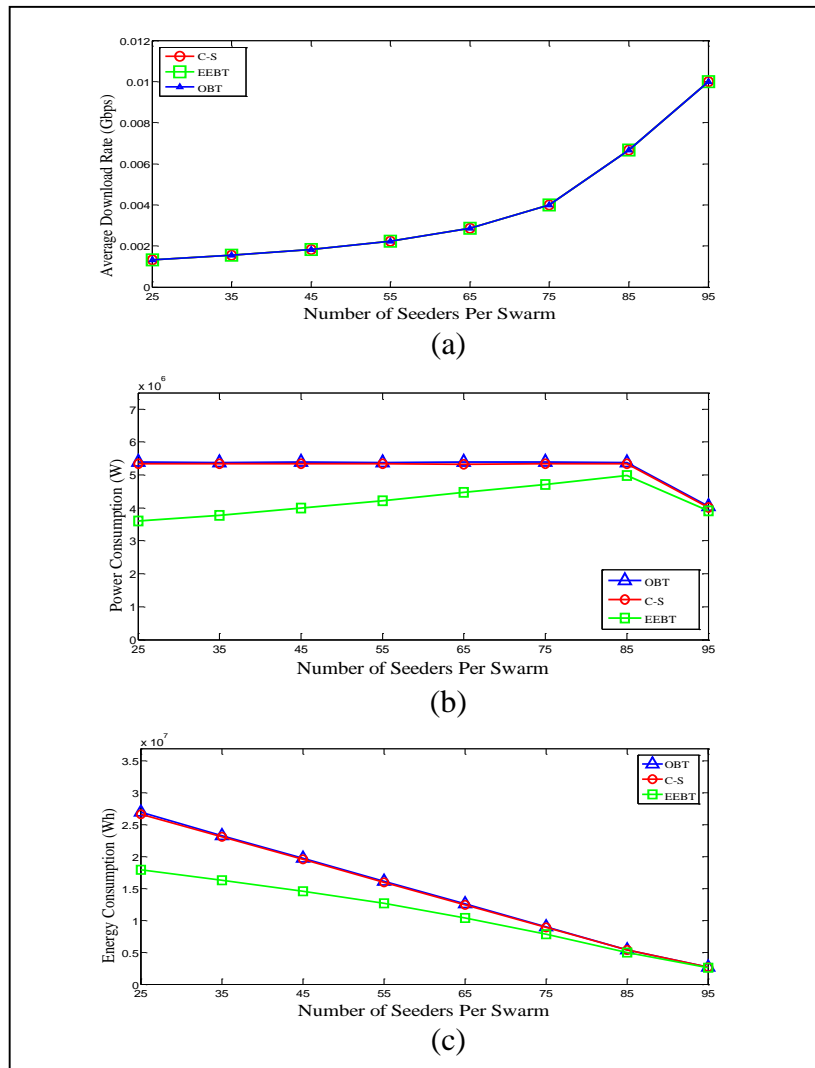


Fig. 3 - 21: AT&T network results (a) Download rate (b) IP/WDM power consumption (c) IP/WDM energy consumption

To evaluate the energy consumption under a particular number of seeders, we multiplied the power consumption by the average download time (calculated by dividing the file size by average download rate). As all schemes achieve similar download rates, the energy consumption, shown in Fig. 3 - 21(c), displays similar trend as the power consumption.

3.9.2 British Telecom European Network (EU BT)

The EU BT Network [94], [97] projected on the map of Europe [98], is depicted in Fig. 3 – 22.

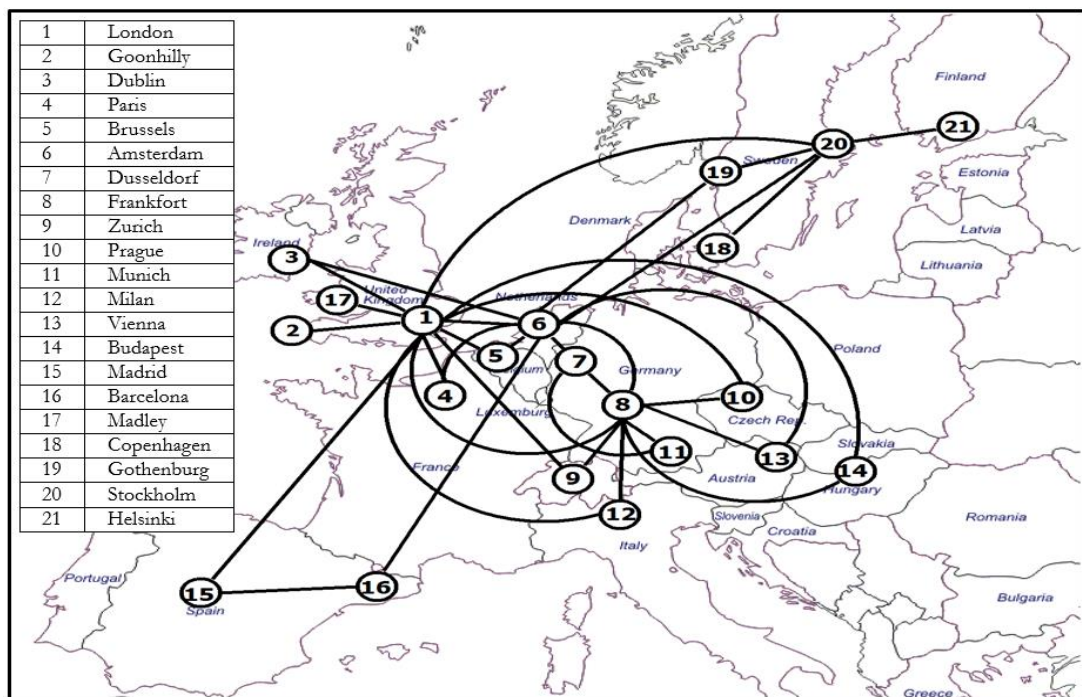


Fig. 3 -22: EU BT network [94], [97], [98]

EU BT has 21 nodes and 34 bidirectional links. The total population of the cities covered by this network is higher than that of the NSFNET, therefore, higher average regular traffic and number of swarms is considered for this network as shown in Table 3 - 2. The 5 data centres of the C/S system are optimally located at nodes 1, 4, 6, 8 and 12 to minimise the power needed using the models in [21].

Fig. 3 - 22 displays the EU BT network power and energy consumption. The average download rate exhibits similar values to those in Fig. 3 - 21(a) since the physical topology has no impact on the optimal download rate. Fig. 3 - 22(a) reveals that EEBT saves 21% of the network power consumption compared to the OBT. The

slightly higher power saving compared to the power savings achieved by the EEBT scheme over the AT&T network is due to the lower number of nodes in the EU BT network, and hence, higher average number of peers per node which increases the ability to localise traffic within the same node.

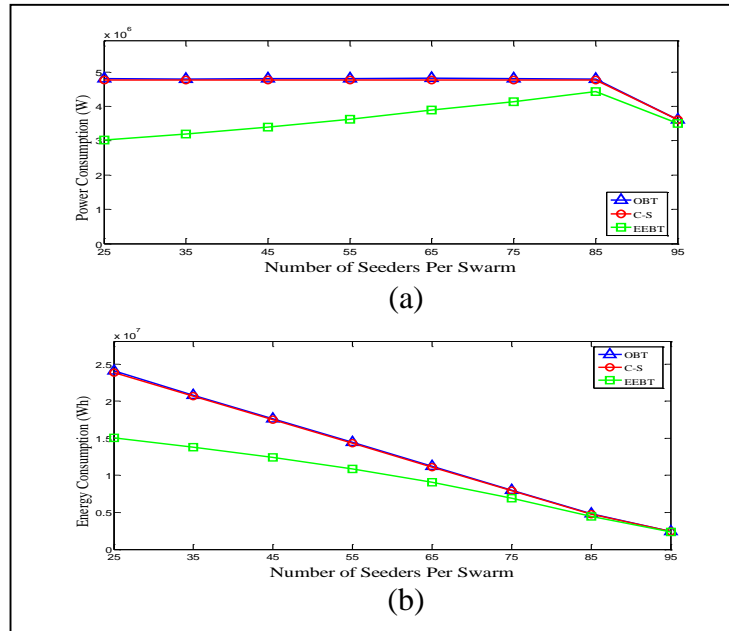


Fig. 3 - 22: EU BT network results (a) IP/WDM power consumption (b) IP/WDM energy consumption

3.9.3 Italian Network

The Italian network (Telecom Italia network) [94], [99] projected on the map of Italy [100], shown in Fig. 3 - 23, consists of 21 nodes and 36 bidirectional links. It has the lowest population among the analysed networks, leading the lowest regular traffic and number of swarms as shown in Table 3 - 2. We consider the C/S system with 5 data centres located optimally at nodes 9, 12, 13, 14, and 15, where these node locations are again determined using the MILP in [21].

As explained above in Section 3.9.2, the average download rate is the same as that observed in Fig. 3 - 21(a) as peers download rate is independent of the physical topology considered. Fig. 3 - 24 reveals that EEBT achieves 22% power and energy savings compared to the OBT scheme. This saving is slightly higher compared to the savings over the EU BT network despite the fact that both networks have similar number of nodes. This is due to the higher average hop count of the Italian network (3 hops) compared to the EU BT network (2 hops) which increases the power

consumed by the transponders and multiplexers/demultiplexers (both consume more power with respect to EDFA).

Therefore, locality in the Italian network will yield higher reduction in the number of utilised transponders and multiplexers/demultiplexers compared to the EU BT network. More saving is expected for non-bypass IP/WDM approach where the number of router ports, the most power consuming devices in the network, is a function of the hop count.

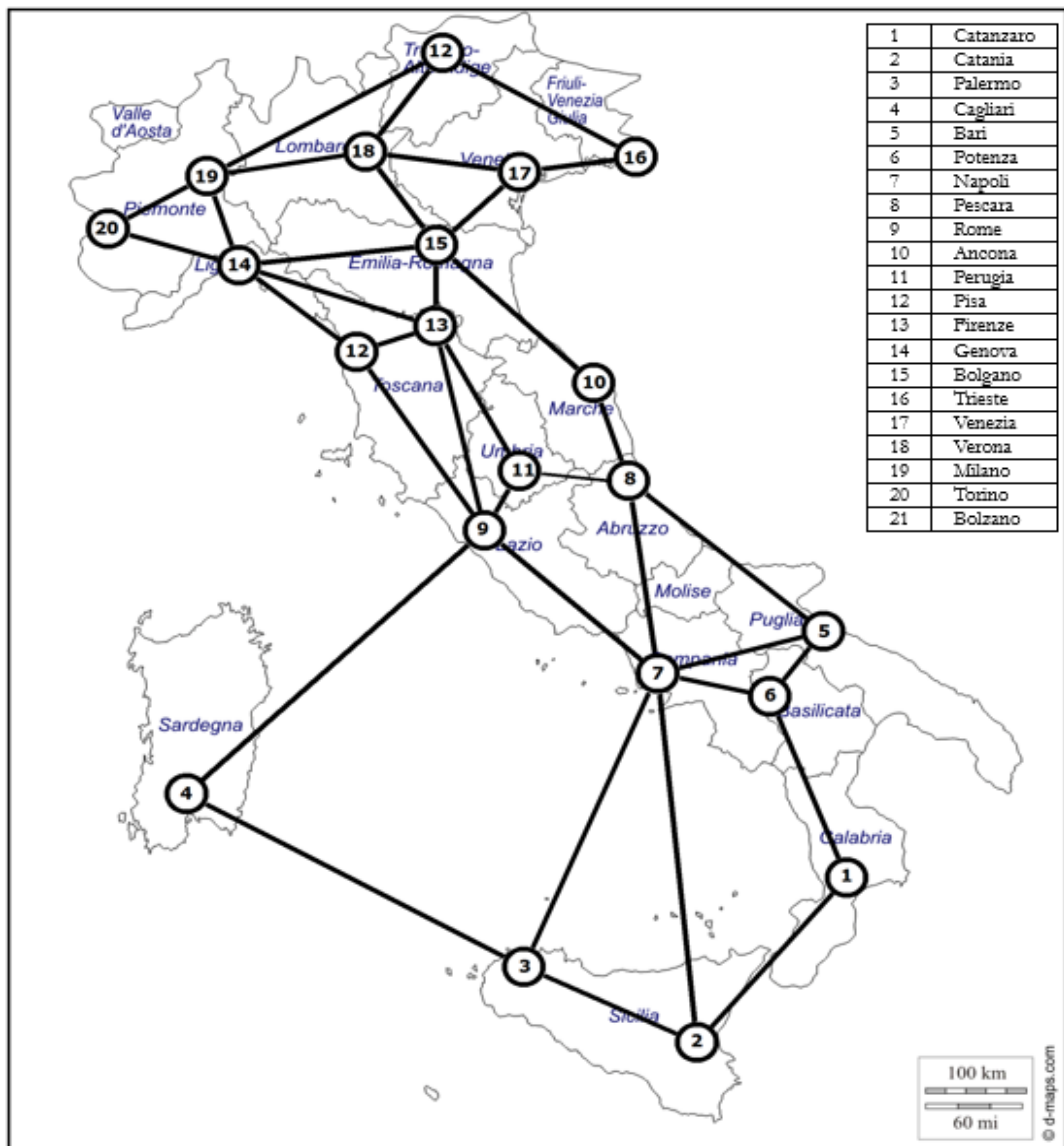


Fig. 3 - 23: The Italian network [94], [99], [100]

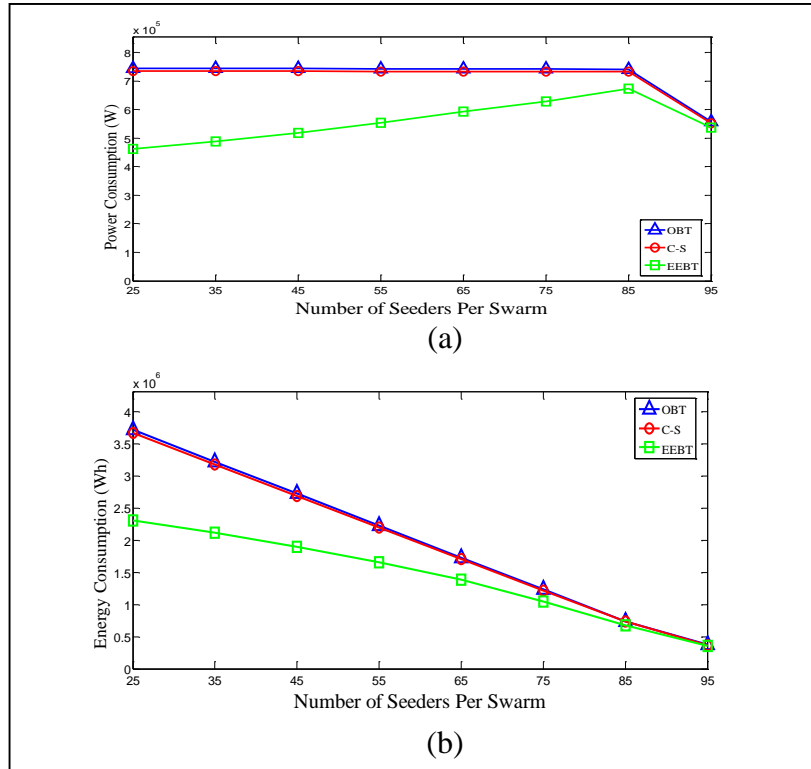


Fig. 3 - 24: Italian network results (a) IP/WDM power consumption (b) IP/WDM energy consumption

From the results above, we see that the size of the network in terms of number of nodes and the average hop count are the main drivers for power saving in localised BitTorrent P2P protocols. Smaller networks with higher average hop counts yield more saving when comparing OBT and C/S for a given swarm with certain number of peers.

3.10 Hybrid CDN-P2P Architecture

In the previous sections we have compared P2P and C/S systems in terms of energy efficiency. We showed that location aware BitTorrent systems can achieve significant energy savings compared to C/S systems. However, BitTorrent systems will suffer in an environment where the content availability is scarce or far. In this section, we develop a MILP model to study and optimise the energy efficiency of a hybrid CDN-P2P architecture where peers can download a video from other peers using a P2P BitTorrent like protocol and/or from a CDN data centre if the P2P capacity is not enough to deliver the video at the required streaming rate. Unlike HP2P in [43] and the heuristics in [44], our CDN-P2P model allows each peer to

download from multiple sources (P2P and/or CDN) simultaneously which requires the servers to be BitTorrent aware as peers will ask these servers for specific pieces of data identified in the metadata file rather than the complete content. The fraction of sources that share content using the P2P protocol are constrained by TFT as in the OBT implementation. We model servers power consumption in CDN data centres while the work in [44] considers the Ethernet switches and edge routers of a fat tree based data centres architecture. The authors in [43] assume a fixed core hop count of 4 while peers in our model, similar to [44], can access data centres at different hop counts. It should be noted however that unlike our work, [44] is not a BitTorrent network in that peer swarms are not formed (such swarms may constrain or support the peer performance according to situation), a file is not broken into pieces for sharing, the BitTorrent TFT mechanism is not implemented, [44] assumes download from a single source who is able to provide the full rate, while BitTorrent specifies download from multiple peers so that the TFT reward mechanism leads to stability (also rewards) and a distributed P2P system. We address these points in our MILP, and furthermore our heuristics and experimental demonstration implement the (BitTorrent mechanisms) and optimal local rarest first mechanism which ensures that the peers have interesting pieces to download.

In this section we extend the MILP model developed in Section 3.2 to consider CDN-P2P hybrid architecture. In the hybrid model, a peer can receive a video by joining a particular swarm that is currently participating in sharing that video and/or from a data centre in case the P2P network capacity is not sufficient to deliver the video with the required streaming rate.

In addition to the sets, parameters and variables defined in Section 3.2, the following sets, parameters and variables are defined:

Sets:

DC Set of nodes with data centres

Parameters:

VSR Video streaming rate

Epb Energy per bit for the server

| | |
|------------|--|
| δ_s | $\delta_s = 1$ if node s has a data centre, otherwise $\delta_s = 0$ |
| γ | Weight of the network power consumption |
| ϵ | Weight of the servers power consumption |

Variables (All are non-negative real numbers):

| | |
|------------------|--|
| L_{cdn}^{sd} | CDN traffic demand between node pair (s,d) |
| $LCDN_{ij}^{sd}$ | The CDN traffic flow between node pair (s,d) traversing virtual link (i,j) |
| CDN_{iks} | Traffic demand between peer i in swarm k and data centre s |

We calculate the network power consumption (NPC) as discussed in Section 3.2. The CDN data centres power consumption (CPC) is deduced by considering the energy per bit of a typical server:

$$CPC = E_{pb} \cdot \sum_{s \in DC} \sum_{d \in N} L_{cdn}^{sd}. \quad (3-38)$$

Note that in this section we only consider traffic proportional energy consumption in data centres and does not account for the power required for redundancy, cooling or underutilisation, which are useful extensions to our MILP models. Therefore, the total power consumption (TPC) is:

$$TPC = NPC + CPC, \quad (3-39)$$

Now we can define the model as: (3-40)

Objective: Minimise $\gamma \cdot NPC + \epsilon \cdot CPC$,

Subject to: Constraints (3-2)-(3-4), (3-6)-(3,9), (3-12)-(3-13) plus the following:

$$L_{cdn}^{sd} = \sum_{k \in Sw} \sum_{i \in Pn_{dk}: i \in L_k} \delta_s \cdot CDN_{iks} \quad (3-41)$$

$$\forall s, d \in N,$$

$$\sum_{j \in N: i \neq j} LCDN_{ij}^{sd} - \sum_{j \in N: i \neq j} LCDN_{ji}^{sd} = \begin{cases} L_{cdn}^{sd} & \text{if } i = s \\ -L_{cdn}^{sd} & \text{if } i = d \\ 0 & \text{otherwise} \end{cases} \quad (3-42)$$

$$\forall s, d, i \in N: s \neq d,$$

$$\sum_{s \in N} \sum_{d \in N: s \neq d} \left(LCDN_{ij}^{sd} + L_{ij}^{sd} + \sum_{k \in Sw} L_{ijk}^{sd} \right) \leq C_{ij} \cdot B \quad (3-43)$$

$$\forall i, j \in N: i \neq j,$$

$$Avdr_{ik} = \sum_{j \in P_k: i \neq j} SLR \cdot U_{jik} + \sum_{s \in DC} CDN_{iks} \quad (3-44)$$

$$\forall k \in Sw \quad \forall i \in L_k,$$

$$Avdr_{ik} = VSR$$

$$\forall k \in Sw \quad \forall i \in L_k. \quad (3-45)$$

Equation (3-40) gives the model objective, i.e. to minimise the total power consumption composed of network and CDN components that are weighted by γ and ϵ , respectively while satisfying the streaming rate constraint for the VoD service. To achieve this objective the model optimises the P2P selection, given by the variable U_{ijk} , as well as the CDN to peers traffic, given by the variable CDN_{iks} .

Constraint (3-41) calculates the transient traffic between IP/WDM nodes due to CDN to peers traffic based on CDN_{iks} . Constraint (3-42) is the flow conservation constraint for the CDN to peers traffic. Constraint (3-43) ensures that the traffic traversing a virtual link does not exceed its capacity. Constraint (3-44) calculates the download rate for each peer according to the upload rate it receives from other peers selecting it and/or the traffic received from the CDN. Constraint (3-45) limits the download rate of a leecher to the required streaming rate for the video.

In the following results, we evaluate four optimisation scenarios to show the trade-off between the different content distribution approaches:

- H-MinNPC Model: A hybrid model that only minimises the IP/WDM network power consumption, i.e. ($\epsilon = 0$).
- H-MinTPC Model: A hybrid that minimises the total power consumption (network and data centres), i.e. ($\gamma = \epsilon = 1$)
- Only-CDN model: Peers download only from the CDN data centres, i.e. $\sum_{j \in P_k: i \neq j} SLR \cdot U_{jik} = 0$.

- Only-P2P model: Peers download only from each other using a BitTorrent like protocol, i.e. $\sum_{s \in DC} CDN_{iks} = 0$.

We evaluate the power consumption of the different scenarios versus an increasing number of seeders in the swarms while the total number of peers is fixed, i.e. versus an increasing download capacity of the P2P system. For CDN, leechers are considered as normal clients that download from CDN directly without P2P connections. Nodes with CDN are the same set of nodes used in Section 3.3.

| | |
|---|--------------------|
| Energy per bit for VoD server (E_{pb}) | 437.5 W/Gbps [101] |
| Video streaming rate (VSR) | 0.003 Gbps |
| Network Power consumption weight (γ) | 1 |
| CDN Power Consumption weight (ϵ) | 0 or 1 |

Table 3 - 3: Input data for the CDN-P2P model

Note that E_{pb} is calculated based on [101] where the server power consumption is 350 W and the capacity is 800 Mbps (0.8 Gbps), therefore, $350 \text{ W}/0.8 \text{ Gbps}=437.5 \text{ W/Gbps}$. Fig. 3 - 25(a) shows the total power consumption (TPC), which is composed of the network power consumption (NPC) and the CDN data centres power consumption (CPC), for the different optimisation scenarios. From Fig. 3 - 25(a) it can be seen that the ‘Only-P2P’ model is not capable of satisfying the required video streaming rate (3 Mbps) with a number of seeders lower than 65. For both hybrid models, the results show that the total power consumption is reduced as the number of seeders increases i.e. the download capacity of the P2P network increases. This is because having more seeders in the swarm, increases the likelihood that leechers will be served locally and therefore decreases the IP/WDM cross traffic as well as the load on CDN data centres.

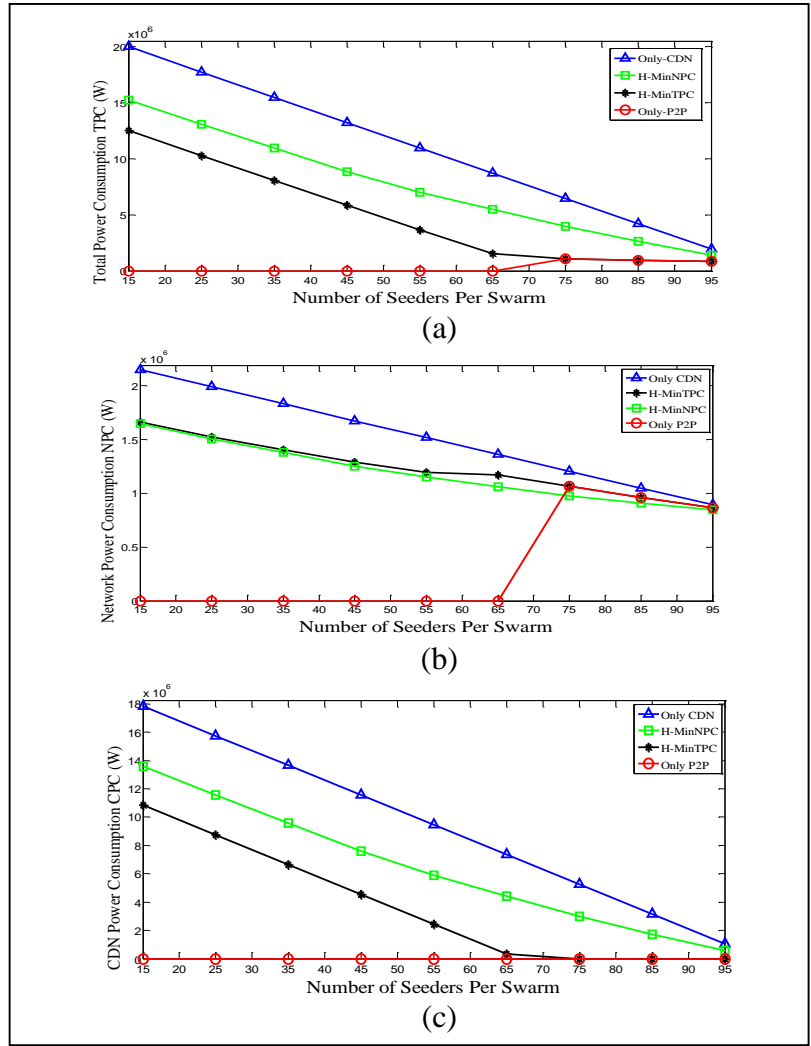


Fig. 3 - 25: CDN-P2P results (a) Total power consumption (b) IP/WDM network power consumption (c) CDN data centre power consumption

The H-MinTPC model is the most energy efficient solution. It consumes 44% and 61% less power compared to the H-MinNPC and Only-CDN models, respectively. This is achieved by utilising the P2P throughput as much as possible by allowing peers to upload at their maximum upload capacity while the CDN is only contacted when the P2P capacity is not enough to satisfy the required streaming rate. A similar approach is reported in [44] for the Minimised Server Bandwidth (MSB) heuristic as peers are looked up before CDN data centres which means that data centres servers are only contacted when peers are not available or have all served their share of requests. However a key distinction between our MILP model and the MSB heuristic of [44] is that we consider a BitTorrent network and not a simple P2P network. In BitTorrent a peer that is selected has to be rewarded later according to the TFT mechanism. This means that our power minimised BitTorrent network MILP may

not allow peers to select very remote peers even if such peers are available due to the “double” journey imposed by TFT, and may therefore select a distant CDN location which does not add a second “reward” journey. It should be recalled that BitTorrent is the most popular P2P implementation as it overcomes a number of key P2P networks problems and provides key advantages. For example if the single source in [44] (and some other P2P implementations) was to leave the network, communication fails, whereas BitTorrent eliminates this single point of failure by allowing peers to connect to multiple peers simultaneously as in our MILP and implementation. BitTorrent provides fairness through TFT, scalability and robustness by dividing the file into pieces that are downloaded. These features have their implications on power consumption and our models include these features.

Note that for a number of seeders equal to or higher than 65, the total power consumption for the H-MinTPC is equal to the P2P total power consumption as no load will be exerted on CDN data centres. On the other hand, the H-MinNPC model saves only about 32% compared to Only-CDN model as it does not consider minimising the power consumption of data centres.

Fig. 3 - 25(b) and Fig. 3 - 25(c) decompose the total power consumption shown in Fig. 3 - 25(a) into its two components: the network power consumption (*NPC*) and the CDN data centres power consumption (*CPC*), respectively. As expected, the Only-CDN model is the least energy efficient at the network side. At higher number of seeders (more than 65); the network power consumption of the Only-CDN model is even higher than the total power consumption of the H-MinTPC model. The network power consumption for the H-MinNPC is slightly lower than the H-MinTPC network power consumption. This is because with H-MinNPC, peers prefer to stream a video from data centres if it is not available locally rather than streaming it from other peers as traffic from data centres does not need to be rewarded back with an equal and opposite traffic as in the case of streaming from other peers (TFT). However, high load will be exerted on data centres resulting in higher CDN power consumption for the H-MinNPC model compared to the H-MinTPC model as shown in Fig. 3 - 25(c). Similar conclusion is reported in [44] for the Closest Source Assignment (CSA) heuristic but due to different reasons, i.e. not due to TFT. In [44] the CDN servers bandwidth might increase as requests are served from the closest

content source available whether it is a peer or a CDN data centre and peers are not deliberately looked up before CDN data centre.

Nevertheless, H-MinNPC is easier to implement in practice as it does not require peers to be aware of other peers in neighbouring IP/WDM nodes and it shows that it is still possible to achieve total power saving compared to Only-CDN model by having peers with lower upload utilisation.

It can be observed in Fig. 3 - 25 that for the hybrid and the Only-CDN models, the major contribution to the total power consumption comes from the CDN data centres because of the inefficient servers used to distribute the VoD service compared to the energy efficient IP/WDM network.

To overcome the inefficiency of the Only-CDN model, servers with higher energy efficiency are needed. To find out the energy per bit of CDN servers required so that the Only-CDN model is as energy efficient as the H-MinTPC model, we equate the total power consumption of the Only-CDN model to that of the H-MinTPC model:

$$(Epb_{future}/Epb_o) \cdot CPC_{OnlyCDN} + NPC_{OnlyCDN} = TPC_{HMinTPC} \quad (3-46)$$

where Epb_o and Epb_{future} are the current and future energy per bit for servers, respectively and $CPC_{OnlyCDN}$ and $NPC_{OnlyCDN}$ are the Only-CDN data centres and network power consumption, respectively. $TPC_{HMinTPC}$ is the total power consumption of the H-MinTPC model.

Hence:

$$Epb_{future} = Epb_o \cdot \frac{TPC_{HMinTPC} - NPC_{OnlyCDN}}{CPC_{OnlyCDN}} \quad (3-47)$$

Note that Epb_{future} is different for different number of seeders per swarm. While for 15 seeders per swarm, Epb_{future} is equal to 254 W/Gbps; Epb_{future} is 9.5 W/Gbps for 65 seeders. However, the servers manufacturing technology still does not support such energy efficiency. Therefore, hybrid CDN-P2P is very efficient at postponing upgrading data centres in terms of capacity and power consumption.

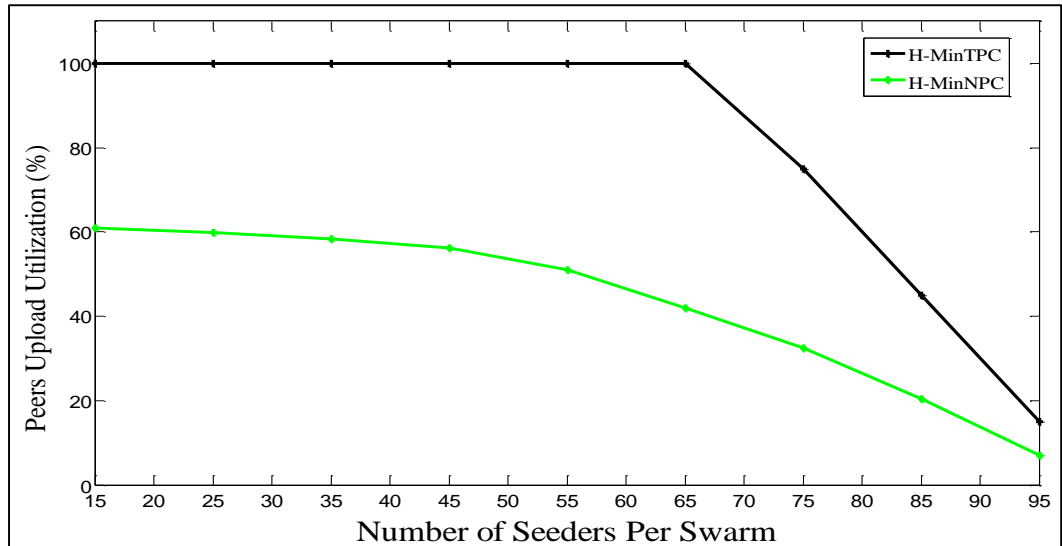


Fig. 3 - 26: File sharing effectiveness

Fig. 3 - 26 shows the average file sharing effectiveness for the hybrid models calculated as:

$$\eta = \sum_{k \in S_w} \sum_{i \in L} \sum_{j \in L: i \neq j} U_{ijk} / (SLN \cdot LN \cdot SN) \quad (3-48)$$

File sharing effectiveness (η , where $0 \leq \eta \leq 1$), is found theoretically to be almost 1 [35] which can be understood as a consequence of the optimality of BitTorrent LRF as discussed in Section 2.5.1. However for video streaming, BitTorrent needs to be modified to satisfy the streaming requirements, which might lead to decreasing η as not all pieces can be downloaded in arbitrary fashion due to streaming constraints. The H-MinTPC model in Fig. 3 - 26 maintains full file sharing effectiveness by allowing peers to contact other peers in neighbouring nodes when the local capacity is not enough until peers have sufficient capacity (at $DN \geq 65$) where lower upload capacity will be enough to satisfy the streaming demand. Conversely, as discussed above the H-MinNPC model limits the majority of peers to their local nodes leading to lower file sharing effectiveness. The H-MinNPC architecture should maintain an average file sharing effectiveness of $\eta = 0.43$ (obtained by averaging peers upload utilisation over the different number of seeders per swarm in Fig. 3 - 26) as with a reduced file sharing effectiveness, which is usually associated with less popular files. The throughput of the P2P system might be insignificant and users might experience poor QoS and therefore, the H-MinNPC model loses its advantage over to the Only-CDN scenario.

Fig. 3 - 27 (left hand side) shows the power consumption of individual data centres at different number of seeders for the H-MinTPC model under the bypass approach. Data centres have dissimilar power consumption levels at a particular number of seeders per swarm because of the unbalanced load on these data centres. CDN providers prefer to balance the load on their data centres to increase the likelihood of serving more nearby users. To evaluate the impact of balancing the data centres loads in the hybrid CDN-P2P architecture, we add a constraint to our model to ensure that all data centres receive the same traffic load:

$$\sum_{d \in \mathcal{N}} L_{cdn}^{sd} = \frac{1}{DCN} \cdot \sum_{i \in DC} \sum_{j \in \mathcal{N}} L_{cdn}^{ij} \quad (3-49)$$

$$\forall s \in DC.$$

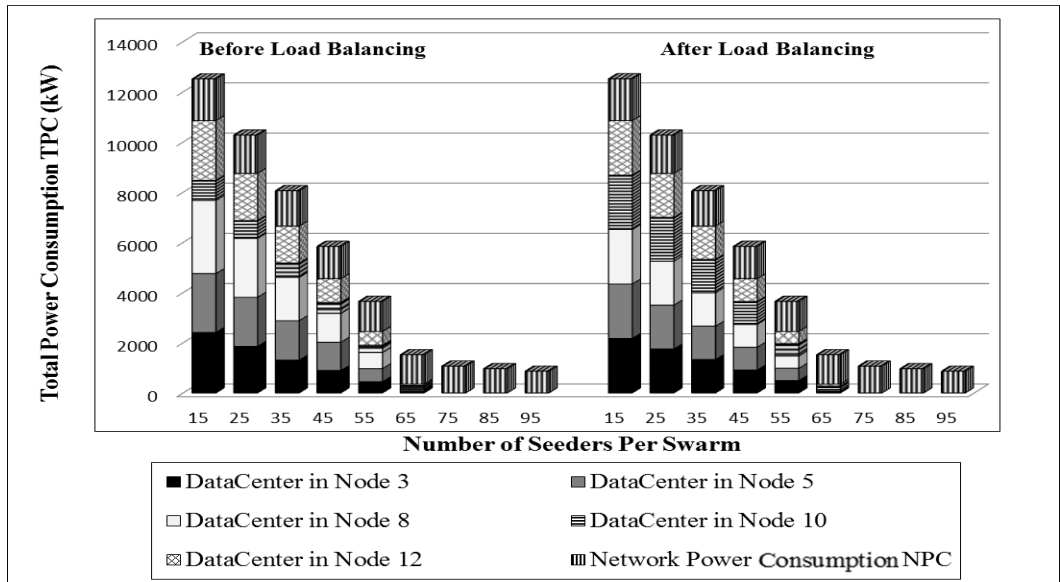


Fig. 3 - 27: Total power consumption (IP/WDM and data centres) with and without load balancing in CDN-P2P

Note that in practice, it might not be possible to reach such sharp balance, however we consider it in our model for illustration purposes. Fig. 3 - 27 (right hand side) shows that balancing the load of data centres has no significant impact on the network power consumption, i.e. the power savings and performance of the hybrid CDN-P2P architecture are not scarified if load balancing is implemented.

Finally, key distinctions between the operator controlled seeders (OCSs) of Section 3.7 and the CDN-P2P include the fact that OCSs increase their rate just to compensate for the number of peers who have left, while the CDN in CDN-P2P may

offer more rate if demanded. The maximum number of available sources to download from in OCSs remains constant and is equal to the swarm size and compensation is achieved by the operator increasing the rate offered by its controlled seeders. In the CDN-P2P network, the CDN sources are in addition to the swarm size.

3.11 Energy Efficient BitTorrent Experimental Demonstration

We further evaluated the EEBT heuristic proposed in Fig. 3 - 8 by building an experimental demonstration to demonstrate its performance and energy consumption over the NSFNET network topology. In the following subsections we discuss the experimental setup and introduce and analyse the results of the experiment.

3.11.1 Experimental Setup

Each node in the NSFNET topology is emulated using a Cisco 10GE, SG 300-10, Layer 3 switch router. Each router is connected to an HP ProLiant DL120G7 server where several instances of the BitTorrent protocol are implemented to represent several peers located at the node. This setup is cost efficient and allows us to distribute peers over the network nodes as required. Table 3 - 4 summarises the details of the hardware we used in our experiment. Fig. 3 - 28 shows the routers and switches placed in two racks and connected to each other to form the NSFNET topology.

| Hardware | Number | Type | Specifications |
|----------|--------|---------------------|---|
| Router | 14 | Cisco SG 300-10 | 10 GE ports [102] |
| Server | 14 | HP ProLiant DL120G7 | Intel® Xeon® E3, RAM 4GB, HD250GB [103] |

Table 3 - 4: Demo hardware components

We implemented the BitTorrent protocol in Python 2.7 using the asynchronous event driven TWISTED library which is the same library the first open source BitTorrent was written in. Our BitTorrent implementation captures the protocol algorithms that control the behaviour of peers such as the choke algorithm (for

leechers and seeders), optimistic unchoke, TFT and LRF. We considered the specifications in [104], [105] as they represent the most popular detailed explanation of BitTorrent online. We implemented a tracker protocol and integrated it with a statistics collection tool to analyse the results of the experiment. Finally we integrated the MATLAB plotting library, Matplotlib [106], with the tracker to display the result instantly.

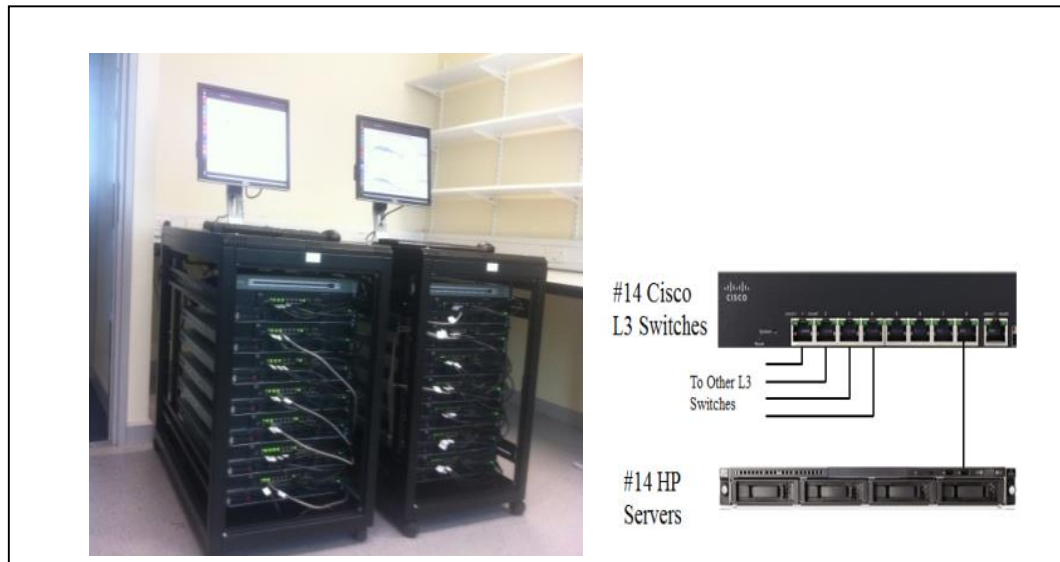


Fig. 3 - 28: Experiment racks and connectivity

The results obtained from the experiment are updated every 1 second on the monitor screen. The network power consumption is calculated based on the traffic demands between network node pairs which can be calculated given the peers' locations and their download rate obtained from the experiment. Given this experimental demand distribution, we use the same power consumption values used in the previous modelling sections (Table 3 - 1) to estimate the power consumption of the experimental setup.

We run the experiment considering a swarm of 56 peers sharing a 40MB file which is divided into pieces of 256kB. Each node has 4 peers, each with an upload capacity of 1 Mbps, and one of them is a seeder.

3.11.2 Experimental Results

The power consumption calculated in the experiment is attributed to the IP layer and optical layer considering the non-bypass approach. Fig. 3 - 29 and Fig. 3 - 30

show the experimental results for the OBT and EEBT, respectively. They also show the results of the model in Section 3.2 considering the peers distribution of the experiment.

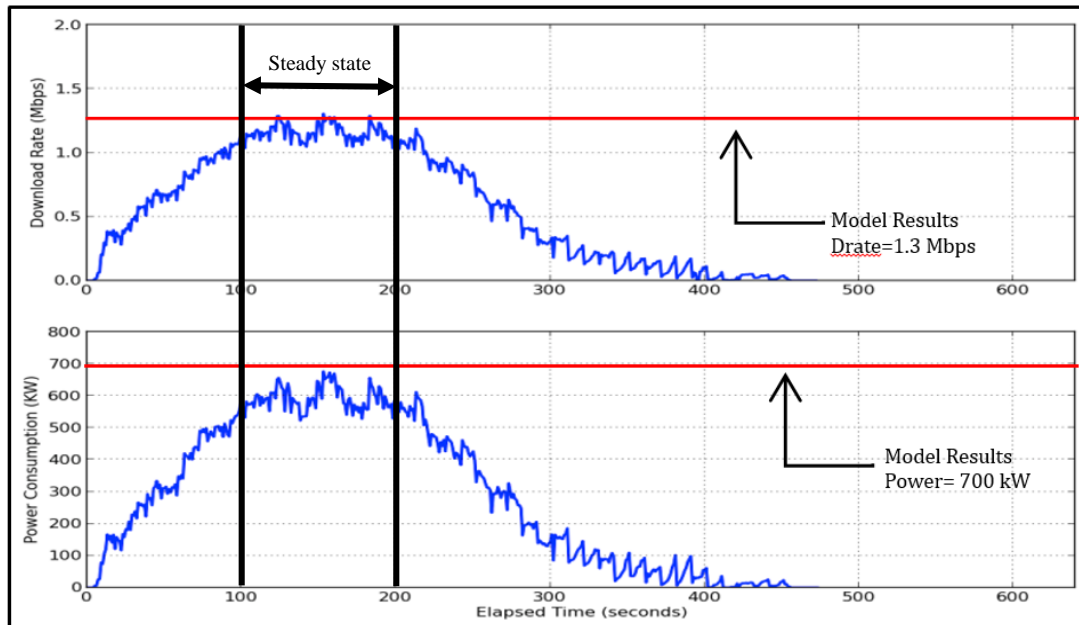


Fig. 3 - 29: Experimental average download rate and IP/WDM power consumption of original BitTorrent experiment (OBT experiment)

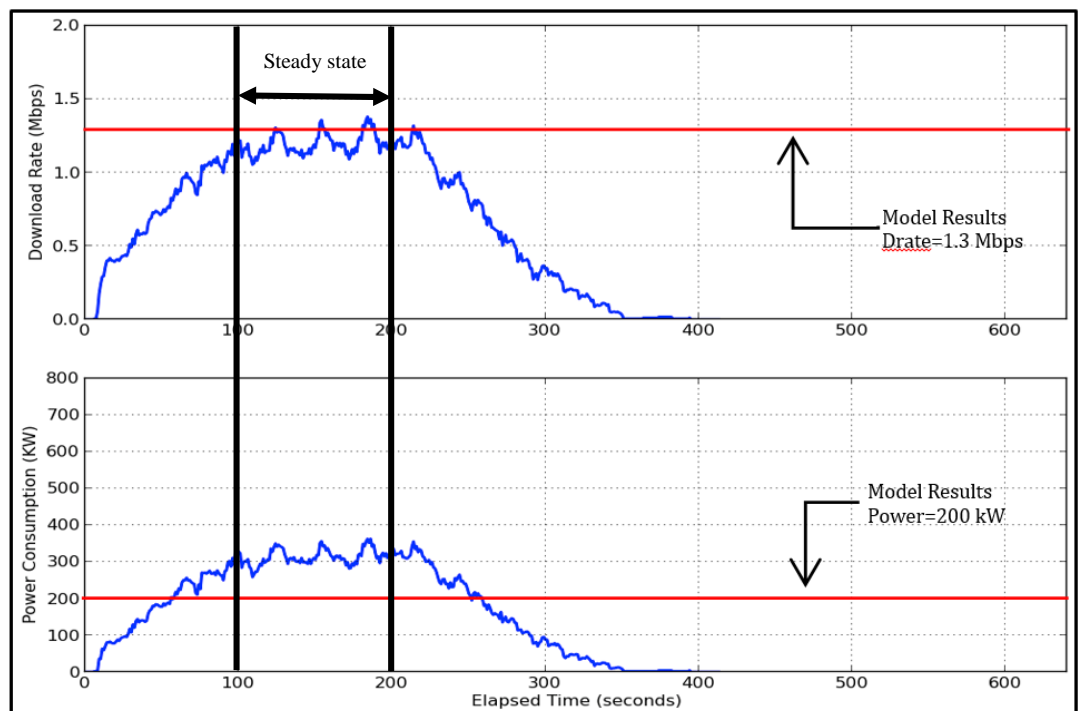


Fig. 3 - 30: Experimental average download rate and IP/WDM power consumption of energy efficient BitTorrent experiment (EEBT experiment)

Both OBT and EEBT achieve a comparable average download rate of about 1 Mbps. At steady state (between 100 and 200 seconds) where all leechers are downloading and uploading at full capacity, the average download rate reaches 1.3 Mbps which is consistent with the theoretical average download rate [83]. This reflects the efficiency of the LRF algorithm in distributing pieces among leechers during steady state. While OBT consumes 400 kW on average, the energy efficient version consumes 240 kW, saving about 40% of power. The power consumption values are averaged over the interval from 50-300 seconds.

As all peers have to download a 40MB (320Mb) file and with average download rate of 1 Mbps, we expect theoretically that all peers have to finish download at 320 seconds. However, the experimental results in Fig. 3 - 29 and Fig. 3 - 30 show a longer average download time of about 400 seconds for both versions of BitTorrent. This is because not all leechers finish exactly at 320 seconds as some uploaders may favour some leechers over others at different times so these leechers receive more than the average download rate of 1 Mbps and other leechers receive less than 1 Mbps and hence their finishing time is delayed beyond the average download time of 320 seconds.

At steady state, the OBT model and the experiment are in good agreement and have almost similar power consumption as shown in Fig. 3 - 29. The power consumption of the EEBT model is however 33% lower (Calculated by taking the steady state average power consumption of the EEBT experiment, 300 kW, as the model only works for steady state case) compared to the experiment as shown in Fig. 3 - 30. This is due to two reasons. Firstly, the model assumes optimal LRF which means that all needed pieces can be found in the local node and therefore neighbouring nodes are only contacted when the average download rate falls below the optimal 1.3 Mbps. In contrast, the experimental testbed has less optimal LRF, as some needed pieces might not be available in the local nodes. Secondly, as mentioned in Table 3 - 2 the average nodal degree in NSFNET is about 2 which makes it more likely to download pieces from a neighbouring node than from the same node as peers in the energy efficient implementation uniformly scan local and neighbouring nodes for peers selections.

Fig. 3 - 31 shows the number of hops travelled by the file pieces to get to the leechers requesting them for the OBT and EEBT experiments. The OBT

experimental results (Fig. 3 - 31(a)) resulted in 5% and 28% of pieces being downloaded from local nodes ($H=0$) and neighbouring nodes ($H=1$), respectively. On the other hand, with the EEBT (Fig. 3 - 31(b)) 30% of the pieces are served from local nodes and 70% of pieces are downloaded from sources located in neighbouring nodes ($H=1$). This is due to uniform neighbourhood scanning as discussed above.

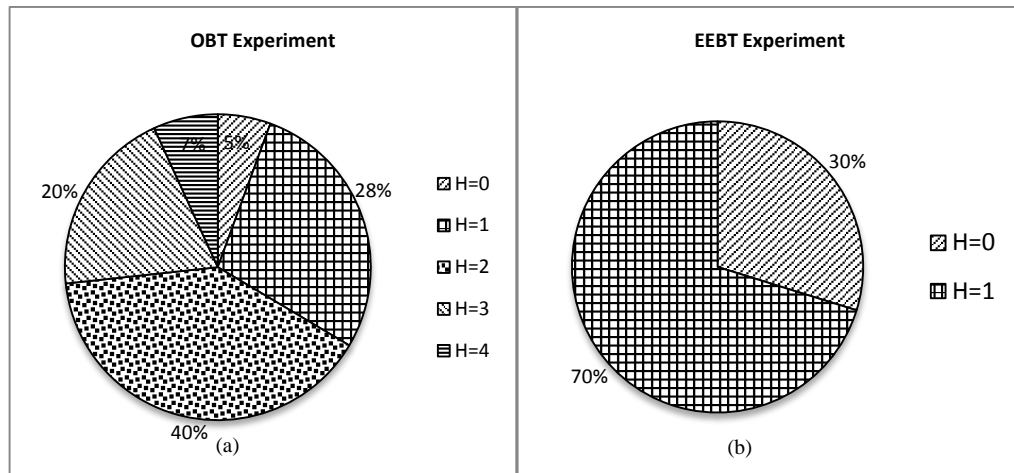


Fig. 3 - 31: Locality for experimental OBT and EEBT

3.12 Summary

In this chapter, we have investigated the power consumption of BitTorrent based P2P file sharing, and compared it to C/S systems. We developed a MILP model to minimise the power consumption of BitTorrent over IP/WDM networks while maintaining its performance. The results indicate that the original BitTorrent protocol, based on random peer selection, has comparable power consumption to the C/S system. The results also reveal that in order to achieve lower power consumption, the energy-efficient BitTorrent model converges to locality in peers selection, resulting in 30% and 36% energy consumption savings compared to the C/S system under the bypass and non-bypass IP/WDM routing approaches respectively. For real time implementation, a simple heuristic is developed based on the model insights. Comparable power savings are achieved with the heuristic with a penalty of 13% reduction in the average download rate. We extended the energy efficient BitTorrent heuristic enhancing its performance by allowing peers to progressively traverse more hops in the network if the number of peers in the local node is not sufficient. Furthermore, a heterogeneous BitTorrent system with two

upload capacity classes is investigated and the results show a 50% reduction in energy consumption compared to a C/S model.

We analysed the energy consumption of BitTorrent considering different peers behaviour scenarios. We showed, by mathematical modelling and simulation, that leechers can cause high network energy consumption if they leave the network after finishing downloading. We introduced the concept of operator controlled seeders (OCSs) to compensate for the negative impact of leechers departure on network energy consumption. The model was extended to optimise the location as well as the upload rates of OCSs to mitigate the performance degradation caused by leechers leaving after finishing the downloading operation.

We have compared the energy consumption of the energy efficient BitTorrent protocol to that of the original BitTorrent protocol and the C/S schemes over bypass IP/WDM networks considering a range of network topologies with different number of nodes and average hop counts. Our results show that for a given swarm size, the energy efficient BitTorrent protocol achieves higher power savings in networks with lower number of nodes as the opportunity to localise traffic increases.

We also compared the power consumption of VoD services delivered using CDN, P2P and a promising hybrid CDN-P2P architecture over bypass IP/WDM core networks. A MILP model was developed to carry out the comparison. We investigated two scenarios for the hybrid CDN-P2P architecture: the H-MinNPC model where the model minimises the IP/WDM network power consumption and the H-MinTPC model where the model minimises the total power consumption including the network and the CDN data centres power consumption.

Finally we carried out an experimental evaluation of the original and energy efficient BitTorrent heuristics. The results show the feasibility to save an average of 40% of IP/WDM network power consumption given our input parameters and swarms distribution in the experiment.

Chapter 4: Energy Efficient Content Distribution in Distributed Clouds over Optical Core Networks

4.1 Introduction

Clouds' dynamic management of physical resources paves the way toward energy efficient internal capability design in parallel with the external networking changing environment. In this chapter we develop a MILP model to study the energy efficiency of cloud content delivery in IP/WDM networks for two different content sizes and compare the results. The model is validated by developing a real time heuristic to design distributed clouds networks tailored for content distribution and subject to content popularity and traffic demands. The heuristic results are compared to the model results in terms of execution time and accuracy. We also study a variant of content delivery in the cloud, Storage as a Service (StaaS), where content access frequency rather than content popularity characterises the service. Again we study and compare the StaaS model results for two different content sizes.

4.2 MILP for Cloud Content Delivery

In this section we introduce the MILP model developed to minimise the power consumption of the cloud content delivery service over non-bypass IP/WDM networks. Given the client requests, the model responds by selecting the optimum number of clouds and their locations in the network as well as the capability of each

cloud so that the total power consumption is minimised. The model also decides how to replicate content in the cloud according to its popularity so the minimum power possible is consumed in delivering content.

We assume the popularity of the different objects of the content follows a Zipf distribution. Zipf is chosen as a representative of the popularity distribution of several cloud content types such as YouTube and others [107] where the popularity of an object of rank i is given as follows:

$$P(i) = \varphi/i$$

where $P(i)$ is the relative popularity of the object of rank i and φ is:

$$\varphi = \left(\sum_{i=1}^N \frac{1}{i} \right)^{-1}.$$

We divide the content in our model into equally sized popularity groups. A popularity group contains objects of similar popularity.

For the IP/WDM network, we use the same sets, parameters and variables defined in Section 3.2, plus the following:

Parameters:

| | |
|------------|---|
| PUE_n | IP/WDM network power usage effectiveness |
| M | A large enough number |
| Δt | Time granularity, which represents the evaluation period. |

The content delivery cloud is represented by the following sets, variables and parameters:

Sets:

| | |
|-------|---|
| U_d | Set of users in node d |
| PG | Set of popularity groups, $\{1 \dots PGN\}$ |

Parameters:

| | |
|------------|--|
| $ PG $ | Number of popularity groups |
| PUE_c | Cloud power usage effectiveness |
| S_{PC} | Storage power consumption |
| S_C | Storage capacity of one storage rack in GB |
| Red | Storage and switching redundancy |
| S_{PPGB} | Storage power consumption per GB, $S_{PPGB} = S_{PC}/S_C$ |
| S_{Utl} | Storage utilisation |
| PGS_p | Popularity group storage size, $PGS_p = (S_C/ PG) \cdot S_{Utl}$ |
| CS_C | Content server capacity |
| CS_{EPB} | Content server energy per bit |
| Sw_{PC} | Cloud switch power consumption |
| Sw_C | Cloud switch capacity |
| Sw_{EPB} | Cloud switch energy per bit, $Sw_{EPB} = Sw_{PC}/Sw_C$ |
| R_{PC} | Cloud router power consumption |
| R_C | Cloud router capacity |
| R_{EPB} | Cloud router energy per bit, $R_{EPB} = R_{PC}/R_C$ |
| $Drate$ | Average user download rate |
| P_p | Popularity of object p (Zipf distribution) |
| ND_d | Node d total traffic demand, $ND_d = \sum_{i \in U_d} Drate$ |
| D_{pd} | Popularity group p traffic to node d , $D_{pd} = ND_d \cdot P_p$ |

Variables (All are non-negative real numbers)

| | |
|----------------|--|
| δ_{sdp} | $\delta_{sdp} = 1$ if popularity group p is placed in node s to serve users in node d , $\delta_{sdp} = 0$ otherwise |
| L_{sdp} | Traffic generated due to placing popularity group p in node s to serve users in node d |
| L_{sd} | Traffic from cloud s to users in node d |
| Cup_s | Cloud s upload capacity |
| δ_{sp} | $\delta_{sp} = 1$ if cloud s stores a copy of popularity group p , $\delta_{sp} = 0$ otherwise |
| $Cloud_s$ | $Cloud_s = 1$ if a cloud is built in node s , $Cloud_s = 0$ otherwise. |
| CN | Number of clouds in the network |
| CSN_s | Number of content servers in cloud s |
| SwN_s | Number of switches in cloud s |
| RN_s | Number of routers in cloud s |
| $StrC_s$ | Cloud s storage capacity |

The cloud power consumption is composed of:

- 1) The power consumption of content servers ($SrvPC_{CD}$):

$$\sum_{s \in N} Cup_s \cdot CS_{EPB}$$

- 2) The power consumption of switches and routers ($LANPC_{CD}$):

$$\sum_{s \in N} Cup_s \cdot (Sw_{EPB} \cdot Red + R_{EPB})$$

- 3) The power consumption of storage ($StPC_{CD}$):

$$\sum_{s \in N} StrC_s \cdot S_PPGB \cdot Red$$

The model is defined as follows:

Objective: Minimise

$$\begin{aligned}
& PUE_n \cdot \left(\sum_{i \in N} Prp \cdot Q_i + Prp \cdot \sum_{m \in N} \sum_{n \in Nm_m} W_{mn} + \right. \\
& \quad \sum_{m \in N} \sum_{n \in Nm_m} Pt \cdot W_{mn} + \\
& \quad \sum_{m \in N} \sum_{n \in Nm_m} Pe \cdot A_{mn} \cdot F_{mn} + \\
& \quad \left. \sum_{i \in N} PO_i + \sum_{m \in N} \sum_{n \in Nm_m} Pmd \cdot F_{mn} \right) + \\
& PUE_c \cdot \left(\sum_{s \in N} Cup_s \cdot CS_EPB + \right. \\
& \quad \sum_{s \in N} Cup_s \cdot (Sw_EPB \cdot Red + R_EPB) + \\
& \quad \left. \sum_{s \in N} StrC_s \cdot S_PPGB \cdot Red \right)
\end{aligned} \tag{4-1}$$

Equation (4-1) gives the model objective which is to minimise the IP/WDM network power consumption and the cloud power consumption.

Subject to:

1) *IP/WDM network traffic*

$$\begin{aligned}
\sum_{j \in N: i \neq j} L_{ij}^{sd} - \sum_{j \in N: i \neq j} L_{ji}^{sd} &= \begin{cases} L_{sd} & \text{if } i = s \\ -L_{sd} & \text{if } i = d \\ 0 & \text{otherwise} \end{cases} \\
\forall s, d, i \in N: s \neq d, &
\end{aligned} \tag{4-2}$$

$$\begin{aligned}
\sum_{s \in N} \sum_{d \in N: s \neq d} L_{ij}^{sd} &\leq C_{ij} \cdot B \\
\forall i, j \in N: i \neq j, &
\end{aligned} \tag{4-3}$$

$$\begin{aligned}
\sum_{n \in Nm_m} W_{mn}^{ij} - \sum_{n \in Nm_m} W_{nm}^{ij} &= \begin{cases} C_{ij} & \text{if } m = i \\ -C_{ij} & \text{if } m = j \\ 0 & \text{otherwise} \end{cases} \\
\forall i, j, m \in N: i \neq j, &
\end{aligned} \tag{4-4}$$

$$\sum_{i \in N} \sum_{j \in N: i \neq j} W_{mn}^{ij} \leq W \cdot F_{mn} \quad (4-5)$$

$$\forall m \in N \quad \forall n \in Nm_m,$$

$$\sum_{i \in N} \sum_{j \in N: i \neq j} W_{mn}^{ij} = W_{mn} \quad (4-6)$$

$$\forall m \in N \quad \forall n \in Nm_m,$$

$$Q_i = 1/B \cdot \sum_{d \in N: i \neq d} L_{id} \quad (4-7)$$

$$\forall i \in N,$$

$$L_{sdp} = \delta_{sdp} \cdot D_{pd} \quad (4-8)$$

$$\forall s, d \in N \quad \forall p \in PG,$$

$$\sum_{s \in N} L_{sdp} = D_{pd} \quad (4-9)$$

$$\forall d \in N \quad \forall p \in PG,$$

$$L_{sd} = \sum_{p \in PG} L_{sdp} \quad (4-10)$$

$$\forall s, d \in N,$$

$$Cup_s = \sum_{d \in N} L_{sd} \quad (4-11)$$

$$\forall s \in N,$$

For the sake of completeness and clarity, we re-introduce IP/WDM flow and capacity constraints, constraints (4-2)-(4-7), in order to refer to them appropriately when needed in this chapter.

Constraint (4-8) calculates the traffic generated in the IP/WDM network due to requesting popularity group p that is placed in node s by users located in node d . Constraint (4-9) ensures that each popularity group request is served from a single cloud only. We have not included traffic bifurcation where a user may get parts of the content from different clouds. Constraint (4-10) calculates the traffic from the cloud in node s and users in node d , to be used in constraints (4-2) and (4-7). Constraint (4-11) calculates each cloud upload capacity based on total traffic sent from the cloud.

2) *Popularity groups and clouds locations:*

$$\sum_{d \in N} \delta_{sdp} \geq \delta_{sp} \quad (4-12)$$

$$\forall s \in N \forall p \in PG,$$

$$\sum_{d \in N} \delta_{sdp} \leq M \cdot \delta_{sp} \quad (4-13)$$

$$\forall s \in N \forall p \in PG,$$

$$\sum_{p \in PG} \delta_{sp} \geq Cloud_s \quad (4-14)$$

$$\forall s \in N,$$

$$\sum_{p \in PG} \delta_{sp} \leq M \cdot Cloud_s \quad (4-15)$$

$$\forall s \in N,$$

$$CN = \sum_{s \in N} Cloud_s, \quad (4-16)$$

Constraints (4-12) and (4-13) ensure that popularity group p is replicated to cloud s if cloud s is serving requests for this popularity group, where M is a large enough unitless number to ensure that $\delta_{sp} = 1$ when $\sum_{d \in N} \delta_{sdp}$ is greater than zero. Constraints (4-14) and (4-15) build a cloud in location s if that location is chosen to store at least one popularity group or more, where M is a large enough unitless number to ensure that $Cloud_s = 1$ when $\sum_{p \in PG} \delta_{sp}$ is greater than zero. Constraint (4-16) calculates total number of clouds in the network.

3) *Cloud Capability*

$$CSN_s = Cup_s / CS_C \quad (4-17)$$

$$\forall s \in N,$$

$$SwN_s = (Cup_s / Sw_C) \cdot Red \quad (4-18)$$

$$\forall s \in N,$$

$$RN_s = Cup_s / R_C \quad (4-19)$$

$$\forall s \in N,$$

$$StrC_s = \sum_{p \in PG} \delta_{sp} \cdot PGS_p \quad (4-20)$$

$$\forall s \in N.$$

Constraints (4-17)-(4-19) calculate the number of content servers, switches and routers required at each cloud based on cloud upload traffic going through these elements. The integer value is obtained using the ceiling function. Note that the number of switches (SwN_s) is calculated considering redundancy. Constraint (4-20) calculates the storage capacity needed in each cloud based on the number of replicated popularity groups.

We use relaxation in our model due to the large number of variables. However, as we are interested in power consumption, relaxation has a limited impact on the final result as the difference will be within the power of less than one wavelength (router port and transponder) which is negligible compared to the total power consumption. The heuristics which produce comparable results provide independent verification for the model (and its relaxation), especially that the routing and placements in the heuristics follow approaches that are independent of the model.

4.3 MILP Model Results

The NSFNET network, depicted in Fig. 3 - 1, is considered as an example network to evaluate the power consumption of the cloud content delivery service over IP/WDM networks. In this work the network is designed considering the peak traffic to determine the maximum resources needed. However we still run the model considering varying levels of traffic throughout the day to optimally replicate content as the traffic varies to obtain the minimum power consumption. One point in the operational cycle (the point that corresponds to the peak demand) is strict network design where the maximum resources needed are determined. At every other point the optimisation is a form of adaptation where resources lower than the maximum are determined and used to meet the demand. In our evaluation users are uniformly distributed among the NSFNET nodes and the total number of users in the network fluctuates throughout the day between 200k and 1200k as shown in Fig. 4 - 1. The values in Fig. 4 - 1 are estimated, based on the data in [21]. The number of users throughout the day considers the different time zones within the US [21]. The reference time zone in Fig. 4 - 1 is EST. We use the model to evaluate the power consumption associated with the varying number of users at the different times of the day, with a two hour granularity.

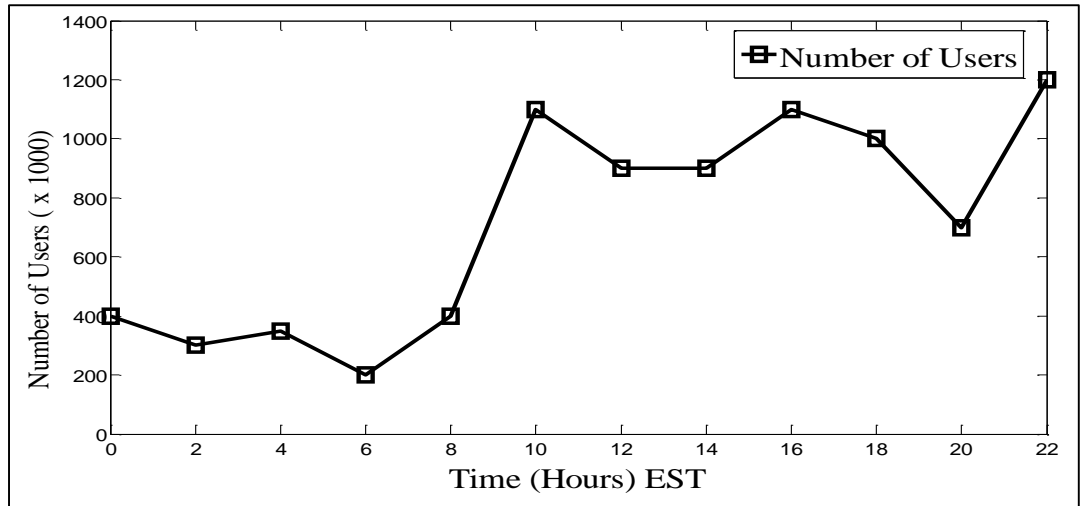


Fig. 4 - 1: Number of users versus time of the day

Table 4 - 1 gives the input parameters of the model. IP/WDM network input data are the same as those reported in Table 3 - 1.

| | |
|--|--------------------|
| Average client download rate ($Drate$) | 5 Mbps [108] |
| Content server capacity (CS_C) | 1.8 Gbps [109] |
| Content server energy per bit (CS_{EPB}) | 211.1 W/Gbps [109] |
| Storage power consumption (S_{PC}) | 4.9 kW [59] |
| Storage capacity (S_C) | 75.6 *5 TB [59] |
| Storage utilisation (S_{Utl}) | 50% |
| Storage and switching redundancy (Red) | 2 |
| Cloud switch power consumption (Sw_{PC}) | 3.8 kW [59] |
| Cloud switch capacity (Sw_C) | 320 Gbps [59] |
| Cloud router power consumption (R_{PC}) | 5.1 kW [59] |
| Cloud router capacity (R_C) | 660 Gbps [59] |
| Cloud power usage effectiveness (PUE_c) | 2.5 |
| IP/WDM network power usage effectiveness (PUE_n) | 1.5 |
| Number of popularity groups (PGN) | 50 |
| Popularity group size (PGS_p) | 0.756 TB |
| Time granularity (Δt) | 2 Hours |

Table 4 - 1: Input data for the clouds models

The energy per bit (EPB) in the table is capacity based as we base it on the maximum power and maximum rate of the server. However note that the model always attempts to fully utilise servers, see constraint (4-17), and switches off unused servers to minimise power consumption. The combination of these two operational factors results in EPB based on capacity being a good representation. The 5 Mbps average download rate is based on the results of a survey conducted in the US in 2011 [108].

A typical Telecom office PUE is 1.5 [59]. Typical data centres PUE varies widely between 1.1 for large data centres able to implement sophisticated water cooling [110] to small data centres with PUE as high as 3 [111]. We have adopted a PUE of 2.5 in this study for the small distributed clouds considered.

We divide the cloud content into 50 popularity groups, which is a reasonable compromise between granularity and MILP model execution time. Note also that distributing the content into multiple locations does not increase the power consumption of the cloud, i.e. the power consumption of a single cloud with all the content is equal to the total power consumption of multiple distributed clouds storing the same content without replication. The reason is that each server has an idle power; however it is either switched on (and through packing is operated near maximum capacity) if needed or switched off. The cloud is made up of a large number of servers (200 for example, see Fig. 4 - 7). The cloud power consumption therefore increases with good granularity in steps equal to the power consumption of a single server. This leads to a staircase (with sloping stairs) profile of power versus load and with the very large number of steps, the profile is almost linear. This form of power management means that placing a given piece of content in different clouds amounts to the same power consumption approximately.

We also assume similar type of equipment and PUE, hence we do not assume a fixed power component associated with placing a cloud in certain location. We also assume that underutilised storage units, switches, and routers) in the cloud are switched off or put in low power sleep mode. Note that savings are averaged over the 12 time points of the day (24 hours). The metrics used are average savings over 24 hours. These are the average network power saving, average cloud power saving and average total power saving.

Note that the variables specified above (with the exception of binary variables) take values that are dictated by the number of users, their data rates, content popularity and scenario considered.

We compare the following different delivery scenario:

- **Single Cloud:** Users are served by single cloud optimally located at node 6 as it yields the minimum average hop count. This scenario is obtained by setting the total number of clouds to 1, i.e. Constraint (4-16) becomes:

$$CN = \sum_{s \in N} Cloud_s = 1.$$

We consider two schemes in this scenario:

- **No Power Management (SNPM):** The cloud and the network are energy inefficient where different components are assumed to consume 80% of their maximum power consumption at idle state.
- **Power Management (SPM):** The cloud and the network are energy efficient where underutilised components are powered off or put into deep sleep at off-peak periods.
- **Max number of clouds with power management:** A cloud is located at each node in the network, i.e. the network contains 14 clouds. In this case the total number of clouds is set to 14, i.e. Constraint (4-16) becomes:

$$CN = \sum_{s \in N} Cloud_s = 14.$$

We consider three schemes in this scenario:

- **Full Replication (MFR):** Users at each node are served by a local cloud with a full copy of the content. This scheme is obtained by setting the number of popularity groups to 1, i.e. $|PG| = 1$.
- **No Replication (MNR):** The content is distributed among all the 14 clouds without replication. This scheme is obtained by ensuring that the

total number of replicas (δ_{sp}) does not exceed the original number of popularity groups ($|PG|$):

$$\sum_{p \in PG} \sum_{s \in N} \delta_{sp} = |PG|.$$

- **Popularity Based Replication (MPR):** The model optimises the number and locations of content replicas among all the 14 clouds based on content popularity.
- **Optimal number of clouds with power management:** The number and location of clouds are optimised.

We consider three schemes in this scenario:

- **Full Replication (OFR):** Each cloud has a full copy of the content. This scheme is obtained by setting $|PG| = 1$.
- **No Replication (ONR):** Content is distributed among the optimum clouds without replication. This scheme is obtained by setting:

$$\sum_{p \in PG} \sum_{s \in N} \delta_{sp} = |PG|.$$

- **Popularity Based Replication (OPR):** The number and locations of content replicas are optimised based on content popularity.

In the following subsections we compare the energy efficiency of the different delivery schemes discussed above considering two popularity group sizes ($PGS_p = 3.78 \text{ TB}$) and ($PGS_p = 0.756 \text{ TB}$). The size of the popularity group reflects the type of data stored in the cloud.

4.3.1 Popularity Group Size $PGS_p = 3.78 \text{ TB}$

Fig. 4 - 2(a) shows the total power consumption of the different content delivery schemes while Fig. 4 - 2(b) and Fig. 4 - 2(c) decompose it into its two components: IP/WDM network power consumption and cloud power consumption, respectively.

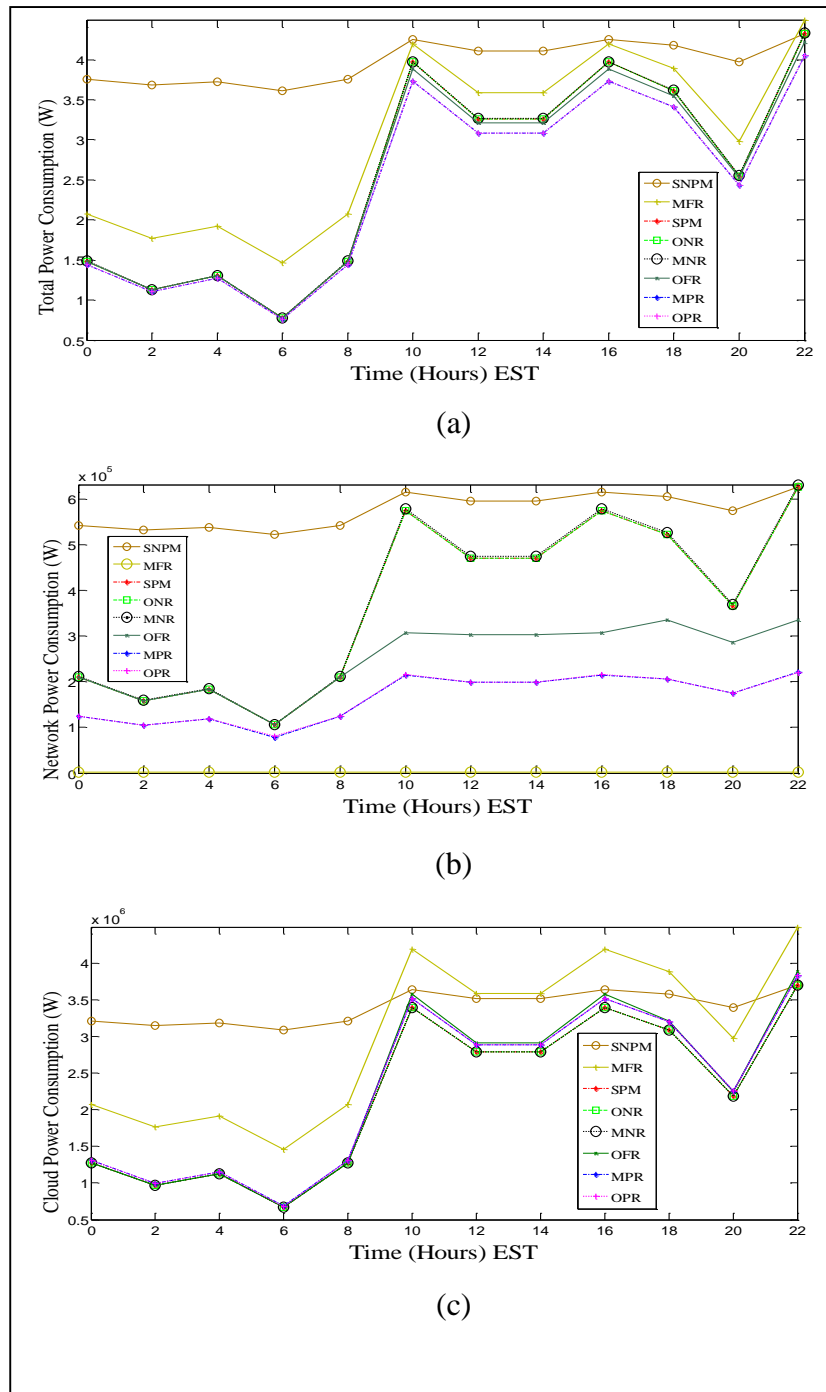


Fig. 4 - 2: $PGS_p = 3.78TB$ (a) Total power consumption (b) IP/WDM power network consumption (c) Cloud power consumption

The SNPM scheme, where all content is placed in a single cloud, results in the highest total power consumption as all the resources are switched on even at off-peak periods where idle power consumption contributes 80% of the total power consumption. Therefore, the small variation in SNPM power consumption throughout the day is due to the 20% load induced power consumption. We use SNPM as our benchmark to calculate the power savings achieved by the other

schemes. The optimal location of the single cloud is selected based on network and cloud power consumption minimisation using our MILP. Node 6 is the optimum location that minimises power consumption based on MILP. It yields the minimum average hop count which is a good choice for power minimisation given that the traffic is uniformly distributed among the nodes. Note that this choice of the reference case is conservative. We could have chosen the reference case as a single cloud, but optimally placed to minimise delay or network CAPEX as is currently done, in which case the energy savings as a result of our work will be higher. The power awareness of the SPM scheme saves 37% and 36.5% of the network and cloud power consumption, respectively, compared to the SNPM scheme.

We also investigate the other extreme scenario represented by the MFR scheme where content is fully replicated into all possible locations (14 nodes of the NSFNET). At the network side (Fig. 4 - 2(b)), the MFR saves 99.5% of the network power consumption as all requests generated in a node are served locally. The other 0.5% of the power consumption is associated with the optical switch as discussed in Fig. 2 - 2. However, having a cloud with full content at each node significantly increases the cloud power consumption due to storage requirements as shown in (Fig. 4 - 2(c)), reducing the total power savings to 25.5%. Therefore the MFR scheme is not efficient if storage power consumption continues to dominate the power consumption of data centres.

Despite their different approaches in optimising content delivery, the MNR, ONR and SPM schemes have similar total power consumption. In terms of the cloud power consumption, the three schemes produce the lowest power consumption as content is not replicated and as mentioned above distributing the content into multiple locations does not increase the power consumption. In the following we discuss the network power consumption of the different schemes.

The ONR scheme finds the optimal number of clouds required to serve all users from a single copy of the content, where different popularity groups are migrated to different clouds based on their popularity. However, our results show that the ONR scheme selects to serve users using a single cloud located at node 6, i.e. ONR imitates the SPM scheme. This is because distributing the content into multiple clouds without replicating it results in higher network power consumption. For instance, if the ONR model decides to build two clouds one at node 1 (far left end of

NSFNET) and the other at node 12 (far right end of NSFNET), then users at nodes located at the left end of the network will have to cross all the way to the right end of the network to download some of their content from the cloud at node 12 as we do not allow this content to be replicated into the cloud in node 1, and vice versa for users located at nodes at the right end of the network asking for content only available at node 1. However, if all popularity groups are kept in node 6 which is the node that yields the minimum average hop count to different nodes in the network (this will be proven later in Section 4.4), then the power consumed in the network to download content will be minimised, resulting in 36.5% and 37% saving in total and network power consumption, respectively compared to SNPM, similar to SPM.

The main insight of the ONR model is that energy efficient content delivery prioritises single cloud solutions over distributed solutions if content is not allowed to be replicated, the content has similar popularity at every node, and we were free to choose the number of clouds. This raises the question of how should we replicate content in a scenario of more than one cloud. The extreme of such a scenario is represented by the MNR where each node in the network contains a cloud. To create a cloud in a certain location, an object should be migrated into that location. However, as discussed earlier migrating content into multiple clouds without replication results in high power consumption in the network. The MNR scheme selects to place content in agreement with the insights of the ONR scheme, where most of the content is located in node 6, while migrating only the least popular objects, associated with the lowest network power consumption, into other nodes. This placement strategy meets the MNR scheme constraints and at the same time minimises the network power consumption needed to access content. The MNR network power consumption slightly deviates from the ONR network power consumption as the least popular contents are not served from the cloud in node 6. The MNR scheme, however maintains the total power saving achieved by the ONR scheme, i.e. 36.5% compared to the SNPM scheme.

As already observed, serving content locally by enforcing replication in all the 14 locations (MFR scheme) yields the highest cloud power consumption and the lowest network power consumption. In the OFR scheme we investigated the impact of removing the constraint on the number of clouds; so the MILP model is free to choose the optimal number of clouds that have a full copy of the content. The OFR

scheme manages to reduce the total number of clouds from 14 to 7. These clouds are switched on and off according to the traffic variation as seen in Fig. 4 - 3. Note that only 4 of these clouds are switched on at the same time of the day. OFR achieves significant power savings at the network side of 56.5% compared to the SNPM scheme, a saving higher than what is achieved by The SPM, ONR and MNR as the content is fully replicated to optimally located clouds. Deploying fewer clouds also increases the total power saving compared to the MFR scheme, resulting in a total saving of 37.5% compared to SNPM scheme.

In spite of deploying multiple clouds in the network, the OFR scheme has increased the total power saving compared to the SPM and ONR schemes where a single cloud is deployed. This is because the network power savings compensate for the increase in cloud power.

From the discussion above we can see that the savings achieved by the OFR scheme are limited by the constraint on the content replication granularity where all content is replicated to a certain location if a cloud is created in that location. The question raised next is how much can the limits of power saving be pushed if the constraints on both the number of clouds and content replicated at each cloud are removed. This approach is implemented by the OPR scheme. The results in Fig. 4 - 2 indicate that the OPR scheme is the most optimum scheme.

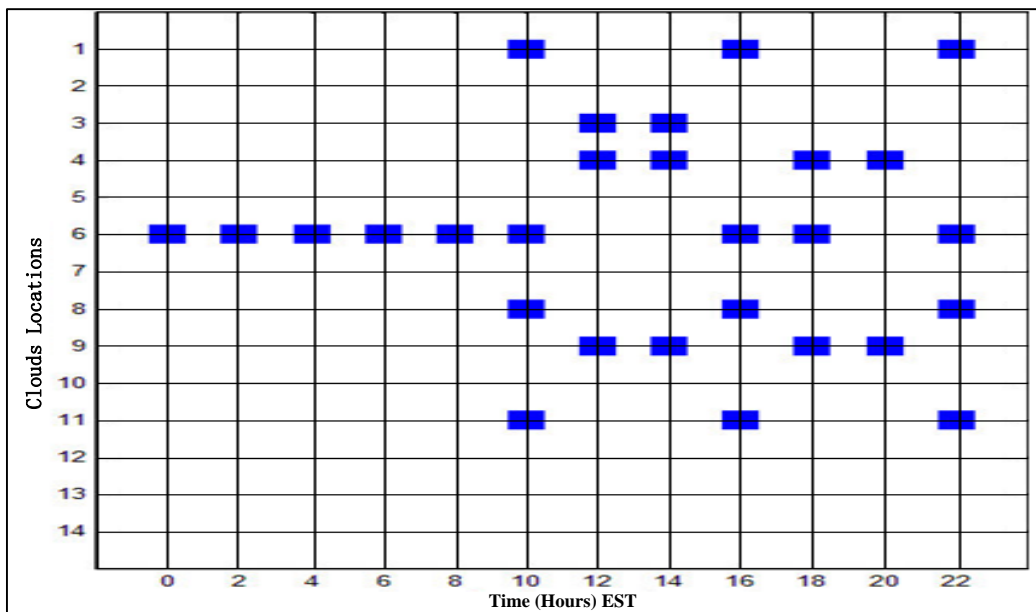


Fig. 4 - 3: OFR powered on clouds at different times of the day ($PGS_p = 3.78 TB$)

OPR saves 72% of the network power consumption and 40% of the total power consumption compared to SNPM. Compared to SPM, the savings are reduced to 49% and 4% of the network and total power consumption, respectively. Unlike the OFR scheme, OPR can build more clouds as the cost of storage is minimised by optimising the content of each cloud based on the content popularity, resulting in a network power saving of 34% and a total power saving of 3% compared to the OFR scheme.

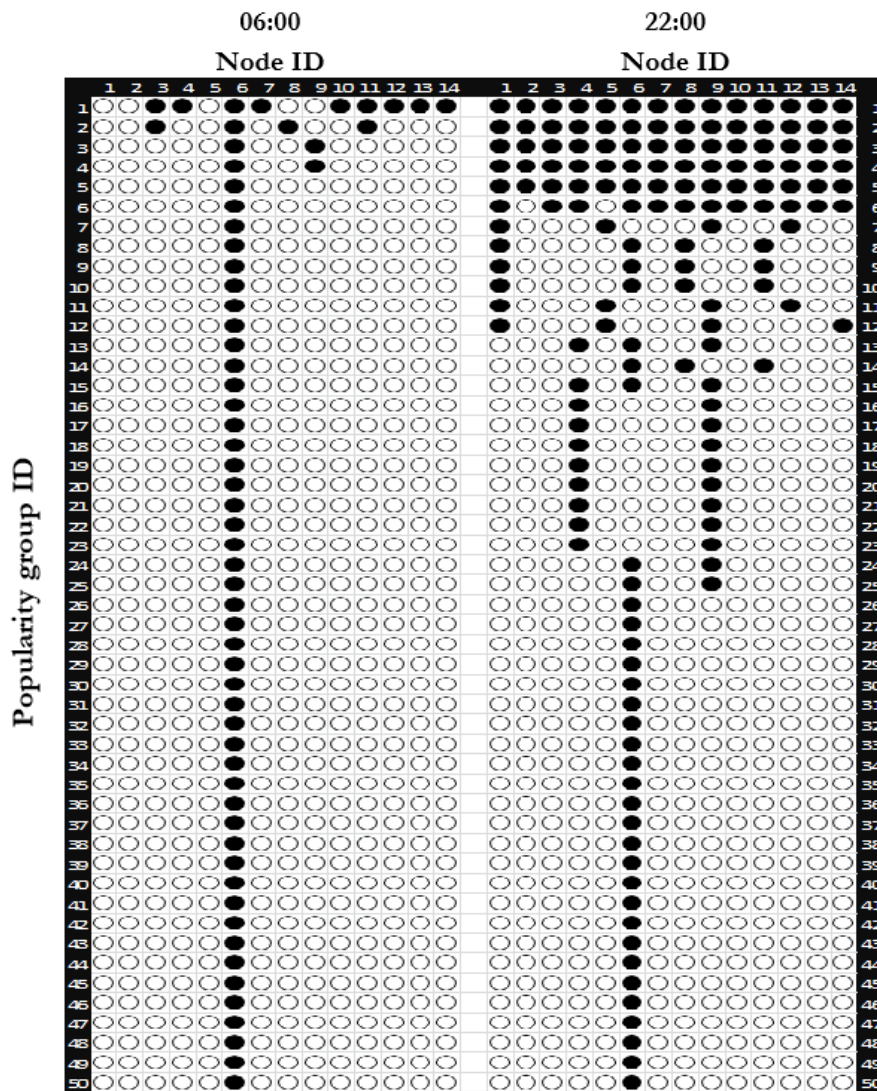


Fig. 4 - 4 Popularity groups placement under the OPR scheme at 06:00 and 22:00 ($PGS_p = 3.78 TB$)

Fig. 4 - 4 shows how the OPR scheme replicates the content at two times of the day, 06:00 (left half of Fig. 4 - 4) and 22:00 (right half of Fig. 4 - 4), which correspond to the lowest and highest load demands, respectively. As the popularity

of the content increases (popularity group 1 is the most popular), it will be replicated (black circle) to more clouds as this will result in serving more requests locally and therefore reducing the network power consumption. At 06:00, most of the content is kept in node 6, while at 22:00, more popularity groups are replicated into more clouds as under higher loads the power consumption of the cloud is compensated by higher savings in the network side.

As content is equally popular among all users and users are uniformly distributed among nodes, OPR will replicate the most popular content into all the 14 nodes most of the day. Therefore OPR has similar power efficiency compared to MPR where content is optimally replicated among all the 14 clouds based on its popularity. However, under a scenario with a non-uniform user distribution, OPR might outperform MPR as it might not be necessary to build 14 clouds.

Fig. 4 - 5 shows the total number of replicas per popularity group for the OPR scheme, obtained by summing the black circles for each popularity group in Fig. 4 - 4. Note that the distribution of the number of replicas follows a Zipf replication at both low and high demand periods.

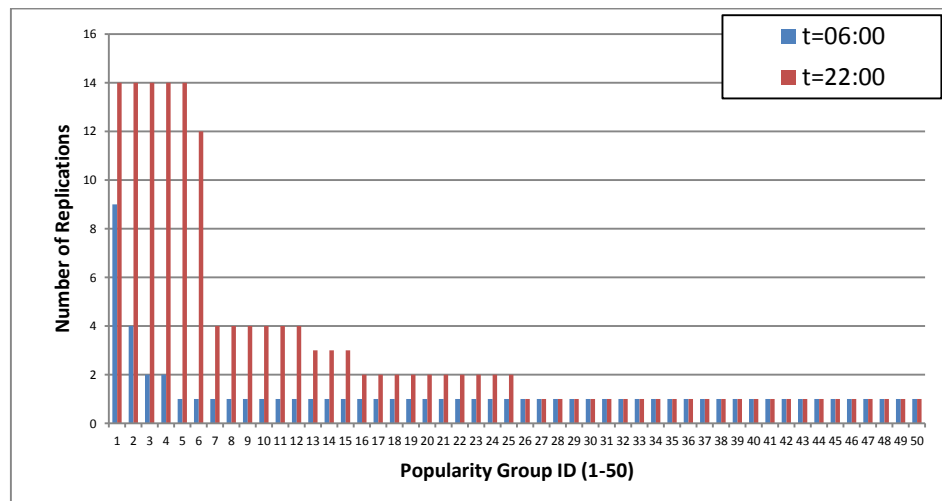


Fig. 4 - 5: Total number of replicas per popularity group under the OPR scheme ($PGS_p = 3.78 TB$)

Fig. 4 - 6 shows the total number of popularity groups replicated at each cloud, obtained by summing the black circles in Fig. 4 - 4 for each cloud; i.e. Fig. 4 - 6 reflects the relative cloud size at each node. At low demand periods (06:00) most of the content is replicated to node 6 only, while at peak period (time 22:00) fewer

popularity groups are replicated to node 6 as the high network power savings at peak period justify replicating the content to more clouds instead of having a single copy in a centralised node.

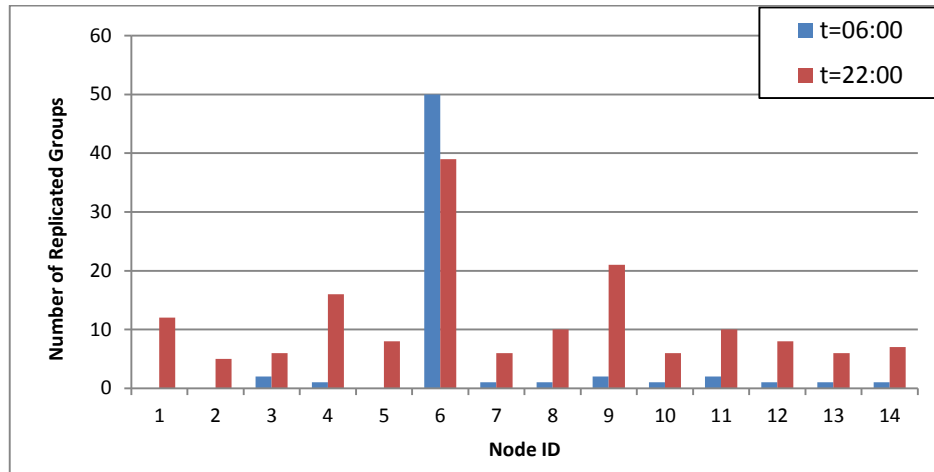


Fig. 4 - 6: Number of popularity groups replicated at each node under the OPR scheme ($PGS_p = 3.78 TB$)

Fig. 4 - 7 shows the number of servers powered on at each cloud at t=06:00 and t=22:00. The number of servers powered on at each cloud at a certain time is proportional to the size of content replicated to the cloud given in Fig. 4 - 6. Note that at node 6 more servers are powered on at t=22:00 compared to t=06:00 while less content is replicated to node 6 at t=22:00. This is because content is more frequently accessed at peak periods. Note that the number of switches and routers at each cloud follows a similar trend to that of the number of servers.

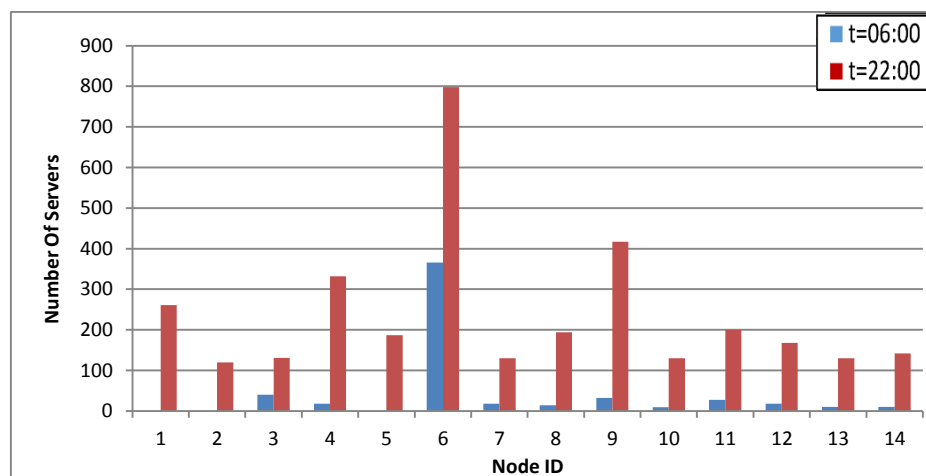


Fig. 4 - 7: Number of powered on servers in each cloud under the OPR scheme ($PGS_p = 3.78 TB$)

4.3.2 Popularity Group Size $PGS_p = 0.756$ TB

In this section we reduce the popularity group size to 20% of the size considered in the results of the previous section, i.e. $PGS_p = 0.756$ TB. A single download rate of 5 Mb/s is used for the two cases of file size. The two file sizes may for example correspond to two movies of different length and/or different resolution. At a constant user rate, the time taken to download the larger file (before playing in this case) is longer. The smaller popularity group size represents a cloud scenario where music, for instance, is more popular than movies. Fig. 4 - 8(a) shows the total power consumption of the different schemes while Fig. 4 - 8(b) and Fig. 4 - 8(c) show the network and cloud power consumptions, respectively.

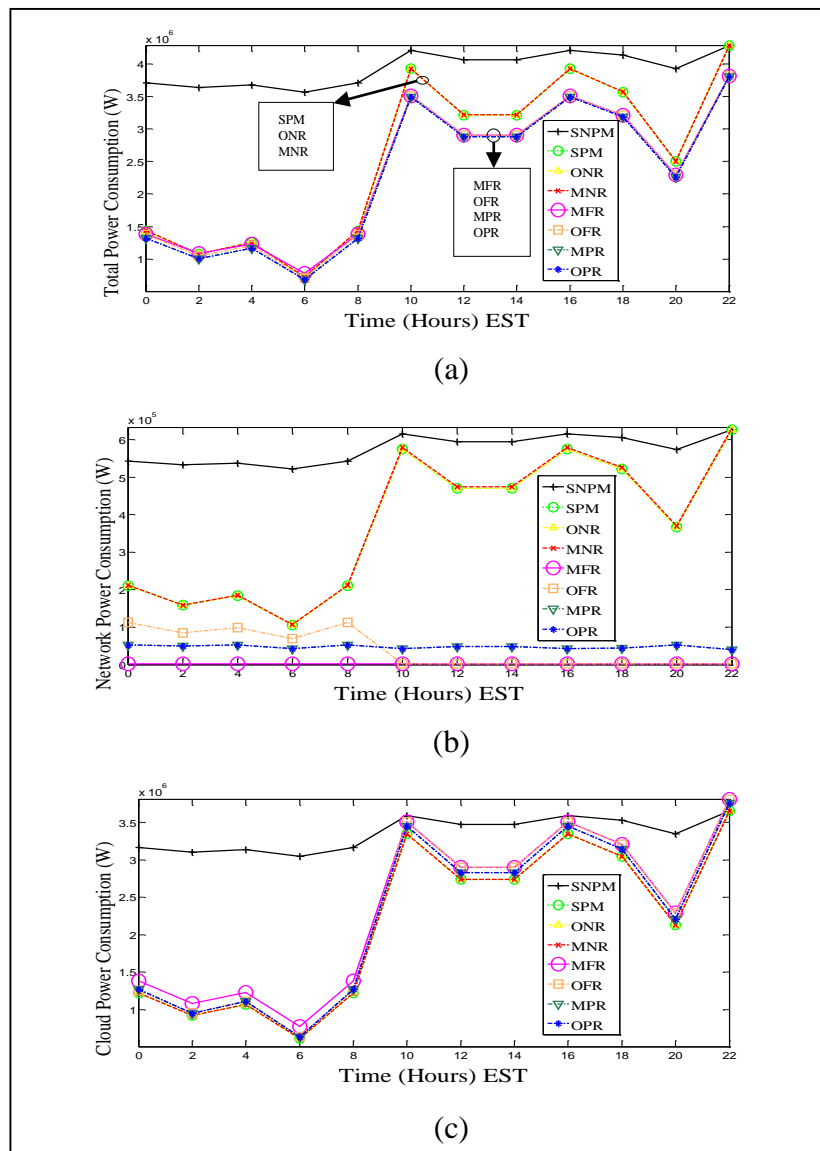


Fig. 4 - 8: $PGS_p = 0.756$ TB (a) Total power consumption (b) IP/WDM network power consumption (c) Cloud power consumption

ONR and MNR still follow the SPM scheme and centralise the content in one cloud at node 6, as observed in Section 4.3.1. Therefore centralising the content is the optimum solution if content is not allowed to be replicated regardless of content size. The ONR results in 37% saving in both total and network power consumption compared to SNPM, and similar to SPM. Similar to Section 4.3.1, the MNR network power consumption slightly deviates from the ONR network power consumption (36.5% rather than 37%) as the least popular contents are not served from the cloud in node 6. The MNR scheme, however maintains the total power saving achieved by the ONR scheme, i.e. 37% compared to the SNPM scheme.

The OFR scheme, Fig. 4 - 9, manages to reduce the total number of clouds from 14 to 6 at off-peak periods of the day (between 00:00 and 08:00). However, at peak periods (between 10:00 and 22:00) the OFR scheme converges to the MPR scheme and builds clouds at all nodes as the power saved in the network is higher than the power lost in storage replication. OFR achieves significant power savings at the network side of 92% compared to the SNPM scheme, higher than those observed in Section 4.3.1. Eventually, the OFR scheme increases the total power saving compared to the SPM, ONR and MNR schemes, where the cloud in node 6 is mainly used, from 37% to 42.5% compared to SNPM, which is also slightly higher saving compared to MFR scheme due to deploying fewer clouds at off-peak periods.

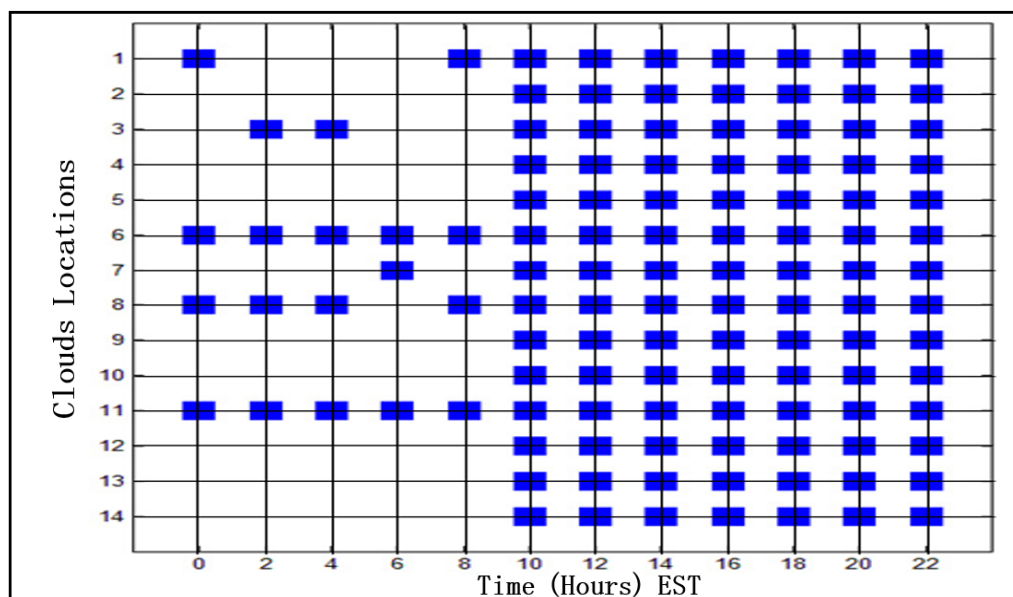


Fig. 4 - 9: OFR powered on clouds at different times of the day ($PGS_p = 0.756 TB$)

The OPR, MPR and OFR schemes in this case have similar power consumption to the MFR scheme (43% total power savings compared to SNPM) which implies that the three schemes tend to replicate the majority of the content in all the 14 clouds most of the time due to the small storage power cost as shown in Fig. 4 - 8(c).

Fig. 4 - 8(b) shows that the network power savings for the different models follow a similar trend to that in Fig. 4 - 8(a). At the network side, the OPR, MPR, OFR and MFR schemes save 92%-99.5% of the network power consumption compared to the SNPM scheme while the SPM, ONR and MNR schemes save 37% of the network power consumption.

Despite their similar average network power saving, OPR and OFR have different behaviour in saving power at the network side. OPR maintains the network power at the lowest level at all times by powering on the optimum number of clouds with the optimum content. However, OFR is less flexible as all the powered on clouds have to have a full copy of the content. Therefore OFR powers on only 4 clouds at low load and consumes higher network power while behaving as MFR and consuming power only in optical switches at high loads (10:00 to 22:00) by powering on 14 clouds (see Fig. 4 - 9) resulting in a daily average network power consumption similar to the OPR scheme.

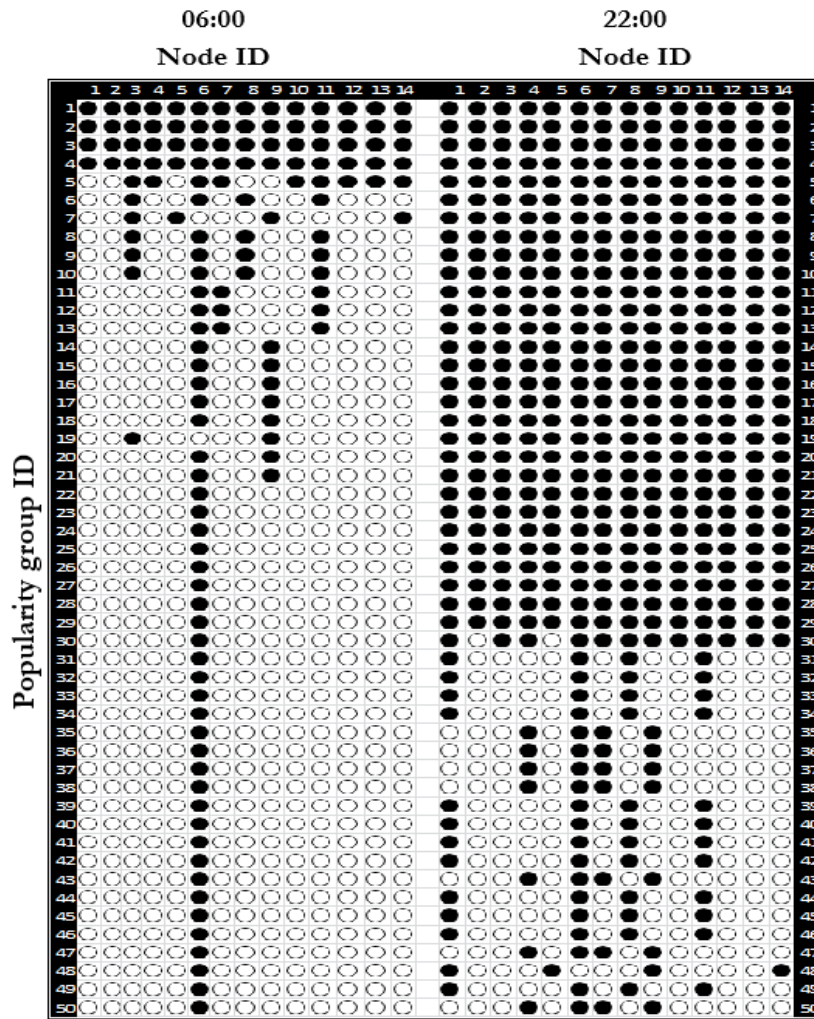


Fig. 4 - 10: Popularity groups placement under the OPR scheme at 06:00 and 22:00 ($PGS_p = 0.756 TB$)

Compared to the results of Section 4.3.1, Fig. 4 - 10 shows that OPR tends to replicate more content to more clouds due to lower power consumption of storage, especially that we fixed the average download rate at 5 Mbps. As content is equally popular among all users and users are uniformly distributed among nodes, OPR will replicate the most popular content into all the 14 nodes most of the day. Therefore OPR has similar power efficiency to MPR where content is optimally replicated among all the 14 clouds based on its popularity.

Fig. 4 - 11 shows the total number of replicas per popularity group for the OPR scheme. At low demand, the number of replications follows a Zipf distribution. However, at high demand (at 22:00), the scheme does not follow a Zipf distribution in replicating content as the high demand and the low power cost of storage allow the majority of the popularity groups to be replicated into all the nodes.

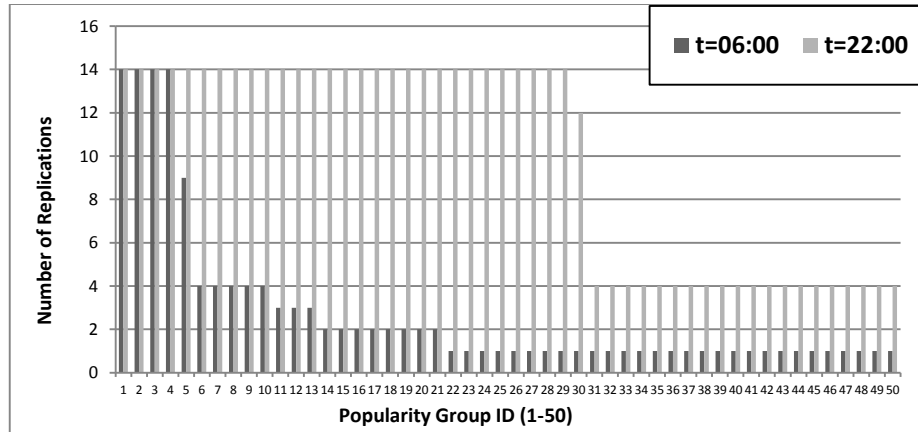


Fig. 4 - 11: Total number of replications per popularity group under the OPR scheme
(PGS_p = 0.756 TB)

Fig. 4 - 12 shows the total number of popularity groups replicated at each built cloud, Due to the low power cost of storage, content is replicated to more clouds at both high and low loads compared to the larger popularity group results in Section 4.3.1.

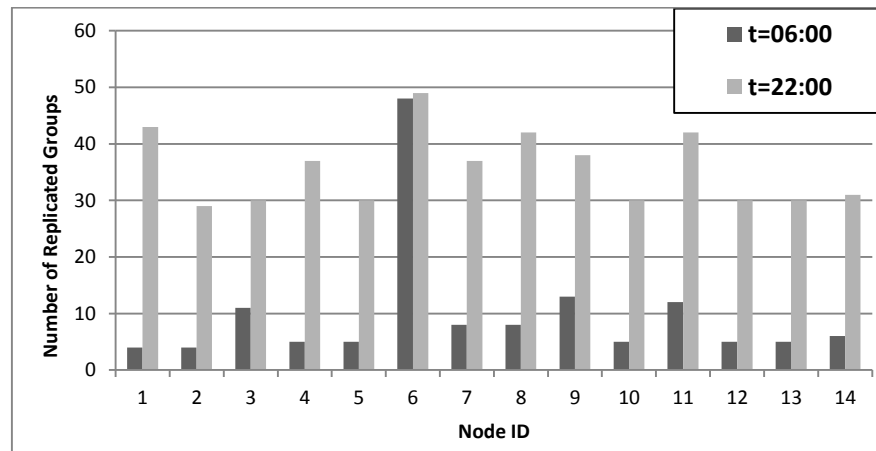


Fig. 4 - 12: Number of popularity groups replicated at each cloud under the OPR scheme
(PGS_p = 0.756 TB)

Fig. 4 - 13 shows the number of servers powered on at each cloud at t=06:00 and t=22:00. Fewer servers are powered on at node 6 at both times compared to the results of Section 4.3.1 as more requests are served from other clouds due to low storage cost. Note that the number of switches and routers at each cloud follows a similar trend to that of the number of servers.

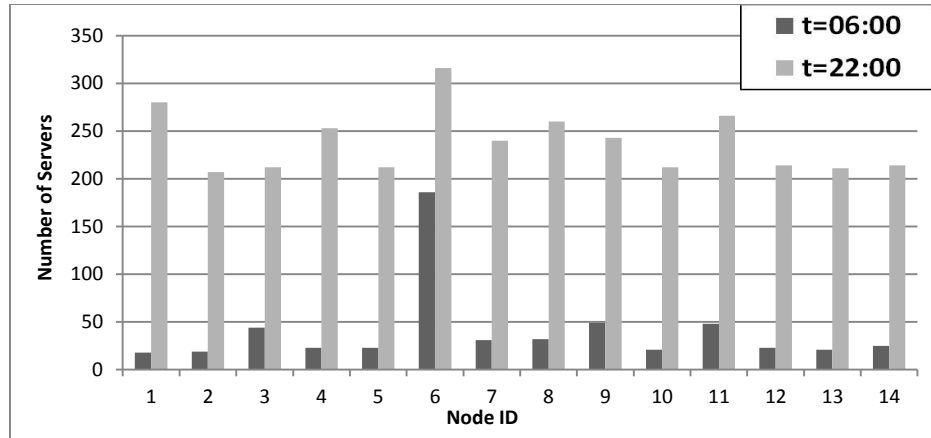


Fig. 4 - 13: Number of powered on servers in each cloud under the OPR scheme ($PGS_p = 0.756 TB$)

From the results above it is observed that OPR is always the best scenario for content delivery. OPR converges to a Single Cloud scenario for content of larger size at low demand periods while it fully replicates contents at all network locations for content of smaller size at high demand periods. OPR can be realised either by replicating popular content to the optimised locations and continuously replacing it as the popularity changes throughout the day; or by replicating all the content to all clouds and only switching on the hard disks storing the content with the highest popularity, selected by the MILP model at each location. The latter storage management approach saves power in the network side; however, it needs knowledge of content popularity to assign separate hard disks to different popularity groups. Table 4 - 2 summarises the power savings achieved by the different cloud content delivery approaches, for the two content sizes considered compared to the SNPM model.

| Scenario | $PGS_p = 3.78TB$ | | $PGS_p = 0.756TB$ | |
|------------|------------------|----------------|-------------------|----------------|
| | Total Saving | Network Saving | Total Saving | Network Saving |
| OPR | 40% | 72% | 43% | 92% |
| MPR | 40% | 72% | 43% | 92% |
| OFR | 37.5% | 56.5% | 42.5% | 92% |
| SPM | 36.5% | 37% | 37% | 37% |
| ONR | 36.5% | 37% | 37% | 37% |
| MNR | 36.4% | 36.5% | 37% | 36.5% |
| MFR | 25.5% | 99.5% | 42% | 99.5% |

Table 4 - 2: The power savings gained by the different content delivery clouds models compared to the SNPM model

4.4 DEER-CD: Energy Efficient Content Delivery Heuristic for the Cloud

As OPR is the most energy efficient scheme among the different schemes investigated in section 4.3, in this section we build a heuristic (Distributed Energy Efficient Resources – Content Delivery, DEER-CD) to mimic the OPR model behaviour in real time. We need to build a mechanism to allow the cloud management to react to the changing network load by replicating the proper content to the optimum locations rather than deciding an average replication scheme that might not fit well with different load patterns throughout the day. The DEER-CD heuristic involves two phases of operation:

1) Offline Phase: Each node in the network is assigned a weight based on the average number of hops between the node and the other nodes and the traffic generated by the node, i.e. the number of users in the node and their download rate. The weight of node s , NW_s , is given as:

$$NW_s = \sum_{d \in N} U_d \cdot D_{rate} \cdot H_{sd}. \quad (4-21)$$

where U_d is the number of users in node d and H_{sd} is the minimum number of hops between node pair (s, d) .

As the network power consumption is proportional to the amount of content transiting between nodes and the number of hops travelled by the content, nodes of lower weight are the optimum candidates to host a cloud. Equation (4-21) can be pre-calculated as it relies on information that rarely changes throughout the day such as the physical topology, average users population and download rate. We construct a sorted list of nodes from lowest to highest weight and use this list to make cloud placement decisions. In the absence of our sorted list approach, an exhaustive search is needed where a PG can be allocated to a single node leading to $|N|$ (number of nodes) combinations being evaluated for network energy efficiency. In addition the PG can be allocated to two nodes leading to the evaluation of $|N| \cdot (|N| - 1)$ combinations, and therefore in total this exhaustive search, which we totally avoid, requires $\sum_{i=1}^{|N|} \frac{|N|!}{(|N|-i)!}$ placement combinations to be assessed. Our sorted list reduces this search to the evaluation of $|N|$ combinations only. For NSFNET with $|N| = 14$,

this is a complexity reduction by a factor of 1.6×10^{10} . Furthermore using a 2.4 GHz Intel Core i5 PC with 4 GB Memory, the heuristic took 1.5 minutes to evaluate the DEER-CD results.

In our scenario the users are uniformly distributed over all nodes and they all have the same average download rate of 5 Mbps. Therefore the nodes' ranking is mainly based on the average number of hops. The list of ordered nodes based on C_s from the lowest to the highest is as follows:

$$\text{LIST} = \{6, 5, 4, 3, 7, 9, 13, 10, 11, 12, 14, 1, 8, 2\}$$

To place a given popularity group in one cloud, node 6 is the best choice as it has the minimum weight. If the model decides to have two replicas of the same popularity group, then they will be located at nodes $\{6, 5\}$. Higher numbers of replicas are located similarly by progressing down the list and replicating content in a larger ordered subset of the set above. We call each subset of the list a placement (J). Therefore, DEER-CD will only have 14 different placements for each popularity group to choose from, which dramatically minimises the number of iterations needed to decide the optimal placement for each popularity group.

2) Online Phase: In this phase, the list generated from the offline phase is used to decide the placement of each popularity group. Fig. 4 - 14 shows the pseudo code of the heuristic.

For each popularity group, the heuristic calculates the total power consumption TPC_{ij} associated with placing each popularity group $i \in PG$ in each placement, $J \subseteq \text{LIST}$. The total power consumption is composed of network power consumption NPC_{ij} and the cloud power consumption CPC_{ij} , at each placement J . Each cloud location candidate in the placement, $s \in J(\text{loop(a)})$, is assigned to serve nodes according to the minimum hop count (loop (b)). (L_{ijsd}) is the traffic matrix generated by placing popularity group i in the set of nodes s that are specified by the associated placement J , d denotes the set of other nodes in the network where users are requesting files in popularity group i . We use THE multi hop non-bypass heuristic developed in [14] to route the traffic between nodes s and d and calculate the network power consumption that is induced due to cross traffic between the nodes associated with each placement (14 possible placements) for each popularity

group (loop (c)). The total power consumption is calculated and the placement associated with the lowest TPC_i among the 14 possible placements is selected to replicate the popularity group (loop (d)).

| | |
|-----------------|---|
| Inputs: | LIST= {6, 5, 4, 3, 7, 9, 13, 10, 11, 12, 14, 1, 8, 2}, PG = {1..PGN} |
| Outputs: | Optimal Placement (J'), Total Power Consumption (TPC) |
| 1. | For each popularity group $i \in PG$ Do |
| 2. | For each placement $J \subseteq LIST$ Do |
| 3. | For each node $d \in N$ Do |
| 4. | For each cloud location candidate $s \in J$ Do |
| 5. | (a) Add { $cost_{sd}$ } = $MinHop(s, d)$ |
| 6. | (b) End For |
| 7. | (c) Get s where: $cost_{sd} = Min\{cost_{sd}\}$ |
| 8. | (d) $L_{ijsd} = D_{id}$ |
| 9. | End For |
| 10. | $NPC_{ij} = MultiHopHeuristic\{N, Nm_i, L_{ijsd}\}$ |
| 11. | $CPC_{ij} = PUE_c \cdot (SrvPC_{CD} + LANPC_{CD} + StPC_{CD})$ |
| 12. | $TPC_{ij} = NPC_{ij} + CPC_{ij}$ |
| 13. | End For |
| 14. | $TPC_i = Min\{TPC_{ij}\}$ |
| 15. | $J' = J$ |
| 16. | End For |
| 17. | Calculate $TPC = \sum_{i \in PG} TPC_i$ |

Fig. 4 - 14: The DEER-CD heuristic pseudo-code

The DEER-CD heuristic is able to build a core network that includes clouds and it is able to handle the resultant traffic to minimise power consumption. It is able to use the number of users in each node, the network hop counts, user data rates and content popularity distribution to specify the location of clouds and their capability in terms of servers, switches, storage and routers. It is able subsequently to route the resultant traffic using multi-hop non-bypass to minimise power consumption. As such it is able to carry out a complete network design and a complete cloud design which is different from dynamic operation over an existing cloud and an existing network. Note that our heuristic in its current form does not consider the capacity constraints explicitly (such as the number of installed fibres and other network elements) as we consider designing the network for peak traffic (t=22:00) first and running the heuristic at times where the traffic is less than the peak traffic (Fig. 4 - 1). The heuristic can however be easily updated to work in a capacitated network.

Fig. 4 - 15(a) shows the total power consumption for the DEER-CD heuristic, while Fig. 4 - 15(b) and Fig. 4 - 15(c) show the IP/WDM network and cloud power consumptions, respectively also under the DEER-CD heuristic. For the larger size popularity group scenario, the OPR model and the DEER-CD heuristic achieve comparable network power savings of 72% and 70%, respectively, compared to SNPM scheme. Also the cloud and total power savings achieved by the OPR model are maintained at 34% and 40%, respectively. This is due to the almost identical popularity groups' placement by the model and heuristic. A Similar observation is noticed for the smaller popularity group where the DEER-CD heuristic maintains the network, cloud and total power savings of 92%, 35% and 43%, respectively, achieved by the OPR model.

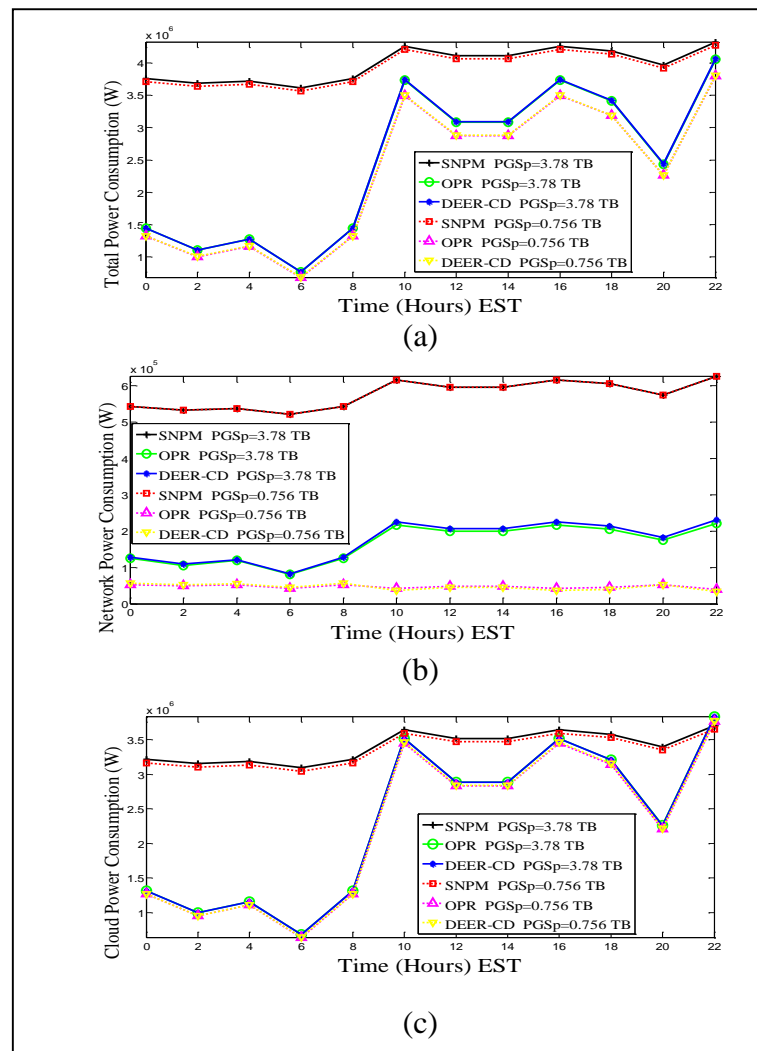


Fig. 4 - 15: (a) Total power consumption of the DEER-CD heuristic (b) IP/WDM network power consumption of the DEER-CD heuristic (c) Cloud power consumption of the DEER-CD heuristic

Fig. 4 - 16 and Fig. 4 - 17 show the number of replications per popularity group for the two popularity group sizes. Similar to the OPR model results in Fig. 4 - 5, the heuristic displays a Zipf like behaviour in replicating popularity groups for the larger popularity group size (Fig. 4 - 16). Similar distributions to those of the model in Fig. 4 - 11 are exhibited by the heuristic for the smaller size where at low demand the content placement follows a Zipf distribution while at higher demand it follows a simple binary distribution. Such behaviour can be harnessed to simplify the content placement heuristic in networks characterised by long periods of peak traffic. Comparing the distribution in Fig. 4 - 17 at (t=22:00) to Fig. 4 - 11 shows that the heuristic creates more replications for popularity groups of lower popularity which results in higher cloud power consumption and lower network power consumption compared to the OPR model as shown in Table 4 - 3 which reports the optimisation gaps between the DEER-CD heuristic and the OPR model for both larger and smaller popularity group sizes at low and high traffic.

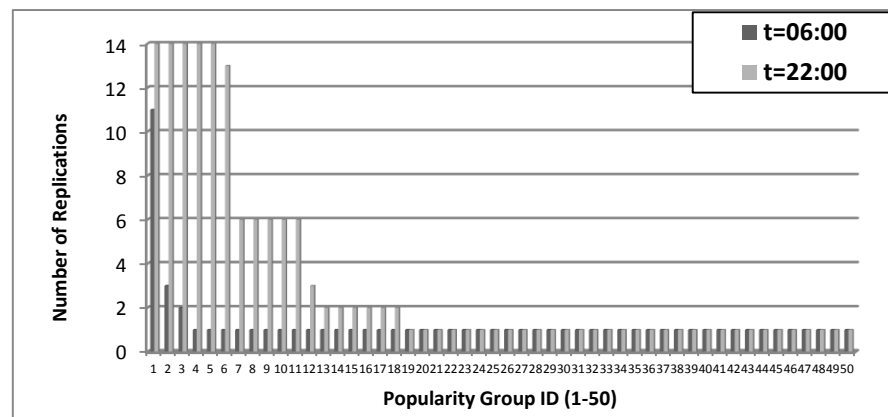


Fig. 4 - 16: Total number of replications per popularity group for DEER-CD ($PGS_p = 3.78$ TB)

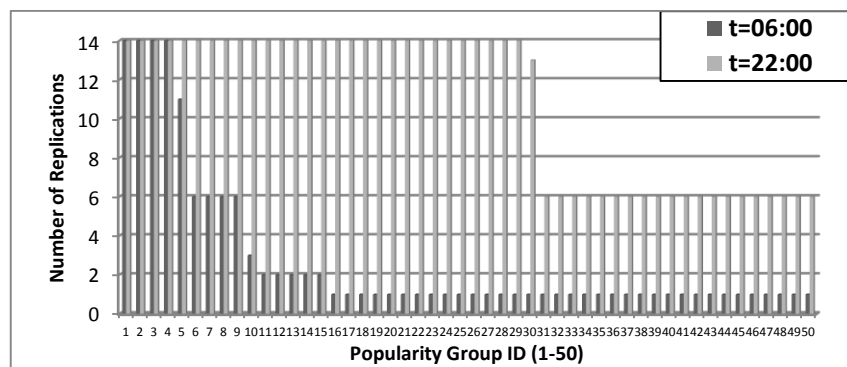


Fig. 4 - 17: Total number of replications per popularity group for DEER-CD ($PGS_p = 0.756$ TB)

| Metric | Gap (%) | | | PG Size |
|---------------|-----------|------------|--------|----------|
| | 06:00 | 22:00 | Avrg. | |
| Total Power | 0.26% | 0.10% | 0.21% | 0.756 TB |
| | 0.22% | 0.26% | 0.25% | 3.78 TB |
| Network Power | 4.06% | -18.30% | -3.72% | 0.756 TB |
| | 2.06% | 4.63% | 3.32% | 3.78 TB |
| Cloud Power | 1.56E-05% | 0.26% | 0.15% | 0.756 TB |
| | 1.46E-05% | -2.61E-05% | 0.01% | 3.78 TB |

Table 4 - 3: Optimisation gaps between the DEER-CD heuristic and MILP

4.5 Energy Efficient Storage as a Service (StaaS)

In energy efficient StaaS, all content is stored in one or more central locations and dynamically migrated to locations in proximity of its owners to minimise the network power consumption. The content can be migrated. However, content migration consumes power at the IP/WDM network as well as in the servers and internal LAN of the clouds. Therefore, StaaS should achieve a trade-off between serving content owners directly from the central cloud/clouds and building clouds near to content owners.

We extend the model in Section 4.2 to capture the distinct features of StaaS. As only the owner or a very limited number of authorised users have the right to access the stored content, the concepts of popularity and replication do not apply to StaaS.

In addition to the sets, parameters and variable defined in Section 4.2, we define the following:

Parameters:

Freq Average file download frequency per hour

Dsize Average file size in Gb.

Rate Average user rate per second, where $Rate = 2 \cdot Freq \cdot Dsize / 3600$

ND_d Node d total traffic demand, $ND_d = \sum_{i \in U_d} Rate$

| | |
|--------------|--|
| <i>Quota</i> | User storage quota in Gb |
| SU_i | Storage Quota utilisation of user i |
| φ | Factor that determines amount of intercloud traffic considered, and is set to 1 or 2 |

Variables (all are non-negative real numbers)

| | |
|------------|--|
| IT_{cd} | Traffic between the central cloud and cloud in node d due to content migration |
| CU_{sd} | Traffic from the cloud in node s to users in node d |
| π_{sd} | $\pi_{sd} = 1$ if cloud s serves users in node d , $\pi_{sd} = 0$ otherwise |
| L_{sd} | Total traffic between node pair (s, d) |

Note that the average user rate, *Rate*, substitutes *Drate* in Section 4.2 and is calculated by dividing total amount of data sent and received which (are measured in Gb, and equal to $2 \cdot Freq \cdot Dsize$) over one hour by the number of seconds in one hour as users need to download the full file before editing and need to upload the full file after finishing (or intermediately). Waiting is not desirable and the file access frequency dictates the data rate. The factor of 2 is introduced to represent the fact that users usually re-upload their files back to the cloud after downloading and editing / processing them.

The model is defined as follows:

Objective: Similar to the one introduced in section 4.2

Subject to: Constraints (4-1)-(4-7), (4-17)-(4-19) plus the following:

1) *Clouds to users traffic:*

$$\sum_{s \in N} CU_{sd} = ND_d \quad (4-22)$$

$$\forall d \in N,$$

$$M \cdot CU_{sd} \geq \pi_{sd} \quad (4-23)$$

$$\forall s, d \in N,$$

$$CU_{sd} \leq M \cdot \pi_{sd} \quad (4-24)$$

$$\forall s, d \in N,$$

$$CU_{cd} = ND_d \cdot \left(1 - \sum_{b \in N: b \neq c} Cloud_b\right) \quad (4-25)$$

$$\forall d \in N : d \neq c,$$

Constraint (4-22) ensures that the traffic demand of all users in each node is satisfied. Constraints (4-23) and (4-24) decide whether a cloud serves users in node d or not, where M is a large enough number, with units of 1/Gbps and Gbps in (4-23) and (4-24), respectively, to ensure that $\pi_{sd} = 1$ when CU_{sd} is greater than zero. Constraint (4-25) sets the traffic between the central cloud and users in other nodes to 0 if those users have a nearby cloud to download their content from.

2) *Clouds locations:*

$$M \cdot \sum_{d \in N} CU_{sd} \geq Cloud_s \quad (4-26)$$

$$\forall s \in N,$$

$$\sum_{d \in N} CU_{sd} \leq M \cdot Cloud_s \quad (4-27)$$

$$\forall s \in N,$$

Constraints (4-26) and (4-27) build a cloud in location s if that location is selected to serve the requests of users of at least one node d , where M is a large enough number, with units of 1/Gbps and Gbps in (4-26) and (4-27), respectively, to ensure that $Cloud_s = 1$ when $\sum_{d \in N} CU_{sd}$ is greater than zero

3) *Clouds storage capacity:*

$$StrC_s = \sum_{d \in N} \sum_{i \in U_d} \pi_{sd} \cdot Quota \cdot SU_i \cdot Red \quad (4-28)$$

$$\forall s \in N,$$

Constraint (4-28) calculates the cloud storage capacity based on the number of users served by the cloud, their storage quota and utilisation, taking redundancy into account.

4) *Inter clouds traffic:*

$$IT_{cd} = \sum_{i \in U_d} Cloud_d \cdot Quota \cdot SU_i / (3600 \cdot \Delta t) \quad (4-29)$$

$$\forall d \in N : d \neq c,$$

Constraint (4-29) calculates the content migration traffic between the central cloud and local clouds. The factor of Δt in the denominator scales the power consumption down to be consistent with our evaluation period of Δt hours.

5) *Total traffic between nodes and clouds upload capacity:*

$$L_{sd} = CU_{sd} + IT_{sd} \quad (4-30)$$

$$\forall s, d \in N,$$

$$Cup_s = \sum_{d \in N} (L_{sd} + \varphi \cdot IT_{sd}) \quad (4-31)$$

$$\forall s \in N.$$

Constraint (4-30) calculates the total traffic between node pair (s, d) as the summation of the inter cloud traffic and clouds to users traffic. Constraint (4-30) substitutes constraint (4-10) in calculating network traffic. Constraint (4-31) calculates clouds upload capacity which includes the clouds to users traffic and the clouds inter traffic when $s=c$. The factor φ is set to 2 if we are interested in total power consumption, as the receiving local cloud will consume similar power in its servers and internal LAN to the central sending cloud during migration. However, it is set to 1 if we are only interested in the actual clouds upload capacity and capability calculated by constraints (4-17)-(4-19). In this section we set $\varphi = 2$ as we are interested in power consumption.

The NSFNET network, the users' distribution and input parameters discussed in Section 4.3 are also considered to evaluate the StaaS model. Node 6 is optimally selected based on the insights of Section 4.3 to host one central cloud.

We analyse 1200k users uniformly distributed among the network nodes which corresponds to time 22:00 in Fig. 4 - 1. The power consumption calculation is averaged over the range of access frequencies considered (10 to 130 downloads per hour). We consider three different schemes to implement StaaS:

- **Single Cloud:** Users are served by the central cloud only.

- **Optimal Clouds:** Users at each node are served either from the central cloud or from a local cloud by migrating content from the central cloud.
- **Max Clouds:** Users at each node are served by a local cloud.

We evaluate the different schemes considering two file sizes of 22.5 MB and 45 MB and a user storage quota of 2 GB. Note that the file sizes reflect content of high resolution images or videos. Files of smaller sizes will result in low network traffic that will not justify replicating content into local clouds. Users' storage utilisation SU_i is uniformly distributed between 0.1 and 1.

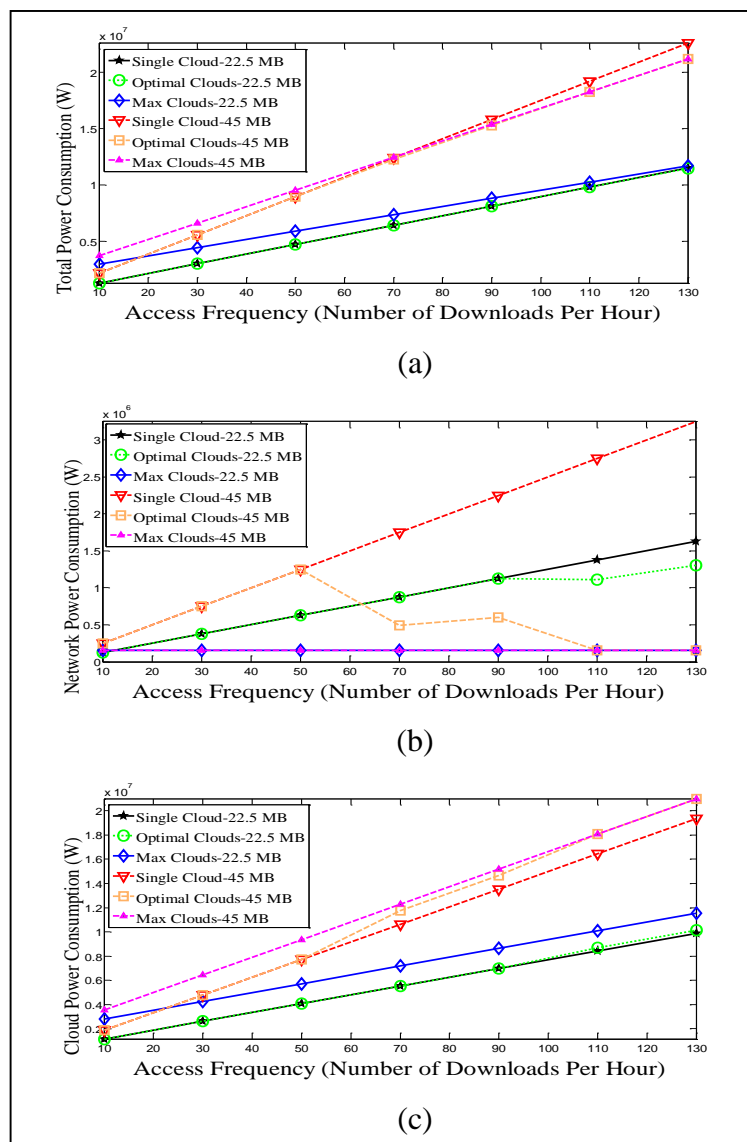


Fig. 4 - 18: Total power consumption of StaaS (b) IP/WDM network power consumption of StaaS (c) Cloud power consumption of StaaS

Fig. 4 – 18(a) shows the total power consumption versus the content access frequency while Fig. 4 – 18(b) and Fig. 4 – 18(c) decompose it into the IP/WDM network power consumption and cloud power consumption, respectively. At lower access frequencies, the optimal clouds scheme selects to serve all users from the central cloud. At higher access frequencies, however, the impact of the file size becomes more relevant. For the larger file size (45 MB) scenario local clouds are built whenever the access frequency is equal to or higher than 50 downloads per hour. On the other hand for the smaller file size of 22.5 MB, users are served from the central cloud up to access frequencies as high as 90 downloads per hour for this smaller file size (22.5 MB) scenario. This is because a larger file size results in higher traffic and consequently larger reduction in traffic between the central cloud and users when serving the requests locally. Therefore it will compensate for the power consumption of content migration. To eliminate the impact of content replication on storage power consumption, this scheme requires switching off the central clouds storage that stores the migrated content after migration. Apple iCloud is an example of a cloud implementation that typically hosts large files representing images and videos. Migration to local clouds is energy efficient in this case as opposed to clouds that typically host small text documents.

On the network side, the Max Clouds scheme has the lowest network power consumption, saving 67% and 83% of the network power consumption compared to the Single Cloud scheme considering the 22.5 MB and the 45 MB average file size, respectively. This is because all users are served locally and the IP/WDM network power consumption is only due to content migration from the central cloud. However, this saving is at the cost of high power consumption inside the clouds to migrate content, resulting in an increase of 28% and 19% in the cloud power consumption for the 22.5 MB and 45 MB cases, respectively, as shown in Fig. 4 – 18(c).

For the 22.5 MB file size scenario, limited total and network power savings are obtained by the Optimal Clouds scheme compared to the Single Cloud scheme (0.1% total and 5% network power saving) as shown in Fig. 4 – 18(b). On the other hand, for the 45 MB file size scenario, more total and network power savings are obtained by the Optimal Cloud scheme compared to the Single Cloud scheme (2% total and 48% network power saving) as shown in Fig. 4 – 18(b).

Fig. 4 - 19 shows the variation in the number and size of clouds with the content access frequency for the 45 MB file size. As the content access frequency increases, migrating content from the central cloud to local clouds becomes more energy efficient compared to delivering content directly from the central cloud and therefore more clouds are needed to serve users locally. Note that the storage size in Fig. 4 - 19 represents the powered-on storage. This results in decreased storage size of the central cloud with higher content access frequency as shown in Fig. 4 - 19. Fig. 4 - 19 also shows that other clouds have almost similar storage size, at high access rates, due to the uniform distribution of users in the network.

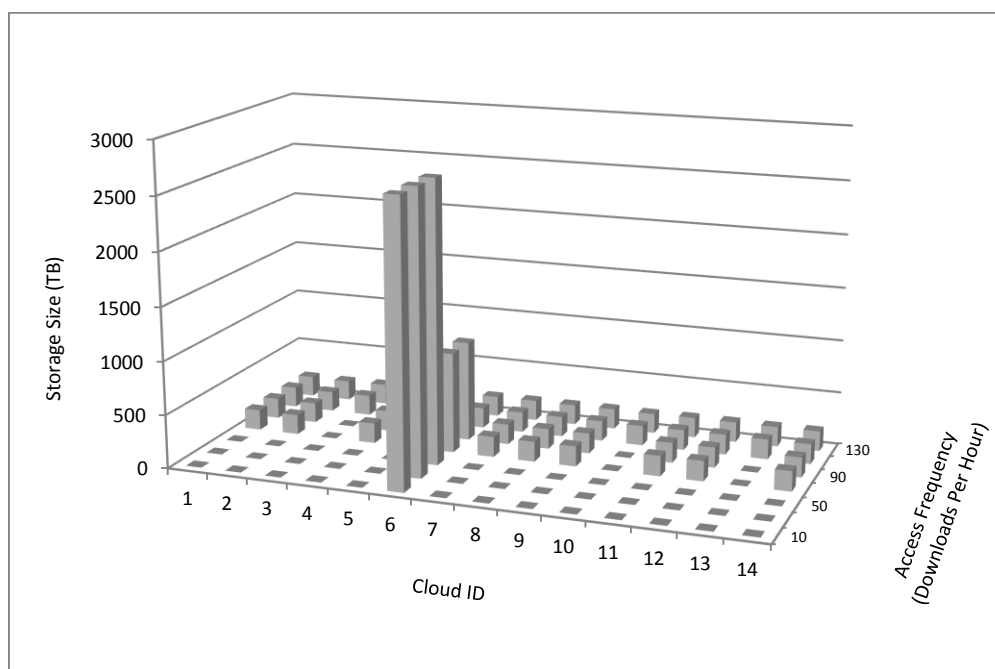


Fig. 4 - 19: Powered on clouds storage size versus content access frequency for the StaaS optimal scheme (45 MB file size)

4.6 Summary

In this chapter, we introduced a framework for designing energy efficient cloud computing services over non-bypass IP/WDM core networks. We investigated network related factors including the centralisation versus distribution of clouds and the impact of demand, content popularity and access frequency on the clouds placement, and cloud capability factors including the number of servers, switches and routers and amount of storage required in each cloud. We studied the

optimisation of two cloud services: Cloud Content Delivery and Storage as a Service (StaaS).

Firstly, we developed a MILP model to optimise cloud content delivery services. Our results indicate that replicating content into multiple clouds based on content popularity yields up to 43% total saving in power consumption compared to power un-aware centralised content delivery. Based on the model insights, we developed an energy efficient cloud content delivery heuristic, DEER-CD, with comparable power efficiency to the MILP results. Second, we extended the content delivery model to optimise Storage as a Service (StaaS) applications. The results show that migrating content according to its access frequency yields up to 48% network power savings compared to serving content from a single central location. The implication of these results is that optimally distributing content according to popularity/access frequency yields the minimum power consumption in the core network as well as the clouds. This is ensured by not over replicating content where clouds power consumption would increase, and not to constrain content in few locations which can cause large amount of traffic to cross the network unnecessarily, resulting in high network power consumption. Therefore, approaches such as OPR represent a win-win state for both cloud and network providers.

Chapter 5: Energy Efficient Virtual Machine Placement in Optical Core Networks

5.1 Introduction

In this chapter we develop a MILP model to optimise the placement of virtual machines in IP/WDM networks for processing applications and to minimise the total energy consumption of the cloud and the network considering different VM distribution schemes. In our analysis, a VM is defined as a logical entity created in response to a service request by one or more users sharing that virtual machine. A user request is defined by two dimensions: (i) the CPU utilisation (normalised workload) of the VM and (ii) the traffic demand between the VM and its user. In this chapter we use the terms CPU utilisation and normalised workload interchangeably. We validate the developed model by a real time heuristic and compare the results of the model and heuristic in terms of execution time and accuracy.

5.2 Mathematical Model

We develop a MILP model to optimise the number, and location of clouds and optimise the placement of VMs within the clouds as demands vary throughout the day to minimise the network and clouds power consumption.

The model considers three VM placement schemes:

- **VM Replication:** More than one copy of each VM is allowed in the network.
- **VM Migration:** Only one copy of each VM is allowed in the network. We assume that the internal LAN capacity inside data centres is always sufficient to support VM migration.
- **VM Slicing:** The incoming requests are distributed among different copies of the same VM to serve a smaller number of users as proposed in [72]. We call each copy a slice as it has less CPU requirements. As VMs with small CPU share might threaten the SLA, we enforce a limit on the minimum size of the VM CPU utilisation. Unlike [72] where CPU and memory bandwidth are considered, we consider the CPU and traffic dimensions of the problem where each slice is placed in a different cloud rather than in a different server inside the same cloud.

In addition to the sets, parameters and variables in Section 4.2, we define the following sets, parameters and variables:

Sets:

| | |
|-------|--------------------------------|
| VM | Set of virtual machines |
| U_v | Set of users requesting VM v |

Parameters:

| | |
|-----------|--|
| NVM | Total number of virtual machines |
| P_{max} | Maximum power consumption of a server |
| W_{max} | Maximum normalised workload of a server |
| ∇ | Server energy per bit, $\nabla = P_{max}/W_{max}$ |
| W_v | Total normalised workload of VM v . |
| D_{dv} | Traffic demand from VM v to node d , $D_{dv} = \sum_{i \in U_d: i \in U_v} D_{rate}$ |
| $MinW$ | Minimum allowed normalised workload per VM |

Variables (all are non-negative real numbers):

| | |
|---------------|---|
| L_{sdv} | Traffic demand from VM v in cloud s to node d |
| δ_{sv} | $\delta_{sv}=1$ if cloud s hosts a copy of VM v , otherwise $\delta_{sv}=0$ |
| CW_s | Total normalised workload of Cloud s |
| W_{sv} | Normalised workload of the slice of VM v in node s |
| PSN_s | Number of processing servers in cloud s |

The power consumption of the cloud considering the machine virtualisation scenario is composed of:

- 1) The power consumption of servers (*SrvPC_VM*):

$$\sum_{s \in N} \nabla \cdot CW_s$$

- 2) The power consumption of switches and routers (*LANPC_VM*):

$$\sum_{s \in N} Cup_s \cdot (Sw_{EPB} \cdot Red + R_{EPB})$$

Note that we do not include the storage power consumption in our models. Although the server power consumption is a function of the idle power, maximum power and CPU utilisation [112], for large number of servers, taking only $\nabla = P_{max}/W_{max}$ as the server energy per bit to calculate its power consumption yields very close approximation as the difference will be only in the last powered on server. Note that a cloud is composed of a large number of servers and through “packing”, each server in our case is either as close to fully utilised as possible or is off. In such a case “idle power plus linear increase in power with load” is equivalent to “linear increase in power with load” as both servers are either operated near the peak or are off and the peak powers are identical. For the overall cloud either a single server (or more generally a very small minority of servers) may be partially loaded. Therefore for a cloud made up of a large number of highly used servers (unused servers are turned off), the power consumption increases in proportion to load approximately. Note that if servers are not fully packed, this approximation becomes less accurate.

This warrants further investigation, however our approach is followed in the literature [109]. As for the content delivery model, we also assume here that other storage and network elements have similar power management as servers.

The model is defined as follows:

Objective: Minimise

$$\begin{aligned}
& PUE_n \cdot \left(\sum_{i \in N} Prp \cdot Q_i + Prp \cdot \sum_{m \in N} \sum_{n \in Nm_m} W_{mn} + \right. \\
& \quad \sum_{m \in N} \sum_{n \in Nm_m} Pt \cdot W_{mn} + \\
& \quad \left. \sum_{m \in N} \sum_{n \in Nm_m} Pe \cdot A_{mn} \cdot F_{mn} + \right. \\
& \quad \left. \sum_{i \in N} PO_i + \sum_{m \in N} \sum_{n \in Nm_m} Pmd \cdot F_{mn} \right) + \\
& PUE_c \cdot \left(\sum_{s \in N} \nabla \cdot CW_s + \sum_{s \in N} Cup_s \cdot (Sw_{EPB} \cdot Red + R_{EPB}) \right)
\end{aligned} \tag{5-1}$$

Subject to: (4-2)-(4-7), (4-10)-(4-11), (4-16), (4-18),(4-19), plus the following constraints:

1) *VMs demand:*

$$\begin{aligned}
& \sum_{s \in N} L_{sdv} = D_{dv} \\
& \forall d \in N \forall v \in VM,
\end{aligned} \tag{5-2}$$

Constraint (5-2) ensures that the requests of users in all nodes are satisfied by the VMs placed in the network. The model also allows a user to be served by multiple copies of the VMs. Similar to (4-10), L_{sdv} can be used to deduce L_{sd} .

2) *Virtual Machines and clouds locations:*

$$\begin{aligned}
& M \cdot \sum_{d \in N} L_{sdv} \geq \delta_{sv} \\
& \forall s \in N \forall v \in VM,
\end{aligned} \tag{5-3}$$

$$\begin{aligned}
& \sum_{d \in N} L_{sdv} \leq M \cdot \delta_{sv} \\
& \forall s \in N \forall v \in VM,
\end{aligned} \tag{5-4}$$

$$\sum_{v \in VM} \delta_{sv} \geq Cloud_s \quad (5-5)$$

$$\forall s \in N,$$

$$\sum_{v \in VM} \delta_{sv} \leq M \cdot Cloud_s \quad (5-6)$$

$$\forall s \in N,$$

Constraints (5-3) and (5-4) replicate VM v to cloud s if cloud s is selected to serve requests for v where M is a large enough number, with units of Gbps, to ensure that $\delta_{sv} = 1$ when $\sum_{d \in N} L_{sdv}$ is greater than zero.

Constraints (5-5) and (5-6) build a cloud in location s if the location is selected to host one or more VMs where M is a large enough unitless number to ensure that $Cloud_s = 1$ when $\sum_{v \in VM} \delta_{sv}$ is greater than zero.

3) *Total cloud normalised workload for replication and migration schemes:*

$$CW_s = \sum_{v \in VM} \delta_{sv} \cdot W_v \quad (5-7)$$

$$\forall s \in N,$$

Constraint (38) calculates the total normalised workload of each cloud by summing its individual VMs normalised workloads.

4) *VM migration constraint*

$$\sum_{s \in N} \delta_{sv} = 1 \quad (5-8)$$

$$\forall v \in VM,$$

Constraint (5-8) is used to model the VM migration scenario where only one copy of each VM is allowed.

5) *VM Slicing constraints:*

$$\sum_{s \in N} W_{sv} = W_v \quad (5-9)$$

$$\forall v \in VM,$$

$$W_{sv} \geq MinW \cdot \delta_{sv} \quad (5-10)$$

$$\forall s \in N \forall v \in VM,$$

$$W_{sv} \leq M \cdot \delta_{sv}$$

$$\forall s \in N \forall v \in VM, \quad (5-11)$$

$$CW_s = \sum_{v \in VM} W_{sv}$$

$$\forall s \in N, \quad (5-12)$$

Constraints (5-9)-(5-12) are used to model the VM slicing scenario. Constraint (5-9) ensures that the total normalised workload of all slices is equal to the original VM normalised workload before slicing. Constraints (5-10) and (5-11) ensure that the locations of the slices of a VM are consistent with those selected in constraints (5-3) and (5-4) and also they ensure that the slices normalised workload does not drop below the minimum allowed normalised workload per slice where M is a large enough number, with units of %, to ensure that $\delta_{sv} = 1$ when W_{sv} is greater than zero. Constraint (5-12) calculates the work load of each cloud by summing the load of the slices of the different VMs hosted by the cloud.

6) *Single Cloud scheme constraint:*

$$\sum_{s \in N} Cloud_s = 1 \quad (5-13)$$

Constraint (5-13) is used to model the Single Cloud scheme which is used as our benchmark to evaluate the power savings achieved by the different VM distribution schemes.

7) *Number of processing servers:*

$$PSN_s = CW_s / W_{max}$$

$$\forall s \in N. \quad (5-14)$$

Constraint (5-14) calculates the number of processing servers needed in each cloud. The integer value is obtained using the ceiling function.

5.3 Cloud VM Model Results:

The VM placement schemes are evaluated considering the NSFNET network and the users distribution discussed in Section 4.3. In addition to the input parameters in Table 3 - 1 and Table 4 - 1, the VM model considers the parameters in Table 5 - 1.

To reflect various users' processing requirements and represent different types of VMs, we uniformly assign normalised workloads to VMs from the set given in Table 5 - 1.

Fig. 5 - 1 shows the server CPU and network bandwidth utilisation of 10 VMs at two times of the day (06:00 and 22:00). Note that network utilisation is calculated by assuming a 10 Gbps servers' interface speed and users traffic rates are kept at 5 Mbps as in Section 4.3.

| | |
|---|--------------------------------------|
| Number of virtual machines (NVM) | 1000 |
| Server maximum power consumption (P_{max}) | 300 W |
| Server maximum normalised workload (W_{max}) | 100% |
| VM v total normalised workload (W_v) | RAND{10,20,30,40,50,60,70,80,90,100} |
| Minimum allowed normalised workload per VM ($MinW$) | 5% |

Table 5 - 1: Input data for the VM models

In a practical cloud implementation the CPU normalised workload needed is estimated by the cloud provider based on users' requirements. Instead of starting with users requests for VMs and assigning them to VMs, we simplify the generation of CPU normalised workload by considering a set of 1000 virtual machines (limit of what MILP can handle) of different types and assign each VM a uniformly distributed normalised workload between 10% and 100% of the total CPU capacity. We then randomly and uniformly assign each VM to serve a number of users.

This approach is less complex to analyze in terms of number of variables and it captures the same picture. This can be understood by noting that a cloud provider will assign the incoming requests to a given VM according to its specialisation up to a certain maximum normalised workload. This results in a distribution of VM normalised workloads and an assignment of users (from different nodes) to a VM which is what our approach also achieves.

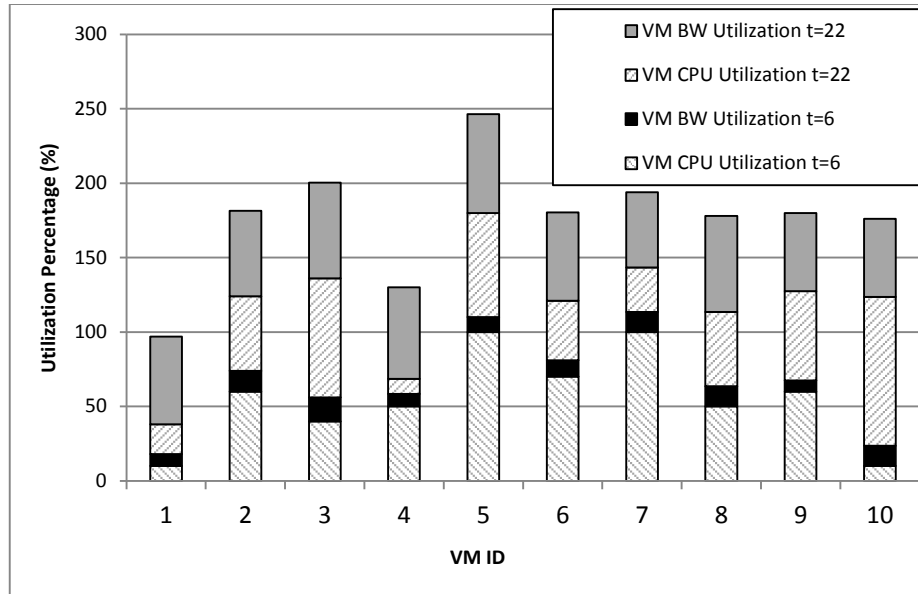


Fig. 5 - 1: Sample VMs CPU and network utilisation

Fig. 5 - 2(a) shows that the VM replication and migration schemes reduce to a single cloud scheme at low demand periods where all users are served from a cloud built in node 6 where all the 1000 VMs reside. For the migration scheme, node 6 is always (low traffic and high traffic) the optimum location for all VMs as it yields the minimum average hop count to all the network nodes given that users are uniformly distributed among nodes and requests for a VM are also uniformly distributed among users. For migration and at higher demands, and if the users connected to each VM have a Geo location clustering tendency, then there will be a benefit at high demand in migrating VMs nearer to such clusters. On the other hand for a uniform distribution of users there is fundamentally no benefit in migrating VMs. Our model concurs with this reasoning and keeps the VMs at node 6 even at high demand under the migration scheme.

Under the replication scheme on the other hand the decision to make extra copies of a VM is driven by the tradeoff between the network power saved as a result of having extra copies of the VM which reduce network journeys, versus the increase in power as a result of the extra VMs. Therefore we found out that the model chooses to replicate lightly loaded VMs (i.e. VMs with load nearer to the 10%, away from 100%) as these consume less power. The replication scheme under uniformly distributed users obtains a limited network saving of 2% (Fig. 5 - 2(b)) compared to the single cloud scheme. This is achieved by replicating a limited number of VMs

(Fig. 5 - 2(c)) with an overall network and VM combined power saving that is near zero, but positive.

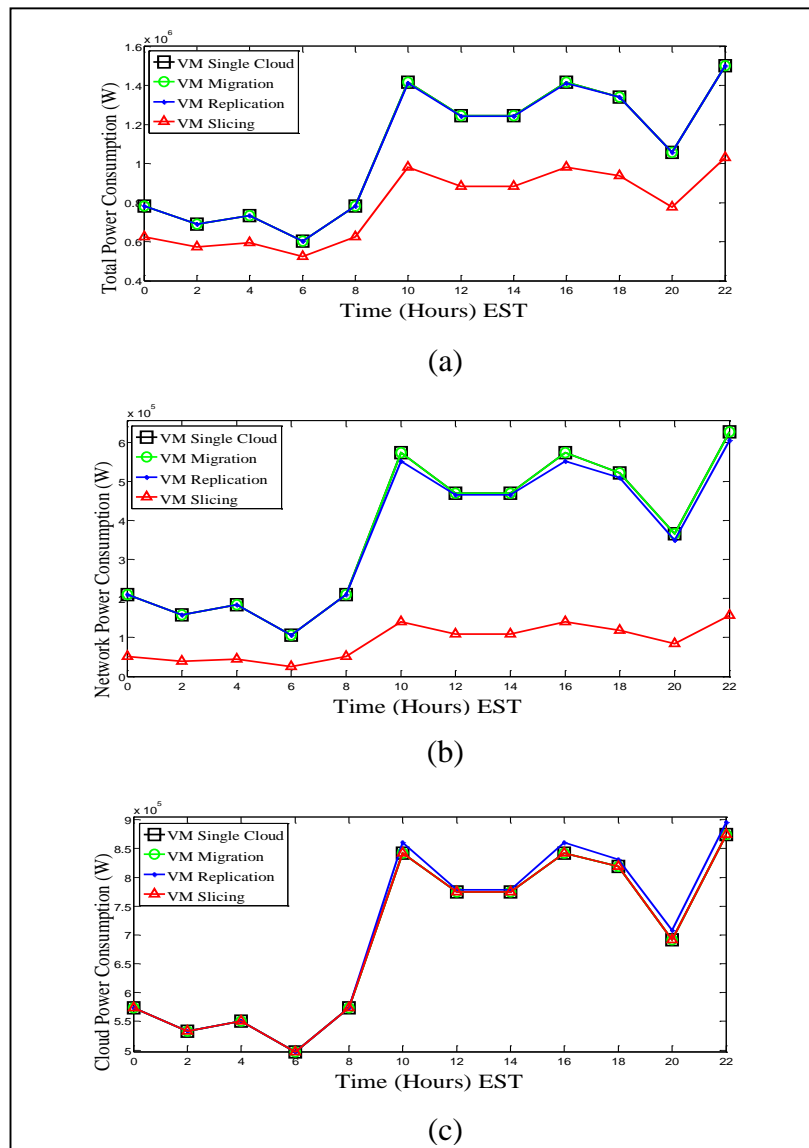


Fig. 5 - 2: Total power consumption of the different VMs scenarios (b) IP/WDM network power consumption of the different VMs scenarios (c) Cloud power consumption of the different VMs scenarios

The VM Slicing scheme is the most energy efficient scheme as slicing does not increase the cloud power consumption (Constraint (5-9)), allowing the VMs slices to be distributed over the network, yielding 25% and 76% total and network power saving, respectively compared to the single cloud scheme as shown in Fig. 5 - 2(a) and Fig. 5 - 2(b).

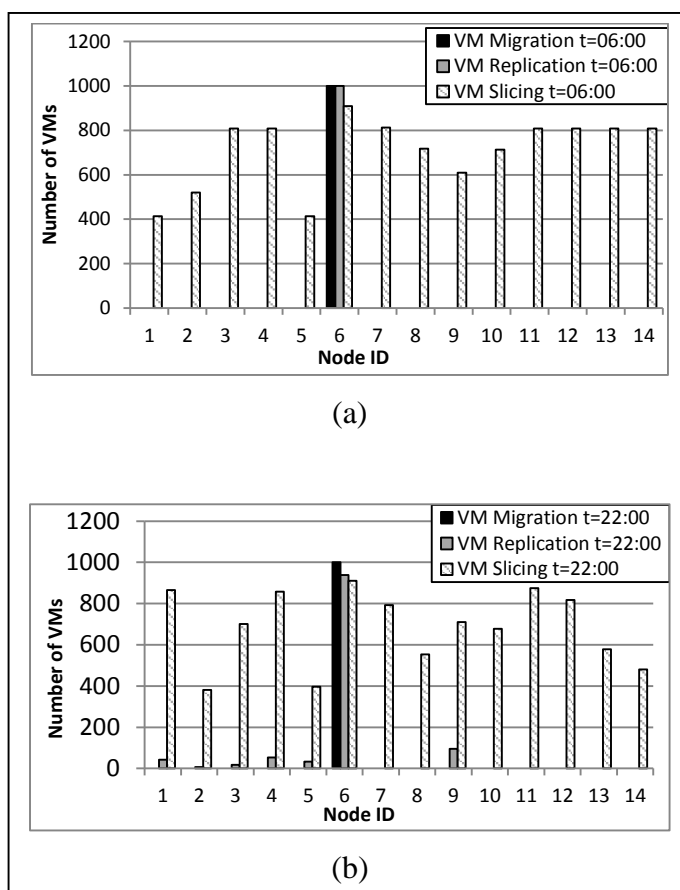


Fig. 5 - 3: (a) VMs distribution scheme at 06:00 (b) VMs distribution scheme at 22:00

Fig. 5 - 3 shows the VMs placement over the network nodes for the three schemes at low and high demands. As discussed above the migration scheme places all VMs at node 6 all the time. At high loads the replication scheme, creates more than one copy of a limited number of VMs. The slicing scheme slices the machines so that each node has about 400-900 VMs at the different times of the day.

Note that the limited impact of the migration and replication schemes is due to the geographical uniformity of the traffic between VMs and nodes. Therefore we also evaluate a scenario with an extreme non-uniform distribution of requests for VMs where only users in a certain neighbourhood request a VM. In this scenario, only users in three neighbouring nodes (one physical hop between each) connect to a particular VM. For each of the 1000 VMs, we generate a uniform normalised workload between 10% and 100% and also generate for the same VM a random number uniformly distributed between 1 and N representing a network node, we then look up the single hop neighbourhood list of that node and select any other two neighbouring nodes. For example at 22:00, when there are 1.2 M users, we choose to

allocate in this example to each VM an equal deterministic share, i.e. 1200 users, and so 400 users will be located in each of the three neighbouring nodes. This means that all users requesting a given VM are highly geographically localised.

Table 5 - 2 shows the power savings achieved by the different schemes compared to the single cloud scheme at two times of the day, 06:00 and 22:00. The power savings of the migration and replication schemes increase compared to the uniform traffic scenario as the popularity of a VM in a certain neighbourhood justifies migrating or replicating it to that neighbourhood. The non-uniformity of traffic also allows the slicing scheme to save more power. The performance under the uniform and extreme non-uniform traffic distributions gives the lower and the upper bounds on the power savings that can be achieved by the different VM placement schemes.

| Scheme | Power Saving | | | |
|-----------------------|--------------|---------|-------|---------|
| | 06:00 | | 22:00 | |
| | Total | Network | Total | Network |
| VM Migration | 8% | 48% | 20% | 49% |
| VM Replication | 8% | 48% | 21% | 59% |
| VM Slicing | 16% | 96% | 40% | 97% |

Table 5 - 2: Power saving of the different schemes compared to single cloud under geographically non-uniform traffic

5.4 DEER-VM: Energy Efficient VM Distribution for the Cloud

The results of the VM models showed that VM slicing is the most energy efficient VM placement scheme. In this section we develop a heuristic to perform VM-Slicing in real time using the same concept used in the DEER-CD heuristic.

| | |
|----------------|---|
| Input: | LIST= {6, 5, 4, 3, 7, 9, 13, 10, 11, 12, 14, 1, 8, 2}, VM = {1..NVM} |
| Output: | Optimal Placement(J'), Total Power Consumption (TPC) |
| 1. | For each Virtual Machine $v \in VM$ Do |
| 2. | For each Placement $J \subseteq LIST$ Do |
| 3. | For each node $d \in N$ Do |
| 4. | For each location candidate $s \in J$ Do |
| 5. | (a) Add {cost _{sd} } = <i>MinHop</i> (s, d) |
| 6. | (b) $CW_{vjs} = W_v$ |
| 7. | (c) End For |
| 8. | (d) Get s where: cost _{sd} = <i>Min</i> {cost _{sd} } |
| 9. | $L_{vjsd} = D_{vd}$ |
| 10. | End For |
| 11. | $NPC_{vJ} = MultiHopHeuristic\{N, Nm_i, L_{vjsd}\}$ |
| 12. | $CPC_{vJ} = PUE_c \cdot (SrvPC_{VM} + LANPC_{VM})$ |
| 13. | $TPC_{vJ} = NPC_{vJ} + CPC_{vJ}$ |
| 14. | End For |
| 15. | $TPC_v = Min\{TPC_{vJ}\},$ |
| 16. | $J' = J$ |
| 17. | End For |
| 18. | Calculate $TPC = \sum_{v \in VM} TPC_v$ |

Fig. 5 - 4: DEER-VM heuristic pseudo-code

The pseudo code of the DEER-VM heuristic is shown in Fig. 5 - 4. Nodes are ordered from the lowest to the highest based on their weight and the heuristic searches the 14 possible placements deduced from the LIST for each VM. The minimum hop count (loop (a)) is used to assign each node, to the nearest node hosting a VM which yields (L_{vjsd}), the traffic generated between nodes (s, d) due to placing VM v according to placement J (loop (b)). Knowing (L_{vjsd}), the heuristic calculates the total power consumption, TPC_{vJ} (loop (c)). VMs are located at the placement associated with the lowest power consumption among the 14 possible placements (loop (d)). The same process is repeated for other VMs till all VMs are placed.

In the absence of our sorted list approach, an exhaustive VM search is needed. In a similar fashion and as outlined for the DEER-CD, for NSFNET with $N=14$ this is a complexity reduction by a factor of 1.6×10^{10} . Furthermore using a 2.4 GHz Intel

Core i5 PC with 4 GB Memory, the heuristic took 35 minutes to evaluate the DEER-VM results.

Fig. 5 - 5(a) reveals that while the VM slicing approach has saved 25% of the total power compared to the Single Cloud scenario, the DEER-VM heuristic achieved 24%. This slightly lower saving is due to the multi hop non-bypass heuristic which is less efficient than the MILP model in routing traffic and therefore its network power consumption has increased by 6.4% as seen in Fig. 5 - 5(b). As slicing the virtual machine does not increase the power consumption of the machine, the results of model and heuristic considering VM slicing maintain the cloud power consumption of the Single Cloud scenario as shown in Fig. 5 - 5(c).

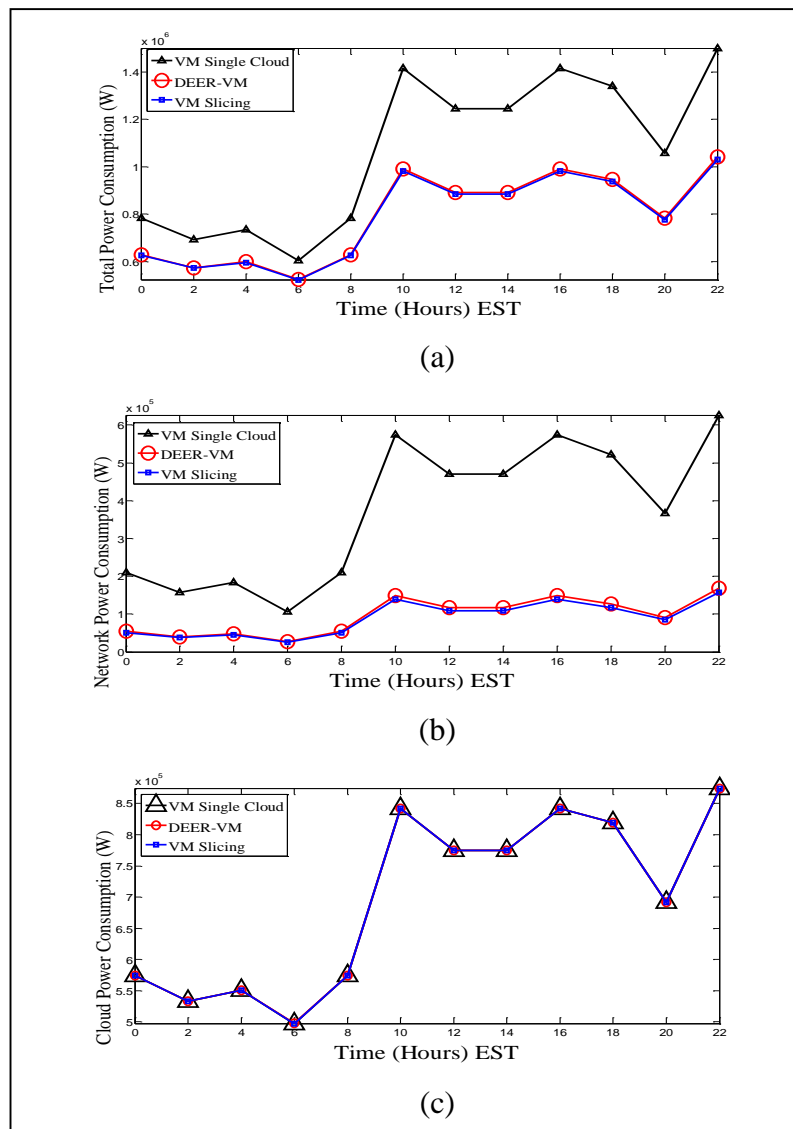


Fig. 5 - 5: DEER-VM total power consumption (b) DEER-VM IP/WDM network power consumption (c) DEER-VM cloud power consumption

Table 5 - 3 reports the optimisation gaps between the DEER-VM heuristic and MILP.

| Metric | Gap (%) | | |
|----------------------|---------|-------|---------|
| | 06:00 | 22:00 | Average |
| Total Power | 0.36% | 1% | 0.73% |
| Network Power | 7% | 6.77% | 6.47% |
| Cloud Power | 0% | 0% | 0% |

Table 5 - 3: Optimisation gaps between the DEER-VM heuristic and MILP

The 24% saving of DEER-VM is due to the IP/WDM network side rather than the cloud side as the CPU normalised workload is the same for both scenarios and the cloud servers' power consumption is normalised workload dependant. Most of the savings come from VMs which generate a lot of traffic in the network compared to their CPU utilisation. Slicing such VMs reshapes the traffic pattern in the network so that users get their service from nearby locations, thereby saving network power consumption. However, if most VMs have high CPU utilisation and low network traffic then slicing VMs will not save power and a Single Cloud scenario will be a better solution, especially taking VMs management cost into account. Therefore, VM slicing can play a major role in saving power consumption in VM based content delivery such as IPTV, and Video on Demand (VoD). The current version of the DEER-VM heuristic is designed to work under a uniform distribution of users as the sorted list is produced only once, however in the case of non-uniformly (geographically) distributed users, the placement of one VM will affect the placement selection of the next one. As such a progressively shorter list has to be sorted at each step. This is a subject we hope to report on in future. Note that the placement decision of one VM (and one PG for the content delivery heuristic in Section 4.4) is independent of the others; therefore, the heuristics can be distributed among different servers to reduce the computation time as different instances will work in parallel.

5.5 Summary

In this chapter, we optimised the placement of Virtual Machines (VMs) in non-bypass IP/WDM networks to minimise the total (Network and Clouds) power consumption. Our results show that slicing the VMs into smaller VMs and placing them in proximity to their users saves 25% of the total power compared to a single virtualised cloud scenario. More savings, up to 40%, can be achieved in a geographically non-uniform traffic scenario. We also developed a heuristic for real time VM placement (DEER-VM) that achieves comparable power savings. The implication of these results is that slicing is the most promising approach for energy saving for VM placement applications. To gain such high saving, slices should have minimum idle workload requirements and cloud providers need to know where each slice is needed in the network so that DEER-VM can allocate the required CPU workload for each slice. Traffic non-uniformity can be harnessed to yield even more power savings even for applications that do not support slicing, such as those VMs that can be only replicated or migrated.

Chapter 6: Renewable Energy for P2P and Distributed Clouds Networks

6.1 Introduction

In the previous chapters we have investigated intra-networking solutions for the problem of energy efficiency of core networks subject to P2P and distributed clouds traffic. Such intra-solutions included, but are not limited to, the optimisation of content location, virtual machine location, and peers selections among BitTorrent peers. However, inter-solutions that extend externally, outside the network, can be harnessed too. One of the most promising such solutions is the consideration of renewable energy. Renewable sources provide clean energy without the cost of environmental impact such as the carbon footprint associated with non-renewable energy such as fossil fuel. Therefore it is an important area of research that we delved into and integrated with our work on content and service distribution in this thesis, from both P2P and distributed clouds perspectives.

In this chapter we study the power consumption of BitTorrent based P2P content distribution systems in IP/WDM networks with renewable energy sources, represented by solar cells. We investigate the impact of optimising the routing table and the peers' selection matrix on the non-renewable power consumption of IP/WDM networks. We also study the impact of renewable energy availability, represented by wind farms, on the optimisation of content delivery in distributed

clouds such as the clouds locations, clouds internal capability and content replication patterns.

6.2 Renewable Energy for P2P Networks

In [20] a MILP model and a heuristic for hybrid power IP/WDM networks were developed, where the energy sources are a mix of renewable and non-renewable sources, to route traffic so the total non-renewable power consumption is minimised taking into account the variation in traffic demands and renewable energy availability throughout the day. The minimum hop routing table (MHRT), yielding the minimum power consumption in non-renewable energy powered IP/WDM networks, is replaced by a green routing table (GRT) that minimises the number of traversed nodes powered by non-renewable energy.

However, when a swarm based content sharing protocol like BitTorrent enters the picture, a new degree of freedom becomes available, (beside the ability to change the routing table), namely the ability to change the peers' selection. As observed in Section 3.3, localising the peers' selection where peers prefer to download from nearby rather than from far peers, a selection that we denote here as local Selection Matrix (LSM), can significantly save power in IP/WDM networks compared to the random selection matrix used as the basis of Original BitTorrent implementations.

In this section we study different routing and peers selection approaches for BitTorrent based P2P protocols over hybrid powered IP/WDM networks. To illustrate the investigated approaches, we consider the network example in Fig. 6 - 1.

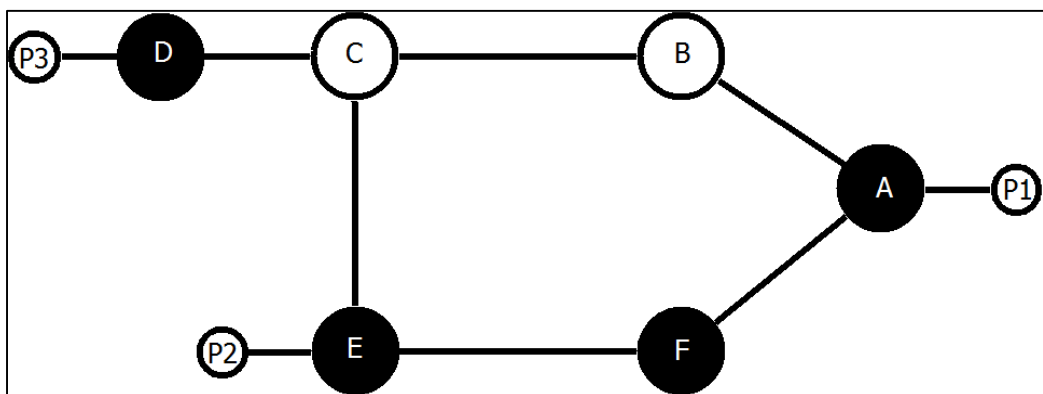


Fig. 6 - 1: Illustrative example

In this network there are 4 nodes powered by non-renewable energy (black nodes) and two powered by renewable energy (white nodes). P1, P2 and P3 are peers that share a piece of data. If P1 needs to upload a piece to P2 then the longer path {A-B-C-E} is lower in non-renewable power consumption compared to the minimum hop path {A-F-E} as the traffic in the longer path goes through 2 black nodes (A and E) compared to 3 black nodes (A, F, and E) in the minimum hop path.

Consider a scenario where P1 has a piece of data that is of interest to both P2 and P3 where any peer can upload only one piece to only one peer at a time. For simplicity we will also assume that any peer can upload only one copy of the piece at all times. If all nodes are powered by non-renewable energy, the optimal solution is the local selection matrix (LSM) where P1 uploads the piece to P2 and then P2 uploads it to P3, taking 6 nodes in total to finish. The LSM results in the minimum power consumption, assuming the traffic is routed using MHRT.

However, with renewable energy sources available at nodes B and C and with the objective of minimising the non-renewable power consumption, the optimal selection changes so that the number of traversed black nodes is minimised. Therefore, P1 uploads the piece to P3 and then P3 uploads the piece to P2, taking 7 nodes to finish. Based on the routing and peers' selection criteria, four solutions exist to upload the piece to P2 and P3, summarised in Table 6 - 1.

| Approach [Routing Policy-Peer Selection] | Paths | #of white Nodes | # of black Nodes |
|--|--------------------------------|------------------------|-------------------------|
| [MHRT-LSM] | {P1-A-F-E-P2}+{P2-E-C-D-P3} | 1 | 5 |
| [MHRT-GSM] | {P1-A-B-C-D-P3}+{P3-D-C-E-P2} | 3 | 4 |
| [GRT-LSM] | {P1-A-B-C-E-P2} +{P2-E-C-D-P3} | 3 | 4 |
| [GRT-GSM] | {P1-A-B-C-D-P3}+{P3-D-C-E-P2} | 3 | 4 |

Table 6 - 1: Different approaches to deliver a data piece from P1 to P2 and P3 in Fig. 6 - 1

The first approach, referred to as MHRT-LSM, constrains the routing and selection matrix to the MHRT and LSM, respectively, resulting in traversing 5 black nodes to deliver the piece to P2 and P3. In the second approach the constraints on the selection matrix are released while maintaining the MHRT so that the model is free to optimise the selection matrix trading locality with non-renewable power saving. Such a selection matrix is referred to as Green Selection Matrix (GSM). This

approach, referred to as MHRT-GSM, reduces the number of black nodes traversed by the traffic demands to 4 nodes. This however comes at the cost of increasing the total number of hops as two white nodes are traversed to avoid traversing a single black node. The third approach, however, maintains the LSM and minimises the non-renewable power consumption by releasing the constraint on the routing table so the routing is optimised similar to [20]. We refer to this approach as GRT-LSM. Note that the second approach has the advantage of simple implementation as implementing changes in the application layer is less complex than the network layer. The fourth approach is the most optimal where both the routing table and selection matrix are optimised, referred to as GRT-GSM.

Note that this example is artificially selected so that the three last approaches yield the same non-renewable power consumption (4 black nodes). The results in Section 6.4 highlight the non-renewable power savings achieved by the different approaches in a more general complicated scenario.

6.3 Renewable Energy for P2P Networks MILP

In this section we extend the MILP model developed in Section 3.2 to evaluate the power consumption of BitTorrent based P2P systems over IP/WDM networks to take into account the presence of renewable energy sources. In the following we introduce the parameters, variable and constraints that are relevant to this section, others are similar to those defined in Section 3.2

Parameters:

| | |
|-----------|--|
| Pre | Power consumption of a regenerator |
| RG_{mn} | Number of regenerators between node pair (m,n) per wavelength. |
| RE_m | Maximum available renewable power at node m |

Variables (All are non-negative real numbers):

| | |
|----------------|---|
| Wb_{mn}^{sd} | A binary variable that indicates the presence of wavelength channels in the physical link (m,n) to serve the traffic demand between nodes (s,d) . |
| PC_m | Total power consumption of node m . |
| $PCRE_m$ | Renewable power consumption of node m . |
| $PCNRE_m$ | Non-renewable power consumption of node m . |
| H_{sd} | Number of physical hops between node pair (s,d) . |

Note that we do not account for virtual links, denoted as (i,j) in Section 3.2 as we directly map traffic demands into physical links to deduce the physical layer routing table, considering non-bypass approach. This is done by replacing (i,j) indexes with (s,d) and setting $C_{ij} = L_{ij}/B$, where L_{ij} is the sum of swarms traffic (L_k^{ij}) and regular traffic (L_r^{ij}) between nodes i and j .

Also we account for the power consumption of the regenerators, as follows:

$$\sum_{m \in N} \sum_{n \in NM_m} PRE \cdot RG_{mn} \cdot W_{mn}$$

The model is defined as follows:

Objective : Maximise

$$\alpha \cdot \sum_{k \in SW} \sum_{i \in L_k} Avdr_{ik} - \sum_{m \in N} PCNRE_m \quad (6-1)$$

Subject to: Constraints (3-2), (3-6)-(3-13), plus the following:

$$PC_m = Prp \cdot Q_m + Prp \cdot \sum_{n \in Nm_m} W_{mn} + \sum_{n \in Nm_m} Pt \cdot W_{mn} + \sum_{n \in Nm_m} Pe \cdot A_{mn} \cdot F_{mn} + \sum_{n \in Nm_m} Pre \cdot RG_{mn} \cdot W_{mn} + PO_m \quad (6-2)$$

$$\forall m \in N,$$

$$PC_m = PCRE_m + PCNRE_m \quad (6-3)$$

$$\forall m \in N,$$

$$PCRE_m \leq Prp \cdot Q_m + Prp \cdot \sum_{n \in Nm_m} W_{mn} + \sum_{n \in Nm_m} Pt \cdot W_{mn} + PO_m \quad (6-4)$$

$$\forall m \in N,$$

$$PCRE_m \leq RE_m \quad (6-5)$$

$$\forall m \in N,$$

$$M1 \cdot W_{mn}^{sd} \geq Wb_{mn}^{sd} \quad (6-6)$$

$$\forall s, d, m \in N \quad \forall n \in Nm_m: s \neq d,$$

$$W_{mn}^{sd} \leq M2 \cdot Wb_{mn}^{sd} \quad (6-7)$$

$$\forall s, d, m \in N \quad \forall n \in Nm_m: s \neq d,$$

$$\sum_{m \in N} \sum_{n \in Nm_m} Wb_{mn}^{sd} = H_{sd} \quad (6-8)$$

$$\forall s, d \in N: s \neq d,$$

$$\sum_{n \in Nm_m} Wb_{mn}^{sd} = 1 \quad (6-9)$$

$$\forall s, d, m \in N: s \neq d,$$

Equation (6-1) gives the model objective where the download rate is maximised while minimising the non-renewable power consumption. Note that the parameter α (Table 6 - 2) is used to scale the average download rate to be comparable to the non-renewable power consumption and ensures compatibility of units in the two terms in (6-1). Constraint (6-2) calculates single node m power consumption. Constraint (6-3) splits the power consumption of node m into renewable power consumption and non-renewable power consumption. Constraints (6-4) and (6-5) put limits on the maximum utilised renewable power at node m . Constraint (6-4) ensures that renewable power is replacing all or part of the power consumption of routers, transponders, and optical switches at node m , while not exceeding the maximum renewable power available in this node as defined by constraint (6-5). Note that the links' EDFAs and regenerators in our model are always powered using non-renewable power as they are distributed in remote sites and also have limited power consumption. Constraints (6-6)-(6-8) calculate all nodes routing tables (H_{sd}). Constraints (6-6) and (6-7) ensure that $Wb_{mn}^{sd} = 1$ whenever $W_{mn}^{sd} > 0$, otherwise, $Wb_{mn}^{sd} = 0$. $M1$ is a large enough unitless number that ensures that the left hand side of (6-6) is either zero or larger than 1. $M2$ is a large enough unitless number that ensures the satisfaction of (6-7) when $W_{mn}^{sd} > 0$. Constraint (6-8) calculates nodes'

routing table (i.e. physical paths between nodes) based on Wb_{mn}^{sd} . Constraint (6-9) prevents bifurcation in the physical layer.

We are also interested in other approaches where pre-specified routing table (MHRT-GSM) and/or selection matrix (GRT-LSM and MHRT-LSM) are to be imposed. In such approaches, the resulting non-renewable power consumption will not be the minimum that can be achieved. These approaches can be realised by replacing the variables Wb_{mn}^{sd} and U_{ijk} by the parameters WP_{mn}^{sd} and UP_{ijk} , respectively, prescribed to the MHRT and LSM, respectively, obtained by running the model with the objective of minimising the total power consumption. In these cases constraints (6-2)-(6-9) have to satisfy the imposed parameters.

6.4 Renewable Energy for P2P Networks MILP Results

The NSFNET network is considered as an example network to evaluate the power consumption of P2P content delivery over hybrid power IP/WDM networks. In this section we use different values for the different IP/WDM networking elements based on the GreenTouch study in [91], [113]. Table 6 - 2 lists the input parameters for the model.

| | |
|---|------------|
| Power consumption of a router port (Prp) | 440 W [91] |
| Power consumption of transponder (Pt) | 148 W [91] |
| Power consumption of an optical switch (PO_i) $\forall i$ | 85 W [91] |
| Power consumption of an EDFA (Pe) | 52 W [91] |
| Power consumption of a regenerator (Pre) | 222 W [91] |
| No. of wavelengths per fibre (W) | 32 |
| Factor of average download rate (α) | 1,000,000 |

Table 6 - 2: Input data for renewable energy in P2P networks model

The content distribution scenario in Section 3.3 is considered where we solve the model for 20 swarms and assume that the network contains 8k replicas of these 20 swarms, i.e. a total of 160k swarms. Each swarm consists of 100 randomly and uniformly distributed peers in the network, 15 of them are seeders with a complete copy of a file while the rest are leechers seeking to download the file. Each peer can have a maximum of four upload slots. All peers are homogeneous in terms of the

upload capacity (1 Mbps). Also BitTorrent accounts for 50% of the total traffic. We set α to a large enough value ($\alpha = 1,000,000$) to ensure all peers use all of their 4 upload slots without dwarfing the power consumption value in the objective function.

Solar energy is used as the renewable energy source and is assumed to be only available at core nodes to power routers, transponders and optical switches, but not regenerators and EDFAs as these are scattered in secondary sites throughout the links. Regardless of the fact that solar energy is fundamentally limited and varies throughout the day, we assume enough solar energy is available to satisfy the power consumption of the node where solar cells are deployed (the impact of solar power diurnal cycle is previously considered in [20]). We have adopted this choice here because in this work we are interested in designing the best approach rather than analysing real time performance variations where renewable energy (wind, solar) variation constraints should be taken into account.

In the following results, the non-renewable power consumption (NRE) and renewable power consumption (RE) of the different approaches discussed in Section 6.2 are evaluated versus an increasing number of nodes with access to renewable energy.

We start with the scenario where all nodes are powered by non-renewable energy sources and gradually power the NSFNET nodes from left to right (from node 1 to node 14, see Fig. 3 - 1), with renewable sources, where 5 nodes powered by renewable energy means nodes 1,2,3,4 and 5 have access to renewable energy. We use the terms green nodes and nodes with renewable energy sources interchangeably in this section.

6.4.1 MHRT-LSM Approach

The results of this approach are obtained by replacing the routing table (Wb_{mn}^{sd}) and the selection matrix (U_{ijk}) variables by the parameters WP_{mn}^{sd} and UP_{ijk} , respectively as discussed in Section 6.3. As this approach does not change any of the decision variables, i.e. traffic demands between nodes and the paths travelled by demands are maintained, the non-renewable power consumption of green nodes in the minimum hop routes is replaced by renewable power, conserving the total power

consumption at the level of the scenario where no renewable energy is available as shown in Fig. 6 - 2.

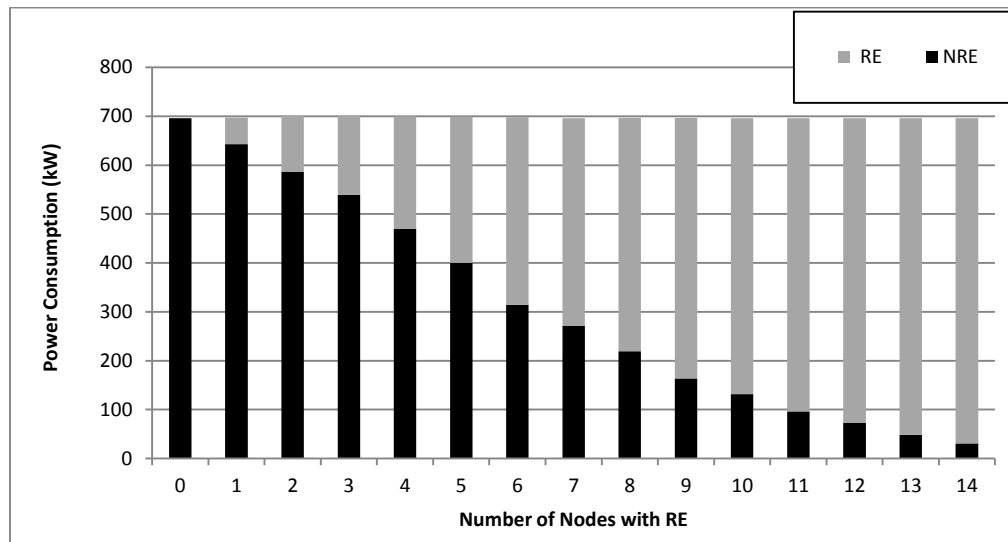


Fig. 6 - 2: Power consumption versus increasing number of green nodes for the MHRT-LSM approach

6.4.2 GRT-GSM Approach

The results of this approach are obtained by running the model introduced in Section 6.3 where it is free to optimise the routing table Wb_{mn}^{sd} and the selection matrix (U_{ijk}) variables for minimum non-renewable power consumption.

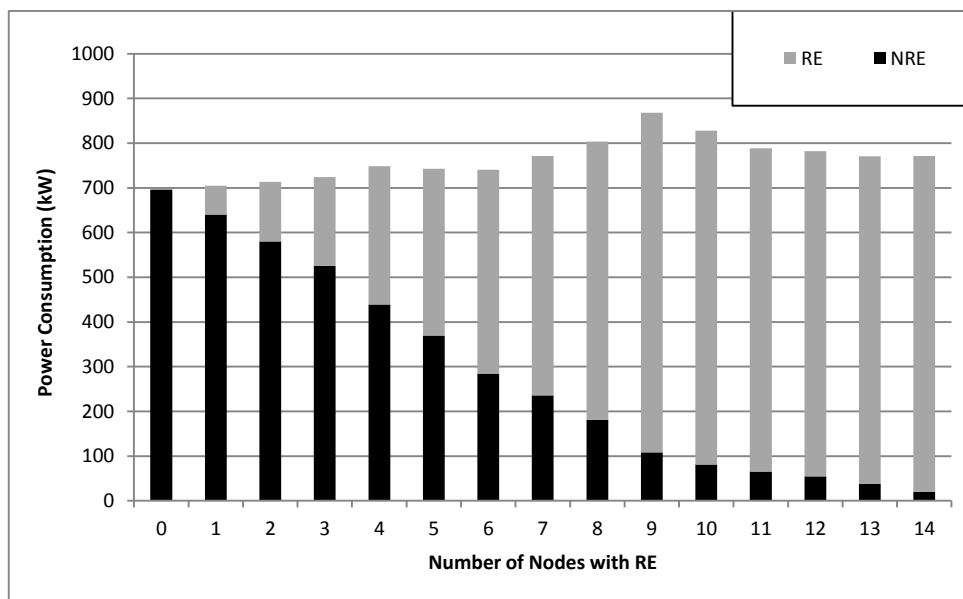


Fig. 6 - 3: Power consumption versus increasing number of green nodes for the GRT-GSM approach

Fig. 6 - 3 shows that optimising both the routing table and the selection matrix does not maintain the total power consumption at the level achieved when all nodes were powered by non-renewable energy. The total power consumption in this case increases as more nodes are powered by renewable energy. This is because the minimum hop routes are replaced by routes of minimum number of non-renewable energy nodes, resulting in increasing the average hop count as explained in Section 6.2, and therefore the total power consumption increases.

The increase in total power consumption continues up to the case where renewable energy is available to 9 nodes after which the total power consumption starts declining. This is because more nodes in the minimum hop routes become powered by renewable energy minimising the need to go through routes of more hops and therefore reducing the amount of renewable power consumed to save a certain amount of non-renewable power. Fig. 6 - 3 shows a maximum saving of 39% (10 Green nodes case) achieved by the GRT-GSM approach compared to the MHRT-LSM approach.

Note that in the case where the NSFNET 14 nodes are fully powered by renewable energy, and as the objective is to minimise the non-renewable power consumption, traffic demands will be routed through shortest distance paths rather than MHRT. This is because shortest distance routing reduces the number of EDFAs and regenerators, the only devices powered by non-renewable energy in our scenario. Therefore the total power consumption at 14 green nodes is higher than that at 0 green nodes.

In the following subsections, we investigate the amount of contribution attributed to the GRT and the GSM in the non-renewable power savings achieved by the GRT-GSM approach by examining the savings achieved by the MHRT-GSM approach where the routing table, Wb_{mn}^{sd} , is replaced by WP_{mn}^{sd} and the GRT-LSM approach where the selection matrix, U_{ijk} , is replaced by UP_{ijk} .

6.4.3 MHRT-GSM Approach

The results of this approach are obtained by replacing the variable Wb_{mn}^{sd} by the parameter WP_{mn}^{sd} while optimising the selection matrix variable, U_{ijk} . Thus, locality is traded for non-renewable power savings.

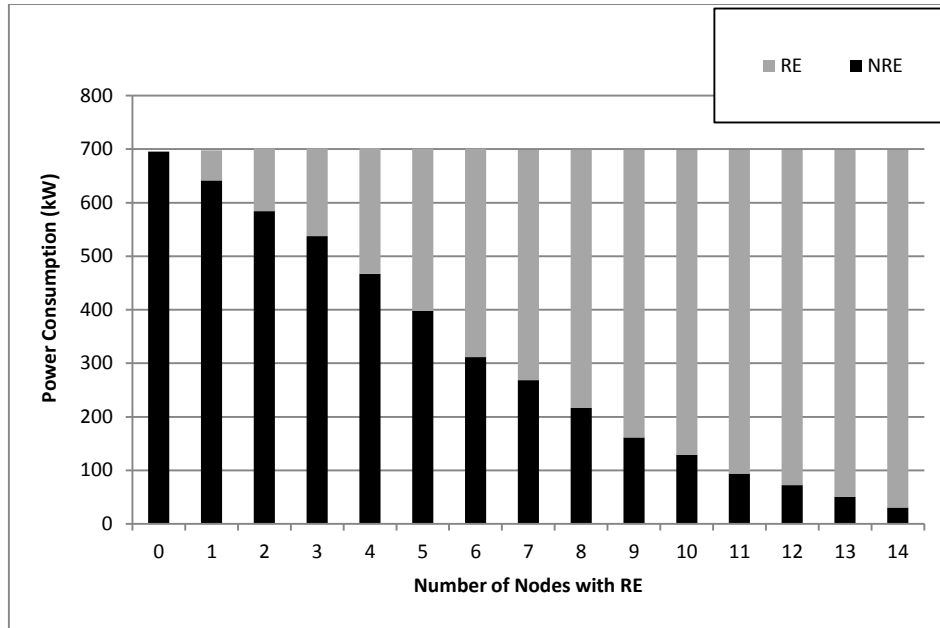


Fig. 6 - 4: Power consumption versus increasing number of green nodes for the MHRT-GSM approach

Fig. 6 - 4, however, shows almost similar renewable and non-renewable power consumption levels to those of the MHRT-LSM approach in Fig. 6 - 2. This is due to the fact that the LSM results in minimum renewable and non-renewable power consumption as peers tend to mostly unchoke other peers located in the same core node and such local selection does not contribute to the power consumption in the IP layer of the IP/WDM network. The local node unchoke accounts for 94% of the selection matrix, leaving the MHRT-GSM approach with 6% of the selections to optimise which represents a small portion of the total network traffic taking regular traffic into account. The non-renewable power savings of this approach compared to the MHRT-LSM approach is limited to a maximum of 2% (11 Green nodes case).

6.4.4 GRT-LSM Approach

The results of this approach are obtained by replacing the variable U_{ijk} by the parameter UP_{ijk} while optimising the routing table variable, Wb_{mn}^{sd} . Fig. 6 - 5 shows that the total power consumption of the GRT-LSM approach parallels the one observed in Fig. 6 - 3, with maximum non-renewable power savings of 37% (10 Green nodes case) compared to the MHRT-LSM approach. This proves the fact that the GRT-GSM approach behaviour is mainly attributed to the optimisation of the

network layer routing table rather than optimising the P2P selection matrix in the application layer.

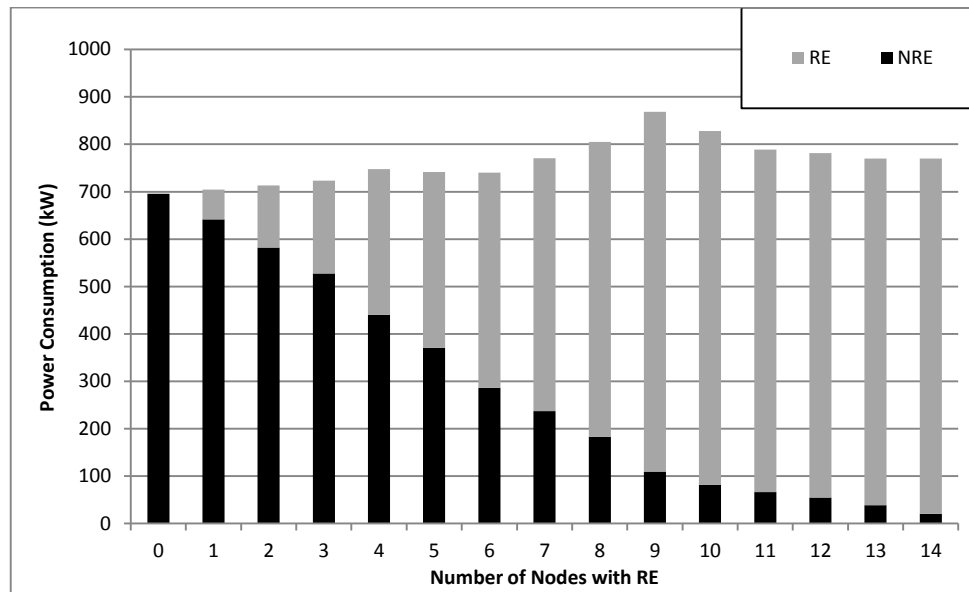


Fig. 6 - 5: Power consumption versus increasing number of green nodes for the GRT-LSM approach

To understand the impact of renewable energy awareness either in the application or network layers, we show the average hop count for the different approaches in Fig. 6 - 6. Note that the hop count for GRT-GSM and GRT-LSM approaches follows similar trend to the total power consumption for these two approaches (Fig. 6 - 3 and Fig. 6 - 5). This shows that the change in the total power consumption is attributed to change in the routes taken by traffic demands where longer paths in terms of number of green hops are preferred over shorter paths of non-renewable powered nodes. The GRT-GSM and GRT-LSM approaches increase the average hop count in the network by 37% compared to the MHRT-LSM approach. On the other hand, the MHRT-GSM approach did not change the minimum average hop count and yielded similar behaviour as that of the MHRT-LSM approach.

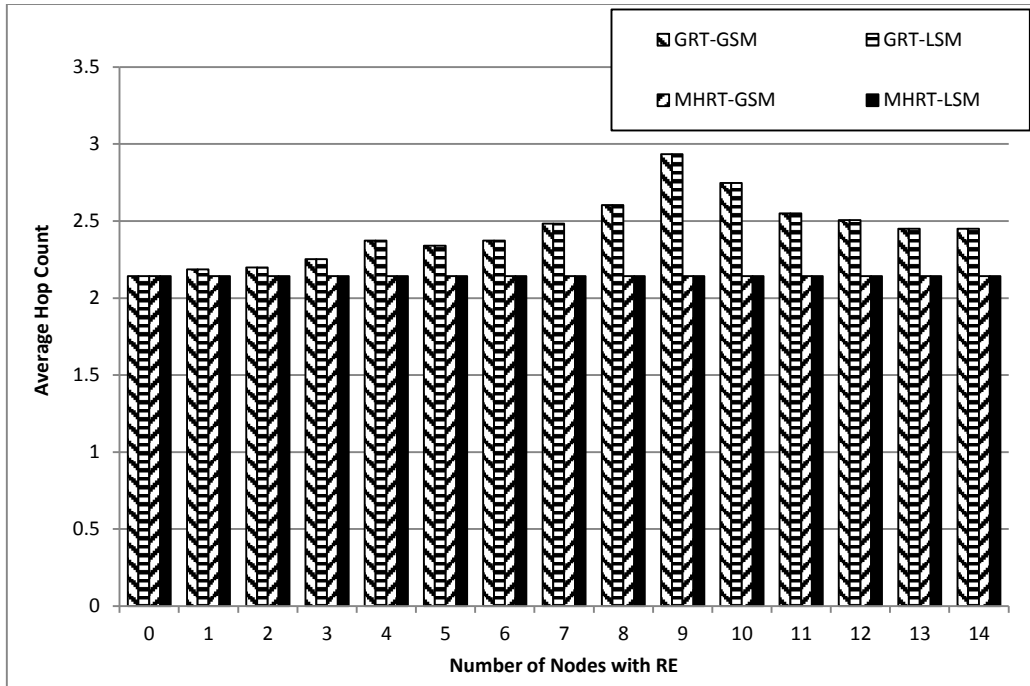


Fig. 6 - 6: Average hop count versus increasing number of green nodes

We summarise the findings above by showing the relative power consumption of each approach considering the MHRT-LSM power consumption as a baseline (100% relative power consumption) as shown in Fig. 6 - 7.

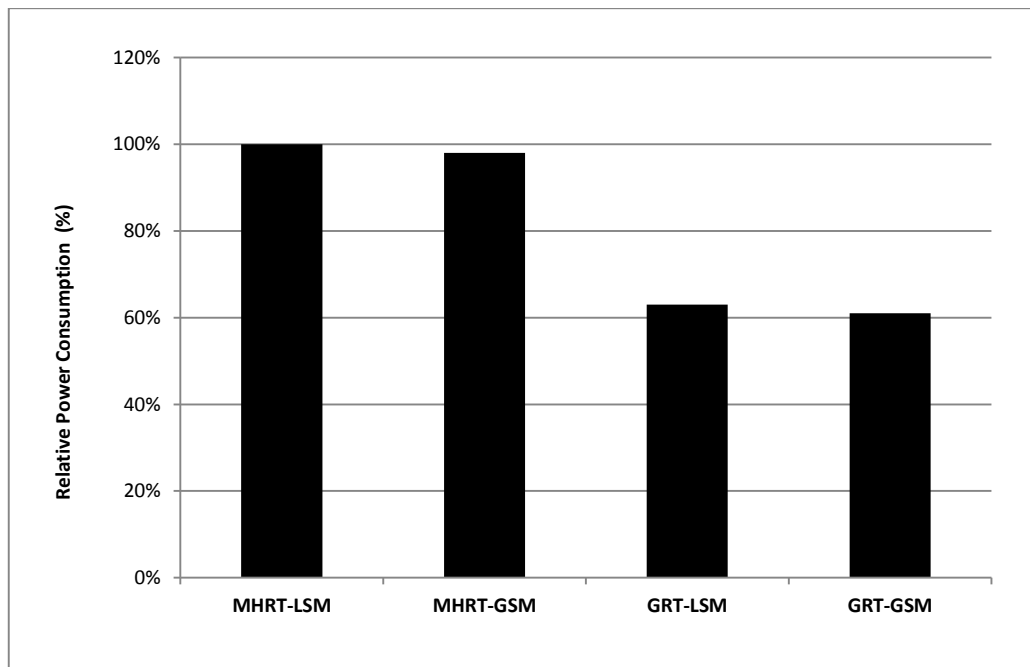


Fig. 6 - 7: Relative power consumption of the four approaches

6.4.5 Quasi Selection Matrix (MHRT-QLSM & MHRT-QGSM) Approaches

We have seen in Fig. 6 - 4 that optimising the selection matrix has a limited impact on optimising the use of renewable energy for the energy efficient BitTorrent where peers tend to localise their peers selection. However, the tendency to localise peers selection introduced by the energy efficient BitTorrent based systems imposes a number of limitations including the loss of robustness, possible peers isolation and not being efficient in distributing “not very popular” content. These limitations might lead the ISP to limit this tendency by restricting the localisation of peers’ selection. In such cases, the use of renewable energy can be further optimised and further non-renewable power savings can be achieved by optimising the peers’ selection matrix where more cross traffic is generated between nodes.

We consider a scenario where peers are not allowed to select other peers in the same node. Such a scenario can be obtained by augmenting constraints (3-2), (3-10)-(3-12) with $NP_{ik} \neq NP_{jk}$, where NP_{ik} is the node where peer i that belongs to swarm k exists. We call the local and green selection matrices in this case; Quasi-LSM (QLSM) (quasi as the local selection of LSM in this case excludes the selection of peers in the same node) and Quasi-GSM (QGSM), respectively.

Fig. 6 - 8 shows non-renewable power savings up to 11% (14 green nodes case) achieved by the MHRT-QGSM approach compared to the MHRT-QLSM approach. However, for the majority of the cases considered, the difference in non-renewable power consumption is limited. This is due to the fact that at limited number of green nodes the QGSM has similar criteria in selecting peers to the QLSM where peers at minimum number of hops are preferred. As more nodes become powered by renewable energy the QGSM will select peers at shortest path distances to reduce non-renewable power consumption at EDFAs and regenerators. More savings of up to 36% (14 green nodes) can be achieved when only P2P traffic is present in the network. Fig. 6 - 8 also includes the previous results of Fig. 6 - 2 (MHRT-LSM) and Fig. 6 - 4 (MHRT-GSM) to show the impact of less locality on the overall non-renewable power consumption as less locality means more traffic crossing the network and consequently more power consumption for the Quasi approaches compared to the original approaches (MHRT-LSM and MHRT-GSM).

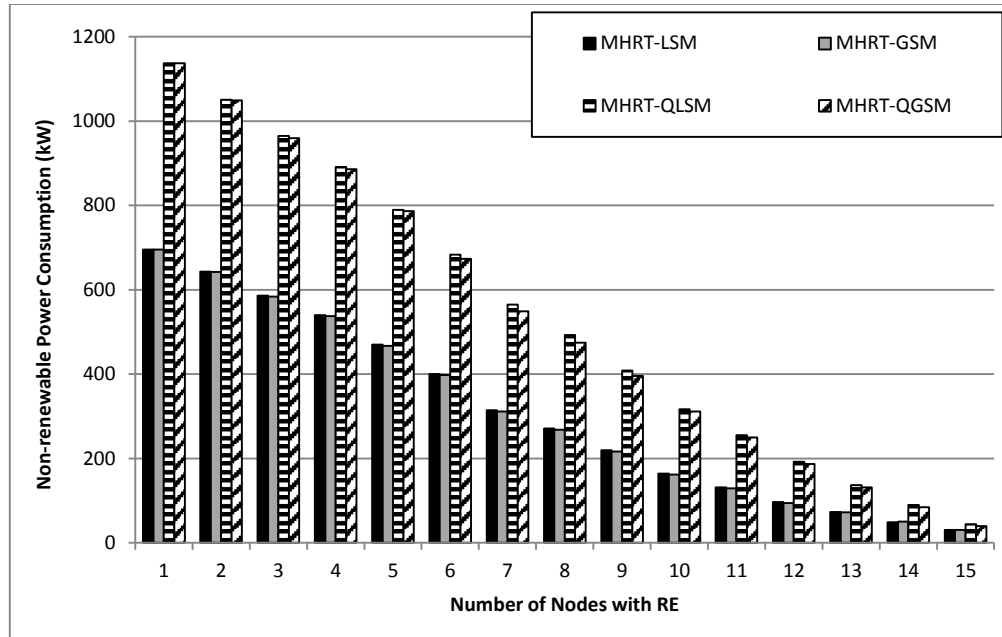


Fig. 6 - 8: Non-renewable power consumption versus increased number of green nodes where no local unchoke is allowed

Regardless of the time complexity issues, implementing a renewable energy tapping heuristic in the application layer is favourable compared to imposing changes in the network layer as any miss-coordination between nodes can cause service failure.

6.5 Renewable Energy for Distributed Clouds Networks

In our analysis in this section, renewable energy is only available to clouds while the IP/WDM network is powered by non-renewable energy. We have chosen wind farms as the source of renewable energy as they are very promising in terms of production capacity and the price per megawatt hour compared to non-renewable energy [114]. The decision of a cloud provider to migrate/replicate its content near to renewable energy sources is governed by the trade-off between the non-renewable power savings achieved by powering the cloud using renewable energy and the power consumption of the network through which users requests traverse to the new cloud location. The aim of the study in this section is to investigate this trade-off taking into account the power losses in electrical power transmission lines delivering renewable energy from wind farms to clouds as well as investigating the associated optimal content replication pattern.

6.6 Renewable Powered Content Delivery Cloud Model

In the energy efficient content delivery cloud model developed in Section 4.2, the model selects, based on users requests, the optimal number and location of clouds as well as the capability of each cloud so that the total power consumption is minimised. The model also decides how to replicate content in the cloud so that the minimum power is consumed in delivering content. In this section we extend the model in Section 4.2 to consider the availability of renewable energy sources to power the cloud. We assume the following:

- The IP/WDM network is powered by non-renewable energy.
- Wind farm power is available to power clouds. However, to maintain service availability in case of limited wind farm power, clouds also have access to non-renewable energy sources.
- There is no restriction on the number of wind farms powering a given cloud.
- Only a fraction, ρ , of the wind farm power is available to power the clouds. We considered examples where ρ takes the values 0, 0.001, and 0.005. These 3 cases refer to the two extremes of interest, namely no renewable energy is available ($\rho=0$), the renewable energy available is enough to power the clouds ($\rho=0.005$), and a case in between these two ($\rho=0.001$).
- The electric power transmission loss (PL_{ws}) to deliver power from wind farms to clouds is assumed to be 15% per 1000 km [21].
- As in Section 4.2, the popularity of the different objects of the content follows a Zipf distribution. We also divide the content in our model into equally sized popularity groups where each group contains objects of similar popularity.

We consider the following sets, parameters and variables

Sets:

WF Set of Wind Farms

Parameters:

| | |
|-----------|--|
| PL_{ws} | Fraction of electric power lost due to transmission power losses between wind farm w and the cloud in node s . |
| WP_w | The maximum output power of wind farm w . |
| ρ | The fraction of wind farms power available to clouds. |

Variables (All are non-negative real numbers):

| | |
|---------------|--|
| Δ_{ws} | The amount of renewable power of wind farm w assigned to power the cloud in node s . |
| $TNNRP$ | Total IP/WDM network non-renewable power consumption. |
| $CNRP_s$ | Cloud s non-renewable power consumption. |
| $TCNRP$ | Total clouds non-renewable power consumption. $TCNRP = \sum_s CNRP_s$ |
| CRP_s | Cloud s renewable power consumption. |
| $TCPC_s$ | Cloud s total power consumption. |
| $TPLOSS$ | Total transmission power losses |

Three constituents are to be minimised in our model:

- a. **Total IP/WDM Network Non-Renewable Power consumption ($TNNRP$):**
This is composed of the same elements as in Section 4.2, however, we include regenerators power consumption as in Section 6.3, and also consider the non-bypass approach.
- b. **Total Clouds Non-Renewable Power consumption ($TCNRP$):** This is composed of the same elements as in Section 4.2.
- c. **Transmission Power LOSSes between wind farms and clouds ($TPLOSS$):**
These is calculated as follows: $\sum_{w \in WF} \sum_{s \in N} \Delta_{ws} \cdot PL_{ws}$

The model is defined as follows:

Objective: Minimise

$$\sigma \cdot TNNRP + \theta \cdot TCNRP + \omega \cdot TPLOSS \quad (6-10)$$

Subject to: All constraints in Section 4.2, plus the following:

$$\begin{aligned} TCPC_s &= CNRP_s + CRP_s \\ \forall s \in N, \end{aligned} \quad (6-11)$$

$$\begin{aligned} CRP_s &= \sum_{w \in WF} \Delta_{ws} \cdot (1 - PL_{ws}) \\ \forall s \in N, \end{aligned} \quad (6-12)$$

$$\begin{aligned} \sum_{s \in N} \Delta_{ws} &\leq WP_w \cdot \rho \\ \forall w \in WF. \end{aligned} \quad (6-13)$$

Equation (6-10) gives the model objective which is to minimise the IP/WDM network non-renewable power consumption, the cloud non-renewable power consumption and transmission power losses subject to weights σ, θ , and ω , respectively where the values of the weights are decided by the relevant approach as will be discussed in Section 6.7. Constraint (6-11) dictates the combination of renewable and non-renewable energy sources that will power a cloud s . Note that $TCPC_s$ is a single cloud s power consumption (servers, storage and internal LAN power consumption) calculated according to Section 4.2 neglecting the sum over the index s . Constraint (6-12) calculates the renewable power delivered to each cloud from the different wind farms subject to transmission losses. Constraint (6-13) ensures that for each wind farm the total renewable energy allocated to power clouds does not exceed the total renewable energy available to power the clouds.

6.7 Renewable Powered Content Delivery Cloud Results

The NSFNET network, depicted in Fig. 6 - 9 is considered as an example network to evaluate the power consumption of the cloud content delivery service over non-bypass IP/WDM networks with wind farms located at nodes 4, 6 and 8, which are current US wind farm locations [21].

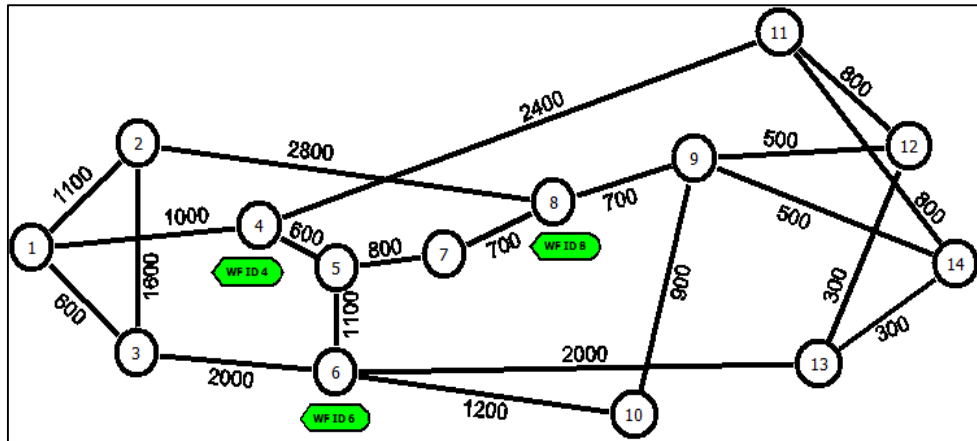


Fig. 6 - 9: The NSFNET network with wind farms locations

In our evaluation, users are uniformly distributed among the NSFNET nodes and the total number of users in the network is 1,200k, estimated based on the data in [21]. The maximum output power of the three wind farms 4, 6 and 8 is 300, 700, and 400 MW [21], respectively.

For input data, we use the same IP/WDM network values considered in Table 6 - 2. The cloud parameters are the same values as in Table 4 - 1. The MILP model is solved using the 64 bit AMPL/CPLEX software on an Intel Core i5, 2.4 GHz PC with 4 GB memory.

We study three approaches to optimise the use of wind farms renewable energy to power content delivery clouds:

6.7.1 Approach 1: $\sigma = 1, \theta = 1$ and $\omega = 1$

This approach considers equally minimising the three elements of equation (6-10). Fig. 6 - 10 shows the clouds power consumption for different values of ρ . At $\rho=0$, all the power supplied is non-renewable and the model decides to replicate content into all the 14 possible locations according to the content popularity (OPR) where the majority of content is kept and served from the cloud in node 6 (Fig. 6 - 11, blue bars) as this location has the lowest number of hops to other nodes, hence, lowest network power consumption. At $\rho=0.001$ the model decides to keep the distribution of content almost the same as the case with $\rho=0$ (Fig. 6 - 11, red bars). In this case only clouds located at nodes with wind farms are powered by renewable energy as this results in the lowest transmission power losses and therefore efficiently utilises the limited renewable energy available. At $\rho=0.005$, the amount of renewable energy is

sufficient to power clouds at all nodes without the need for non-renewable energy. However, to reduce the transmission losses, the model limits the number clouds to 3 clouds each with a full copy of the content. (Fig. 6 - 11, green bars).

Note that at $\rho=0.005$, cloud 8 (i.e. the cloud built at node 8) has the highest power consumption (Fig. 6 - 10) in spite of the fact that all clouds have the same storage capacity (Fig. 6 - 11, green bars). This is because cloud 8 serves more users than the other two clouds as it is closer, in terms of minimum hop and/or minimum distance, to more nodes. This approach minimises the transmission power losses by limiting number of built clouds. However, this comes at the cost of increasing the network power consumption by 33% compared to $\rho=0$. The next approach investigates compromising transmission losses for more power saving at the network side.

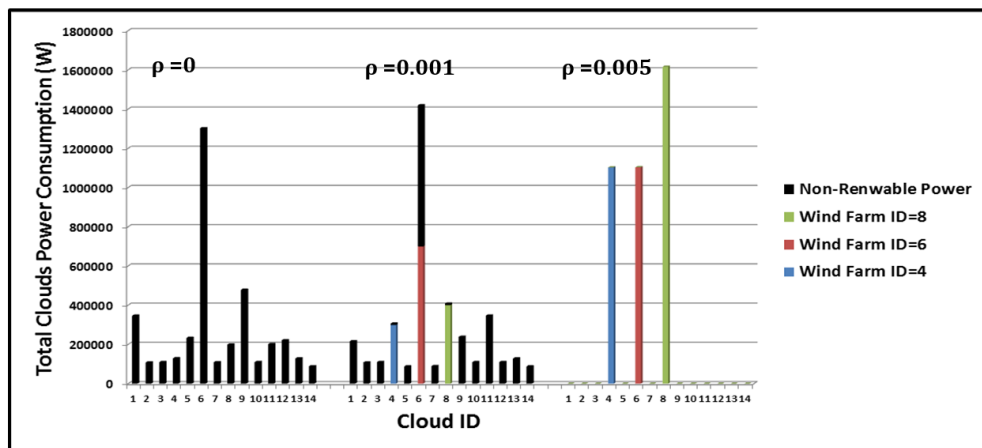


Fig. 6 - 10: Clouds power consumption (Approach 1)

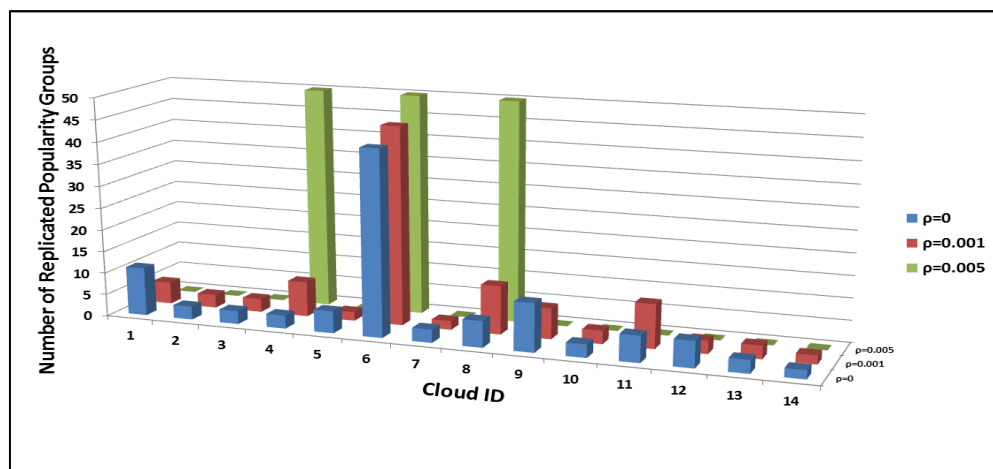


Fig. 6 - 11: Number of popularity groups (Approach 1)

6.7.2 Approach 2: $\sigma = 1, \theta = 1$ and $\omega = 0$

By setting $\omega = 0$, the model minimises the network and cloud non-renewable power consumption without explicitly considering transmission losses in the objective function. The results of this approach are shown in Fig. 6 - 12 and Fig. 6 - 13. Note that the replication scheme has not changed at $\rho=0$ and $\rho=0.001$ compared to Approach 1, resulting in similar total power consumption. This is because although transmission losses are not considered explicitly in the objective, constraint (6-12) will ensure that transmission losses are minimised to efficiently utilise the limited renewable energy available. With enough renewable energy ($\rho=0.005$), the model decides to fully replicate content in all the 14 nodes (Fig. 6 - 13, green bars). This configuration yields the minimum network power consumption as users requests are served from local clouds; therefore, only optical switches will be needed, resulting in only 1,785W of network power consumption. However, note that clouds 4 and 6 are not powered by their nearby wind farms 4 and 8, respectively. This is because enough renewable energy is available to power clouds at all nodes from any of the wind farms and as the transmission losses are not taken into account in the objective function, 1.5 MW of renewable power is lost in transmitting the renewable power from wind farms to clouds which is drastically higher than the non-renewable power saved at the IP/WDM network side (210 kW). In the next approach we investigate the minimum transmission losses required to maintain the minimum network power consumption.

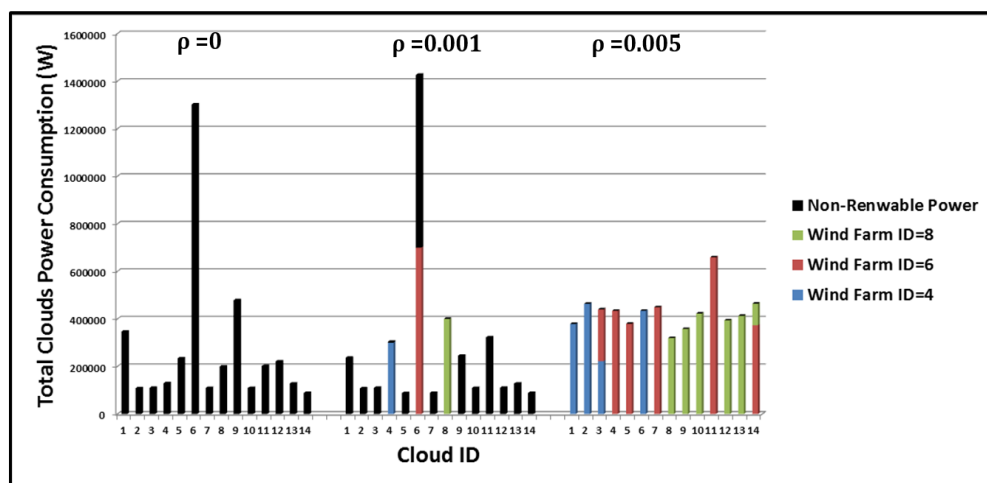


Fig. 6 - 12: Clouds power consumption (Approach 2)

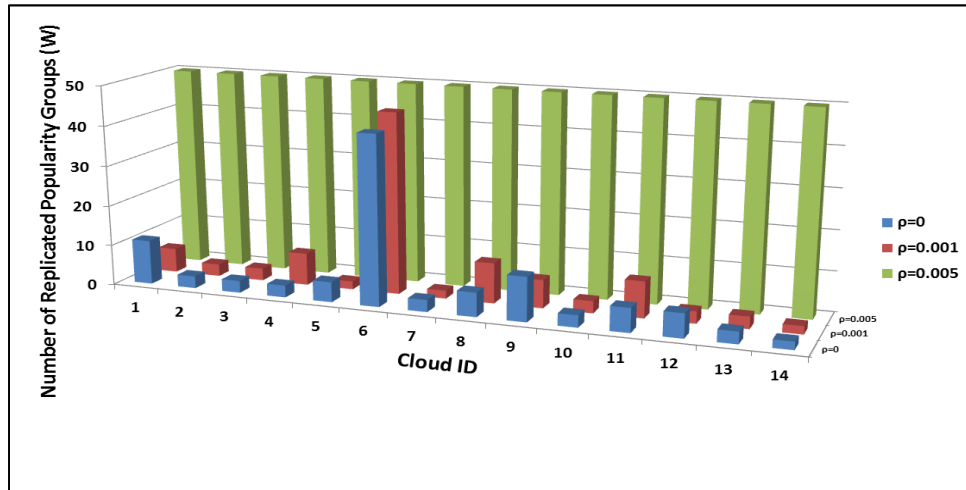


Fig. 6 - 13: Number of popularity groups (Approach 2)

6.7.3 Approach 3: $\sigma = 100$, $\theta = 1$ and $\omega = 1$

In this approach, the network power consumption is given a higher weight in the objective function than the cloud non-renewable power consumption and the transmission losses. The results of this approach are shown in Fig. 6 - 14. In all cases, clouds with fully replicated content are created at all nodes to keep the network power consumption to its minimum. At $\rho=0.001$, as the amount of renewable energy available to power the clouds is not enough to power full replication at each cloud, wind farms power is mainly assigned to local clouds and other clouds are powered by non-renewable energy. The full replication at clouds powered totally or partially by non-renewable energy increases, increasing the total non-renewable power consumption by 25% compared to Approaches 1 and 2.

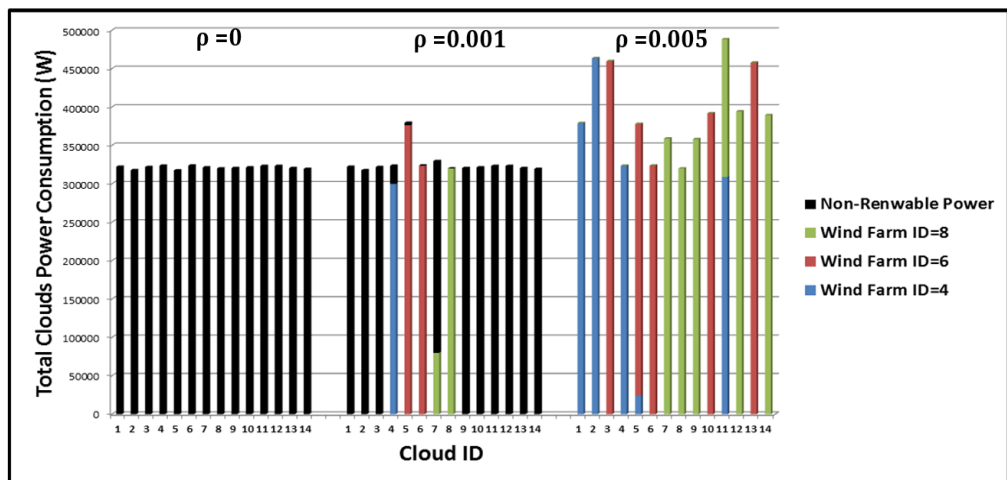


Fig. 6 - 14: Clouds power consumption (Approach 3)

At $\rho=0.005$, the model manages to achieve the minimum network power consumption while saving 35% of transmission power compared to Approach 2. However, this is still larger than the power saved in the IP/WDM network side as 4.73W of renewable power have to be lost in transmission to save 1W of non-renewable power at the IP/WDM network.

Therefore, if total power consumption is the only metric to compare these different approaches, Approach 1 will be the appropriate solution as it yields the minimum transmission losses. However, if the aim is to reduce CO₂ emission, which is a product of non-renewable energy generation, Approach 1 can be implemented when there is a limited amount of renewable energy while Approach 3 is implemented where sufficient renewable power is available.

6.8 Summary

In this chapter, first, we studied different approaches of optimising the utilisation of renewable energy in BitTorrent-based P2P systems over hybrid powered IP/WDM networks where the energy sources are a mix of renewable and non-renewable sources. These approaches are based on different combinations of routing and peers selection. The MILP results show that the renewable energy sources can be efficiently tapped in a P2P system by optimising the routing table so that the number of traversed nodes powered by non-renewable power is minimised while local peers selection is maintained. Optimising the routing has resulted in non-renewable power savings up to 37% compared to the minimum hop routing with renewable energy. The non-renewable power savings associated with the peer selection optimisation is limited to 2%, given our input parameters, due to the tendency to localise peers selection. This leads to an overall 39% power saving when both the routing policy and peers selections are optimised. On the other hand, the tendency to localise peer selection might imposes a number of limitations including the loss of robustness and peers isolation, leading ISPs to limit this tendency by restricting the local peers selection. Our model results show that in a scenario where peers are not allowed to select other peers located in the same node, the optimisation of peers' selection can further contribute to the non-renewable power saving.

Second, we developed a MILP model to study the impact of renewable energy availability, represented by wind farms, on the location of clouds and the content replication schemes of cloud content over IP/WDM networks. In our analysis, we assume that renewable energy is only available to power clouds while the IP/WDM network is powered by non-renewable energy. Our results show that popularity based replication in clouds is the most energy efficient content replication scheme when the clouds are powered only by non-renewable energy sources or when renewable energy availability is limited. With abundant renewable energy, a cloud with a full copy of the content can be built at each node. However, the model should achieve a trade-off between the transmission power losses to deliver renewable energy from wind farms to clouds and the non-renewable power consumption of the IP/WDM network. We discussed this trade-off and showed how to optimise the transmission power losses of renewable energy while minimising the non-renewable network power consumption.

Chapter 7: Conclusions and Future Work

This chapter summarises the work that has been performed in this thesis and states its original contributions. Furthermore, potential future threads of research that can be pursued as a result of work in this thesis are suggested.

7.1 Summary of Contributions

In this thesis, an investigation is reported considering the problems of joint optimisation of energy consumption of optical core networks represented by an IP/WDM network, P2P, and distributed clouds systems. Different research problems have been investigated where each problem has been formulated as a MILP model, and then a heuristic. Experimental demonstrations were developed to assess the work in real time environments.

In Chapter 3, first, we evaluated the energy consumption of BitTorrent; the most popular P2P application over bypass and non-bypass IP/WDM networks and compared it to C/S systems. We developed a MILP model to minimise the power consumption of the BitTorrent systems and to evaluate their performance. The results indicated that the original BitTorrent protocol, based on random peer selection, is energy unaware, and therefore has a similar energy consumption at the network side as a typical C/S model when considering similar delivery scenarios. However, the energy-efficient BitTorrent protocol we introduced, which exploits locality, can reduce the energy consumption of BitTorrent in IP/WDM networks by 30% and 36% compared to the C/S networks under the bypass and non-bypass

approaches, respectively, while maintaining the optimal download rate. Investigating the behaviour of our energy efficient BitTorrent model showed that the model converges to locality where peers select each other based on their location rather than randomly. We built a heuristic to mimic the MILP model behaviour and comparable energy savings were achieved with a reduction of 13% in the achieved download rate. The results of an enhanced EEBT heuristic showed that to match the performance of the OBT protocol, peers have to cross more hops if the number of peers in the local node is not sufficient, which decreases the energy saving to 11% compared to 17% when peers are limited to one hop across the network.

Second, we also showed that a heterogeneous BitTorrent system with two upload capacity classes resulted in a 50% energy consumption reduction compared to the C/S model, as the overall time required to finish downloading was minimised.

Third, we evaluated the impact of leechers' behaviour on the network performance and energy consumption. We developed a model that optimises the upload rate of operator controlled seeders to compensate for leechers leaving the network after finishing downloading. Our proposed approach with operator controlled seeders produced results that approach the performance of the altruistic case where all leechers stay to seed after finishing downloading. Comparable energy savings were achieved by the energy-efficient heuristic with about an 8% reduction in average download rate. We have also shown that to mitigate the impact of leechers leaving the network after finishing downloading, optimising the location as well as the upload rate of operator controlled seeders maintains the download rate. Moreover, this saves 15% energy compared to the case where leechers stay after finishing the downloading process.

Fourth, we investigated the impact of physical topology on the energy consumption of BitTorrent systems. The results show that the EEBT was able to achieve higher energy savings in networks with fewer nodes for a given swarm size as the probability of finding sufficient peers locally to connect with increases. For two networks with the same number of nodes, the energy efficiency is a function of the average hop count as the number of network devices in the optical layer increases with the hop count.

Fifth, we investigated the power consumption of VoD services using CDN, P2P, and the promising hybrid CDN-P2P architecture over bypass IP/WDM networks. We developed a MILP model to analyse the performance of the hybrid CDN-P2P architecture. Our results indicated that the location aware hybrid CDN-P2P is a promising architecture not only in terms of cost and performance, but also in terms of energy consumption. We investigated two scenarios for the hybrid CDN-P2P architecture: the H-MinNPC model where the model minimises the IP/WDM network power consumption and the H-MinTPC model where the model minimises the total power consumption including the network and CDN datacentres. While, the H-MinTPC saved 61% of the total power consumption compared to the CDN-Only architecture, the savings achieved by the H-MinNPC were limited to 32%. The energy efficiency introduced by the hybrid CDN-P2P architecture can effectively defer the upgrade of CDN datacentres in terms of capacity and energy efficiency. The results also show that to maintain the power savings achieved by the H-MinNPC model, the P2P system should maintain an average file sharing effectiveness of $\eta=0.43$. Furthermore, we showed that attempts by content providers to balance the load among their datacentres will not affect the overall energy savings and performance of the hybrid architecture.

Finally, we conducted an experimental evaluation of OBT and EEBT. The results show about a 40% saving in power consumption for the EEBT while the average download rate was maintained at 1 Mbps.

In Chapter 4 we introduced a framework for energy efficient cloud computing services over non-bypass IP/WDM core networks. We analysed two cloud services, namely: Content Delivery and Storage as a Service (StaaS). Mixed Integer Linear Programming (MILP) optimisation was developed for this purpose to study network related factors, including the number and location of clouds in the network and the impact of demand, popularity, and access frequency, on the cloud placement as well as cloud capability factors, including the number of servers, switches and routers, and amount of storage required at each cloud. We studied different replication schemes and analysed the impact of content storage size. Optimising the cloud content delivery revealed that replicating content into multiple clouds based on content popularity (OPR scheme) was the optimum scheme to place content in core networks where at low traffic most of the content was kept in node 6 of the NSFNET

network, while at high traffic more popularity groups were replicated into more clouds, as under higher loads, the power consumption of the cloud was offset by higher savings on the network side.

First, we showed that OPR resulted in 72% and 40% network and total (network and cloud) power savings, respectively, compared to a power un-aware centralised content delivery scenario. The results also showed that higher network and total power savings of 92% and 43%, respectively, can be achieved for clouds of smaller sized content, such as music files. With such small file sizes, the MPR scheme, which builds clouds everywhere, is shown to have a similar performance as OPR; however, under a scenario with a non-uniform user distribution or with a fixed (idle) power component for placing the cloud in a certain location, OPR is expected to outperform MPR as it might not be necessary to build 14 clouds.

Second, for real time implementation, we developed an energy efficient content delivery heuristic, DEER-CD, based on the model insights. Comparable power savings were achieved by the heuristic.

Third, the results of the StaaS scenario show that at lower access frequencies, the optimal cloud scheme serves all users from the central cloud, while at higher access frequencies content is migrated to serve users locally, which results in savings of 48% and 2% of the network and total power compared to serving content from a single central cloud for an average file size of 45MB. Limited total power savings were obtained for smaller file sizes.

In Chapter 5 we studied the problem of virtual machine placement in the context of distributed clouds over an IP/WDM network considering VM workload induced power consumption and VM traffic induced power consumption in the network. Optimising the placement of VMs showed that VM Slicing was the best approach compared to migration or replication schemes. However, this was under the assumption that the minimum normalised workload per slice is 5%. For VMs with larger minimum normalised workloads per slice, slicing might approach VM migration in power saving as it would be difficult to have more local slices. VM slicing saves 76% and 25% of the network and total power, respectively, compared to a single virtualised cloud scenario. Comparable power savings were obtained by

placing VMs using a heuristic (DEER-VM) developed to mimic the model behaviour in real time.

In Chapter 6 we studied the impact of renewable energy availability on P2P and distributed cloud networks. First, we investigated the utilisation of renewable energy sources in BitTorrent based P2P protocols over hybrid power IP/WDM networks. We studied different approaches of routing and peer selection. Our results showed that BitTorrent based P2P systems can efficiently utilise renewable energy sources by optimising the routing table so the number of traversed nodes powered by non-renewable power was minimised while local peer selection was maintained. Such optimisation resulted in non-renewable power savings up to 37% compared to the minimum hop routing with renewable energy. Limited savings, 2%, were obtained from the optimisation of the selection matrix due to the tendency of localised peer selection. We also investigated scenarios where the peer selection localisation was restricted by ISPs to mitigate the impact of locality on robustness and content sharing efficiency. The results showed that further non-renewable power savings of up to 11% and 36% for the cases where regular traffic is or is not considered, respectively, could be achievable.

Second, we studied the impact of renewable energy availability, represented by wind farms, on cloud location optimisation and content replication schemes of content delivery clouds over non-bypass IP/WDM networks. We developed a model to achieve a trade-off between the non-renewable power savings gained by powering the cloud with renewable energy and the power consumption of the network through which users' requests travel to the new cloud location, taking into account the power losses in electrical transmission lines delivering renewable energy from wind farms to the clouds. We optimised the use of renewable energy under different scenarios. We have shown that building mini clouds in different network locations based on content popularity is the most energy efficient approach when clouds are powered by non-renewable sources or when renewable energy is restricted. However, a trade-off between transmission losses and non-renewable power consumption in the IP/WDM network exists when there is enough renewable energy to power all the clouds. With typical transmission losses as well as network and cloud power consumption, building clouds in proximity to wind farms reduces transmission losses; however it would be at the cost of consuming more non-renewable power at the network side.

On the other hand, if the transmission losses were not considered, but the renewable energy available were distance dependent, then building a cloud in each node results in savings in network power consumption if enough renewable energy is available. However, if the network power consumption were the only driving force, then creating clouds with full content would be the optimal configuration regardless of the availability of renewable energy.

The results and approaches of this work are subject to certain number of limitations and assumptions.

First, MILP takes very long time to solve large problems. This can be few hours, to few days. This limits the ability to test the ideas presented in this work for larger sets of input parameters such as large number of swarms or popularity groups.

Second, MILP models accuracy is only validated by heuristics, which is a reasonable validation as heuristics are in close agreement with the MILP models and work independently of the MILP models. However, it is necessary to validate MILP results using other techniques such as evolutionary algorithms and simulated annealing to further establish the findings of this work.

Third, not all MILP models have been validated by heuristics, such as the work on CDN-P2P. Therefore, further investigation is needed to assess the power savings obtained in real time environments.

Fourth, the experimental demonstration for EEBT which is based on the EEBT heuristic principles features only one particular peers distribution, which is 4 peers in each of the NSFNET nodes, one of them is a seeder and the other peers are leechers. However, other arrangements have to be investigated, such as the presence of one seeder only which would represent a challenge for the traffic localisation principle. Therefore, the power savings reported warrant further investigation especially consideration of averaging / performance over larger set of peers placements.

Fifth, it is assumed that the only performance requirement included in this work is the total download rate the end users achieve given the different approaches. However, other QoS and reliability requirements that can be investigated include latency, average blocking rate, and backup paths. Some of those requirements, such as low latency, might require traffic balance among different network links, which

conflicts with the aim of reducing power consumption by powering off the maximum number of network resources. Therefore, a trade-off has to be established which would eventually lead to lower power savings.

Sixth, The ICT technology is not mature enough currently to produce products with linear relationship between resource utilisation and power consumption, which is an assumption in this work. Therefore, the power savings reported represent the minimum bounds of what can be achieved in core networks and clouds. More technical efforts at the circuit and components levels are needed to reach such as minimum bounds in single communication devices. However, when operating with a large number of ICT devices (such as large number of servers or large number of router ports), such assumption of linear relation becomes more realistic given that these devices work at their peak loads.

The work in this thesis has led to a considerable impact. The experimental testbed in Section 3.11 was demonstrated at the GreenTouch consortium members meeting held 5-8 November 2012 at the Alcatel-Lucent Bell Lab facility in Stuttgart, Germany. I also delivered a presentation to explain the work I have conducted in energy efficient P2P content delivery in core optical networks. The demonstration was attended by many GreenTouch consortium members where I answered several questions and received researchers and industrial experts' feedback. It served as a first step towards the adoption of our energy efficient content distribution work in GreenTouch. Our content distribution architecture and protocols have now been adopted by GreenTouch.

The concepts introduced in Chapters 4 and 5 (distributed clouds), Mixed Integer Linear Programming Models and Heuristics have been adopted by GreenTouch as the basis for the GreenMeter v2.0 energy efficient content distribution. GreenMeter v2.0 was released in June 2015 [115]. The GreenMeter provides the architecture, protocols and hardware designs to be used by the GreenTouch industrial members (vendors and operators) and the wider industry to improve energy efficiency in their networks. GreenTouch has 50+ member organisations including vendors: Alcatel-Lucent (and Alcatel-Lucent Bell Labs), Huawei, Fujitsu; and Service providers including France Telecom, AT&T, Swiss Com, China Mobile, NTT. It led to invited talks at INFOCOM 2013, SoftCOM 2013, JANET Networkshop 2014, NOC 2014, OSA Photonics in Switching 2014, and ICC 2014. The concepts introduced in

Section 4.2 have been experimentally demonstrated at the GreenTouch celebration event hosted by Bell Labs Alcatel-Lucent in New York City on June 18, 2015. The analytic models, the heuristics and hardware demo produced results that are in close agreement. The demo represents the NSFNET core network where each node is represented by a server for hosting content and by a router for data forwarding. The demo results show increase in traffic as more users join the network, but also increase in network power consumption as a result. Users are served in this case from one central location. The results also show that after some time and when we introduce distributed data centres or clouds, a reduction in network power consumption is observed. The details of this demo are not included in this thesis.

7.2 Future Work

In this section several future directions for the topic of energy efficient P2P and cloud networks in the Internet are proposed.

7.2.1 Extensions Based On Stated Limitations

The first possible future work is to address the limitations of this thesis mentioned above. One conceivable direction is to validate the findings of this work that are investigated using MILP mathematical modelling by using another optimisation technique, such as genetic algorithms. Another possible direction is to consider other metrics in the objective function such as latency, reliability, blocking rate ...etc. In addition, experimental evaluation can be extended toward CDN-P2P where both work on distributed clouds and P2P can be brought together.

7.2.2 Re-Connect the Network Dots, From Core to Aggregation to Access

An intuitive extension to this work is to include other layers in the hierarchy of telecommunication networks, namely aggregation and access layers. This can reformulate the problem in a wider context where resource placement can be jointly optimised from the core to access networks, either wireless/wired or hybrid access networks. This is better, in terms of optimisation scope and energy efficiency gains, than isolating each layer and optimising it separately from other layers.

7.2.3 Multi-Level Resource Swarms of IP/WDM Networks

We can re-define the concept of swarms to cover a wider scope. Rather than being PCs participating in sharing one file, they can be any collection of IP/WDM nodes sharing certain types of components. For example, we can divide the IP/WDM network into different levels of routers, OXCs, and regenerators. If a multi-level node works in a P2P fashion with other nodes, it can provide a service and ask for a reward from other nodes at different times. For instance, a certain IP/WDM node A, can route the traffic of another node B via the least utilised path, reducing blocking. At another time, node A can be rewarded by node B through providing traffic regeneration for node A traffic passing through node B using one of node B's regenerators. Clouds can add another level over each IP/WDM node and can manage node interactions in this P2P control network.

7.2.4 Game Theoretical Approach for Clouds over IP/WDM networks

Clouds located in IP/WDM networks may belong to several cloud service providers rather than one owner. These providers can cooperate with each other, such as forming coalitions, to respond to users' requests. The IP/WDM network itself can be an active player in these games, participating in the optimal placement of request resources and the set of responding clouds. This means that ISPs can play a role in cloud computing resource management, resulting in a win-win state. On one hand, the IP/WDM network will feed better status information for the clouds, while on the other hand, the IP/WDM network will have better predictions for traffic variation resulting from the clouds' responses to users' requests. Other benefits can be investigated as well.

7.2.5 Energy Efficient Publish/Subscribe for IoT in IP/WDM Networks

Rather than P2P, the publish/subscribe approach of data exchange builds a C/S overlay layer between IoT devices, which enables the overlay multicasting of IoT status updates to their users (subscribers). The IoT traffic is aggregated from the access network towards datacentres where the algorithms that decide where to send the update messages are implemented. These algorithms can be abstracted in virtual machines and migrated/replicated or sliced as necessary to several IP/WDM nodes to

save energy. In addition, the TCP connection between publishers and VMs can be jointly optimised with VM placement to yield further energy saving.

7.2.6 Optimising the Number of Upload Slots' and Their Data Rate for BitTorrent

The BitTorrent MILP model can be extended to optimise the default number of upload slots, which are assumed to be 4 in this work, for energy efficiency. Also the data rate of each slot, which is assumed to be fixed at 0.25 Mbps can be optimised. This requires substantial change for the formulation of the MILP model as the current formulation would lead to a non-linear solution, beyond the scope of what CPLEX can achieve. Therefore, peer selection, uploads slots number, and upload slots rate can be jointly optimised to yield further energy savings.

7.2.7 Big Data in IP/WDM Networks

Big data can originate from several sources, such as transportation systems, the healthcare sector, home automation, sensor networks, surveillance networks ...etc. Most of these sources are located deep in the access networks. However, the raw data generated needs to be aggregated and transported to data centres for information processing to extract useful knowledge. The aggregated raw data travels through access networks, aggregation networks and core networks before reaching data centers. This incurs high power consumption at core networks as they receive large amount of raw traffic. We can mitigate the impact of big data by progressively processing the raw data at the edge of the core networks and also at the intermediate nodes between the edge nodes and the data centers. This is expected to lead to large amount of power savings in core IP/WDM networks.

7.2.8 Integrating Queuing Theory with MILP for Content Distribution in Distributed Clouds in IP/WDM Networks

The work can be extended by integrating queuing theoretical models with the MILP formulation. This will enable the optimisation of servers' CPU utilisation, which is assumed to be fixed in this work. Optimised server's CPU utilisation opens a new degree of freedom in the MILP model that can be harnessed to evaluate the impact of latency and average blocking rate bounds of the problem, yielding more realistic results for the models. For instance, users can define a minimum bound for

the time by which their job in the VMs are to be accomplished, which would require more servers' CPU utilisation to comply with this delay constraint.

List of Abbreviations

| | |
|-------|-------------------------------------|
| AMPL | A Mathematical Programming Language |
| AT&T | American Telephone & Telegraph |
| C/S | Client/Server |
| CAPEX | Capital Expenditures |
| CCN | Content Centric Network |
| CDN | Content Delivery Networks |
| CP | Content Provider |

| | |
|---------|---|
| CPU | Central Processing Unit |
| CRS | Carrier Routing System |
| CSA | Closest Source Assignment |
| DEER-CD | Distributed Energy Efficient Resources – Content Delivery |
| DEER-VM | Distributed Energy Efficient Resources – Virtual Machine |
| DVFS | Dynamic Voltage and Frequency Scaling |
| DWDM | Dense Wavelength Division Multiplexing |
| ECONET | Low Energy Consumption Networks |
| EDFA | Erbium-Doped Fibre Amplifiers |
| EEBT | Energy Efficient BitTorrent |
| EPB | Energy Per Bit |
| EST | Eastern Standard Time |
| EUBT | European British Telecom |
| GB | Giga Bytes |
| Gbps | Giga bit per second |

| | |
|--------|--|
| GRT | Green Routing Table |
| GSM | Green Selection Matrix |
| HP | Hewlett Packard |
| HTTP | HyperText Transfer Protocol |
| ICT | Information and Communication Technologies |
| IoT | Internet of Things |
| IP/WDM | Internet Protocol/Wavelength Division Multiplexing |
| IPTV | Internet Protocol Television |
| ISP | Internet Service Provider |
| IT | Information Technology |
| ITU | International Telecommunication Union |
| LAN | Local Area Network |
| LRF | Local Rarest First |
| LSM | Local Selection Matrix |
| MB | Mega Bytes |

| | |
|-----------|--------------------------------------|
| Mbps | Mega bit per second |
| MFR | Maximum Full Replication |
| MHRT | Minimum Hop Routing Table |
| MILP | Mixed Integer Linear Programming |
| MNR | Maximum No Replication |
| MPR | Maximum Popularity based Replication |
| MSB | Minimised Server Bandwidth |
| Mux/Demux | Multiplexers/Demultiplexers |
| MW | Mega Watt |
| NP | Nondeterministic Polynomial |
| NRE | Non-Renewable Energy |
| NSFNET | National Science Foundation Network |
| OBT | Original BitTorrent |
| OCS | Operator Controlled Seeder |
| OEO | Optical Electrical Optical |

| | |
|------|--------------------------------------|
| OFR | Optimum Full Replication |
| ONR | Optimum No Replication |
| OPR | Optimum Popularity based Replication |
| OXC | Optical Cross Connect |
| P2P | Peer to Peer |
| PAP | Peer Assisted Patching |
| PC | Personal Computer |
| PG | Popularity Group |
| PUE | Power Usage Effectiveness |
| QGSM | Quasi Green Selection Matrix |
| QLSM | Quasi Local Selection Matrix |
| QoS | Quality of Service |
| RAND | Random |
| QoS | Quality of Service |
| RE | Renewable Energy |

| | |
|-------|-------------------------------|
| SLA | Service Level Agreement |
| SNPM | Single No Power Management |
| SPM | Single with Power management |
| TB | Tera Bytes |
| TCP | Transmission Control Protocol |
| TFT | Tit For Tat |
| VANET | Vehicular Ad Hoc Networks |
| VM | Virtual Machine |

References

- [1] GSMA Intelligence, “Mobile broadband reach expanding globally ” Available <https://gsmaintelligence.com/research/2014/12/mobile-broadband-reach-expanding-globally/453/>. Last accessed 04/04/2015.
- [2] Internet world stats, Available <http://www.internetworldstats.com/stats.htm>. Last accessed 04/04/2015.
- [3] Cisco, “Cisco Visual Networking Index: Forecast and Methodology, 2014–2019” white paper, Available http://www.cisco.com/c/en/us/solutions/collateral/service-provider/ip-ngn-ip-next-generation-network/white_paper_c11-481360.html. Last accessed 04/04/2015.
- [4] N. Lyndon, H. Graham, L. Dave, F. Agata, and S. Elena, “Future of the Internet of Services for Industry: the ServiceWeb 3.0 Roadmap” *Future Internet Assembly (FIA 2009)*, 23-24 Nov 2009, Stockholm, Sweden.
- [5] I. Monga, “Going Green Introduction to Network energy- efficiency research” *Lawrence Berkeley National Lab* 16/Jan/ 2013.
- [6] J. Choi, J. Han, E. Cho, T. T. Kwon, and Y. Choi, “A Survey on content-oriented networking for efficient content delivery” *IEEE Communications Magazine*, vol. 49, pp. 121-127, 2011.
- [7] A. Zaslavsky, C. Perera, and D. Georgakopoulos, “Sensing as a service and big data” *arXiv preprint arXiv:1301.0159*, 2013.
- [8] University of Melbourne News, “High speed broadband will create energy bottleneck and slow Internet, new University of Melbourne study” Available <http://archive.uninews.unimelb.edu.au/view-22711.html>. Last accessed 04/04/2015.
- [9] Ericsson, “Energy and Carbon Report” Nov/2014, Available <http://www.ericsson.com/res/docs/2014/ericsson-energy-and-carbon-report.pdf>. Last Accessed 09/06/201.

- [10] CNN, “50,000 BitTorrent users sued alleged illegal downloads” Available http://money.cnn.com/2011/06/10/technology/bittorrent_lawsuits/. Last accessed 04/04/2015.
- [11] N. Qadri, M. Fleury, M. Altaf, B. R. Rofoee, and M. Ghanbari, “Resilient P2P multimedia exchange in a VANET” *Wireless Days (WD), 2nd IFIP*, pp. 1-6, 2009.
- [12] Z. Luo, T. Zhang, S. Han, and J. Liang, “A coordinated p2p message delivery mechanism in local association networks for the Internet of Things” *IEEE 7th International Conference on e-Business Engineering (ICEBE)*, pp. 319-325, 2010.
- [13] Cisco, “Converge IP and DWDM Layers in the Core Network” *White Paper 2007*, Available <http://www.webtorials.com/main/resource/papers/cisco/paper114/ConvergeIPandDWDMLayersintheCoreNetwork.pdf>. Last Accessed 09/06/2015.
- [14] G. Shen and R. Tucker, “Energy-minimized design for IP over WDM networks” *IEEE/OSA Journal of Optical Communications and Networking*, vol. 1, no. 1, pp. 176–186, 2009.
- [15] J. Berthold, A. A. M. Saleh, L. Blair, and J. M. Simmons, “Optical Networking: Past, Present, and Future” *IEEE/OSA Journal of Lightwave Technology*, vol. 26, pp. 1104-1118, 2008.
- [16] U. Lee, I. Rimac, and V. Hilt, “Greening the internet with content-centric networking” *1st International Conference on Energy-Efficient Computing and Networking. e-Energy 10*, pp. 179-182, 2010.
- [17] R. Bolla, R. Bruschi, F. Davoli, and F. Cucchietti, “Energy efficiency in the future internet: A survey of existing approaches and trends in energy-aware fixed network infrastructures” *IEEE Communications Surveys & Tutorials*, vol. 13, no. 2, pp. 223–244, 2011.
- [18] “Econet” Available <http://www.econet-project.eu/>. Last Accessed: 02/04/2015.
- [19] <http://www.greentouch.org/>. Last Accessed: 18/06/2015.
- [20] X. Dong, T. El-Gorashi, and J. M. H. Elmirghani, “IP Over WDM Networks Employing Renewable Energy Sources” *IEEE/OSA Journal of Lightwave Technology*, vol. 29, no. 1, pp. 3–14, 2011.
- [21] X. Dong, T. El-Gorashi, and J. M. H. Elmirghani, “Green IP Over WDM Networks With Data Centers” *IEEE/OSA Journal of Lightwave Technology*, vol. 29, no. 12, pp. 1861–1880, 2011.
- [22] X. Dong, T. El-Gorashi, and J. Elmirghani, “On the energy efficiency of physical topology design for IP over WDM networks” *IEEE/OSA Journal of Lightwave Technology*, vol. 30, no. 12, pp. 1931–1942, 2012.

- [23] Z. Yi, P. Chowdhury, M. Tornatore, and B. Mukherjee, “Energy Efficiency in Telecom Optical Networks” *IEEE Communications Surveys & Tutorials*, vol. 12, pp. 441-458, 2010.
- [24] P. Gill, M. Arlitt, Z. Li, and A. Mahanti, “The flattening internet topology: Natural evolution, unsightly barnacles or contrived collapse?” *Passive and Active Network Measurement*, ed: Springer, pp. 1-10, 2008.
- [25] E. K. Lua , J. Crowcroft, M. Pias, R. Sharma, and S. Lim, “A survey and comparison of peer-to-peer overlay network schemes” *IEEE Communications Surveys & Tutorials*, vol. 7, no. 2, pp. 72–93, 2005.
- [26] B. Cohen, “Incentives build robustness in BitTorrent” *Workshop on Economics of Peer-to-Peer systems*, vol. 6, pp. 68-72. 2003.
- [27] Envisional Ltd, “Technical report: An Estimate of Infringing Use of the Internet”, January 2011. Available http://documents.envisional.com/docs/Envisional-Internet_Usage-Jan2011.pdf. Last Accessed 9 Dec 2013.
- [28] Sandvine Corporate, “Global Internet Phenomena Report”, 2011. Available http://www.wired.com/images_blogs/epicenter/2011/05/SandvineGlobalInternetSpringReport2011.pdf. Last accessed 9 Dec 2013.
- [29] R. Bindal, P. Cao, and W. Chan, “Improving traffic locality in BitTorrent via biased neighbor selection” *The 26th International Conference on Distributed Computing Systems, ICDCS06*, vol. 06, pp. 66–66, 2006.
- [30] A. Legout, G. Urvoy-Keller, and P. Michiardi, “Rarest first and choke algorithms are enough” *6th ACM SIGCOMM conference on Internet measurement*, pp. 203–216, 2006.
- [31] J. He, A. Chaintreau, and C. Diot, “A performance evaluation of scalable live video streaming with nano data centers” *Computer Networks*, vol. 53, no. 2, pp. 153–167, 2009.
- [32] D. Xu, S. Kulkarni, C. Rosenberg, and H. K. Chai, “A CDN-P2P hybrid architecture for cost-effective streaming media distribution” *Computer Networks*, vol. 44, no. 3, pp. 353–382, 2004.
- [33] G. Anastasi, I. Giannetti, A. Passarella, “A BitTorrent Proxy for Green Internet File Sharing: Design and Experimental Evaluation”, *Computer Communications*, vol. 33, no. 7, pp. 794-802, May 2010.
- [34] H. Hlavacs, R. Weidlich, and T. Treutner, “Energy efficient peer-to-peer file sharing”, *The Journal of Supercomputing*, vol. 62, no. 3, pp. 1167–1188, Apr. 2011.

- [35] D. Qiu and R. Srikant, "Modeling and performance analysis of BitTorrent-like peer-to-peer networks" *ACM SIGCOMM Computer Communication Review*, vol. 34, no. 4, pp. 367–378, 2004.
- [36] S. Nedeveschi, S. Ratnasamy, and J. Padhye, "Hot Data Centers vs. Cool Peers" *Workshop on Power Aware Computing and Systems (HotPower '08)*, San Diego, CA, Dec 2008.
- [37] U. Mandal, C. Lange, A. Gladisch, P. Chowdhury, and B. Mukherjee, "Energy-efficient content distribution over telecom network infrastructure" *13th International Conference on Transparent Optical Networks (ICTON)*, June 2011.
- [38] A. Feldmann, M. Kind, A. Gladisch, G. Smaragdakis, C. Lange, and F. J. Westphal, "Energy trade-offs among content delivery architectures" *9th Conference of Telecommunication, Media and Internet Techno-Economics (CTTE)*, Ghent, Belgium, June 2010.
- [39] W. Huang, C. Wu, and F. C. M. Lau, "The Performance and Locality Tradeoff in BitTorrent-Like P2P File-Sharing Systems" *IEEE International Conference on Communications*, pp. 1–5, May 2010.
- [40] S. Kang and H. Yin, "A Hybrid CDN-P2P System for Video-on- Demand", *IEEE International Conference on Future Networks*, pp. 309-313, 2010.
- [41] Z. Lu, J. Wu, and W. Fu, "Towards a Novel Web Services Standard-Supported CDN-P2P Loosely-Coupled Hybrid and Management Model" *IEEE International Conference on Services Computing (SCC)*, pp. 297-304, 2010.
- [42] P. Shi, H. Wang, Y. Gang, and X. Yuan, "ACON: Adaptive construction of the overlay network in CDN-P2P VoD system" *IEEE 3rd International Conference on Communication Software and Networks (ICCSN)*, pp. 182–187, 2011.
- [43] C. A. Chan, E. Wong, A. Nirmalathas, and C. Jayasundara, "Energy Efficient Delivery Methods for Video-rich Services over Next Generation Broadband Access Networks" *IEEE International Conference on Communications (ICC)*, pp. 1-5, 2011.
- [44] U. Mandal, C. Lange, A. Gladisch, and B. Mukherjee, "Should ISPs adopt hybrid CDN-P2P in IP-over-WDM networks: An energy-efficiency perspective?" *IEEE International Conference on Advanced Networks and Telecommunications Systems (ANTS)*, pp. 6–11, 2012.
- [45] N. Bessis, E. Asimakopoulou, T. French, P. Norrington, and F. Xhafa, "The Big Picture, from Grids and Clouds to Crowds: A Data Collective Computational Intelligence Case Proposal for Managing Disasters" *5th IEEE International Conference on P2P, Parallel, Grid, Cloud and Internet Computing (3PGCIC-2010)*, Fukuoka, Japan, November 4-6, 2010.

- [46] Cisco Systems, “Cisco Global Cloud Networking Survey 2012” Available http://www.cisco.com/en/US/solutions/ns1015/2012_Cisco_Global_Cloud_Networking_Survey_Results.pdf. Last accessed 13 Nov 2013.
- [47] T. Hansen, “The Future of Knowledge Work” Intel Corp, White Paper, October 2012. Available <http://blogs.intel.com/intellabs/files/2012/11/Intel-White-Paper-The-Future-of-Knowledge-Work4.pdf>. Last accessed 13 Nov 2013.
- [48] B. P. Rimal, E. Choi, and I. Lumb, “A Taxonomy and Survey of Cloud Computing Systems” *Fifth International Joint Conference on INC, IMS and IDC*, pp. 44-51, 2009.
- [49] Q. Zhang, L. Cheng, and R. Boutaba, “Cloud computing: State-of-the-art and research challenges” *Journal of internet services and applications*, vol. 1, no. 1, pp. 7–18, 2010.
- [50] Amazon EC2, <http://aws.amazon.com/ec2/>. Last accessed 02/04/2015.
- [51] Google App Engine, <https://cloud.google.com/appengine/>. Last accessed 02/04/2015.
- [52] google Apps, <https://www.google.com/work/apps/business/>. Last Accessed 02/04/2015.
- [53] DropBox, <https://www.dropbox.com/business/pricing>. Last accessed 10 Nov.2013.
- [54] F. Rocha, S. Abreu, and M. Correia, “The Final Frontier: Confidentiality and Privacy in the Cloud” *IEEE Computer*, vol. 44, no. 9, pp. 44-50, 2011.
- [55] IBM Global Technology Services, “Security and high availability in cloud computing environments” Available http://www-935.ibm.com/services/za/gts/cloud/Security_and_high_availability_in_cloud_computing_environments.pdf. Last accessed 13 Nov 2013.
- [56] A. Beloglazov and R. Buyya, Y. Lee, and A. Zomaya, “A taxonomy and survey of energy-efficient data centers and cloud computing systems” *Advances in Computers*, vol. 82, pp. 47-111, 2011.
- [57] “U.S. Environmental Protection Agency’s Report to Congress on Server and Data Center Energy Efficiency” August 2, 2007. Available http://hightech.lbl.gov/documents/data_centers/epa-datacenters.pdf. Last Accessed 9 Dec 2013.
- [58] B. Heller, S. Seetharaman, P. Mahadevan, Y. Yiakoumis, P. Sharma, S. Banerjee, and N. McKeown, “ElasticTree: saving energy in data center networks” presented at the *Proceedings of the 7th USENIX conference on Networked systems design and implementation*, San Jose, California, 2010.

- [59] J. Baliga, R. W. A. Ayre, K. Hinton and R. S. Tucker, "Green cloud computing: Balancing energy in processing, storage, and transport" *IEEE*, vol. 99, no. 1, pp.149 -167 2011.
- [60] M. F. Habib, M. Tornatore, M. D. Leenheer, F. Dikbiyik and B. Mukherjee, "Design of disaster-resilient optical datacenter networks" *IEEE/OSA Journal of Lightwave Technology*, vol. 30, no. 16, pp. 2563-2573, Aug. 2012.
- [61] B. Kantarci and H. T. Mouftah, "Designing an Energy-Efficient Cloud Network [Invited]" *IEEE/OSA Journal of Optical Communications and Networking*, vol. 4, no. 11, p. B101-113, Oct. 2012.
- [62] J. Buysse, C. Cavdar, M. de Leenheer, B. Dhoedt, and C. Develder, "Improving energy efficiency in optical cloud networks by exploiting anycast routing" *SPIE Conference Series*, vol. 8310, Nov. 2011.
- [63] J. Buysse, K. Georgakilas, A. Tzanakaki, M. De Leenheer, B. Dhoedt, and C. Develder, "Energy-Efficient Resource-Provisioning Algorithms for Optical Clouds" *IEEE/OSA Journal of Optical Communications and Networking*, vol. 5, no. 3, p. 226, Feb. 2013.
- [64] A. H. Mohsenian-Rad and A. Leon-Garcia, "Energy-information transmission tradeoff in green cloud computing" *IEEE Globecom'10*, 2010.
- [65] W. Jiang, R. Zhang-Shen, J. Rexford, and M. Chiang, "Cooperative content distribution and traffic engineering in an ISP network" *SIGMETRICS '09*, p. 239, 2009.
- [66] L. Chiaraviglio and I. Matta, "An energy-aware distributed approach for content and network management" *Computer Communications Workshops (INFOCOM WKSHPS 2011)*, *IEEE*, pp.337-342, April 2011.
- [67] K. Guan, G. Atkinson, D. Kilper, and E. Gulsen, "On the Energy Efficiency of Content Delivery Architectures" *IEEE ICC Green Communications (GreenComm) Workshop*, Kyoto, Japan, June 2011.
- [68] W. Deng, F. Liu, H. Jin, B. Li, and D. Li, "Harnessing renewable energy in cloud datacenters: opportunities and challenges" *IEEE Network*, vol. 28, pp. 48-55, 2014.
- [69] U. Mandal, M. Habib, S. Zhang, B. Mukherjee, and M. Tornatore, "Greening the cloud using renewable-energy-aware service migration" *IEEE Network*, vol. 27, pp. 36-43, 2013.
- [70] M. Gattulli, M. Tornatore, R. Fiandra, and A. Pattavina, "Low-emissions routing for cloud computing in IP-over-WDM Networks with data centers" *IEEE Journal on Selected Areas in Communications*, vol. 32, pp. 28-38, 2014.

- [71] D. Huang, D. Yang, and H. Zhang, "Energy-aware virtual machine placement in data centers" *2012 IEEE Global Communications Conference (GLOBECOM)*, pp. 3243–3249, Dec. 2012.
- [72] H. Goudarzi and M. Pedram, "Energy-Efficient Virtual Machine Replication and Placement in a Cloud Computing System" *IEEE 5th International Conference on Cloud Computing (CLOUD)*, pp. 750–757, Jun. 2012.
- [73] B. Kantarci, L. Foschini, A. Corradi, and H. T. Mouftah, "Inter-And- Intra Data Center VM-Placement for Energy-Efficient Large-Scale Cloud Systems" *IEEE GLOBECOM Workshop on Management and Security technologies for Cloud Computing (ManSecCC)*, pp. 1-6, 2012.
- [74] M. Pioro and D. Medhi, "Routing, Routing, Flow, and Capacity Design in Communication and Computer Networks" *Morgan Kaufman*, 2004.
- [75] NPTEL, "Operations Research Applications - Linear and Integer Programming", Available <http://www.nptel.ac.in/courses/110106059/13>. Last accessed 25/08/2015.
- [76] Robert Fourer, David M. Gay, and Brian W. Kernighan, "Production Models: Maximizing Profits" in *AMPL: A Modeling Language for Mathematical Programming, Second edition, ISBN 0-534-38809-4*.
- [77] Xpress-optimizer reference manual , Available <http://brblog.typepad.com/files/optimizer-1.pdf>. Last Accessed: 02-04-2015.
- [78] Introduction to Integer Linear Programming , Available <http://wpweb2.tepper.cmu.edu/fmargot/introILP.html>. Last Accessed: 09/06/201.
- [79] H. Goudarzi, M. Ghasemazar, and M. Pedram, "SLA-based Optimization of Power and Migration Cost in Cloud Computing" *12th IEEE/ACM International Symposium on Cluster, Cloud and Grid Computing (CCGrid)*, pp. 172–179, May 2012.
- [80] J. Llorca, K. Guan, G. Atkinson, and D. C. Kilper, "Energy efficient delivery of immersive video centric services" *IEEE INFOCOM*, pp. 1656–1664, 2012.
- [81] AMPL, Available <http://ampl.com/>. Last Accessed 02-04-2015.
- [82] L. Ye, H. Zhang, F. Li, and M. Su, "A measurement study on BitTorrent system" *International Journal of Communications, Network and System Sciences*, vol. 3, p. 916, 2010.
- [83] K. Eger, T. Hoßfeld, A. Binzenh, and G. Kunzmann, "Efficient Simulation of Large-Scale P2P Networks: Packet-level vs. Flow-level Simulations", *The second workshop on Use of P2P, GRID and agents for the development of content networks (ACM)*, pp. 9-16, 2007.

- [84] R. Kumar, Y. Liu, and K. Ross, “Stochastic fluid theory for P2P streaming systems” *IEEE INFOCOM*, pp. 919–927, 2007.
- [85] X. Yang and G. De Veciana, “Service capacity of peer to peer networks” *Twenty-third Annual Joint Conference of the IEEE Computer and Communications Societies (INFOCOM)*, pp. 2242–2252, 2004.
- [86] <http://www.nsfnet-legacy.org/about.php>. Last accessed 25/08/2015.
- [87] Cisco Systems, “Cisco CRS-1 8-Slot Single-Shelf System” Available http://www.cisco.com/en/US/prod/collateral/routers/ps5763/ps6112/product_data_sheet0900aecd801d53a1.pdf.
- [88] Glimmerglass, “Data sheet of Glimmerglass Intelligent Optical System 500.” Available <http://www.glimmerglass.com/products/intelligent-optical-systems/>.
- [89] Cisco Systems, “Cisco ONS15501 Erbium Doped Fiber Amplifier Data Sheet” Available http://www.cisco.com/en/US/products/hw/optical/ps2011/products_data_sheet_09186a008008870d.html.
- [90] Cisco Systems, “Data sheet of Cisco ONS 15454 100-GHz 4-CH Multi/Demultiplexer” Available http://www.cisco.com/en/US/prod/collateral/optical/ps5724/ps2006/product_data_sheet09186a00801a5572_ps5791_Products_Data_Sheet.html.
- [91] GreenTouch, “Green Meter Research Study: Reducing the Net Energy Consumption in Communications Networks by up to 90% by 2020” A *GreenTouch White Paper, Version 1, June 26, 2013*” available http://www.greentouch.org/uploads/documents/GreenTouch_Green_Meter_Research_Study_26_June_2013.pdf. Last accessed 14 Nov. 2013.
- [92] A. Legout, N. Liogkas, E. Kohler, and L. Zhang, “Clustering and sharing incentives in bittorrent systems” *ACM SIGMETRICS Performance Evaluation Review*, pp. 301–312, 2007.
- [93] GreenTouch, “Core Switching and Routing Working Group Overview, Research Targets and Challenges” *GreenTouch Open Forum, 17 Nov 2011*. Available <http://www.greentouch.org/uploads/documents/GreenTouch%20CS&R%20Working%20Group%20Presentation%20-%20Seattle%202011%20-%20v10.pdf>. Last Accessed 11 Nov 2013.
- [94] S. Knight, H. X. Nguyen, N. Falkner, R. Bowden, and M. Roughan, “The Internet Topology Zoo” *IEEE Journal on Selected Areas in Communications*, vol. 29, no. 9, pp. 1765–1775, Oct. 2011.
- [95] Topology Zoo, “ATT North America” Available <http://topology-zoo.org/maps/AttMpls.jpg>. Last accessed 14 Dec 2013.

- [96] D-maps, “United States of America (USA) / United States of America” Available http://d-maps.com/carte.php?num_car=11857&lang=en. Last accessed 14 Dec 2013.
- [97] Topology Zoo, “BT Europe” Available <http://topology-zoo.org/maps/BtEurope.jpg>. Last accessed 14 Dec 2013.
- [98] d-maps, “Europe” Available http://d-maps.com/carte.php?num_car=30073&lang=en. Last accessed 14 Dec 2013.
- [99] T. E. H. El-Gorashi, A. Mujtaba, W. Adlan, and J. M. H. Elmirghani, “Storage area networks extension scenarios in a wide area WDM mesh architecture under heterogeneous traffic” *IEEE 11th International Conference on Transparent Optical Networks, ICTON'09*, pp. 1–8, 2009.
- [100] d-maps, “Italy / Repubblica Italiana” Available http://d-maps.com/carte.php?num_car=18137&lang=en. Last accessed 14 Dec 2013.
- [101] J. Baliga , R. Ayre , K. Hinton and R. S. Tucker “Architectures for energy-efficient IPTV networks”, *OFC/NFOEC'09*, 2009.
- [102] Cisco Systems, “Data sheet of Cisco 300 Series Switches.” Available http://www.cisco.com/en/US/prod/collateral/switches/ps5718/ps10898/data_sheet_c78-610061.html. Last Accessed 9 Dec 2013.
- [103] HP, “Data sheet of HP ProLiant DL120 G7 Server series.” Available: http://www.hp.com/hpinfo/newsroom/press_kits/2011/poweryourdream/HP_ProLiant_DL120_G7_Datasheet.pdf. Last Accessed 9 Dec 2013.
- [104] B. Cohen, “The BitTorrent Protocol Specification”. Available http://www.bittorrent.org/beps/bep_0003.html. Last Accessed 9 Dec 2013.
- [105] J. Fonseca, B. Reza, and L. Fjeldsted “BitTorrent Protocol -- BTP/1.0”. Available <http://jonas.nitro.dk/bittorrent/bittorrent-rfc.html>. Last Accessed 9 Dec 2013.
- [106] <http://matplotlib.org>. Last Accessed 9 Dec 2013.
- [107] M. Soraya, M. Zamani, and A. Abhari, “Modeling of multimedia files on the web 2.0” *IEEE Canadian Conference on Electrical and Computer Engineering, CCECE 2008*, pp.1387-1392, May 2008.
- [108] Pando Networks, “Global Internet Speed Study” Available <http://www.pandonetworks.com/company/news/pando-networks-releases-global-internet-speed-study>. Last accessed 5 Jan 2014.
- [109] V. Valancius, N. Laoutaris, L. Massoulie, C. Diot, and P. Rodriguez, “Greening the internet with nano data centers” *CoNEXT*, pp 37-48, 2009.

- [110] Google, “Efficiency: How we do it” Available <http://www.google.co.uk/about/datacenters/efficiency/internal/>. Last accessed 13 Nov. 2013.
- [111] P. Mathew, S. Greenberg, D. Sartor, J. Bruschi, and L. Chu, “Self-benchmarking Guide for Data Center Infrastructure: Metrics, Benchmarks, Actions” Available <http://hightech.lbl.gov/benchmarking-guides/docs/datacenter-benchmarking-guide.pdf>. Last accessed 13 Nov. 2013, 2010.
- [112] A. Beloglazov, J. Abawajy, and R. Buyya, “Energy-aware resource allocation heuristics for efficient management of data centers for Cloud computing” *Future Generation Computer Systems*, vol. 28, no. 5, pp. 755–768, May 2012.
- [113] J. M. H. Elmirghani, T. Klein, K. Hinton, A. Q. Lawey, and X. Dong, “GreenTouch GreenMeter Core Network Power Consumption Models and Results” *IEEE Online Conference on Green Communications (OnlineGreencomm)*, pp. 1-8, 2014.
- [114] J. Paton, “Australian Wind Energy Now Cheaper Than Coal, Gas, BNEF Says” Feb 7, 2013. Available <http://www.bloomberg.com/news/articles/2013-02-06/australia-wind-energy-cheaper-than-coal-natural-gas-bnef-says>. Last accessed 09/06/2015.
- [115] GreenTouch, “Reducing the Net Energy Consumption in Communications Networks by up to 98% by 2020”, white paper, Version 2.0, August 15, 2015. Available <http://www.greentouch.org/uploads/documents/White%20Paper%20on%20Green%20Meter%20Final%20Results%20August%202015%20Revision%20-%20vFINAL.pdf>. Last accessed 25/08/2015.